

**Imperial College
London**

**Tau-proximity ligation assay reveals extensive
previously undetected pathology prior to
neurofibrillary tangles in preclinical
Alzheimer's disease**

Elisavet Velentza-Almpani

Submitted for the Degree of Doctor of Philosophy

May 2023

Department of Brain Sciences, Imperial College London

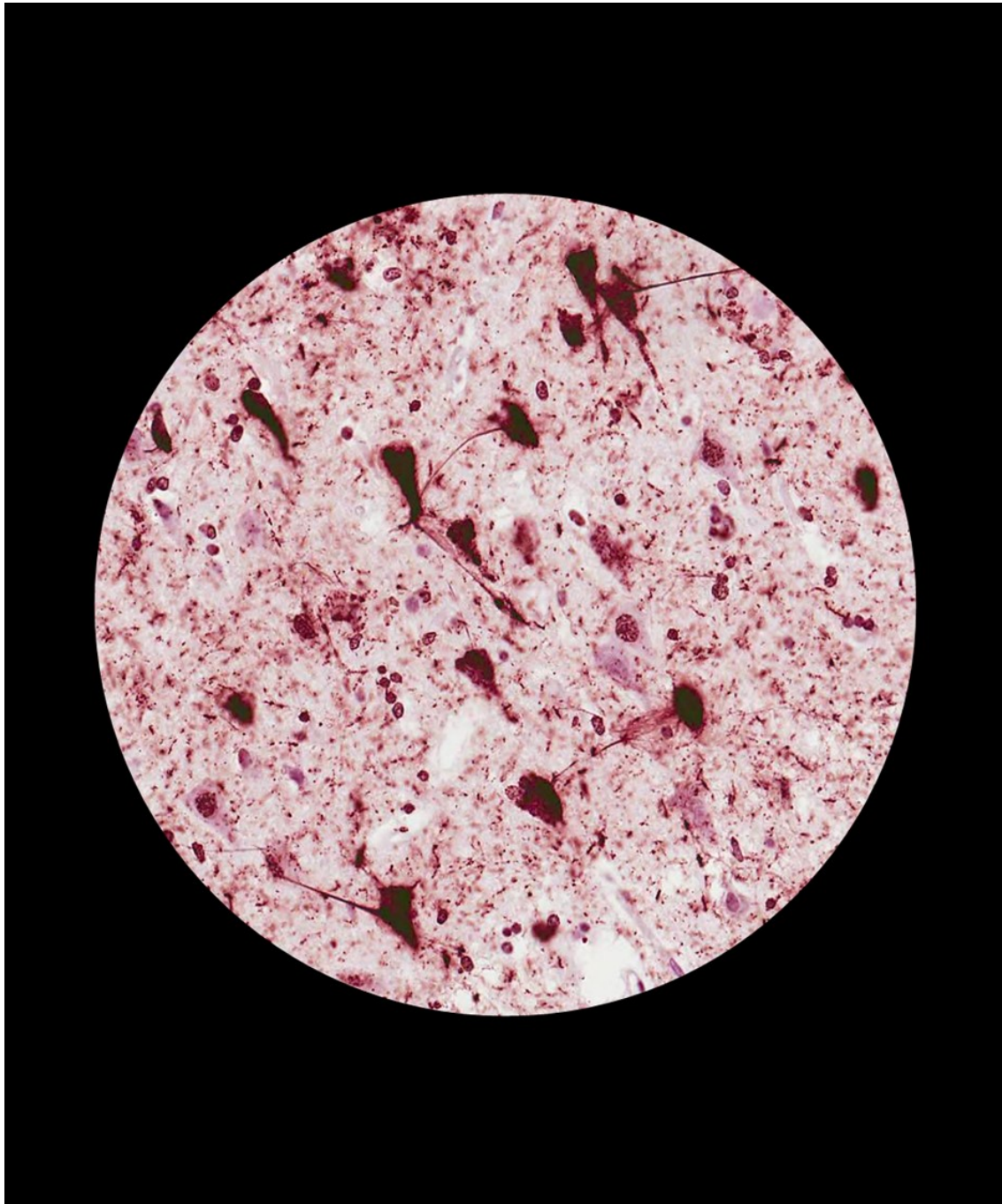


Illustration: Tau-PLA labelling of tau multimers in post-mortem human brain.

Declaration of Originality

The work presented in this thesis is my own and everyone else who has contributed is appropriately referenced and acknowledged.

Copyright Declaration

The copyright of this thesis rests with the author. Unless otherwise indicated, its contents are licensed under a Creative Commons Attribution-Non-Commercial 4.0 International Licence (CC BY-NC).

Under this licence, you may copy and redistribute the material in any medium or format. You may also create and distribute modified versions of the work. This is on the condition that: you credit the author and do not use it, or any derivative works, for a commercial purpose.

When reusing or sharing this work, ensure you make the licence terms clear to others by naming the licence and linking to the licence text. Where a work has been adapted, you should indicate that the work has been changed and describe those changes.

Please seek permission from the copyright holder for uses of this work that are not included in this licence or permitted under UK Copyright Law.

Acknowledgments

The following dissertation, entitled "Tau-proximity ligation assay reveals extensive previously undetected pathology prior to neurofibrillary tangles in preclinical Alzheimer's disease," was conducted in the Laboratory of Neuropathology and Neurophysiology, Department of Brain Science, Imperial College London, under the guidance of Dr. Javier Alegre-Abarategui and Prof. Nicholas D. Mazarakis.

Throughout the arduous and challenging four-year journey that led to the completion of this work, I was privileged to have had the support and assistance of numerous individuals who enabled me to reach my destination. I would like to express my sincere gratitude to all those who stood by me and helped me to overcome the obstacles and difficulties that I encountered.

First and foremost, I am grateful to Dr. Javier Alegre-Abarategui for offering me the opportunity to work in his laboratory and for entrusting me with such an intriguing and promising scientific project. I would also like to extend my appreciation to my co-supervisor, Prof. Nicholas D. Mazarakis, for his valuable contributions and guidance. The knowledge, support, and mentorship provided by both supervisors have been instrumental in my development as a researcher. Their encouragement and advice throughout the rigorous and challenging years of my Ph.D. have been invaluable.

I would also like to acknowledge the contributions of my Ph.D. progress review panel, Dr. Magdalena Sastre, Prof. Bill Wisden, and Dr. Amin Hajitou, who offered valuable insights and suggestions on my current and future experimental work.

I am deeply grateful to Michael J Fox, Alzheimer's Research UK, and the NIHR Imperial Biomedical Research Centre for their financial support of this project. I would also like to thank Parkinson's UK, the Medical Research Council Centres of Excellence in Neuroscience (COEN), and the British Neuropathological Society for their assistance. The Multiple Sclerosis and Parkinson's Tissue Bank of Imperial College London and the Oxford Brain Bank provided the control and patient brain tissue samples and assisted with the immuno-labelling procedures. In addition, I would like to thank Dr. Michael Goedert for kindly providing the P301S mouse line. Lastly, I want to express my gratitude to the donors and families from the Tissue Banks for their valuable donations that enabled the research to take place.

I would also like to express my appreciation to my former and current colleagues at the laboratory, including Maria Otero Jimenez, James Spence, Sandra Gray-Rodriguez, Dr. Radhi Anand, Ildiko Farkas, Dr. Djordje Gveric, and Dr. Bibiana Mota, as well as the MSc and BSc students, for their collaboration, encouragement, and friendship. I would also like to extend my gratitude to Prof Steve Matthews and Dr. Amit Kumar from the Department of Chemistry for their help with the protein purification experimental procedure. Furthermore, I would like to thank all our collaborators from Oxford University, particularly Dr. Nora Bengoa-Vergniory, for their collaboration in publishing our research. My sincere appreciation also goes to Prof. Steve Gentleman and Dr. Mariana Vargas-Caballero for accepting to be members of my examination committee.

I would like to extend my deepest gratitude to Mr. Mohamed Ahmed, whose unwavering support significantly aided my studies throughout these years.

I am deeply indebted to my family, who instilled in me the values of perseverance, hard work, and determination, and provided me with unwavering support throughout my academic journey. Giannis, Eleni, Angela, and Leo, I extend my sincerest gratitude and boundless appreciation to each of you for believing in my potential and bolstering my aspirations in every way possible. Your guidance has been invaluable in shaping me into the person I am today, and for that, I am eternally grateful. You have taught me the importance of setting goals, working diligently, maintaining integrity, and remaining patient and persistent. Once again, thank you for standing by my side, sharing my concerns, and offering unwavering support throughout my journey.

In addition, I extend my heartfelt appreciation to my friends for their unyielding motivation, encouragement, and support. Your unwavering support has been a constant source of strength and inspiration, and I am deeply grateful for your presence in my life.

To my family...

Abstract

Tauopathies, with Alzheimer's disease (AD) the most common neurodegenerative disorder, are caused by the abnormal folding and aggregation of proteins that seed themselves and spread throughout the brain in a prion-like manner causing irreversible neuronal cell death and progressive neurological symptoms. The intracellular aggregates of the hyperphosphorylated tau in neurofibrillary tangles (NFTs), together with the extracellular deposits of amyloid beta, are the fundamental neuropathological characteristics of AD. It is unclear which tau species cause the toxicity and have seeding capacity, responsible for the prion-like spread of tau pathology. While neuronal loss correlates with the number of NFTs in AD, it is disproportionately higher, suggesting oligomeric tau species rather than NFTs being the toxic species. This also suggests that a proportion of tau pathology is not being detected by standard histopathological markers (which focus on the detection of phosphorylated tau), particularly since tau fibrillisation can occur independently of tau post-translational modifications. We have now developed a new assay, tau proximity ligation assay (tau-PLA), for the histopathological visualisation of a range of tau pathology, including previously invisible early tau multimers, *in situ* with anatomical and subcellular detail. Tau-PLA detected self-interacting tau *in vitro* and *in situ* in animal and post-mortem AD human brain with high specificity, recognising different patterns of tau pathology. In contrast with standard histopathological markers, tau-PLA detected a previously unreported early type of tau pathology revealing an extensive diffuse tau distribution in non-pathological brain regions of the brain along the Braak tau pathway. It also revealed that tau multimerization is one of the earliest detectable molecular events of AD tau pathology preceding tau hyperphosphorylation and misfolding. Tau Real-Time Quaking-Induced Conversion showed that the early tau multimers have high seeding activity and might be the toxic species contributing to the disease progress. Therefore, our findings open a new window to the study of early tau pathology, with potential implications in early diagnosis and the design of therapeutic strategies.

List of Abbreviations

ABC	Avidin-biotin complex
AD	Alzheimer's disease
ALP	Autophagy-lysosome pathway
ARUK	Alzheimer's Research UK
AV	Average
BiFC	Bimolecular fluorescence complementation
DAB	3'3-diaminobenzidine
DAPI	4',6-diamidino-2-phenylindole
ddH ₂ O	double-distilled water
DMEM	Dulbecco's Modified Eagle Medium
DNA	Deoxyribonucleic acid
DPX	Distrene-Plasticiser-Xylene
EDTA	Ethylenediaminetetraacetic acid
FFPE	Formalin-fixed paraffin-embedded
FPLC	Fast protein liquid chromatography
GFAP	Glial Fibrillary Acidic protein
GFP	Green fluorescent protein
H&E	Haematoxylin and eosin
HEK293	Human Embryonic Kidney 293
HEPES	Hydroxyethyl piperazineethanesulfonic acid
HRP	Horseradish peroxidase
Iba1	Ionized calcium-binding adaptor molecule 1
IF	Immunofluorescence
IHC	Immunohistochemistry
ITC	Inferior temporal cortex
LB	Luria-Bertani Broth
MAPT	Microtubule-associated protein tau
MTC	Middle temporal cortex
NFT	Neurofibrillary tangles
NT	Neuropil threads
NP	Neuritic plaque

OC	Occipital Cortex
OCT	Optimal cutting temperature
PBS	Phosphate buffered saline
PBS – Tw	Phosphate buffered saline with Tween
PBS – Tx	Phosphate buffered saline with Triton-X
PFA	Paraformaldehyde
PHFs	Paired helical filaments
PLA	Proximity Ligation Assay
PR	Parastriate area
PTMs	Post-translational modification
RT	Room temperature
SDS	Sodium dodecyl sulfate
SEC	Size exclusive chromatography
SFs	Straight filaments
SPs	Senile plaques
ST	Striate area
STC	Superior temporal cortex
TC	Temporal cortex
TEM	Transmission electron microscopy
ThT	Thioflavin T
UPS	Ubiquitin-proteasome system

Contents

Declaration of Originality	2
Copyright Declaration.....	3
Acknowledgments.....	4
Abstract	7
List of Abbreviations	8
List of Figures	15
List of tables.....	17
Chapter 1: Introduction	18
1.1 Alzheimer’s Disease.....	18
1.1.1 Epidemiology of AD	18
1.1.2 Risk factors for AD.....	19
1.1.3 Neuropathology of AD	22
1.1.4 Symptoms of pre-clinical and clinical AD	27
1.1.5 Treatments for AD.....	29
1.2 Tau protein	32
1.2.1 Tauopathies.....	32
1.2.2 <i>MAPT</i> gene and tau structure	33
1.2.3 Post-translational modifications of tau protein	35
1.2.4 The physiological role of tau protein	38
1.2.5 Tau pathology	40
1.3 Early-type tau aggregates	45
1.3.1 Strains of tau protein.....	45
1.3.2 Seeding activity of tau protein	46
1.4 Current methods for the detection and investigation of tau pathology	49
1.4.1 Immunoassays.....	49
1.4.2 Cell-based assays	50
1.4.3 Protein amplification-based assays	51
1.5 Hypothesis and Aims.....	52

Chapter 2: Materials and methods	54
2.1 Materials	54
2.2 Methods.....	59
2.2.1 Methods of Molecular Biology.....	59
2.2.1.1 Bacterial DMSO stocks.....	59
2.2.1.2 Inoculation of bacterial culture	59
2.2.1.3 Plasmid DNA purification	59
2.2.1.4 Determination of plasmid DNA total concentration and purity.....	60
2.2.1.5 Agarose gel electrophoresis	60
2.2.1.6 Diagnostic Restriction Digest	61
2.2.1.7 DNA Sequencing	61
2.2.1.8 Recombinant τ 306 tau fragment purification.....	61
Inoculation of starter culture from plate colonies	62
Autoinduction of protein expression	62
Fast protein liquid chromatography (FPLC)	63
Acetone precipitation of τ 306 fractions	64
Size exclusion chromatography (SEC)	64
Polyacrylamide gel electrophoresis.....	64
Protein Collection.....	65
RT2.2.1.9 Protein assembly	65
2.2.1.10 Tau Real-Time Quaking-Induced Conversion (RT-QuIC).....	66
Kinetic Calculations and statistical analysis	68
2.2.2 Methods of Cellular Biology	68
2.2.2.1 Cell Culture.....	68
Cell culture conditions	68
Cell thawing	68
Cell passaging	69
2.2.2.2 Tau Bimolecular fluorescence complementation (BiFC) assay.....	69
2.2.2.3 Tau FKBP-FRB-rapamycin assay.....	70

2.2.2.4 Imaging	70
2.2.3 Tissue work.....	71
2.2.3.1 Animal work	71
Tissue Collection.....	71
Microtome sectioning.....	71
Ethics declarations.....	72
2.2.3.2 Human tissue work	72
Neuropathological assessment of the cases.....	72
Exclusion Criteria.....	73
Summary of cases included in the study	73
Microtome sectioning.....	77
Cryo-sectioning	77
Brain Tissue Homogenisation	77
Ethics declarations.....	78
2.2.3.3 Tau – Proximity Ligation Assay (tau-PLA).....	78
Tau-PLA probes preparation.....	78
Tissue preparation for tau-PLA.....	78
Tau-PLA brightfield staining	79
Tau-PLA co-immunofluorescence	80
6x His tag Proximity Ligation Assay (6x His tag-PLA).....	80
2.2.3.4 Immunohistochemistry (IHC) of FFPE sections.....	81
2.2.3.5 Haematoxylin & Eosin staining	81
2.2.3.6 Imaging and neuropathological analysis.....	82
Chapter 3: tau-PLA detects tau-tau interactions in <i>in vitro</i> systems.....	85
3.1 Introduction.....	85
3.2 Hypothesis and Aims	87
3.3 Tau-PLA detects tau-BiFC complexes	87
3.4 Tau-PLA detects intracellular tau complexes but no monomeric.....	89
3.5 Tau-PLA detects tau multimerisation of recombinant tau but no monomers.....	90

3.6 Discussion	92
3.6.1 Limitations.....	93
3.6.2 Conclusions	94
Chapter 4: <i>In situ</i> specificity of tau-PLA in animal and post-mortem human brain tissues	95
4.1 Introduction.....	95
4.2 Hypothesis and Aims	96
4.3 <i>In situ</i> specificity of tau-PLA in transgenic and <i>MAPT</i> KO mice	96
4.4 <i>In situ</i> specificity of tau-PLA in human tissue.....	100
4.4.1 Tau-PLA is a result of productive tau-PLA.....	100
4.4.2 Tau-PLA is an antibody-dependent assay	101
4.5 Discussion.....	102
4.5.1 Limitations.....	103
4.5.2 Conclusions	104
Chapter 5: tau-PLA recognised disease-related tau multimers.....	105
5.1 Introduction.....	105
5.2 Hypothesis and Aims	106
5.3 Tau-PLA labels a range of structures in the AD brain.....	107
5.4 NFT maturity characterised by Tau-PLA	108
5.5 Tau-PLA detects tau small complexes in glial cells	110
5.6 Discussion.....	111
5.6.1 Limitations.....	112
5.6.2 Conclusions	113
Chapter 6: Extensive and early tau multimerisation revealed by tau-PLA in the development of tau pathology.....	114
6.1 Introduction.....	114
6.2 Hypothesis and Aims	116
6.3 Braak Staging of post-mortem human brain tissue according to BrainNet Europe diagnostic protocol.....	116

6.4 Spatiotemporal distribution of tau-PLA labelled structures across Braak Stages	118
6.5 Tau-PLA reveals early tau-tau interactions, prior to tau hyperphosphorylation and misfolding	125
6.6 Tau-PLA highlights tau multimerisation as one of the earliest events occurring during NFT maturity	133
6.6 Discussion	135
6.6.1 Limitations	137
6.6.2 Conclusions	138
Chapter 7: Investigation of the seeding activity of self-interacting tau molecules....	139
7.1 Introduction	139
7.2 Hypothesis and Aims	140
7.3 Characterisation of τ 306 plasmid construct	141
7.4 τ 306 protein fragment purification and aggregation	142
7.5 Tau RT-QuIC reveals high seeding activity of early tau multimerisation.....	143
7.6 Discussion	149
7.6.1 Limitations	151
7.6.2 Conclusions	152
Chapter 8: General Discussion.....	153
8.1 Limitations	159
8.2 Future directions	160
8.3 Conclusions	161
Appendix.....	162
References	170

List of Figures

Figure 1.1. Macroscopic image of post-mortem normal and AD human brain	23
Figure 1.2. Tau aggregated species	24
Figure 1.3. AD senile plaques.....	25
Figure 1.4. Human microtubule-associated protein tau	34
Figure 2.1. Macroscopically neuroanatomical regions of post-mortem human brain .	72
Figure 2.2. Automated analysis scale used for analysis.....	83
Figure 2.3. Semi-quantitative scale used for analysis.....	84
Figure 3.1 Schematic representation of tau Proximity Ligation Assay (tau-PLA).....	86
Figure 3.2 Tau-PLA detects tau-BiFC complexes	88
Figure 3.3 Tau-PLA can detect the rapamycin-induced interactions between the tau molecules of the tau-FKBP-FRB system.....	90
Figure 3.4 Tau-PLA detects tau multimerisation of recombinant tau but no monomers	91
Figure 4.1 Demonstration of the in situ specificity of tau-PLA in mouse brain tissue	98
Figure 4.2 Age-dependent accumulation of tau-PLA signal in P301S transgenic mice	99
Figure 4.3 Fluorescent tau-PLA in mouse brain tissue.....	100
Figure 4.4 Tau-PLA is a result of productive tau-PLA	101
Figure 4.5 Application of 6xHisTag-PLA in post-mortem human brain tissue	102
Figure 5.1 Tau-PLA recognises a range of tau structures, from large lesions to small-sized diffuse tau pathology	108
Figure 5.2 NFT maturity characterized by tau-PLA	109
Figure 5.3 Tau-PLA detects tau small complexes in glial cells.....	110
Figure 6.1 Tau aggregates labelled with AT8-IHC across the different Braak Stages as defined by BrainNet Europe diagnostic protocol.....	117
Figure 6.2 Tau-tau interactions labelled with tau-PLA across the different Braak Stages as defined by BrainNet Europe diagnostic protocol	118

Figure 6.3 Tau-PLA revealed that cases in Braak 0 group presented heterogeneity as far as it concerns the levels of tau-PLA load in brain regions that are affected quite early in the development of pathology.....	119
Figure 6.4 Quantification of tau-PLA labelled diffuse pathology and tau-PLA and AT8-IHC labelled large perikaryal neurofibrillary-type lesions in hippocampal regions, TC, and OC	120
Figure 6.5 Quantification of large lesions labelled with tau5-IHC in the hippocampal and temporal region	122
Figure 6.6 Quantification of lesions labelled with 4G8-IHC in the hippocampal and temporal region	123
Figure 6.7 Scanned tau-PLA labelled post-mortem human brain tissue sections.....	124
Figure 6.8 Tau aggregates labelled with different phosphor-tau and conformational antibodies across the different Braak Stages as defined by BrainNet Europe diagnostic protocol	1274
Figure 6.9 Quantification of AT180-, T217-, PHF-1, S422-, MC1- and Alz50-IHC labelled large perikaryal neurofibrillary-type lesions in hippocampal regions, TC, and OC.....	128
Figure 6.10 Widespread tau multimerization occurs early and prior to tau hyperphosphorylation and tau misfolding across EC, TC, and OC.....	132
Figure 6.11 Tau multimerisation is one of the earliest detectable events occurring during the maturity of NFTs.....	134
Figure 7.1 Characterisation of τ 306 plasmid construct.....	142
Figure 7.2 Transmission electron microscopy of recombinant τ 306 soluble monomers and τ 306 aggregated species	143
Figure 7.3 PLA-/AT8-, PLA+/AT8-, and PLA+/AT8+ groups.....	144
Figure 7.4 ThT fluorescence data of RT-QuIC analysis.....	146
Figure 7.5 Tau RT-QuIC analysis.....	148

List of tables

Table 2.1 – Primary antibody list.....	55
Table 2.2 – Secondary antibody list.....	58
Table 2.3 – RT-QuIC reaction buffer master mix.....	67
Table 2.4 - Summary of patient information	74
Table 2.5 – Additional brain tissue information	74
Table 2.6 - Solutions and Regents	162
Table 2.7 - Commercial Kits.....	169

Chapter 1: Introduction

1.1 Alzheimer's Disease

1.1.1 Epidemiology of AD

AD is worldwide the most prevalent and common cause of dementia affecting a vast number of individuals (60-80% of cases with dementia) (Silva and Haggarty, 2020). Recent studies showed that approximately 58 million individuals in America of the age of 65 and above live with AD, with the number of cases predicted to reach 88 million in 2050 (He W. et al., 2016; "U.S. Census Bureau. 2014 National Population Projections," 2021). Although the incidence rate of AD has been reported to be decreasing through the years due to improvements and the acquired knowledge in the field of medicine and technology, the number of individuals with AD is increasing significantly as the population aged 65 years old and over is rising (He W. et al., 2016; Rajan et al., 2021; "U.S. Census Bureau. 2014 National Population Projections," 2021). The number of individuals with AD is increasing with age, defining age as one of the principal risk factors for the development of AD (Tahami Monfared et al., 2022). A percentage of 5% of individuals with age 65-74 years suffers from AD, with this percentage being increased to 13% and 32% in individuals with age 75-84 and >85 years, respectively (Rajan et al., 2021). Although AD predominantly appears in old people, known as late-onset (sporadic) Alzheimer's dementia, young population can also be affected with the number of patients presenting the early-onset (familial) form being limited (Hendriks et al., 2021). Together with the global rise of people living with AD, the financial expenses for the investigation, diagnosis, and treatment of the disease are expected to be doubled reaching more than \$2 trillion by 2030, unless new ways and means for preventing, delaying, and curing the disease are developed ("2020 Alzheimer's disease facts and figures," 2020; Holtzman et al., 2011). Differences in the prevalence of AD have also been reported between the two genders (Rajan et al., 2021). Studies have shown that females are more likely to develop AD and other dementias than males of the same age. The fact that the lifespan of female individuals is longer than males contributes to the higher prevalence of AD in women ("2022 Alzheimer's disease facts and figures," 2022; Chêne et al., 2015). The findings concerning the risk

of developing AD for age-matched female and male patients are mixed suggesting that the differences reported between the two genders are dependent as well on the age and the geographic region (Tahami Monfared et al., 2022). Genetic factors affect in a different manner women and men with the majority of the studies highlighting that the ApoE-e4 gene has a strong link to AD (Ungar et al., 2014). The geographic region, racial identity, lifestyle, and education also contribute to the reported differences in the prevalence of AD as these conditions affect differently the risk of developing AD (Launer et al., 1999; Russ et al., 2013; Tahami Monfared et al., 2022). The number of individuals dying from AD has increased dramatically since 2000 affecting mostly the older ages (Rajan et al., 2021; Tejada-Vera, 2013). Data from 2019 reported AD to be the 6th leading cause of death, falling to 7th in 2020 and 2021 after the appearance of COVID-19, with COVID-19 being one of the most dominant death causes during these years (Rajan et al., 2021; The US Burden of Disease Collaborators et al., 2018; Xu et al., 2020). The long duration of the disease from the moment of diagnosis to death (8-10 years, together with the increase in the average lifespan of humans and the high levels of morbidity contribute dramatically to the public health impact of the disease (Rajan et al., 2021; The US Burden of Disease Collaborators et al., 2018)

1.1.2 Risk factors for AD

Different risk factors have been described so far to contribute to the development of AD. Although a small percentage of AD cases are familial, caused by inherited gene mutations, the vast majority of AD cases are sporadic and are the result of various factors that increase the risk for the disease (“2022 Alzheimer’s disease facts and figures,” 2022). One of the strongest risk factors is age (Hebert et al., 2010). The risk of developing AD is higher in individuals with age over 65 (Tahami Monfared et al., 2022). As mentioned previously the percentage of patients living with AD is increasing with age with the percentage of patients over 85 years old being 33.2% (Hebert et al., 2010). Genetics also play a pivotal role in the development of sporadic AD (“2022 Alzheimer’s disease facts and figures,” 2022). One strong genetic candidate is the ApoE-e4 gene (Loy et al., 2014). Three are the alleles of ApoE gene e2, e3, and e4. People with at least one e4 allele have a higher risk of getting AD, with the individuals homozygous for the e4 allele having up to 12 times more chance of developing the

disease (Michaelson, 2014). The e4 allele has been reported to be linked with the increased possibility of forming a-beta plaques (Jansen et al., 2015). Various factors like ethnicity, racial differences, or regional background affect the appearance of e4 allele in the adult population affecting consecutively the likelihood of developing AD (Rajan et al., 2021). Initiation of AD pathology due to neuronal e4 involves several pathophysiological mechanisms, including: the activation of microglia to induce neuroinflammation, direct promotion of neuronal degeneration, involvement in multiple signaling pathways that encourage the production and accumulation of A β and Tau proteins, interference with lipid elimination resulting in cellular lipid accumulation, and disruption of neuron cholesterol transport, ultimately reducing the formation of myelin sheaths (Weuve et al., 2018). Recent studies focusing on e4 expression among individuals with different ethnic and geographic background have reported conflicting outcomes and therefore further investigation into the AD genetic mechanisms is essential (Bakulski et al., 2021; Weuve et al., 2018). A link between people with Trisomy 21 – Down Syndrome and AD has also been reported (Lott and Dierssen, 2010). Individuals with Trisomy 21 have an extra chromosome 21. *APP* gene, located in chromosome 21, leads to the production of the amyloid precursor protein (APP) (Selkoe and Hardy, 2016). In patients with AD, APP cleavage leads to the generation of a β protein which tends to aggregate forming the a β plaques, one of the main pathological hallmarks of the disease (Selkoe and Hardy, 2016). Therefore, individuals with 3 copies of chromosome 21, produce higher levels a β , having a higher risk for AD (Lott and Dierssen, 2010). People with Trisomy 21 develop AD at a younger age with the possibility of developing AD to increase with age (Lott and Dierssen, 2010). With life expectancy of adults living with Trisomy 21 rising, AD is considered one of the main causes of morbidity in individuals with Down Syndrome (Hithersay et al., 2019). A small number of AD cases are results of dominantly inherited gene mutations, with the mutations being detected in the genes: *APP*, Presenilin 1 (*PSEN1*), and Presenilin 2 (*PSEN2*) leading to early-onset AD (Goldman et al., 2011; Ryman et al., 2014). Apart from these factors that cannot be easily controlled to delay and reduce the possibility of the appearance of the symptoms, other more manageable risk factors include: cardiovascular disorders, lifestyle, diet, education, and brain trauma (“2022 Alzheimer’s disease facts and figures,” 2022). These factors may not affect directly the risk of developing AD, but they might act indirectly affecting other factors linked more tightly to AD (Weuve et al., 2018). The brain is a small but demanding organ having

high demands in oxygen (1/5 of the body's total oxygen supply), and hence, an efficient blood supply is essential for the normal function of the brain (Mergenthaler et al., 2013). The heart supplies the brain with blood through the carotid and vertebra arteries and disturbances in the health of the heart affect the function of the brain (Samieri et al., 2018). Therefore, the factors that increase the chances of a cardiovascular disorder affect indirectly the risk of developing AD (Samieri et al., 2018). These could be diabetes, blood pressure, hypertension, and high cholesterol (Abell et al., 2018; Anstey et al., 2017; Biessels and Despa, 2018). On the other hand, the disease itself affects normal blood flow and heart function (“2022 Alzheimer’s disease facts and figures,” 2022). Since 1952 infections from microbes such as Herpes viruses, *Porphyrromonas gingivalis*, *Candida albicans* and others are also considered to be important risk factors for AD. These microbes are associated with the tau and A β fragments levels, as well as with *APOE* expression, by having the potential to directly harm neurons or indirectly initiate neuroinflammation, as demonstrated by previous studies (Lannuzel et al., 1997; Li et al., 2015), while viral infections can additionally impact the metabolism, accumulation, and elimination of proteins associated with Alzheimer's disease (Eimer et al., 2018; Fan et al., 2020; Kamer et al., 2015; Sjogren et al., 1952). Detection of the genetic material of these pathogens in the brain or CSF of the patients could be a potential biomarker for the diagnosis of the disease (Fan et al., 2020). Lifestyle and diet are also important risk factors for AD. Individuals following a balanced diet, exercising, and avoiding smoking and drinking reduce the risk of mild cognitive impairment and Alzheimer’s dementia (Buchman et al., 2019; Sanches Machado d’Almeida et al., 2018). Education and brain training also support brain health. Although the underlining mechanisms, in this case, are not well defined, it is hypothesised that education and performance of cognitive tasks help the brain to use more efficiently the neuronal networks (Stern et al., 2020). Here it is essential to mention that from a socioeconomic aspect, education tends also to provide a lifestyle that ensures a better nutrition and medical care (McDowell et al., 2007). Other risk factors include trauma brain injury (TBI), mental health, and environmental factors (Barnes et al., 2018; Cherbuin et al., 2015; Fann et al., 2018; Weuve et al., 2021).

1.1.3 Neuropathology of AD

Neurons are the fundamental components of the nervous system, each consisting of a) the cell body that contains the nucleus, b) the axon, a long process that extends out from the cell body and forms branches that connect to other neurons, muscles, or other cell types, and c) the dendrites, numerous shorter processes that receive information from other neurons through synapses (Luo et al., 2015; Zayia and Tadi, 2022). Healthy neurons are essential for the transmission of electrical impulses and chemical molecules (neurotransmitters) to and from the brain to execute multiple functions forming the cellular basis for the production of movements, senses, and memories (Giménez, 1998). The healthy structure and function of the neuronal cells are highly affected in the diseased brain. Although the neuropathological diagnosis of AD is still a challenge for the neuropathologists, an early and correct diagnosis is essential for the delay and treatment of the disease. In macroscopical assessment, the AD brain is characterized by weight and volume loss as the atrophy expands through the cortices affecting mostly the association cortices and the structures of the limbic system (Perl, 2010). Ventricle expansion is also observed with the frontal and temporal horns being severely involved (Piguet et al., 2009). The enlargement of the temporal horn has an impact on the hippocampal region, contributing to the development of cognitive and memory impairment in patients (Serrano-Pozo et al., 2011). Finally, pons involvement is a common pathological feature of AD, characterized by degeneration of the pigmented neuronal cells in the area of locus coeruleus (Serrano-Pozo et al., 2011). These macroscopic characteristics are non-AD specific and can be also observed in other neurological conditions like age-associated diseases, and therefore microscopic evaluation of the brain tissue is essential for accurate confirmation of AD diagnosis (DeTure and Dickson, 2019) (Fig. 1.1).

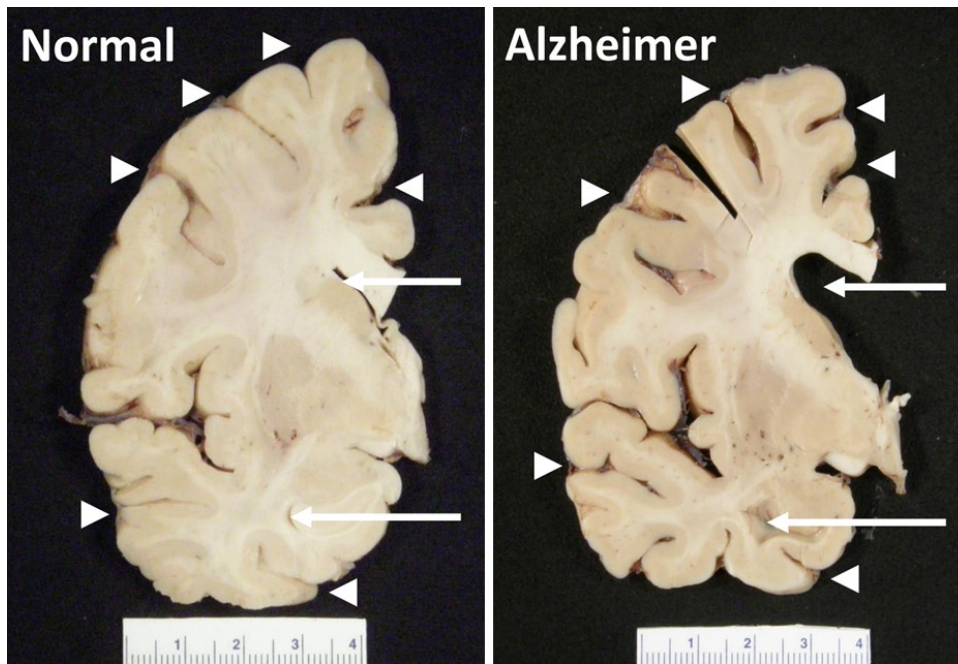


Figure 1.1. Macroscopic images of post-mortem normal and AD human brain. AD brain is characterised by cortical atrophy with the gyri being shrunk and the sulcal spaces being widened (arrowheads). Enlargement of the ventricles is also observed (arrows). These pathological features are not AD-specific and can also be detected in other neurological conditions. (DeTure and Dickson, 2019).

Intracellular accumulation of abnormal tau in neurofibrillary tangles (NFTs), neuropil threads (NTs) (straight and paired helical filaments that consisting of abnormally phosphorylated tau, primarily found in distant dendritic regions), and neuritic plaque (NP)-associated tau (degenerating neural matter encircling accumulations of amyloid beta) (Fig. 1.2), together with the extracellular amyloid beta deposition and the enhanced levels of neuroinflammation and neurodegeneration are the fundamental features of the AD (Selkoe and Hardy, 2016; Spillantini and Goedert, 2013). Additional characteristics of the disease are cerebral amyloid angiopathy (CAA), granulovacuolar degeneration (GVD) due to the small vacuoles with a dense core in the cytoplasm of the neurons that contain tau molecules, and the appearance of Hirano bodies: accumulation of filamentous actin and actin-binding proteins found in the dendrites of the neurons (DeTure and Dickson, 2019; Hirano, 1994; Serrano-Pozo et al., 2011).

Tau protein, produced by the *MAPT* gene, is physiologically a soluble protein that binds to the microtubules of the axons providing neuronal stability, promoting axonal growth, contributing to neuronal transportation, and contributing to synaptic plasticity and

hence ensuring the healthy and normal function of neurons (Pallas-Bazarra et al., 2016; Panda et al., 2003). This normal function and structure of tau are highly affected in the AD brain. Tau lesions vary in structure, composition, size, and cellular and anatomical location. These tau accumulations can be soluble forming multimeric complexes and protofibrils, or insoluble aggregates that form tau fibrils consisting of paired-helical filaments (PHFs) and straight filaments (SFs), or even extracellular tau depositions following neuronal death (ghost tangles) (Grundke-Iqbal et al., 1986; Lasagna-Reeves et al., 2014; Lee et al., 1991) (Fig. 1.2).

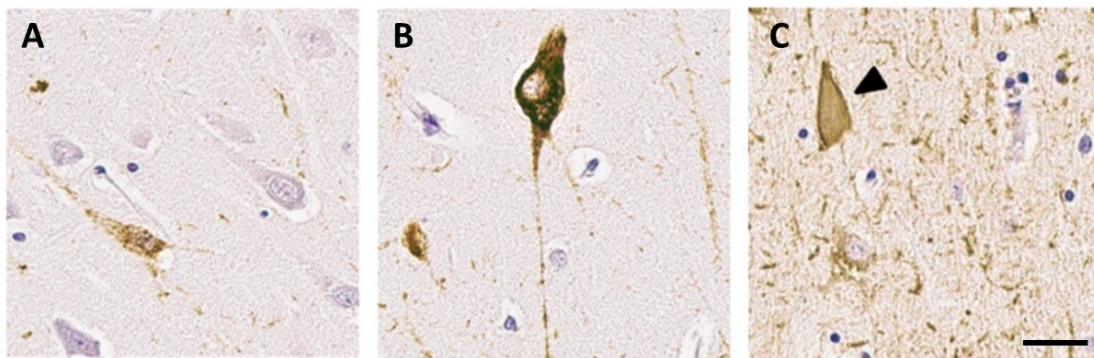


Figure 1.2. Tau aggregated species. Microscopic analysis of post-mortem human AD brain tissue stained with a phospho-tau antibody (AT8) . A) Soluble multimeric tau species and intraneuronal pre-tangle materials, B) mature intraneuronal neurofibrillary tangles and neuropil threads, and C) ghost tangles spotted in the extracellular space (arrowhead). Scale bar 50 μ m. (Bengoa-Vergniory et al., 2021)

In the AD brain, tau pathology progresses gradually in synaptically connected brain regions and is apparent long before the appearance of the clinical symptoms, being responsible for synaptic loss and neuronal cell death (Alafuzoff et al., 2008; Braak et al., 2006). Based on the ability of the AT8 antibody to capture the hyperphosphorylated tau in the epitope Ser202/Thr205, Braak and his colleagues developed a staging system for AD. According to this system, the intraneuronal hyperphosphorylated tau propagates from the transentorhinal and the entorhinal cortex in Braak stage I and II respectively to the fusiform gyrus in Braak stage III and neocortical association areas in Braak stage IV. The pathology then expands to the frontal, parietal, and occipital cortices in Braak stage V ending up in the striate region of OC in Braak stage VI (Braak

et al., 2006). The staging system was further optimized by Alafuzoff and his research group in 2008 to overcome the restrictions of the previous methods. In the updated staging system the stages were defined based on the AT8-positive NTs (Alafuzoff et al., 2008). Braak stage I is characterized by at least low levels of AT8-immunopositive NTs in the transentorhinal cortex. In Braak stage II the pathology expands to the posterior hippocampus with at least moderate levels of AT8-immunopositive NTs being observed in the EC. Pathology then expands to the inner layers of EC, fusiform cortex, and neocortex in Braak stage III continuing to the deeper layers of TC in Braak stage IV. Finally, parastriate and striate areas of the OC are displayed in Braak stages V and VI, respectively (Alafuzoff et al., 2008).

Amyloid deposition is also one of the main hallmarks of AD (DeTure and Dickson, 2019). Amyloid plaques are the result of the abnormal cleavage of the amyloid precursor protein (APP) by the β -secretase (BACE1) and γ -secretase leading to the production of A β fragments, as well as the outcome of A β overproduction or/and insufficient clearance mechanisms (Kumar et al., 2015; Thal et al., 2006). These plaques are consisting of A β 40 and A β 42 peptides with the A β 42 being more prone to aggregation (Masters et al., 2015). These fragments fold creating β -sheets and hence promoting the formation of A β plaques (Sipe and Cohen, 2000). The two types of plaques observed in the AD brain are the diffuse and the dense core plaques (Thal et al., 2006). Diffuse A β plaques are loosely packed and usually lack tau filaments. On the other hand, the dense core plaques are densely packed and contain neuritic components and for this reason are called neuritic plaques (NPs) (Thal et al., 2006) (Fig. 1.3).

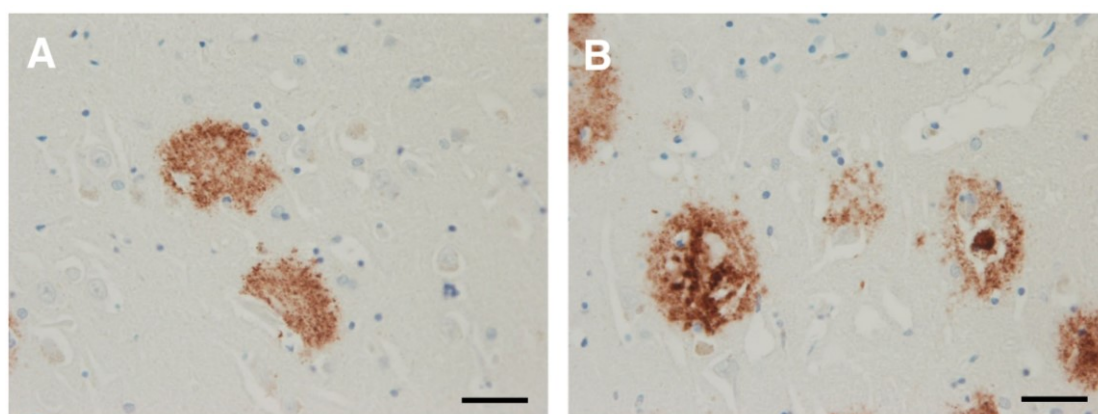


Figure 1.3. AD senile plaques. Microscopic analysis of post-mortem human AD brain an antibody against A β fragments (4G8). A) Diffuse A β plaques and B) dense core plaques spotted in the AD post-mortem human brain tissue. Scale bar 40 μ m. (DeTure and Dickson, 2019).

NPs are usually surrounded by activated astrocytes and microglia inducing immune response and neurodegeneration (Dickson, 1997; Yasuhara et al., 1994). A β deposition is also detected within the blood vessels of the brain and the leptomeninges causing CAA (Serrano-Pozo et al., 2011). In contrast to the A β located in the brain parenchyma, the A β located within the blood vessels is mostly consisting of A β 40 (Perl, 2010). Evidence support that tau lesions correlate better with the clinical symptoms than A β plaques. It is also suggested that tau and A β pathologies occur before the appearance of brain atrophy and other macroscopically visible changes (Jack et al., 1999).

Inflammatory response is also evident in the AD brain. Microglial cells are the primary immune cells of the CNS, with phagocytotic activity, that clear the brain from A β and tau aggregated species and cell debris, promote neuroprotection, and maintain the integrity of the synapses and neurons (Heneka et al., 2015). The levels of microglial receptors linked to their phagocytotic activity (e.g. TREM2) and their ability to recruit other cell types (e.g. CX3CR1) are reported to be elevated in the AD brain (Heneka et al., 2015; Ho et al., 2020). Astrocytes are glial cells responsible for maintaining the integrity and healthy function of neurons (Sofroniew and Vinters, 2010). Activation of astrocytes is also observed in the AD brain, with their physiological role focusing on preserving cell homeostasis and normal activity (Preman et al., 2021). Although glial cells contribute to the protection of the diseased brain, chronic activation of the inflammatory response can be harmful resulting in synaptic loss, protein aggregation, and neurodegeneration (Di Benedetto et al., 2022; Walker et al., 2019). Mitochondrial dysfunction and extensive oxidated stress have also been observed in the AD brain. The energy deficits and the release of reactive oxygen species caused by the abnormal mitochondria affect the integrity and activity of te neuronal and glial cells reducing their viability.

The neuropathological diagnosis is still a challenge for neuropathologists as AD could be easily misdiagnosed or co-exist with other neurological disorders. Therefore,

detailed evaluation and assessment of the brain tissue are essential. A number of diagnostic criteria have been proposed for the neuropathological evaluation of AD based on the 2012 National Institute on Aging-Alzheimer's Association Guideline. The criteria include the determination of tau Braak staging, A β Thal phase (A β staging system based on the detection of immunopositive amyloid deposits in cortical and subcortical areas), and neuritic plaque CERAD (Consortium to Establish a Registry for Alzheimer's Disease) score (Hyman et al., 2012; Mirra et al., 1991). Brain tissue from individuals with or without dementia is accessed based on these criteria to conclude whether the patients with AD and determine the severity and stage of the disease (Hyman et al., 2012; Mirra et al., 1991).

1.1.4 Symptoms of pre-clinical and clinical AD

AD, the most common cause of dementia, is a neurodegenerative disorder that progresses gradually from the moment of the appearance of the first neuropathological signs in the brain until the development of severe clinical symptoms creating an AD continuum. Three main stages have been described to characterize AD. These are pre-clinical AD, mild cognitive impairment caused by AD, and AD dementia (McKhann et al., 2011; Sperling et al., 2011; Vermunt et al., 2019). In the pre-clinical stage, the patients usually exhibit changes in the brain as the appearance of the first AD biomarkers is occurring (Sperling et al., 2020). However, no clinical symptoms have yet developed, with the individuals maintaining a normal life (Vermunt et al., 2019). A β deposits and tau aggregates are the main pathological features detected in the brain, CSF, or blood of the patients (Olsson et al., 2016; Sperling et al., 2020). Due to the fact that patients don't present any pathological clinical image, the diagnosis of the disease at this stage is difficult (Sperling et al., 2011). To overcome this limitation, scientists are now focusing on developing new methods for the detection of early AD biomarkers in the pre-clinical brain. However, more research is required in this field until the discovery of a tool that could be widely used by medical centers and hospitals in order to capture the pathology in such an early stage (Olsson et al., 2016). A number of individuals exhibiting biological brain alternations related to AD could later on develop MCI then AD (Bennett et al., 2006). In this stage, pathological changes continue to occur in the neuronal system, however the clinical image of the patients alters with the

appearance of very mild cognitive symptoms (Vermunt et al., 2019). These symptoms could be mild cognitive and memory impairments that don't affect the daily life of the patients and cannot be easily spotted by the surrounding environment ("2022 Alzheimer's disease facts and figures," 2022). Approximately 33% of individuals with MCI could develop dementia within five years (Ward et al., 2013). AD dementia can be mild, moderate, or severe depending on the neuropathological image of the brain and the severity of the clinical phenotype ("2022 Alzheimer's disease facts and figures," 2022; Ward et al., 2013). In the mild form of AD, although the patients can perform the majority of their daily tasks, some help in more complicated activities is required (Petersen et al., 2018). Moving to the moderate form, the number of clinical symptoms is increased with the patients exhibiting more difficulties in the performance of several tasks, in remembering things, in the language, as well as, in the way they behave and react (Petersen et al., 2018). The last stage is the severe form of dementia due to AD, where the patients are unable to survive without having any care or assistance as the symptoms are dramatically severe affecting every aspect of their daily life (Petersen et al., 2018). Patients are unable to complete most of their everyday tasks as their ability to recall memories, recognise faces, or even communicate is significantly reduced (Romero et al., 2014). Their ability to move can be also be impaired with most of the patients start developing other physical dysfunctions and health issues (Romero et al., 2014). Receiving food efficiently and breathing properly are also a challenge for patients with the severe form of AD, making them more susceptible for lung infections (Romero et al., 2014). Although the disease is progressing gradually from the one stage to the other, the duration of each stage varies depending from multiple factors including the age, gender, genetic and environmental factors (Vermunt et al., 2019). It is also essential to highlight that not all the individuals with pre-clinical AD or patients with MCI develop MCI or AD dementia, respectively (Vermunt et al., 2019). Individuals exhibiting brain changes related with dementia might suffer exclusively from AD, or other neurological disorders, or even more commonly from mixed dementia (AD co-existing with other non-AD neurological causes) (Kawas et al., 2015).

1.1.5 Treatments for AD

So far, no current treatments have been developed to stop or reverse AD. All the therapeutic approaches that have been developed since today aim to delay the appearance of clinical symptoms and to ameliorate their severity, offering the patients a better quality and duration of life (Yiannopoulou and Papageorgiou, 2020). Communication and examination of the symptoms and behaviour of the patients, as well as psychological support and educational approaches, are used by the physicians, doctors, and caregivers to assist the patients to deal with the disease and cope with their daily routine and tasks (Yiannopoulou and Papageorgiou, 2020). Pharmacological treatment of AD using approved Food and Drug Administration (FDA) drugs is another approach to the management of the disease symptoms (Cummings et al., 2018). Such an approach includes the use of acetylcholinesterase inhibitors (AChEIs). The three FDA-approved drugs are donepezil, rivastigmine, and galantamine (Cummings et al., 2019). These molecules prolong the activity of the acetylcholinesterase enzyme by preventing acetylcholine (ACh) breakdown in the synapses (Yiannopoulou and Papageorgiou, 2013). The AD brain is characterised by a deficiency in the levels of ACh and therefore, preventing the breakdown of this neurotransmitter is vital for the healthy function and survival of the neurons (Akıncıoğlu and Gülçin, 2020). Analysis of these three drugs' efficiency supported that patients presented delay in the appearance of the clinical symptoms, with some of them showing even an improvement in their cognitive ability (Farlow et al., 2000). However, side effects affecting the function of the gastrointestinal tract and heart have been reported (Yiannopoulou and Papageorgiou, 2020). For moderate or severe cases of AD, memantine, an N-methyl-D-Aspartate (NMDA) receptor antagonist is used. NMDA receptor is a glutamate receptor and ion channel that has been found to be overactive as a consequence of the pathologically high levels of glutamate in the AD brain, resulting in neuronal dysfunction and neurodegeneration (Parsons et al., 2007). Thus, by modulating ion influx and glutamate transmission, memantine ameliorates the cognitive impairment and behavioural disturbances of the patients (Zhou et al., 2019). A combination of AChEIs and memantine is also a common approach used for AD management (Na et al., 2019). Antidepressants are also used for the psychological support of patients suffering from psychological symptoms, anxiety, or/and depression (Bessey and Walaszek, 2019). However, a careful and controlled administration and use of these drugs are essential as adverse effects might appear in

some cases (Bessey and Walaszek, 2019). Therefore, each patient must be carefully examined and the medication provided should be based on his age, disease severity, symptoms, clinical history, and general health (By the American Geriatrics Society 2015 Beers Criteria Update Expert Panel, 2015). Food supplements and vitamins are also administered to the patients (Blok et al., 2017). Apart from the medical and technological progress in the last decades, the discovery and development of a new efficient drug for the cure of AD present a significantly high failure rate, with AD treatment still being a challenge for scientists (Fan et al., 2020). Today ongoing studies are focusing on the different aspects of AD pathology and molecular mechanisms aiming to develop new disease-modifying strategies that will overcome the limitations of the previously developed drugs. These approaches include the development of agents that target A β formation such as β - or γ -secretase inhibitors, as well as, α -secretase modulators, components that prevent the formation of senile plaques and tau aggregated species, and immunotherapies against A β or abnormal tau (Yiannopoulou and Papageorgiou, 2020). A β and tau immunotherapies aim the degradation and clearance of their targets and can be either active or passive. In active immunotherapy A β or phosphorylated tau peptides, synthetic or not, are used for the development of vaccines that induce the production of antibodies in the patients receiving the treatment. On the other hand, passive immunotherapy is achieved by using monoclonal or polyclonal antibodies against these targets (Folch et al., 2016; Goñi et al., 2013). Up to today, small progress has been made in the development and FDA approval of successful immunotherapeutic methods; however, significant improvements have been achieved to overcome the different limitations encountered in the past (Wisniewski and Goñi, 2015; Yiannopoulou and Papageorgiou, 2020). Lecanemab-irmb, an A β -directed antibody, is an example of a recently approved FDA immunotherapy (fda.gov). As the enhanced levels of inflammatory response is one of the main features of AD, anti-inflammatory drugs have also been developed (McGeer et al., 2016). Studies has shown that nonsteroidal anti-inflammatory drugs used for other diseases, like TNF- α inhibitors, could delay the appearance of the clinical symptoms being a potential therapeutic approach for AD (Chang et al., 2017). Stem cell-based therapies are being developed (Cummings et al., 2019). Although the development of AD therapeutic methods and drugs is essential for AD treatment, early diagnosis is the key for delaying and managing AD. Therefore, development of more efficient and drastic diagnostic tools and strategies is one of the main aims of the scientists today (Atri, 2019). Well-

established relationship between properly trained caregivers and the patients, as well as emotional and psychological support, are vital for the improvement of the quality of the life of the individuals living with AD. Finally, financial support of the caregiving system and AD research is essential (“2022 Alzheimer’s disease facts and figures,” 2022).

1.2 Tau protein

1.2.1 Tauopathies

Proteinopathies are neurological disorders caused by the abnormal folding and aggregation of proteins that seed themselves and spread through the brain in a prion-like manner causing, as they expand, irreversible cell death and progressive neurological symptoms (Goedert et al., 2017; Lee et al., 2001). The abnormal and pathological aggregation and misfolding of the microtubule-associated protein tau in the central nervous system (CNS) in the neuronal and glial cells is the main hallmark of neurodegenerative disorders termed tauopathies (Goedert, Eisenberg, & Crowther, 2017; Lee, Goedert, & Trojanowski, 2001). Tauopathies are divided into primary and secondary tauopathies (Silva and Haggarty, 2020). Disorders, where tau is the dominant pathological characteristic and has a direct impact on neurodegeneration, are known as primary tauopathies, while tauopathies where tau is not the only responsible pathological feature and other proteins also contribute to the development of the disease are called secondary (Silva and Haggarty, 2020; Spillantini and Goedert, 2013). Pick's Disease (PiD), Progressive Supranuclear Palsy (PSP), Corticobasal Syndrome (CBD), Aging-Related tau Astroglialopathy (ARTAG), Primary age-related Tauopathy (PART), Behavioural variant of Frontotemporal Dementia (bvFTD), and Argyrophilic Grain Disease (AGD) are some well-known examples of primary tauopathies (Kovacs, 2020; Silva and Haggarty, 2020; Spillantini and Goedert, 2013). Alzheimer's Disease (AD) and Chronic Trauma Encephalopathy (CTE) are secondary tauopathies with AD being the most prevalent dementia and the most common neurodegenerative disorder (Hernández et al., 2018; Mez et al., 2017; Spillantini and Goedert, 2013). The division of tauopathies in these two subgroups doesn't mean that tau plays a less important role in the pathophysiology of secondary tauopathies (Jadhav et al., 2019). Tauopathies are also characterised as familial or sporadic (Hutton, 2006; Lee et al., 2001). Although a significant number of familial cases has been reported, with mutations in the *MAPT* gene being responsible for the abnormal structure, behaviour, and function of tau protein that leads to toxicity and cell death (Hutton, 2006), the majority of tauopathies are sporadic presenting neurological and phenotypic diversity (Lee et al., 2001). Different mechanisms have been proposed so far to contribute to tau-induced neurotoxicity and neurodegeneration and can be divided into two non-mutually

exclusive main groups: the loss of tau function and the gain of toxic function (Feinstein and Wilson, 2005; Trojanowski and Lee, 2005). The loss of tau normal function can be caused by abnormal post-translational modifications (PTMs) and conformational changes of tau. This results in the inability of tau protein to bind properly to the microtubules of neuronal axons affecting the structure, stability, and function of neurons, creating disturbances in axonal transport, leading to synaptic dysfunction, and promoting toxicity and neuronal cell death (Feinstein and Wilson, 2005; Tepper et al., 2014). Gain of toxic function of tau is a result of abnormal PTMs of tau, impaired tau folding, and deficits in tau clearance leading to the generation of tau molecules that are prone to aggregate forming insoluble structures and fibrils that prevent the normal function of neurons (Kuret et al., 2005; Mandelkow and Mandelkow, 2012; Ramachandran and Udgaonkar, 2011). Although nowadays the knowledge about tauopathies and their pathology has significantly increased, a deeper understanding of the molecular mechanisms of tau pathology is needed to allow the development of new biomarkers and therapies for AD and related tauopathies (Silva and Haggarty, 2020).

1.2.2 *MAPT* gene and tau structure

The microtubule-associated protein tau is encoded in humans by a single gene called *MAPT* and is a protein required for microtubule assembly in the neuronal axons. The *MAPT* gene is located on the 17q21 chromosome and is characterised by impressive evolutionary conservation (Sündermann et al., 2016). Although tau is predominately expressed in the central and peripheral nervous system, its expression has been described also in the breast, pancreas, kidneys, heart and skeletal muscles, and salivary glands (Kent et al., 2020). Tau is a physiologically unfolded soluble protein consisting of three main domains with different biochemical and functional properties (Brandt, 1996; Iqbal et al., 2009). These domains are an N-terminal acidic domain, a proline-rich domain, and a microtubule-binding domain in the C-terminal part of the tau molecule (Brandt, 1996; Goedert et al., 1989) (Fig. 1.4). The N-terminal domain is mainly responsible for the transmission of neuronal signals, contributes to the interaction of tau with the cell membrane, and regulates the microtubule dynamics. The C-terminal domain is responsible for tau ability to bind to the microtubules, with the domains within or close to this region affecting the microtubule-binding process of tau

through multiple tau modifications (Brandt, 1996). Proline-rich domain contributes to the interaction of tau with actin (He et al., 2009). The *MAPT* gene comprises 16 exons, three of which (exons 2,3, and 10) are involved in alternative splicing resulting in the generation of 6 tau isoforms (Goedert et al., 1989; Wang and Mandelkow, 2016). Tau isoforms differ in the number of N-terminal inserts (0N, 1N, or 2N) and the number of microtubule-binding repeats (3R and 4R) (He et al., 2009; Silva and Haggarty, 2020). Expression of exons 2 and 3 is responsible for the number of N-inserts, with exon 2 encoding N1 insert and exon 3 encoding N2 insert (Trabzuni et al., 2012). Translation of exon 10 leads to the expression of the second microtubule-binding repeat resulting in the production of the 4R instead of the 3R isoform (Park et al., 2016) (Fig. 1.4).

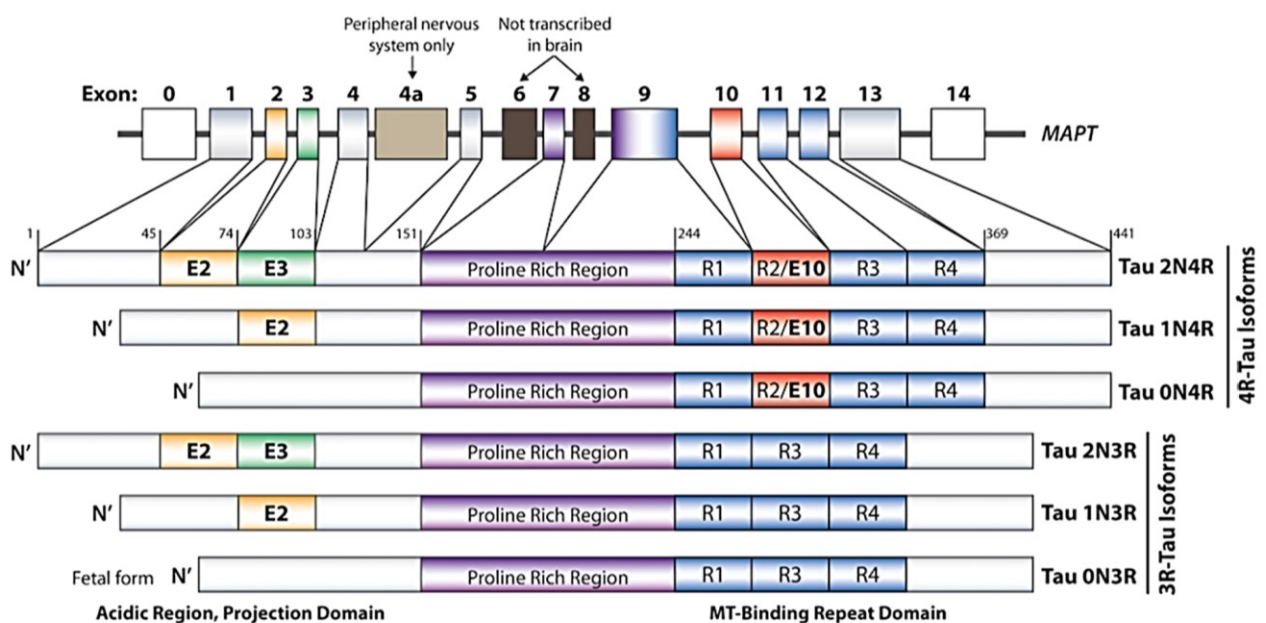


Figure 1.4. Human microtubule-associated protein tau. Schematic representation of *MAPT* gene and tau isoforms. The *MAPT* gene comprises 16 exons three of which (exons 2,3, and 10) contribute to alternative splicing, resulting in the generation of 6 tau isoforms. The human tau protein consists of three main domains, an N-terminal acidic domain, a proline-rich domain, and a microtubule-binding domain. Tau isoforms differ in the number of N-terminal inserts (0N, 1N, or 2N) and the number of microtubule-binding repeats (3R and 4R) (Silva and Haggarty, 2020).

The expression of tau protein in the brain is developmentally regulated with all six isoforms being expressed differently during human brain development. A balanced ratio of 1:1 characterises the healthy adult brain with the 4R isoform increasing the ability of tau to bind stronger to the microtubules (Goedert et al., 1989). The shortest 3R isoform (0N3R) is dominant in the fetal brain contributing to axonal growth and plasticity, as well as the formation of new synaptic connections (Lacovich et al., 2017). Expression of the other isoforms occurs in the later developmental stages of the human brain. In addition, N1 isoforms are dominant in the adult brain with N2 isoforms being encoded at a lower level (Goedert et al., 1989). The presentation of various isoforms of this protein in the mature mouse brain differs with the adult mice lacking the 3R isoforms. Furthermore, there is dissimilarity in the N-terminal sequence of the Tau protein between mice and humans, with murine tau interacting with different endogenous proteins (Hernandez et al, 2020). Tau conformational architecture is characterized by the lack of a stable precise three-dimensional structure as quick and often morphological alternations and modifications are required to maintain its physiological activity (Dunker et al., 2008). This fact makes tau prone to lose its physiological function and obtain a pathological behavior, being responsible for the appearance of several tau-related disorders (tauopathies), with AD being the most common of them (Kovacech et al., 2010).

1.2.3 Post-translational modifications of tau protein

PTMs of a protein refer to the biochemical alterations that occur to one or more amino acid residues of a protein after its expression that further define its structure, properties, and function. These modifications usually occur through an enzyme-mediated addition of chemical particles or through the mechanism of proteolytic cleavage (Ramazi and Zahiri, 2021). Tau is a protein that undergoes various modifications including phosphorylation, acetylation, ubiquitination, proteolytic truncation, methylation, glycosylation, and others. These modifications can increase its morphological and physiological functional diversity, but they also make it prone to obtain pathological behaviors resulting in the loss of normal function or the gain of toxic function. Specific amino acid residues are more susceptible to specific modifications. For example, serine,

threonine, and tyrosine are susceptible to phosphorylation, lysine to ubiquitination, acetylation, and glycosilation, histidine to truncation, etc (Alquezar et al., 2021).

During tau phosphorylation, a phosphate group is added to one or more amino acid residues of the tau molecule. The addition of this group is performed by kinases, while the removal is by phosphatases. This modification changes the chemical properties of the protein by adding a group that increases the hydrophilicity of the targeted protein, an event that affects multiple cellular mechanisms and functions (Humphrey et al., 2015). Tau phosphorylation in specific sites occurs normally in the brain. However, the majority of these events tend to be pathological, leading to the development of different tauopathies (Cook et al., 2014; Hanger et al., 2009). The insufficient clearance of these abnormal tau molecules affects the degradation mechanisms and therefore its clearance affects proteostasis and homeostasis of the cells (Matsuo et al., 1994). Numerous enzymes have been described to contribute to these events including the kinases: glycogen synthase kinase-3 (GSK-3), microtubule affinity-regulating kinases (MARKs), cyclin-dependent kinase 5 (CDK5), casein kinase 1 (CK1), 5' AMP-activated protein kinase (AMPK), protein kinase A (PKA), as well as phosphatases: protein phosphatase 1 (PP1), protein phosphatase 2A (PP2A), protein phosphatase 5 (PP5) (Alquezar et al., 2021). Changes in the charge of tau also affect its ability to bind to the microtubules resulting in tau relocation from the neuronal axon to the cytoplasm and dendrites (Li and Götz, 2017). Further investigation on the molecular mechanisms and pathways that induce tau hyperphosphorylation and thus acquisition of a pathological status is needed.

Acetylation is another type of tau modification that includes the introduction of an acetyl group to a lysine of tau molecules. The addition and removal of this group are performed by the enzymes acetyltransferases and deacetylases, respectively (Drazic et al., 2016). Acetylation affects the charge of tau protein by neutralizing the positive charge of lysine residues, through which it binds to the negatively charged microtubules, and therefore alters protein folding, location, activity, as well as interactions with other proteins. These changes also have an impact on other PTMs of tau affecting processes like tau degradation and clearance (Alquezar et al., 2021; Lim et al., 2014; Narita et al., 2019). Studies in animal and post-mortem human brain tissue have revealed increased levels of tau acetylation in diseased brains with the acetylation occurring early in the development of tau pathology in tauopathies (Chen et al., 2020;

Min et al., 2010; Morris et al., 2015). The role of acetyltransferases and deacetylases is considered controversial with studies supporting that both enzymes contribute to the increase and reduction of tau accumulation (Carlomagno et al., 2017; Cook et al., 2014; Ding et al., 2008; Min et al., 2018).

Ubiquitination is also one of the PTMs that modifies tau protein. During this modification, a ubiquitin-protein consisting of one or more ubiquitin molecules is introduced to a lysine residue of tau protein. Ubiquitination is catalysed by three enzymes, the activating enzyme E1, the conjugating enzyme E2, and the ligating enzyme E3 that attach a ubiquitin chain to tau protein promoting tau degradation through the ubiquitin-proteasome system (UPS) or the autophagy-lysosomal pathway (APS). Seventeen out of forty-four lysine amino acid residues of the full-length human tau have been reported to exhibit ubiquitination (Harris et al., 2020; Nathan et al., 2013; Suresh et al., 2016). Tau fibrillar lesions purified from the brain of patients with AD and related tauopathies have been found to be ubiquitinated, with the ubiquitination occurring after tau phosphorylation and multimerisation, indicating that the process of ubiquitination is occurring as a response of the cells to deal with the abnormal tau molecules driving them to degradation (Alquezar et al., 2021; Bancher et al., 1991; Perry et al., 1987). On the other hand, pieces of evidence are proposing that the addition of ubiquitin molecules can also promote tau assembly (Dickey et al., 2006).

Proteolytic cleavage and truncation of tau is another tau PTM that is catalysed by proteases. This modification plays a pivotal role in the viability of the cells as it regulates tau structure and function, and therefore various molecular and cellular mechanisms like protein degradation (Alquezar et al., 2021). The role of proteolytic truncation is controversial as this mechanism can either promote tau aggregation by affecting other physiological PTMs and degradation processes of abnormal tau or promote clearance of pathological tau complexes protecting cell viability (Chesser et al., 2013). Proteases involved in this process are calpains and caspases (Quinn et al., 2018).

Methylation has also been described to modify tau protein. Both DNA and protein can exhibit methylation through the addition of a methyl group. DNA methylation is a chemical process that regulates gene expression by promoting transcriptional silencing (Moore et al., 2013). Tau protein methylation is usually occurring on lysine or arginine

amino acid residues, changing the electrostatic behavior of the protein and therefore affecting its location, activity, and various other cellular mechanisms (Alquezar et al., 2021; Falnes et al., 2016).

Another PTM of tau is glycosylation, through which a carbohydrate is added to a protein and can be either enzyme-mediated glycosylation or glycation (non-enzyme-mediated glycosylation). Glycosylation occurs in asparagine, serine, or threonine residues is catalysed by glycosyltransferases, and is usually important for the physiological biosynthesis and function of the protein. In contrast, glycation refers to a non-enzymatic addition of a monosaccharide to the target protein (Taniguchi et al., 2016; Welsh et al., 2016). Glycosylation by the addition of sugar on the oxygen molecule of a threonine or serine residue of tau protein, known as O-glycosylation, is considered to have a protective role since this modification occurs to residues vulnerable to phosphorylation (Smet-Nocca et al., 2011). This is in line with the finding supporting that tau O-glycosylation is reduced in the AD brain (Robertson et al., 2004). Glycation on the other hand has been reported to be elevated in the tau aggregates purified from the brain of the AD cases, but not in the monomeric tau (Ko et al., 1999). Glycation is reported to affect the affinity for microtubules, as well as the process of ubiquitination (Yan et al., 1994).

More PTMs have also been described including nitration and oxidation (Alquezar et al., 2021). To sum up, PTMs of tau play a determining role in the three-dimensional architecture, properties, and cellular functions of the protein, having either a protective or a damaging impact on the neurons and the other cell types, contributing to the progress of the various tauopathies.

1.2.4 The physiological role of tau protein

The main role of tau is focused on its interaction with the microtubules in the neuronal axons. Tau protein is responsible for microtubule assembly and stabilization by binding with high affinity to tubulin dimers leading to the formation of microtubule polymers of various lengths (Amos, 2004; Dent and Baas, 2014). The majority of the neuronal tau protein is spotted in the axons and plays a vital role in axonal growth and maturation, controlling microtubule dynamics. Research studies on tau knock-out models have

revealed that depletion of tau disturbs neuronal growth and maturation, prevents axonal elongation, impairs axonal structure and integrity, and prevents the recruitment of other factors that are essential for the microtubule stability and axon formation (Dawson et al., 2001; Harada et al., 1994; Liu et al., 1999; Ramirez-Rios et al., 2016; Sotiropoulos et al., 2017). Additional studies have proved that tau is essential for neurons to preserve a single, non-branched axon, while reduced tau levels have been described to the full-of-branches dendrites (Yu et al., 2008). It has also been reported that tau prevents the cleavage of the microtubules by blocking the action of the protein katanin, a microtubule-severing protein (Luptovčiak et al., 2017; Yu et al., 2008). Although tau plays a determining role in axonal dynamics, the lack of tau has been described to trigger the increase of the expression of the other microtubule-associated proteins to execute and make up the initial function of tau (Ma et al., 2014; Tint et al., 1998). Microtubules participate as well in the transport of various proteins, molecules, and organelles across the neurons. Tau is a regulator of this mechanism with disturbances in the function and levels of the protein blocking the movement of the axonal motor proteins, impairing their activity, or even inducing their detachment from the microtubules (Kent et al., 2020; Siahaan et al., 2019). Although the majority of the studies have described diverse actions of tau in the control of axonal transport dynamics, a number of them supported that tau depletion or overproduction does not affect the transport rate through the axon (Holper et al., 2022; Yuan et al., 2008). The role of tau is not restricted only to axonal growth and stability. Tau contributes as well to synaptic activity and plasticity, with the impairments in this activity harming the synapses, affecting the spine density, and inducing synaptic protein deficits (Velazquez et al., 2018; Zhou et al., 2019). Tau's role in the post-synaptic region is of utmost importance, as it regulates long-term potentiation (LTP), demonstrated by its ability to hinder hippocampal LTP when neurons are exposed to tau, particularly in rat hippocampal synapses (Ondrejčak et al., 2018). Furthermore, research suggests that tau holds significant physiological significance within synapses; heightened tau levels in dendrites impact memory and synaptic plasticity. When tau is not properly located, it leads to a reduction in miniature excitatory postsynaptic currents (mEPSCs) in rats, as outlined in the study conducted by Hoover et al. (2010). Apart from neuronal tau, tau is also expressed by oligodendrocytes. It has been reported that tau contributes to the production of myelin protein and the process of myelination, as patients suffering from AD and related tauopathies usually present hypomyelination and disturbances in the

myelin formation (Ferrer et al., 2020). In line with this are studies with animal models of human tauopathies supporting the existence of disease-induced myelination impairments (Jackson et al., 2018). Tau is also essential for the growth and stability of oligodendrocyte processes (Klein et al., 2002). It is evident that tau plays a vital role in the activity and morphological architecture of oligodendrocytes, and thus the integrity and viability of neurons (Kent et al., 2020). Although the majority of tau is cytoplasmic, tau can also be detected in the nuclei of the cells interacting with the DNA or the RNA, preserving the genomic integrity (Camero et al., 2014; Maina et al., 2018; Rady et al., 1995). Tau protein found in the nucleus of cells usually lacks phosphorylation, with the hyperphosphorylation of the protein impairing its ability to interact with the nucleic acids, and thus affecting multiple physiological molecular mechanisms and functions of the cells (Lu et al., 2013). Tau plays an important role in preserving the integrity and structure of chromosomes, protecting the oligonucleotides from the harmful effects of the oxygen-reactive species, promoting the repair of the damaged DNA or RNA, and controlling the process of transcription by suppressing or inducing gene expression (Kent et al., 2020; Maina et al., 2018; Rossi et al., 2013; Violet et al., 2014). Finally, studies in *MAPT* KO mice have reported that tau, as a structural protein, contributes to the regulation of the cell division cycle, acting as a suppressor of tumorigenesis (Han et al., 2020). Therefore, we can declare that tau proteostasis can also be associated with the risk of tumor formation (Kent et al., 2020). Overall, these pieces of evidence highlight the importance of the maintenance of the physiological architecture, folding, modification, and activity of tau protein both in the neurons and the other cell types, preventing the development and progress of the various tauopathies.

1.2.5 Tau pathology

Although a significant number of cases with tauopathies are familial and are caused due to *MAPT* gene mutations, the majority of the cases are sporadic, characterised by neurological and phenotypic diversity (Lee et al., 2001). Tau protein, due to the lack of a precise stable conformation, is susceptible to morphological changes and can subsequently sustain pathological properties (Kovacech et al., 2010). In the last decades, studies support that early-type tau aggregates, rather than late-type tau lesions, are the main responsible species that lead to the development of tauopathies (Bengoa-

Vergniory et al., 2021; Gómez-Isla et al., 1997). Tau multimerisation, abnormal PTMs, conformational changes, insufficient tau clearance, and tau cellular and anatomical relocation are potential mechanisms through which tau obtains pathological and toxic behaviours causing neurotoxicity and cell death (Silva and Haggarty, 2020). Multiple molecular and cellular mechanisms have been proposed to contribute to tau-induced toxicity and neurodegeneration and can be divided into two non-mutually exclusive groups: the loss of tau function and the gain of toxic function (Feinstein and Wilson, 2005). Loss of tau function affects the ability of tau to bind properly to the microtubules resulting in disturbances in the neuronal cell function, axonal growth and transportation, and synaptic efficacy (Tepper et al., 2014). The loss of tau physiological function can be the outcome of abnormal PTMs and conformational changes (Tepper et al., 2014). Similarly, PTMs, tau misfolding, and insufficient tau clearance can lead tau to obtain toxic properties leading to the production of tau molecules that are prone to aggregate preventing the normal function of the neurons (Kuret et al., 2005; Mandelkow and Mandelkow, 2012).

Different molecular mechanisms have been described to cause tau-induced toxicity with the most common of them being tau PTMs. Tau inhibits multiple PTMs like phosphorylation, acetylation, ubiquitination, and truncation (Silva and Haggarty, 2020). Disturbed tau modifications can affect tau charge, and thus its affinity for axonal microtubules (Kellogg et al., 2018). Hyperphosphorylation of tau is the main cause of tau abnormalities. Numerous phosphorylation sites have been detected so far, with most of them being spotted at serine (Ser) and threonine (Thr) residues (Neddens et al., 2018). One of the most affected epitopes is the Ser202/Thr205 which can trigger tau fibrillisation and large tau lesion formation (Ercan-Herbst et al., 2019; Lasagna-Reeves et al., 2012). Hyperphosphorylation in Thr231, Ser422, Ser396/Ser404, and Thr217 are events that occur early in the development of the AD pathology with some of them (e.g., Thr321) being linked with the increase of tau ability to seed itself and propagate to the synaptically connected cells (Ercan-Herbst et al., 2019; Mondragón-Rodríguez et al., 2014; Smolek et al., 2016). Targeting kinases, phosphatases, or other enzymes that are responsible for tau modification can be potential targets for the treatment of tauopathies. Therefore, kinases like GSK-3, MARKs, CDK5, CK1, AMPK, and PKA, as well as phosphatases like PP1, PP2A, and PP5 can be some potential candidates (Inobe et al., 2015; Qian et al., 2010; Silva and Haggarty, 2020). Although

hyperphosphorylation of tau reduces tau affinity for microtubules, several studies still question whether tau hyperphosphorylation occurs before or after tau dissociation from microtubules (Kent et al., 2020). In a recent study, researchers proved that disease-like pseudo-phosphorylation although reduced the ability of tau to bind to the microtubules, it didn't affect the detachment rate of tau (Niewidok et al., 2016). In line with this is another study supporting disruption-induced tau dissociation and relocation to the cytoplasm, followed by phosphorylation (Miyasaka et al., 2010).

Tau acetylation is also a modification that regulates tau ability to bind to the microtubules. Hyperacetylation of tau is mostly occurring in the microtubule-binding domain in the C-terminal of tau and has been proven to prevent tau from interacting with microtubules, affecting axonal stability and neuronal integrity (Cook et al., 2014; Min et al., 2015).

Tau ubiquitination is also important to maintain tau normal function and avoid fibril formation. The majority of ubiquitination sites are located in the proline-rich domain (Abreha et al., 2018). Changes in tau folding or truncation can affect the process of ubiquitination and consequently tau proteasomal degradation. This insufficient tau clearance leads to tau accumulation in the neurons (Cripps et al., 2006).

Tau truncation can also induce tau aggregation and seed as it can affect tau folding and conformational structure (García-Sierra et al., 2008). Animal and human studies have shown that several enzymes contribute to tau cleavage including caspase 3, caspase 6, calpain 1, and calpain 2 (Silva and Haggarty, 2020). Caspase 6 has been found to be elevated in the brain of AD patients, with the active enzyme being detected in the NFTs and NTs jeopardizing neuronal morphology and function (Guo et al., 2004). Respectively, calpain 2 has been proven to be related to disturbances in the cytoskeleton and structure of axons (Grynspan et al., 1997). The use of inhibitors against such enzymes has improved AD pathogenesis (Li et al., 2022). However, it is essential to highlight that under physiological conditions these enzymes are required for tau and other protein clearance (Quinn et al., 2018). These modifications of tau affect also tau structure and folding, leading to the generation of different tau strains that present distinct biochemical and physiochemical properties resulting in the development of diverse pathological phenotypes in the various tauopathies (Fitzpatrick et al., 2017; Kaufman et al., 2016a). The different tau strains have different seeding capacities and

they can spread themselves to various anatomical brain areas affecting specific cell types based on their properties (Holmes et al., 2014; Sanders et al., 2014). Tau species can propagate from one neuronal cell to the other through synapses and therefore can seed themselves in synaptically connected brain regions (Kaufman et al., 2016a). Tau molecules can also be released from the different cell types in the extracellular space, naked or in vehicles. Finally, *in vitro* studies have proven that the cellular uptake of tau is a mechanism that contributes to tau propagation and affects the viability of the cells, making them more vulnerable to stressors (Brunello et al., 2016; Simón et al., 2012).

To maintain a healthy structure and function, each cell needs an efficient protein degradation system. This system is responsible for the clearance of abnormal proteins protecting the cells from the toxicity that protein aggregation can cause (E. Wong and Cuervo, 2010). In tauopathies like AD, this system has been proven to be affected and impaired by the aggregation of abnormal tau species (Bain et al., 2019; Nixon and Yang, 2011). Protein ubiquitination is essential for protein degradation by the UPS. The formation of a ubiquitin chain at a lysine residue of the targeted protein is required to drive the protein in the proteasome (Finley, 2009). However, in AD, tau lesions appeared to be mono-ubiquitinated, a fact that prevents successful tau degradation by the proteasome complex (Morishima-Kawashima et al., 1993). Both *in vitro* and *in vivo* studies in AD mouse models have reported the inability of the UPS to clear the abnormal or aggregated tau species (David et al., 2002; Oddo et al., 2004). In addition, as mentioned previously, several PTMs can affect the folding and architecture of tau protein, impairing the process of degradation (Nachman et al., 2020). Impairment of the APS has also been described to be linked to abnormal tau molecule degeneration, with research studies supporting that the use of lysosomal proteases inhibitors induces tau multimerisation and lesion formation (Bi et al., 1999; Ikeda et al., 1998; Esther Wong and Cuervo, 2010). However, it is still a question whether impairment in the clearance of tau is a cause of tauopathies, or is an outcome of deficits in other molecular and cellular mechanisms, or both (Silva and Haggarty, 2020).

Mutated and aggregated tau molecules can also cause mitochondrial impairment. Disruption of axonal transportation due to tau abnormalities prevents their movement across the axons leaving neuronal processes with fragmented and dysfunctional mitochondria. In turn, these energy deficits caused by the absence of functional mitochondrial can trigger tau accumulation in these regions (Kopeikina et al., 2011;

Wee et al., 2018). The release of oxygen-reactive species from the damaged mitochondria affects the PTMs of tau protein including the production of abnormal tau conformers and species (Silva and Haggarty, 2020; Thornton et al., 2011).

Impairment in RNA-splicing contributes also to tau pathology. Deficits in the process of tau alternative splicing can lead to the production of impaired tau isoforms with pathological properties. Studies in the P301S mouse model of human tauopathy revealed that disruption of the tau splicing system had an impact on the expression of genes associated with the function of synapses and neurotransmitter release affecting glutamate transmission and calcium influx in the axons (Apicco et al., 2019). In addition, multiple studies have indicated that TIA1, an RNA-binding protein, induces tau accumulation contributing to tau pathology (Apicco et al., 2018; Jiang et al., 2019; Vanderweyde et al., 2016).

As tau deposits can be detected in oligodendrocytes (coiled bodies), the process of myelination can also be affected. It is evident that diseased individuals present impairments in the production of myelin, demyelination of axons, neurodegeneration, and cognitive deficits (Ferrer et al., 2020).

Finally, tau toxicity is highly related to the accelerated inflammatory response (Wendeln et al., 2018). Pathological tau is responsible for the enhanced inflammation, release of pro-inflammatory cytokines and factors like TNF- α , and overactivation of brain immune cells (microglia and astrocytes), promoting neuronal dysfunction, neurotoxicity, and cell death (Heneka et al., 2015; Keren-Shaul et al., 2017).

1.3 Early-type tau aggregates

1.3.1 Strains of tau protein

Until recently NFTs and NTs were considered to be primarily responsible for the progression of tauopathies (Andrade-Moraes et al., 2013; Holmes et al., 2014). However, studies have shown that neurodegeneration and cognitive deficits occur before the formation of NFTs (Haroutunian et al., 2007). In line with this, recent studies support that early-type tau aggregates are the toxic species, resulting in neuronal loss and contributing to the progression of the diseases (Holmes et al., 2014; Lasagna-Reeves et al., 2011a). Formation of NFTs and late-type tau lesions requires the transition of physiological tau protein to an abnormally modified and misfolded, prone to aggregate monomeric tau molecule (Boyko and Surewicz, 2022). Recent research studies support that the formation of abnormal tau liquid assemblies through a mechanism that involves liquid-liquid separation of abnormal tau (Boyko and Surewicz, 2022; Kanaan et al., 2020; Kang et al., 2021). These aggregated liquid droplets, which can be either homotypic (mixture of tau proteins) or heterotypic (mixture of tau with other cellular components), are usually driven by electrostatic forces and interactions of the pathological tau protein and are regulated by PTMs and other crowding elements (Boyko and Surewicz, 2022). Therefore, it is clear that abnormal tau has the ability to form different tau strains, with distinct physiochemical and biochemical properties, that are prone to assembly forming multiple pathogenic aggregates that lead to the development of the diverse pathological phenotypes in the various tauopathies (Kaufman et al., 2017). The existence of the different tau isoforms, the multiple epigenetic tau modifications, and the mutations in the *MAPT* gene are the key drivers for the development of the various strains (Gerson et al., 2016). These tau assemblies can vary in morphology, size, composition, location, and folding and can be either soluble including oligomers, protofibrils, and annular protofibrils, or insoluble consisting of PHFs and SFs (Gerson et al., 2016; Gómez-Isla et al., 1997; Grundke-Iqbal et al., 1986). Even within a defined aggregated state, tau can exhibit different conformations characterised by distinct regional and cell-type specificity (Sanders et al., 2014; Yamada, 2017). Studies have shown that tau aggregates purified from different tauopathy brains induce pathology which is similar to the human source cases when injected into transgenic mice expressing both the wild-type or mutant human tau

protein (Boluda et al., 2015; Clavaguera et al., 2013). However, strain-induced pathology is proven to be conformation-specific rather than source-specific (Kaufman et al., 2016a). In the case of AD, the various tau forms may correlate with the different stages of the disease (Lasagna-Reeves et al., 2014). Tau aggregated conformers can be observed in the neurons, the extracellular space, and glial cells (Baner et al., 1989; Silva and Haggarty, 2020). These tau forms can be soluble small aggregates, pre-tangle materials, large fibrillar lesions, or ghost tangles, each of them presenting a characteristic pathological behaviour (Moloney et al., 2021). Understanding and further investigation of these tau strains, the mechanisms that lead to their production, and the way they behave can help the design of more specialised and targeted methods for the treatment and diagnosis of tauopathies.

1.3.2 Seeding activity of tau protein

In the various tauopathies, tau-tau interactions affect specific cell types and anatomical brain regions following a disease-specific pattern (Kaufman et al., 2016b). In AD, tau pathology propagates from the transentorhinal and entorhinal cortex to the fusiform gyrus and neocortical association areas, expanding to the frontal, parietal, and occipital cortices, with tau spreading through the synaptically connected neuronal cells, in a prion-like manner, from the one brain area to the other (Alafuzoff et al., 2008; Braak et al., 2006). The anatomical pathway through which tau propagates in the AD brain is highly linked to the clinical phenotype and correlates better with the symptoms of the patients than A β pathology (Hyman et al., 1984; Lasagna-Reeves et al., 2014). *In vitro* studies have shown that the addition of tau aggregates in reaction solutions full of tau monomers induced the multimerisation of tau (Holmes et al., 2014; Kaufman et al., 2017). Similarly, injection of tau specimens extracted from patients suffering from the different tauopathies in cell cultures and animal models induced the accumulation of endogenous tau (Boluda et al., 2015; Clavaguera et al., 2013; Kaufman et al., 2016b; Liu et al., 2021). In these cases, the tau aggregates weren't only conformational-specific, but they also had strain-specific seeding capacities and were able to propagate at distinct rates underlining the pathology of each tauopathy, a fact that indicates that the morphological architecture and folding of each strain define its seeding properties and cellular targets (Clavaguera et al., 2013; Hromadkova et al., 2022). In a recent

study, Kraus and colleagues proved that tau oligomeric species purified from the AD brain had higher seeding capacity compared to the oligomers extracted from the post-mortem brain of patients with PSP (Kraus et al., 2019). In addition, it has been reported that the seeding capacity of each strain is highly linked to its toxicity, with tau toxicity increasing proportionally to their seeding activity (Kaufman et al., 2016a). As mentioned previously, tau strains also vary in size, from soluble aggregated species to insoluble fibrillar aggregates (Gerson et al., 2016). Multiple studies using cellular and animal models showed that soluble tau oligomers, rather than fibrillar lesions, are more susceptible to intracellular propagation and thus they induce higher levels of toxicity damaging the different cell types (Lasagna-Reeves et al., 2011b; Rauch et al., 2018). In line with this theory is a study performed by Dujardin and his group in which they managed to prove, using tau seeding FRET biosensor assay, that soluble tau oligomers are the most toxic species and the mainly responsible for the spread of tau pathology in the AD brain (Dujardin et al., 2020). In addition, *in vitro* and *in vivo* studies have revealed that tau transmission can be also achieved through the release of tau molecules in the extracellular space. The extracellular tau can be secreted from the different cell types, under physiological or pathological conditions, and can be found naked or in vesicles (Simón et al., 2012; Yamada, 2017; Yamada et al., 2014). Tau release to the surrounding environment can also occur after cell death (Arriagada et al., 1992; Brunello et al., 2020). Numerous studies using cell-based assays have reported trans-cellular propagation of oligomeric tau supporting cell's ability to secrete and uptake tau aggregated conformers to and from the extracellular area (Holmes et al., 2013; Kaufman et al., 2017; Kfoury et al., 2012). Furthermore, the detection of elevated levels of tau in the cerebrospinal fluid (CSF) of AD patients, supports further the involvement of extracellular tau protein in the progression of the disease (Arriagada et al., 1992). However, this increase in the levels of tau detected in the CSF and blood has been described to AD cases and not to the other related tauopathies, indicating that these elevated levels of tau in the CSF and blood correlate better with the A β rather than tau pathology (Goodwin et al., 2020). Cellular uptake of extracellular tau is also a mechanism that contributes to tau propagation and affects the viability of the cells, making them more vulnerable to stressors (Brunello et al., 2016; Simón et al., 2012). Endocytosis, phagocytosis, and pinocytosis are some of the main mechanisms used by the cells in order to uptake tau (Rauch et al., 2018; Silva and Haggarty, 2020; Stopschinski et al., 2018). Heparan sulfate proteoglycans have been reported in several

studies to be the responsible mediators for tau cellular uptake contributing to tau propagation (Holmes et al., 2013). Apart from the neuronal contribution to tau transmission, glial cells are also involved in the propagation of tau molecules (Silva and Haggarty, 2020). Microglial cells are the primary immune cells of the brain. Although tau expression in these cell types has not been described, microglia using phagocytosis, internalize the pathological tau species and debris for degradation participating in tau transmission through the brain. Still, the exact mechanisms through which microglial cells spread tau is unclear (Brunello et al., 2020). Studies using tau seeds extracted from the post-mortem brain of patients with PSP and CDB revealed that astrocytes and oligodendrocytes can develop tau pathology, with tau molecules seeding themselves through these cell types respectively (Lee et al., 2001). Tau accumulations in oligodendrocytes are usually found in the form of coiled bodies. Oligodendrocytes contribute to the transmission of abnormal tau strains using their cellular processes indicating that oligodendrogliopathy has a strong impact on tau spreading in the various tauopathies (Ferrer et al., 2019). To sum up, all these studies support that tau oligomeric species are the key drivers of the progression of each tauopathy with the various tau strains characterised by high heterogeneity in their conformations/structures and seeding ability, affecting in different ways the various cell types and anatomical brain region. Although it is clear that different mechanisms contribute to the generation of the multiple tau strains/conformers, further investigation is still needed to determine whether the pathway of pathological tau propagation across the brain is due to the synaptic connections of neurons or because some cell types and brain areas are more vulnerable to tau aggregates or due to a combination of these two events. Despite the fact that tau can propagate between cells, no transmission of pathological tau between individuals or animals has been reported so far in epidemiological studies (Irwin et al., 2013, Silva and Haggarty, 2020). In any case, deeper knowledge about the molecular and cellular mechanisms through which tau spreading is achieved and regulated is essential for the discovery of new potential targets and the development of new therapeutic approaches.

1.4 Current methods for the detection and investigation of tau pathology

1.4.1 Immunoassays

The discovery and development of a wide range of techniques for the detection and investigation of tau pathology is the main focus of researchers. For the direct visualisation of aggregated tau species, numerous antibodies have been developed that recognise different epitopes of these abnormal tau molecules. As most tau residues exhibit PTMs, with phosphorylation being the most common molecular mechanism of tau modification, most of the antibodies used for the investigation of tau pathology target this abnormal and pathological characteristics (Ercan-Herbst et al., 2019; Lim et al., 2014). Until today, AT8 antibody is the gold standard for the staging and diagnosis of AD, binding to the phosphor-epitope Ser202/Thr205 and enabling the detection of late-type phosphorylated tau aggregates such as NFTs, NTs, and neuritic plaques-associated tau (Alafuzoff et al., 2008; Braak et al., 2006; Otvos et al., 1994). Antibodies capable of detecting early-type tau pathology, including oligomeric tau species exhibiting modifications that occur early in the process of tau fibrillisation, have also been developed. Such validated antibodies are the monoclonal phosphor-tau antibodies AT180 (pThr231), PHF-1 (pSer396/pSer404), S422 (pSer422), S198 (pSer198), and S199 (pSer199), etc (Arbaciauskaite et al., 2021; Ercan-Herbst et al., 2019; Li et al., 2016). Other antibodies like MC1 and Alz50 have also been used for the investigation of tau conformational changes (Dujardin et al., 2018; Holmes et al., 2014). Although antibodies together with the use of modern imaging techniques have been proven to be crucial for the investigation of the progress of the various tauopathies using post-mortem brain tissue, more recent and less invasive techniques are used for the detection of the pathology in patients living with the disease. Such techniques are PET (Positron Emission Tomography), MRI (Magnetic Resonance Imaging), and CSF biological immunoassays (Arbaciauskaite et al., 2021; Ercan-Herbst et al., 2019; Li and Cho, 2020). These immunoassays, like enzyme-linked immunosorbent assay (ELISA), single-molecule array (SiMoA), multi-arrayed fibreoptics (EIMAL), and others, enable the detection of both soluble and insoluble molecules and can discriminate tau conformers that differ between the various tauopathies (Ercan-Herbst et al., 2019; Li

and Cho, 2020). At this point, we need to highlight that although a large number of antibodies have been developed, further antibody validation is needed (Arbaciauskaite et al., 2021).

1.4.2 Cell-based assays

Although the aforementioned techniques have allowed us to capture the pathology and proceed to AD diagnosis in an early stage before the appearance of any symptoms, the prognosis of the AD progression and the clinical fate through these methods are still a challenge (Dujardin et al., 2020). For this reason, the discovery and development of assays that focus on the investigation of tau spreading capacity have been in the spotlight of recent research studies (Lathuiliere and Hyman, 2021). As mentioned previously, each tauopathy is characterised by different tau strains that vary in size, morphology, location, and biochemical and biophysical properties, behaving distinctly and having a specific seeding capacity (Gerson et al., 2016; Kaufman et al., 2016a; Lasagna-Reeves et al., 2014). Thus, the progression of each disease and the impact the brain pathology has on the clinical phenotype differ among the patients. Therefore, such techniques that aim for the detection and investigation of tau seeding activity can be useful tools for the early prognosis of AD and related tauopathies when applied to the biological fluids of the patients (Lathuiliere and Hyman, 2021). Several cell-based and protein amplification assays have been developed in the last decades. Cell-based assays like biomolecular fluorescence complementation assay (BiFC) and fluorescence resonance energy transfer (FRET) biosensor assays aim to investigate and capture the seeding activity of tau protein extracted from the brain of patients with tauopathies (Lim et al., 2014). Although these methods might be unable to capture tau-tau interactions *in situ*, findings support that they are characterised by higher specificity compared to the conventional methods, being able to detect the pathology in earlier stages (Lathuiliere and Hyman, 2021). BiFC assays is a cell-based sensor assay where the investigation of tau multimerisation is based on the use of two non-fluorescent fragments of GFP. Fluorescent complementation of these two non-fluorescent fragments of GFP and production of a fluorescent construct is achieved when these two splits of GFP are brought in proximity to each other following the interaction of the proteins they are fused to. The first GFP split encodes the first 10 beta-strains of the full-length GFP,

while the second one encodes the 11th beta-strain of GFP. These splits are fused to the proteins of interest (Brunello et al., 2020; Kerppola, 2013). A relevant cell-based assay for the investigation of the tau strains purified from the human brain tissue of the patients is FRET. This assay is based on the energy transfer between two fluorophores that are tagged to recombinant monomeric tau molecules. Every time these molecules interact/ are in proximity to each other, energy is transferred from the donor to the receiver fluorophore (Rizzo et al., 2004). Based on this assay, Kaufman and colleagues analysed the seeding capacity of tau strains spotted in the AD brain. In this case, cell lines expressing CFP and YFP fused with monomeric tau were treated with brain homogenate from AD and healthy control cases. The outcome of this study revealed enhanced seeding activity in the AD tissue. In contrast to other conventional methods like IHC, with this assay researchers managed to capture elevated levels of tau seeding activity in brain regions that appeared to be devoid of tau pathology (Kaufman et al., 2016b). Similarly, in another study, FRET captured tau seeding activity in mouse models of human tauopathy revealing that tau multimerisation is one of the earliest detectable events, occurring during the progress of the disease, before the appearance of tau deposits in the hippocampus of mice at 6 m.o. (Holmes et al., 2014).

1.4.3 Protein amplification-based assays

Due to the fact that tau protein is characterised by the ability to propagate and spread itself through the extracellular space (Kocisko et al., 1994), protein amplification assays have also been developed for the investigation of infectious protein seeding activity (Kraus et al., 2019; Lathuiliere and Hyman, 2021; Metrick et al., 2020; Saijo et al., 2017). A novel recently developed assay is Real-Time Quaking-Induced Conversion (RT-QuIC). In this assay protein extracts from brain tissue or biofluids like CSF are mixed with recombinant monomeric protein substrates and Thioflavin T (ThioT) and the solution is shaken under defined conditions. The protein extracts act as a template for the accumulation of monomeric substrates and the process of aggregation is monitored in real-time with the quantification of the fluorescence produced by ThioT (Atarashi et al., 2007). In the past years, scientists managed to build a sensitive and selective RT-QuIC assay that allows the detection of tau aggregates seeding activity (Kraus et al., 2019; Saijo et al., 2017). The specificity of the assay for the various

tauopathies is based on the selection of the substrate molecule. Therefore, different substrates are used for the different disorders to achieve the maximum specificity of the assay. For example, K19 which is a 3R fragment is used for Pick's disease, a 3R tauopathy, allowing the detection of tau self-aggregation with high sensitivity in both brain homogenate and CSF (Saijo et al., 2017). Respectively, the use of another substrate, τ 306, a tau fragment comprises of residues 306-378 of the full-length 4R tau isoform with a point mutation to the residue 322, has been used for the investigation of the seeding activity in the AD cases (Kraus et al., 2019; Metrick et al., 2020). With this, RT-QuIC is characterised by high specificity, being able to distinguish the 3R, 4R, and 3R/4R tau aggregated extracts from the brain of the patients (Saijo et al., 2017). It can also detect tau-tau interactions in the CSF making the assay a potentially powerful tool for the diagnosis of AD and other tauopathies (Lathuiliere and Hyman, 2021; Saijo et al., 2017). Analysis of AD and healthy post-mortem human brains with tau RT-QuIC showed that specimens extracted from familial and sporadic AD brains presented higher seeding activity and shorter lag phase compared to non-AD brain tissue (Kraus et al., 2019). The use of amplification assays has also been described in animal models where aggregation of endogenous tau was detected in the brain of transgenic mouse models after the injection of abnormal tau species extracted from the brain tissue of individuals with tauopathies (Holmes et al., 2014). These studies highlight that tau strains extracted from the post-mortem brain tissue of individuals with different tauopathies induced pathology similar to the source cases when injected into animals (Boluda et al., 2015; Clavaguera et al., 2013). Similar observations have been reported in studies using CSF samples from AD patients (Dujardin et al., 2020; Skachokova et al., 2019). Overall, these assays with further optimisations could be potential tools for the early diagnosis and prognosis of tauopathies, aiming at the investigation of tau self-aggregation in the biofluids of the individuals. Still, deeper knowledge and further validation are needed.

1.5 Hypothesis and Aims

Considering that the process of tau multimerization is a crucial stage in the formation of abnormal tau aggregates, our hypothesis centred on the prospect of directly observing this molecular occurrence in its natural context, essentially visualising interactions between tau molecules, as a means to gain insight into the initial pathological stages of

AD. In our research, we have introduced a novel method called tau-PLA, which exclusively identifies tau-tau interactions without detecting individual monomers under *in vitro* conditions. Beyond its ability to highlight neurofibrillary-like lesions in the human brain, tau-PLA identifies a novel form of early, small-sized diffuse pathology that has not been reported previously. Our findings reveal that this diffuse pathology accumulates significantly from the earliest phases of AD-related pathology, particularly in previously unnoticed medial temporal and hippocampal regions, even before the appearance of neurofibrillary tangles (NFTs) and neuropil thread (NT) pathology identified by conventional tau immunohistochemistry, with tau multimers presenting enhanced levels of seeding activity. Through these discoveries, we believe we are shedding fresh insights and paving the way for potential new avenues in exploring the early pathological processes of AD.

Chapter 2: Materials and methods

2.1 Materials

Table 2.1 – Primary antibody list

Primary antibody	Host	Clonality	Immunogen	Dilution	Source	% H ₂ O ₂	Blocking	Wash Buffer
4G8	Mouse	Monoclonal	aa 18-22 of beta-amyloid	1:1000	BioLegend, SIG-39200	3% in PBS	1/10 NHS in PBS	PBS
ALZ50	Mouse	Monoclonal	aa 2-10 and 312-342 of human basal forebrain homogenate	1:100	Peter Davies, The Feinstein Institute for Medical Research, Manhasset, NY	3% in PBS	5% milk in TBS	TBS - 0.05% Tx
Alpha-synuclein 42	Mouse	Monoclonal	aa 15-123 of rat synuclein-1	1:4000	BD Bioscience, 610787	0. 3% in PBS	1/10 NHS in PBS	PBS
Anti-6x His tag	Rabbit	Monoclonal		1:200	Abcam, ab213204	0. 3% in PBS	1/10 NGS in PBS	PBS
AT8	Mouse	Monoclonal	pSer202/pThr205 of partially purified human tau	1:1000	ThermoFisher, MN1020	0. 3% in PBS	1/10 NHS in PBS	PBS

AT180	Mouse	Monoclonal	pThr321 of human tau40	1:1000	ThermoFisher, MN1040	0.3% in PBS	1/10 NHS in PBS	PBS
GFAP	Rabbit	Polyclonal	bovine spinal cord GFAP	1:1000	Dako, Z0334	-	IF Blocking Buffer	TBS - 0.05% Tx
Iba1	Rabbit	Polyclonal	Iba1 (microglia / macrophages)	1:1000	Wako, 019-19741	-	IF Blocking Buffer	TBS - 0.05% Tx
MC1	Mouse	Monoclonal	aa 312-322 of human tau40 conformation-dependent antibody	1:100	Peter Davies, The Feinstein Institute for Medical Research, Manhasset, NY	3% in PBS	5% milk in TBS	TBS - 0.05% Tx
PHF-1	Mouse	Monoclonal	pSer396/pSer404 paired helical filaments of tau	1:1000	Peter Davies, The Feinstein Institute for Medical Research, Manhasset, NY	3% in PBS	5% milk in TBS	TBS - 0.05% Tx
PS422	Rabbit	Polyclonal	pSer422 of human tau-derived peptide	1:500	ThermoFisher, 44-764G	0.3% in PBS	1/10 NGS in PBS	PBS

PT217	Rabbit	Polyclonal	pThr217 of human tau40	1:1000	ThermoFisher, 44-744	0. 3% in PBS	1/10 NGS in PBS	PBS
Tau5	Mouse	Monoclonal	aa 210-241 of human tau40	1:200	Abcam, ab80579	0. 3% in PBS	1/10 NGS in PBS	PBS

Table 2.2 – Secondary antibody list

Secondary antibody	Host	Dilution	Source
Goat anti-rabbit IgG Antibody (H+L), Biotinylated	Goat	1:100	Vector Laboratories, BA-1000
Horse Anti-Mouse IgG Antibody (H+L), Biotinylated	Horse	1:100	Vector Laboratories, BA-2000
Goat anti-Rabbit IgG (H+L) Highly Cross-Adsorbed Secondary Antibody, Alexa Fluor 488	Goat	1:200	Invitrogen, A32731

2.2 Methods

2.2.1 Methods of Molecular Biology

2.2.1.1 Bacterial DMSO stocks

For bacterial DMSO stocks, 1 ml of bacterial starter culture was mixed with 70 μ l filtered DMSO (SIGMA-ALDRICH, D2650) in CryoTube vials (NUNC, 366656). The vials were then vortexed, frozen in dry ice, and stored at -80 °C.

2.2.1.2 Inoculation of bacterial culture

To initiate a bacterial culture, bacterial DMSO stocks were transferred from the -80 °C freezer to dry ice. Under sterile conditions, DMSO stocks were streaked out on kanamycin-selective LB/agar plates and the plates were then incubated in a Memmert Incubator at 37°C overnight.

2.2.1.3 Plasmid DNA purification

The first step for the purification of the plasmid DNA includes the amplification of the plasmid DNA in a bacterial culture. Therefore, using a sterile tip, a single colony from a freshly streaked selective plate was picked to inoculate a starter culture of 5 ml LB medium, containing kanamycin. The starter culture was incubated at 250 rpm at 37 °C for 16 hours. After 16 hours of incubation, bacterial growth was visible. 1.5 ml of bacterial culture was then transferred to new sterile Eppendorf tubes and bacterial cells were then harvested by centrifugation at 8000 rpm for 3 minutes at RT using the Heraeus Pico 17 Microcentrifuge (ThermoScientific). The plasmid DNA collected from the bacterial cells was performed using QIAprep® Spin Miniprep Kit, according to the manufacturer's instructions. The purified plasmid DNA was then eluted in a suitable volume (30-50 μ l) of endotoxin-free Buffer TE (10 mM Tris-Cl-pH 8.0, 1 mM EDTA) provided by the kit. The Eppendorf tubes including the purified plasmid DNA were stored at -20 °C.

2.2.1.4 Determination of plasmid DNA total concentration and purity

The concentration and purity of plasmid DNA were determined by measuring absorbance at 260 nm and 280 nm. The purity of the DNA was determined by the ratio of absorbance at 260 nm and 280 nm. A ratio of 1.8 – 2.1 indicates pure DNA (Lucena-Aguilar et al., 2016). The DNA concentration was calculated according to the following equation:

$$\text{DNA concentration } (\mu\text{g}/\mu\text{l}) = \text{A}_{260} * \text{Dilution} / (\text{Depth of well}) * (\text{Extinction coefficient})$$

(Depth of well 0.6, extinction coefficient 20)

The plasmid DNA was diluted in 1:50, 1:100, and 1:200 in TE Buffer. For each sample, 105 μl were loaded in duplicates in a 96 well-plate. Two wells of TE Buffer were included as blank. The measurements were obtained by using a plate reader (GloMax®-Multi Detection System, Promega). The concentration of the plasmid DNA was determined based on the previously mentioned equation and the purity was according to the ratio of absorbance at 260 nm and 280 nm.

2.2.1.5 Agarose gel electrophoresis

To verify the plasmid DNA that has been isolated, agarose gel of different concentrations was used. The concentration of agarose gel is dependent on the molecular size of the DNA plasmid. For plasmid DNA size between 500 to 10000 bp, 1g of agarose (SIGMA-ALDRICH, A9539) was dissolved in 100 ml of 1xTAE Buffer by heating for 2-3 minutes in the microwave. After adding 10 μl of ethidium bromide solution (EtBr, 10 mg/ml, SIGMA-ALDRICH, E1510), the solution was allowed to cool for 15-20 minutes. The gel was then placed in a gel tank containing 1xTAE. 4 μl of 6x Gel Loading Dye Purple (NEB, B7024S) was added to 20 μl of the plasmid DNA samples, and the samples were loaded in the wells of the agarose gel. The ladder used for the electrophoresis was the Quick-load purple 1 kb DNA ladder. The gel was run at 100V for 60 minutes and the DNA bands were observed in a UV transilluminator (BioDoc-IT Imaging System, UVP).

2.2.1.6 Diagnostic Restriction Digest

The identity of plasmid DNA was determined through restriction enzyme digestion. The plasmid DNA sequence was analysed in DNA Dynamo Software to determine which restriction enzymes were appropriate for the plasmid DNA. The plasmid DNA was then diluted 1:10 in ddH₂O. 2 µl of the 3.1 NEB Buffer (New England BioLabs, B7203), 0,5 µl of appropriate restriction enzymes (New England BioLabs), 500 ng of the diluted plasmid DNA and the appropriate volume of ddH₂O to reach a final volume of 20 µl/Eppendorf tube were mixed into an Eppendorf. Following a 2-hour incubation in a 37 °C water bath, 4 µl of 6x Gel Loading Dye Purple (NEB, B7024S) was added to the tube and the DNA sample was then loaded into a well of the agarose gel for electrophoresis at 100V for 1 hour. The DNA bands were observed in a UV transilluminator (BioDoc-IT Imaging System, UVP) to examine if the number and the sizes of the DNA bands were the ones expected according to the restriction enzymes we had used.

2.2.1.7 DNA Sequencing

Following the restriction enzyme digestion, the plasmid DNA sequence was confirmed with Sanger Sequencing performed by GENEWIZ, from Azenta Life Sciences, a genomics service company. 20 µl of DNA sample was transferred in an Eppendorf tube and sent to GENEWIZ company. T7 promoter and T7 terminator primers were provided from GENEWIZ and used for the sequencing. The results obtained from Sanger Sequencing were analysed with DNA Dynamo and SnapGene Software.

2.2.1.8 Recombinant τ 306 tau fragment purification

The tau construct used in this study, provided by Saijo Eri, was τ 306 tau fragment (residues 306–378 using the numbering for full-length human tau isoform htau40) with a point mutation at residue 322 cysteine to serine and a stop codon at C terminal residue 379. The cloning cassette was cloned into pET-28a bacterial vector right after the 5' N-terminal poly-histidine tag and thrombin site by GenScript using CloneEZ seamless cloning technology (Saijo et al., 2017). T306 fragment purification from BL21(DE3)

strain of *Escherichia coli* was performed based on the protocol previously described in (Saijo et al., 2017) following the overnight express autoinduction method (Studier, 2005).

Inoculation of starter culture from plate colonies

DMSO stock with the bacterial cells expressing τ 306 tau fragment was transferred from -80 °C to dry ice and was streaked out on kanamycin-selective LB/agar plates. The plates were then incubated in a Memmert Incubator at 37°C overnight. The following day, using a sterile tip, a single colony from a freshly streaked selective plate was picked to inoculate a starter culture of 5 ml LB medium, containing kanamycin. The starter culture was incubated at 250 rpm at 37 °C for 16 hours in the New Brunswick™ Excella® E24 Incubator Shaker (Eppendorf). Bacterial cell growth was estimated by optical density (OD) measurements at a wavelength of 600nm using UV-Vis Spectrophotometer (Labtech). Therefore, 800 μ l of kanamycin-selective LB media were mixed with 200 μ l of starter culture, and the OD₆₀₀ was measured.

Autoinduction of protein expression

Autoinduction of protein expression was achieved using Isopropyl- β -D-thiogalactopyranoside (IPTG) following the overnight express autoinduction method (Studier, 2005). For the autoinduction, 50 ml falcons with 20 ml of kanamycin-selective LB media were inoculated with the appropriate volume of starter culture to achieve OD₆₀₀ ~ 6.0-0.7. 20 μ l of IPTG were added in each 20 ml bacterial culture and the falcons were incubated at 250 rpm at 37 °C for 3 hours in the New Brunswick™ Excella® E24 Incubator Shaker (Eppendorf). 400 μ l of kanamycin (50 μ g/ μ l) were added in big Culture flasks (2.5 L) with half-baffle for bacteria growth (SIGMA-ALDRICH Z710822) with 400 ml autoinduction bacterial culture media 2ZYM – 2 x LAC. The flasks were then inoculated with 1 ml IPTG-bacterial culture and incubated at 250 rpm at 37 °C overnight. Bacterial cells were harvested by centrifugation at 5000 rpm for 15 minutes at 4°C using the pre-cooled Avanti® J-E Centrifuge (Beckman

Coulter) with J-LITE® JLA-16.250 Fixed-angle Rotor (Beckman Coulter). The bacterial pellet could be stored at 4°C for a day or -20°C for long-term storage.

Fast protein liquid chromatography (FPLC)

The bacterial pellet was resuspended with 50 ml FPLC Buffer A supplemented with 500 µl PMSF Protein Inhibitor (20 mg/ml). Pellet was dissolved with vigorous shaking in the 4°C cold room. Resuspensions were then transferred into two 50 ml polypropylene tubes (Falcon) and kept on ice for the following steps. The tubes were then placed in a Sonicator (Ultrasonic) and the cell resuspensions were probe sonicated in ethanol/ice bath for a total of 1 minute (three cycles of 2 seconds sonication + 2 seconds pause) at a power setting of 25%. This step was repeated 3-5 times until the pellet was completely dissolved. Tubes were centrifuged at 18000 rpm for 45 minutes at 4°C and the supernatant was collected. In the meanwhile, the nickel column (His Trap FF crude, 17-5286-01, GE Healthcare) for FPLC was prepared. The FPLC machine used was ÄKTA Pure chromatography system (GE Healthcare) and Unicorn 1.0 Software. FPLC system was washed and preloaded with Buffer A and Buffer B as appropriate and the nickel column was attached in line with the FPLC. 10 column volumes (50 ml) of Buffer A at a flow rate of 1 ml/minute were used for pre-equilibration of the His-tag nickel column. A fraction collector was set up to collect 2 ml fractions. When the column was equilibrated, the samples were loaded and the flow rate was set up at 1 mL/min. The column was firstly washed with Buffer A until the A280 returns to baseline. Then the column was loaded with 13% Buffer B with 7 column volumes, followed by 5 column volumes with 21% Buffer B wash to elute contaminants peak. 10 fractions (2.5 ml/fraction) of τ 306 protein fragments were collected after elution of the τ 306 peak with a linear gradient from 21% Buffer B to 100% Buffer B over 8 column volumes. 2 µl of 2 M dithiothreitol (DTT) was added to each collection tube to obtain a final concentration of 2 mM.

Acetone precipitation of τ 306 fractions

Acetone precipitation was used to precipitate and concentrate the protein fragments. Fractions including the τ 306 protein fragments were pooled in a bottle. Pre-chilled acetone (SIGMA-ALDRICH, 179124) was added in a protein: acetone ratio of 1:4 and mixed. Bottles were kept for 10 minutes at -80 °C and then placed at 4°C overnight to achieve protein precipitation. The content of the bottles was then split into 50 ml polypropylene tubes (Falcon) and centrifuged at 18000 rpm at 4 °C for 30 minutes. The supernatant was discarded and the pellet was left to air-dry to remove the remaining acetone. Then the pellet was resuspended by adding 2 ml of 8 M guanidine hydrochloride in PBS (elution buffer) to each pellet.

Size exclusion chromatography (SEC)

To further remove the contamination caused by other proteins of different molecular weights, size exclusion chromatography was performed. As previously, the SEC column (HiPrep Sephacryl S-300 HR, Cytiva) was placed in ÄKTA Pure chromatography system (GE Healthcare) and was washed and equilibrated. Firstly, the column was washed with 1 column volume with ddH₂O, followed by equilibration with 2 column volumes of 25 Mm Ammonium Hydrogen Carbonate buffer. As τ 306 is a prone-to-aggregate protein fragment, SEC was performed in the 4°C cold room. After the column was equilibrated, the sample was loaded with the flow rate set up at 1 mL/minute. When the sample was loaded, we switched back to the buffer and let it flow to elute our protein. 2.5 ml fractions of elution were collected in tubes. To collect the fractions with the τ 306 protein fragment, polyacrylamide gel electrophoresis was then performed.

Polyacrylamide gel electrophoresis

Polyacrylamide gel electrophoresis was performed to determine which fractions included the τ 306 protein fragment. 4–20% Mini-PROTEAN® TGX™ Precast Protein Gels (BIORAD, 4561096) were used for polyacrylamide gel electrophoresis. 20 μ l

samples were collected from each fraction and mixed with 4 μ l Gel Loading Dye, Purple (6X) (NEB, B7024S) per sample. The samples were then loaded to the 4-20% gradient protein gel immersed in 1 x Running Buffer. A PageRuler™ Prestained Protein Ladder, 10 to 180 kDa (ThermoFisher, 26616) was also loaded in the gel together with the samples. Samples were run at 200 V for 1 hour. When the running step was over, the gel was carefully transferred to a box containing Quick Coomassie Stain (Protein Ark) and incubated for at least 20 minutes until the bands become visible. The τ 306 protein fragment bands were expected to appear at 10 kDa.

Protein Collection

All the fractions including the τ 306 protein fragment were then collected and pooled together in a 50 ml falcon. An extra 25 Mm Ammonium Hydrogen Carbonate buffer was added to make up the final volume of 50 ml, diluting in this way the protein extract and avoiding spontaneous protein aggregation due to high protein concentration. The falcon with the protein extract was then frozen in liquid nitrogen and stored at -80 °C. The Lyophilisation step followed next. The lid of the falcon tube was replaced with one that had holes to allow the NH₃ and CO₂ from the ammonium hydrogen carbonate to evaporate and be removed from the purified protein. The tube was then placed in SP VirTis AdVantage Pro Freeze Dryer (SP Scientific) to lyophilise the protein. After 3 overnights the lyophilisation of the protein fragment was complete. The weight of the lyophilised protein was measured with a bench scale and stored at -20 °C, avoiding freezing-thawing cycles. When was about to be used, lyophilised protein was dissolved in freshly prepared and pre-chilled 1 x PBS. Protein was adjusted to 0.75 mg/mL in 1 x PBS for the RT-QuIC assay and 1 mg/mL in 1 x PBS for the protein assembly experiment. Diluted protein was stored at -20 °C until further use.

RT2.2.1.9 Protein assembly

For tau-441 2N4R (rPeptide, T-1001-1): 40 μ M tau-441 2N4R was shaken in 100 Mm Sodium Acetate pH 7.0, 40 μ M Heparin (SIGMA-ALDRICH, H6279), and 2mM DTT (Fisher Scientific, FERR0861) at 250 rpm at 37 °C for 360 hours to induce aggregation,

as per (Poepsel et al., 2015). Tau-441 2N4R protein was filtered through an Amicon Ultra-0.5 Centrifugal Filter Unit - 100 kDa molecular weight cut-off (Millipore, UFC510024) prior to use to remove any aggregated fragments. Tau-441 2N4R aggregates were stored at -80 °C until further use.

For τ 306 fragment: 1 mg/ml τ 306 fragment was shaken in 10 mM HEPES pH 7.0 (SIGMA-ALDRICH, H3375), 400 mM NaCl (SIGMA-ALDRICH, S7653), and 40 μ M Heparin (SIGMA-ALDRICH, H6279) at 250 rpm at 37 °C for 360 hours to induce aggregation, as per (Kraus et al., 2019). T306 fragment was filtered through an Amicon Ultra-0.5 Centrifugal Filter Unit - 100 kDa molecular weight cut-off (Millipore, UFC510024) prior to use to remove any aggregated fragments. T306 aggregates were stored at -80 °C until further use.

For alpha-synuclein: 2 mg/ml of alpha-synuclein (rPeptide, S-1001-2) was shaken at 250 rpm at 37 °C for 120 hours to induce fibril formation. Alpha-synuclein fibrils were stored at -80 °C until further use.

Samples were sent for Transmission electron microscopy (TEM) to Dunn School of Pathology, University of Oxford, and imaged by Errin Johnson as follows: Ten μ l of 40 μ M samples for tau, 1 mg/ml τ 306, and 1 mg/ml for alpha-synuclein aggregates were applied to carbon-coated TEM grids (TAAB) after glow discharge and incubated on the grids for 2 minutes at RT. Then staining with uranyl acetate 2% was performed for 10 seconds and the samples were dried immediately and stored at RT as previously described in [Bengoa 2021]. FEI Tecnai 12 TEM microscope (120 kV) with a Gatan US1000 camera was image acquired.

2.2.1.10 Tau Real-Time Quaking-Induced Conversion (RT-QuIC)

The tau RT-QuIC with τ 306 tau substrate assay was performed as previously described [Saijo 2017, Kraus 2018]. T306 tau substrate (0.75 mg/ml) in PBS was thawed at RT and filtered through an Amicon 100 kDa molecular weight cut-off filter column (Millipore, UFC510024) at 3300 x g for 5 minutes at RT to use to remove any aggregated τ 306 species. Tau RT-QuIC reaction buffer included 10 mM HEPES, pH 7.4, 400 Mm NaCl, 40 μ M heparin, 10 μ M ThT, and 0.1 mg/ml τ 306 (substrate). The RT-QuIC buffer was prepared according to the following table:

Table 2.3 – RT-QuIC reaction buffer master mix

Reagent	µl/reaction	Final Concentration in 100 µl reaction
ddH ₂ O	41.75	
50 Mm HEPES pH 7.4	20	10 mM
2M NaCl	20	400 mM
10 mg/ml Heparin	2.25	40 µM
500 mM ThT	2	10 µM
0.75 mg/ml τ306	14	20 µM
Total	98	

All components, except the τ306 substrate, were mixed in a 15 ml falcon tube and vortexed. After vortexing, 14 µl of 0.75 mg/ml τ306 were added to the tube. 98 µl of the master mix was transferred to each well of a 96-well plate. For brain homogenates, frozen brain tissue from the different samples were placed in Eppendorf tubes and weighed. 10% W/V brain homogenates in Protease and Phosphatase Inhibitor in TBS homogenisation buffer were created using Tissue Ruptor (Qiagen, 9002755) and disposable probes (Qiagen, 990890). After the solution was homogenous, the homogenates were centrifuged at 13300 rpm for 15 minutes at 4 °C. Supernatant was transferred to new tubes and stored at -80 °C. Brain homogenate samples were serially diluted in 10-fold steps in the KO/N₂/HEPES buffer consisting of 10 mM HEPES, pH 7.4, 0.53% tau KO mouse brain homogenate, and 1 x N-2 supplement. Tau KO mouse brain homogenate and N-2 supplement are an important addition to the diluent sample buffer as they prevent the spontaneous aggregation of τ306 fragment. 2 µl of brain homogenate dilution was transferred into triplicate wells including 98 µl of master mix each for a final volume of 100 µl per well in a 96 well plate. After being sealed, the plate was placed in the BMG Omega FLUOStar plate reader and incubated at 42 °C with intermittent shaking, consisting of 1 minute of orbital shaking at 500 rpm and 1-minute rest. ThT fluorescence reads (450-10 nm excitation, 480-10 nm emission, bottom read) were collected every 15 min.

Kinetic Calculations and statistical analysis

The RT-QuIC assay cut-off was determined to be 52 hours and had a reproducible endpoint before the spontaneous amyloid aggregation in the wells with the tau KO mouse brain homogenate. The endpoint of 52 hours was used for any data points with ThT fluorescence values at or greater than 52 hours. Fmax (maximum ThT fluorescence), lag time (reaction time to exceed a ThT fluorescence threshold of the average baseline fluorescence + 5 SD), time to reach maximum ThT fluorescence, and Vmax (maximum slope) were analysed. Differences in these parameters across the three groups with dilution 1×10^{-1} were assessed using One-way ANOVA with Bonferroni's Multiple Comparison Test. Statistical significance was defined as $p < 0.05$.

2.2.2 Methods of Cellular Biology

2.2.2.1 Cell Culture

Cell culture conditions

Human Embryonic Kidney 293 (HEK293) cells were used for *in vitro* assays. Cells were cultured in T175 flasks (NUNC, 159910) at 37°C in a 5% CO₂ humidified atmosphere. For HEK293 cell culture, complete Dulbecco's Modified Eagle's Medium-high glucose (SIGMA-ALDRICH, D6546) was used, supplemented with 10% Fetal calf serum (FCS) (SIGMA-ALDRICH, F7524), 1% 200 mM L-glutamine (SIGMA-ALDRICH, G7513), and 1% 100 U/ml Penicillin/Streptomycin (SIGMA-ALDRICH, P4333).

Cell thawing

Cryo-vial tubes containing 1 ml of HEK293 cells in complete DMEM were preserved in liquid nitrogen storage. For cell thawing, the tubes with the frozen cells were rapidly transferred to a 37 °C water bath for a few seconds-minutes. Under sterile conditions, thawed cells were transferred in a T175 flask containing 24 ml of pre-warmed complete DMEM medium, and the flask was placed into an incubator at 37°C in a 5% CO₂ humidified atmosphere. When the cells were attached, the medium was completely

removed and replaced by fresh pre-warmed complete medium. The medium was replaced with a fresh one every two days.

Cell passaging

For passaging the cells when flasks were confluent, the medium was removed from the flask, the cells were washed with 10 ml pre-warmed Dulbecco's Phosphate buffered saline (SIGMA, D8537). The cells were then detached after incubation for 3 minutes with 4 ml pre-warmed 1x Trypsin-EDTA. After detaching the cells, 6 ml of the complete medium was added into the flask to neutralise the 1x Trypsin-EDTA. Cells were then transferred into a 15 ml falcon tube and centrifuged for 5 minutes at 750 rpm. After removing the supernatant, the pellet was dissolved in 10 ml of fresh pre-warmed complete medium and the cells were seeded in new flasks containing pre-warmed complete medium in different ratios based on the desired cell confluency. Cells were then cultured at 37°C in a 5% CO₂ humidified atmosphere.

2.2.2.2 Tau Bimolecular fluorescence complementation (BiFC) assay

Tau BiFC plasmid constructs: pmGFP10C-tau (Addgene, 71433) and pmGFP11C-tau (Addgene, 71434) were kindly provided by Henri Huttunen. The assay was performed with our collaborators Nora Bengoa-Vergniory and Ana Maria Silva at Oxford University. Poly-D-lysine coated coverslips were placed in 24 well plates and were seeded with 2×10^5 HEK293 cells per well. Cells were placed in the incubator and incubated overnight. The following day, cells were transfected with 100 ng of each BiFC plasmid construct using Lipofectamine and Plus Reagents (ThermoFisher, A12621) according to the manufacturer's instructions. Cells were then fixed for the tau-PLA experiment. For cell fixation, after cells were washed with 250 μ l Dulbecco's PBS (SIGMA, D8537), were fixed with 250 μ l ice-cold 4% Paraformaldehyde for 45 minutes in the dark in a laminar flow hood. Once cells were fixed, PFA was removed and the cells were washed with 2 x 250 μ l Dulbecco's PBS. Fixed samples could be stored in Dulbecco's PBS wrapped with foil at 4°C for a short period of up to 3 weeks.

2.2.2.3 Tau FKBP-FRB-rapamycin assay

FK506 Binding Protein (FKBP)-tau and FK506 Rapamycin binding (FRB)-tau constructs were generated in the Department of Physiology, Anatomy, and Genetics, Oxford University, and the assay was performed with our collaborators Nora Bengoa-Vergniory and Ana Maria Silva at Oxford University. As previously, Poly-L-lysine coated coverslips were placed in 24 well plates and were seeded with 2×10^5 HEK293 cells per well. Cells were placed in the incubator and incubated overnight. The following day, cells were transfected with 25 ng of FKBP-tau and FRB-tau plasmid constructs using Lipofectamine and Plus Reagents (ThermoFisher, A12621) according to the manufacturer's instructions. Cells were incubated at 37°C for 4 hours before being washed with 250 μ l Dulbecco's PBS. The transfection reagents were replaced with complete DMEM media supplemented or not with 400 nM rapamycin (Calbiochem) for 1 hour for the + rapamycin or – rapamycin conditions respectively. Cells were then fixed for the tau-PLA experiment. For cell fixation, after cells were washed with 250 μ l Dulbecco's PBS were fixed with 250 μ l ice-cold 4% Paraformaldehyde for 45 minutes in the dark in a laminar flow hood. Once cells were fixed, PFA was removed and the cells were washed with 2 x 250 μ l Dulbecco's PBS. Fixed samples could be stored in Dulbecco's PBS wrapped with foil at 4°C for a short period of up to 3 weeks. 1 hour after transfection, cells were fixed for the tau-PLA experiment. For cell fixation was performed as previously.

2.2.2.4 Imaging

For fluorescence imaging analysis of fixed cells, the DV Elite system based on an Olympus IX71 fully motorized widefield deconvolution inverted microscope (60x objective) was used. Representative Z-stack images (0.250 μ m intervals) were captured using a CoolSNAP HQ2 cooled charge-coupled device (CCD) camera (Photometrics) and SoftWoRx 5.0 software (Applied Precision). For the Tau FKBP-FRB-rapamycin assay, Fiji software was used for the quantification of tau-PLA puncta per PLA-positive cell. N = 20 cells per condition. GraphPad Software was used for the statistical analysis and comparison of the groups. Unpaired two-tailed Student's t-tests were performed with statistical significance being defined as $p < 0.05$.

2.2.3 Tissue work

2.2.3.1 Animal work

MAPT KO mice missing exon 1 in the *MAPT* gene after replacement with the neomycin-resistant cassette, P301S transgenic mice expressing the shortest human four-repeat tau isoform (0N4R) with the P301S mutation, under the control of the murine *thy1* promoter, and wild-type aged matched littermates C57BL/6, were used in this study. Histological analysis was performed in 6 months old female and male *MAPT* KO (N=2) P301S tau (N=6), and C57BL/6 (N=6) mice, together with 3 (N=2) and 9 (N=2) month old P301S mice.

Tissue Collection

Both transgenic and wild-type mice were deeply anesthetized via intraperitoneal injection of 100 µl Euthatal® 200 mg in 1 ml Solution for Injection Pentobarbital Sodium (Merial). Following anesthesia, mice were perfused transcardially with 1xPBS. Brains were extracted and the right and left hemispheres were separated. The right hemisphere was used for histological analysis, while the left was for biochemical. The right hemisphere was fixed in 4% paraformaldehyde in PBS for 48 hours at 4°C, followed by paraffin embedding and microtome sectioning. Paraffin embedding was performed at the Multiple Sclerosis and Parkinson's Tissue Bank, ICL. The left hemisphere was stored at -80°C for future use.

Microtome sectioning

Formalin-Fixed Paraffin-Embedded (FFPE) left hemispheres were sectioned into 10 µm thick slices using a microtome (ThermoFisher). The sections were then placed onto SuperFrost Plus Microscope Slides (VWR, 631-0108) and incubated at 37°C overnight in the lab incubator to air-dry. Then stored at RT.

Ethics declarations

Work with animal models was approved by the UK Home Office and performed according to the Animals (Scientific Procedures) Act of 1986 and European Union Directive 2010/63/EU.

2.2.3.2 Human tissue work

Formalin-Fixed Paraffin-Embedded (FFPE) and frozen blocks from the hippocampal region, temporal cortex, and occipital cortex (Fig. 2.1) from individuals without neurological disease or *intra vitam* diagnosis of AD were supplied by the Multiple Sclerosis and Parkinson's Tissue Bank of Imperial College London and Oxford Brain Bank. FFPE tissue was sectioned and used for IHC and tau-PLA.

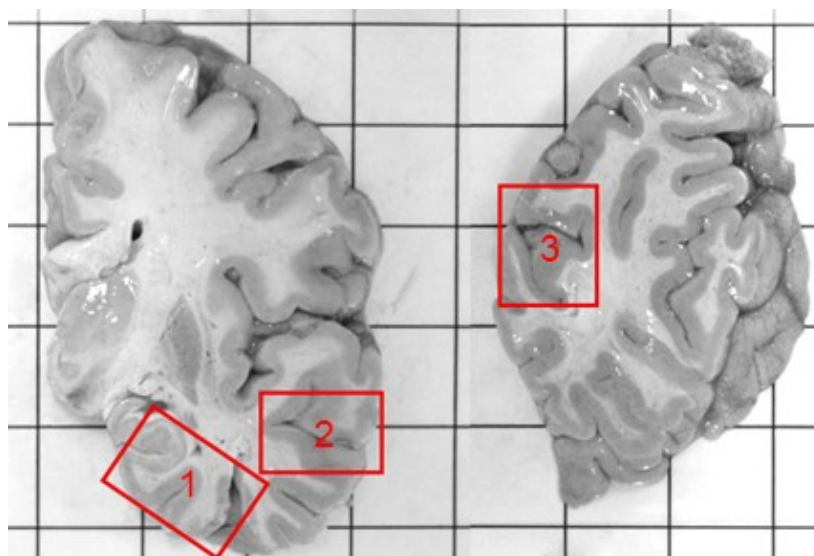


Figure 2.1. Macroscopically neuroanatomical regions of post-mortem human brain. Macroscopically neuroanatomical regions of the 1-posterior hippocampus, fusiform gyrus, and part of inferior temporal gyrus, 2-temporal cortex including parts of middle and superior temporal gyrus, and 3-occipital cortex including calcarine fissure.

Neuropathological assessment of the cases

Cases selected for this study were accessed by the neuropathologists of Multiple Sclerosis and Parkinson's Tissue Bank of Imperial College London and Oxford Brain Bank. The cases were further validated with Haematoxylin & Eosin (H&E) staining

and immunohistochemistry (IHC) for hyperphosphorylated tau with AT8 antibody, beta-amyloid plaques with 4G8 antibody, alpha-synuclein with alpha-synuclein 42 antibody. Post-mortem human brain sections positive for tau staining were diagnosed with AD. The staging of each case was defined according to the modified Braak Staging System (Braak 2006) based on the AT8-immunoreactive neuropil threads (NTs) across the brain regions of the hippocampus, temporal cortex, and occipital cortex (BrainNet Europe diagnostic protocol) (Alafuzoff 2008). Beta-amyloid plaques and alpha-synuclein immunoreactive inclusions were accessed using 4G8- and alpha-synuclein 42-IHC, respectively. The presence of other pathologies was accessed based on H&E staining.

Exclusion Criteria

To select the appropriate AD cases for our research study, we followed a number of exclusion criteria. Firstly, cases with deficient tissue conditions were not included in the study. Cases diagnosed with tauopathies other than AD, like Primary age-related tauopathy (PART), Progressive Supranuclear Palsy (PSP), Corticobasal Degeneration (CDB), Aging-related tau astrogliaopathy (ARTAG), Chronic Traumatic Encephalopathy (CTE), and others were also excluded. In addition, cases with other neurodegenerative disorders were excluded. Finally, cases with vascular lesions were not included too. For control cases, post-mortem brain tissue from healthy individuals with no clinical symptoms and neurological pathology was selected.

Summary of cases included in the study

Based on the exclusion criteria, a total of 67 cases of neurofibrillary Braak stages 0, I, II, III, IV, V, and VI were selected. A summary of patient information (Table 2.4) and additional brain tissue information (Table 2.5) are presented in the following tables. Brain tissue from the hippocampal region, temporal cortex, and occipital cortex was obtained (Fig.2.1).

Table 2.4 - Summary of patient information

	Braak 0	Braak I	Braak II	Braak III	Braak IV	Braak V	Braak VI
N=67	11	12	12	9	7	8	8
Av. death age	54.6	68.7	82.6	89.1	87	85.7	76.5
% Demented Individuals	0%	0%	8.3%	11.1%	59.8%	100%	100%

Table 2.5 – Additional brain tissue information

PMI	Dementia	Age at death	Gender	Amyloid burden (CERAD)	α -syn burden (Braak stage)	Neurofibrillary Braak stage
24	no	65	female	0, no neuritic plaques	0	0
48	no	42	female	0, no neuritic plaques	0	0
48	no	48	female	0, no neuritic plaques	0	0
72	no	51	male	0, no neuritic plaques	0	0
48	no	45	male	0, no neuritic plaques	0	0
48	no	41	female	0, no neuritic plaques	0	0
48	no	56	male	0, no neuritic plaques	0	0
19	no	74	male	0, no neuritic plaques	0	0
29	no	68	male	0, no neuritic plaques	0	0
20	no	52	female	0, no neuritic plaques	0	0
45	no	59	female	0, no neuritic plaques	0	0
48	no	56	male	0, no neuritic plaques	0	I
42	no	56	male	0, no neuritic plaques	0	I
65	no	92	female	0, no neuritic plaques	0	I
12	no	77	female	0, no neuritic plaques	0	I

100	no	88	female	0, no neuritic plaques	0	I
48	no	60	female	0, no neuritic plaques	0	I
48	no	51	male	0, no neuritic plaques	0	I
26	no	77	male	0, no neuritic plaques	0	I
19	no	91	female	1, sparse neuritic plaques	0	I
28	no	50	female	0, no neuritic plaques	0	I
15	no	61	female	0, no neuritic plaques	0	I
23	no	66	male	0, no neuritic plaques	0	I
54	no	92	female	0, no neuritic plaques	0	II
24	no	87	female	0, no neuritic plaques	0	II
48	no	57	female	0, no neuritic plaques	0	II
26	MCI	83	female	3, frequent neuritic plaques	1	II
24	no	89	female	1, sparse neuritic plaques	0	II
48	no	91	female	0, no neuritic plaques	0	II
96	no	79	male	0, no neuritic plaques	0	II
15	no	82	female	0, no neuritic plaques	0	II
26	no	83	male	2, moderate neuritic plaques	0	II
20	yes	82	female	2, moderate neuritic plaques	0	II
25	no	79	male	1, sparse neuritic plaques	0	II
15	no	87	female	2, moderate neuritic plaques	0	II
80	no	83	male	1, sparse neuritic plaques	0	III
86	MCI	90	female	0, no neuritic plaques	0	III

34	no	69	male	1, sparse neuritic plaques	0	III
72	no	92	male	1, sparse neuritic plaques	0	III
18	no	89	male	0, no neuritic plaques	0	III
24	no	92	female	3, frequent neuritic plaques	0	III
24	yes	98	female	3, frequent neuritic plaques	0	III
11	no	95	male	2, moderate neuritic plaques	0	III
40	MCI	94	female	3, frequent neuritic plaques	0	III
48	no	92	male	1, sparse neuritic plaques	0	IV
24	MCI	87	male	1, sparse neuritic plaques	0	IV
120	no	80	male	2, moderate neuritic plaques	0	IV
48	yes	89	male	3, frequent neuritic plaques	0	IV
12.75	yes	85	female	2, moderate neuritic plaques	0	IV
13	yes	89	female	3, frequent neuritic plaques	0	IV
28	no	95	female	2, moderate neuritic plaques	0	IV
31.25	yes	77	female	3, frequent neuritic plaques	0	V
46	yes	75	male	3, frequent neuritic plaques	Amygdala-only	V
66	yes	91	male	3, frequent neuritic plaques	0	V
34	yes	87	male	3, frequent neuritic plaques	0	V
24	yes	85	male	3, frequent neuritic plaques	0	V
45	yes	80	male	3, frequent neuritic plaques	0	V
34	yes	89	male	3, frequent neuritic plaques	0	V
21	yes	92	female	3, frequent neuritic plaques	0	V

7	yes	77	male	3, frequent neuritic plaques	0	VI
28	yes	64	female	3, frequent neuritic plaques	0	VI
13.67	yes	85	female	3, frequent neuritic plaques	0	VI
23	yes	61	female	3, frequent neuritic plaques	0	VI
69	yes	85	male	3, frequent neuritic plaques	0	VI
120	yes	83	male	3, frequent neuritic plaques	0	VI
7	yes	78	male	3, frequent neuritic plaques	0	VI
41	yes	79	male	2, moderate neuritic plaques	0	VI

Microtome sectioning

Formalin-Fixed Paraffin-Embedded (FFPE) tissue was sectioned into 5 µm thick slices using a microtome (ThermoFisher). The sections were then placed onto SuperFrost Plus Microscope Slides (VWR, 631-0108) and incubated at 37°C overnight in the lab incubator to air-dry. Then stored at RT.

Cryo-sectioning

Frozen blocks of human brain tissue were transferred from a -80°C freezer to dry ice. Cryostat temperature was set up at -20°C. The frozen tissue blocks were adhered to the specimen mount by adding a drop of O.C.T. compound (VWR, 361603E) and left to equilibrate to the cryostat temperature for 15 minutes. Thick sections of frozen tissue were collected and placed into pre-cooled Eppendorf tubes until collecting ~ 100 mg of frozen tissue per tube. Tubes were then transferred to dry ice and stored at -80°C.

Brain Tissue Homogenisation

Frozen tissue samples were homogenised in ice-cold PBS (10% w/v) using a Tissue Ruptor (Qiagen, 9002755) and disposable probes (Qiagen, 990890). In detail, frozen tissue was transferred from -80°C to ice. 10% W/V brain homogenates in homogenisation buffer (Protease and Phosphatase Inhibitor in TBS) were created using

a Tissue Ruptor and disposable probes. When the solution became homogenous, the homogenates were centrifuged at 13300 rpm for 15 minutes at 4 °C. Supernatant was transferred to new tubes and stored at -80 °C.

Ethics declarations

Work with human post-mortem tissue was performed according to the Imperial College London Multiple Sclerosis and Parkinson's Tissue Bank's Research Ethics Committee Approval Ref. No 07/MRE09/72, the Oxford Brain Bank's Research Ethics Committee Approval Ref. No. 15/SC/0639, and the Multiple Sclerosis and Parkinson's Tissue Bank's Research Ethics Committee Approval Ref. No. 08/MRE09/31+5.

2.2.3.3 Tau – Proximity Ligation Assay (tau-PLA)

Tau-PLA probes preparation

The tau-PLA was performed using Duolink PLA kits (Table 2.7) according to the manufacturer's instructions. The tau conjugated were prepared according to the Duolink PLA Probemaker protocol. Tau5 monoclonal pan-tau antibody (anti-tau5, 1 mg/ml, no BSA or azide) (Abcam, ab80579), which recognises epitopes 218-225 of full-length human tau, was used together with the Duolink PLA Plus (SIGMA-ALDRICH, DUO92009) or Minus (SIGMA-ALDRICH, DUO92010) kits for the generation of the conjugates. Briefly, 20 µl of the anti-tau5 was incubated with a vial of Duolink PLA Plus or Minus oligonucleotides and 2 µl of conjugation buffer overnight (16 hours minimum) at RT. The following day, conjugates were incubated for 30 minutes at RT with 2 µl Probemaker stop solution and stored at 4°C after adding 24 µl in Probemaker storage buffer.

Tissue preparation for tau-PLA

For fluorescent tau-PLA, transfected HEK293 cells were fixed in 4% PFA as described previously. For brightfield tau-PLA, 10 µm thick paraffin-embedded mouse tissue and 5 µm thick paraffin-embedded human tissue were prepared by heating for 45 minutes at 70°C followed by dewaxing and rehydration. For the dewaxing, slides were left for 3 minutes in 100% xylene, followed by 3 minutes of incubation in Histo-Clear (Fisher

Scientific, 50-899-90147). The slide rehydration was performed in 100-70% graded ethanols. Slides were initially incubated in 100% ethanol for 3 minutes twice. This step was repeated for 95% and 70% ethanols and the slides were then incubated for 3 minutes in ddH₂O. Blocking of the endogenous peroxide was performed by incubating the slides with 10% H₂O₂ for 1 hour at RT in the dark and the slides were then washed with ddH₂O for 5 minutes. For antigen retrieval, microwave heating in citrate buffer (pH 6.0) for a total of 10 minutes was used. Detailed, slides were placed in a microwavable box with citrate buffer (pH 6.0) and microwaved in a 900 W microwave for 4 minutes, followed by 5 minutes rest. Slides were microwaved again for 1.5 minutes with 5 minutes resting after. This step was repeated 3 more times. The box was then placed in ice to cool down for 30-40 minutes. After washing the slides with ddH₂O the slides were washed twice with TBS - 0.1% Tw Wash Buffer.

Tau-PLA brightfield staining

Samples, after being washed with TBS - 0.1% Tw Wash Buffer, were incubated with Duolink blocking solution for 1 hour at 37°C. Tau-PLA conjugates were diluted in PLA Probe diluent (1 PLUS : 1 MINUS : 250 diluent) and samples were incubated with 120 µl per slide overnight at 4°C. After being washed with TBS - 0.05% Tw Wash Buffer three times for 5 minutes, the samples were incubated 120 µl per slide PLA ligation solution for 1 hour at 37°C. Following the ligation step, the samples were washed as previously and incubated 120 µl per slide PLA amplification solution for 2.5 hours at 37°C. For fluorescent tau-PLA, after samples were washed with TBS - 0.05% Tw Wash Buffer three times for 5 minutes, were mounted in Vectashield with 1 µg/ml DAPI counterstain. For brightfield tau-PLA, the detection step was performed after washing the samples and covering the sections with 120 µl per slide PLA detection solution for 1h at RT. After washing, the samples were incubated with the 120 µl per slide PLA substrate solution for 20 minutes at RT. The reaction was terminated by dipping the slides into a box with ddH₂O and washing them for a couple of minutes before being counterstained with Mayer's haematoxylin solution (SIGMA-ALDRICH, MHS16). Dehydration with 70-100% graded ethanols and xylene was performed and the slides were then mounted with DPX mounting reagent (SIGMA-ALDRICH, 44518) and left to air-dry overnight in the laminar hood.

For recombinant protein analysis, 10 µl of 40 µM tau-441 2N4R aggregates, 1 mg/ml τ306 aggregated fragments, and 1mg/ml alpha-synuclein fibrils were spotted on poly-L-lysine coated coverslips, left for 30 minutes at RT, then PFA-fixed for 10 minutes as described in a previous chapter and treated as above for fluorescent tau-PLA.

Tau-PLA co-immunofluorescence

For tau-PLA co-immunofluorescence, immunofluorescence was performed after the antigen retrieval step, before blocking the slides for PLA. Slides were incubated with 120 µl per slide primary antibody (GFAP, Iba1, Tau5) (Table 2.1) for 1 hour at RT before being washed with TBS - 0.05% Tw Wash Buffer three times for 5 minutes. Slides were then incubated with 120 µl per slide secondary antibodies (Table 2.2) for 1 hour at RT and then washed with TBS - 0.05% Tw Wash Buffer as previously.

6x His tag Proximity Ligation Assay (6x His tag-PLA)

6x His tag-PLA was performed similarly to tau-PLA. Briefly, anti-6x His tag (Abcam, ab213204) was used together with the Duolink PLA Plus (SIGMA-ALDRICH, DUO92009) or Minus (SIGMA-ALDRICH, DUO92010) kits for the generation of the conjugates. Dewaxing was performed as previously by heating, dewaxing in xylene and histoclear, rehydrating in 100-70% graded alcohols, blocking of the endogenous peroxide with 10% H₂O₂ for 1 hour at RT, and performing antigen retrieval via microwave heating in citrate buffer (pH 6.0) for a total of 10 min. Samples were incubated with Duolink blocking solution for 1 hour at 37 °C and then with 6x His tag-PLA conjugates diluted in PLA Probe diluent (PLUS : 1 MINUS : 200 diluent) overnight at 4°C. After being washed, the samples were incubated with PLA ligation solution for 1 hour at 37°C. After washes, incubation with the PLA amplification solution for 2.5 hours at 37°C was performed. Tissue sections were then washed and incubated with a PLA detection solution for 1 hour at RT. After washing, the samples were incubated with the PLA substrate solution for 20 minutes at RT. Samples were then counterstained with haematoxylin for 4 minutes, washed with tap water for 5 minutes, dehydrated with 70-100% graded alcohols and xylenes, and mounted with DPX mounting reagent.

2.2.3.4 Immunohistochemistry (IHC) of FFPE sections

10 µm thick paraffin-embedded mouse tissue and 5 µm thick paraffin-embedded human tissue were prepared by heating for 45 minutes at 70°C followed by dewaxing in xylene and rehydration in 100-70% graded ethanols, as described previously. Sections were then blocked with H₂O₂ for 1 hour (Table 2.1) at RT in the dark. After being washed with ddH₂O for 5 minutes, antigen retrieval was performed. Antigen retrieval was achieved via microwave heating with citrate buffer pH 6.0 for a total of 10 minutes (AT180, PS422, PT217, Anti-6x His tag), or with incubation in 80% formic acid (SIGMA-ALDRICH, 399388) for 15 minutes (4G8, alpha-synuclein 42), or no treatment (AT8, MC1, ALZ50, PHF-1). The slides were then washed with washing buffer (Table 2.1) three times for 5 minutes. Blocking of non-specific binding sites was performed by incubating the slides with normal serum for 1 hour in PBS at RT. Then the sections were incubated with the primary antibody (Table 2.1) overnight at 4°C. The following day, after the slides were washed with washing buffer three times for 5 minutes, sections were incubated with a biotinylated IgG secondary antibody (Table 2.2), for 1 hour RT. After being washed three times for 5 minutes, the slides were incubated with Vectastain ABC reagents (Vector Labs) according to the manufacturer's instructions. Slides were washed once again and detection was performed using a 3,3'-diaminobenzidine (DAB) substrate based on according to manufacturer's protocol. When the stain was developed, the reaction was terminated by dipping the slides into a box with tap water. Slides were washed with running tap water for a couple of minutes and were counterstained with Mayer's Haematoxylin solution (SIGMA-ALDRICH, MHS16). The slides were washed with tap water for 5 minutes. Dehydration with 70-100% graded ethanols and xylene was performed as previously and the slides were then mounted with DPX mounting reagent (SIGMA-ALDRICH, 44518) and left to air-dry overnight in the laminar hood.

2.2.3.5 Haematoxylin & Eosin staining

For Haematoxylin & Eosin staining, the 5 µm thick paraffin-embedded human brain tissue was prepared by heating the slides for 45 minutes at 70°C followed by dewaxing in xylene and rehydration in 100-70% graded ethanols, as described previously. Slides were then immersed in Mayer's Haematoxylin (SIGMA-ALDRICH, MHS16) for 4

minutes and then washed with tap water for 5 minutes to enhance the staining. Slides were then immersed in 1% eosin for 5 minutes before being washed with ddH₂O for 5 minutes. Dehydration with 70-100% graded ethanols and xylene was performed as previously and the slides were then mounted with DPX mounting reagent (SIGMA-ALDRICH, 44518) and left to air-dry overnight in the laminar hood.

2.2.3.6 Imaging and neuropathological analysis

For the brightfield imaging analysis of the stained sections, a Leica Aperio AT2 slide scanner and Aperio-Imagescope (40x objective) were used. Three representative images were blindly taken from the analysed brain regions and neuropathological analysis was performed using the ImageJ software (Rasband WS, ImageJ, U.S. National Institutes of Health, USA. <http://imagej.nih.gov/ij/>). Images were thresholded and the number of particles in the total covered area was quantified (Fig. 2.2). Particle size was adjusted as follows: 1.5–3.5 μm^2 for the diffuse tau-PLA signal labelling of small structures (Fig. 2.2 A), and 12.5–100 μm^2 for the large perikaryal lesions, mostly representing NFTs and NTs (Fig. 2.2 B). The mean of each sample and brain region was calculated and analysed. Semi-quantitative analysis was performed by collecting blindly three representative images for each sample and brain region according to a semi-quantitative scale between 1 and 6 (Fig. 2.3). GraphPad Software was used for the statistical analysis and comparison of the groups. One-way ANOVA with Dunnett's post hoc test and unpaired two-tailed Student's t-test was performed with statistical significance being defined as $p < 0.05$.

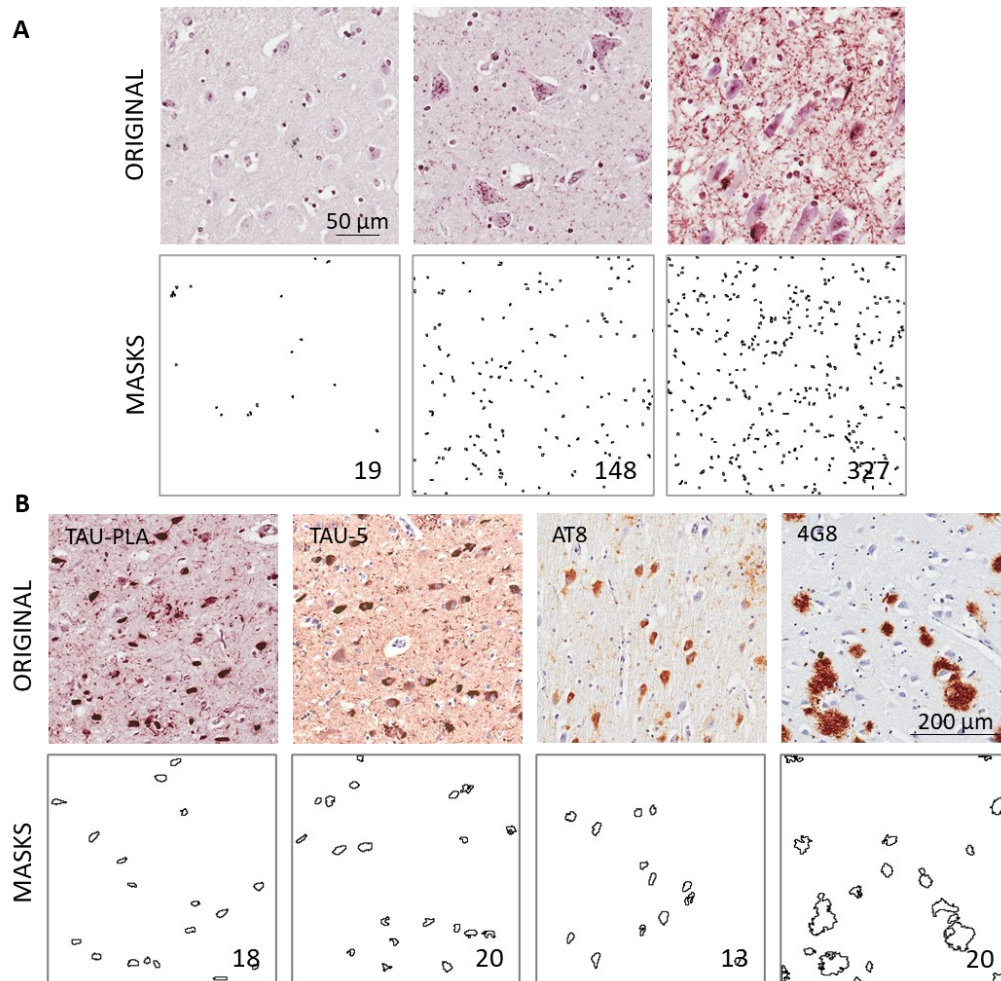


Figure 2.2. Automated analysis scale used for analysis. A) Original images and images after analysis with quantification using an automated analysis scale using ImageJ Software with particle size being adjusted at 1.5–3.5 μm^2 . Images represent tau-PLA labelled structures of different densities; insets show the final counts. B) Original images and images after analysis with quantification using an automated analysis scale using ImageJ Software with particle size being adjusted at 12.5–100 μm^2 . Images represent tau structures with 4 different immunolabellings; insets show the final counts.

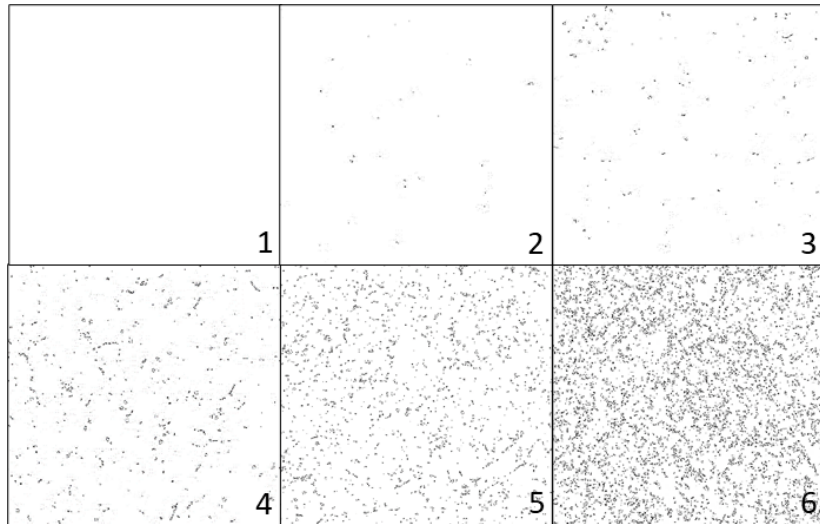


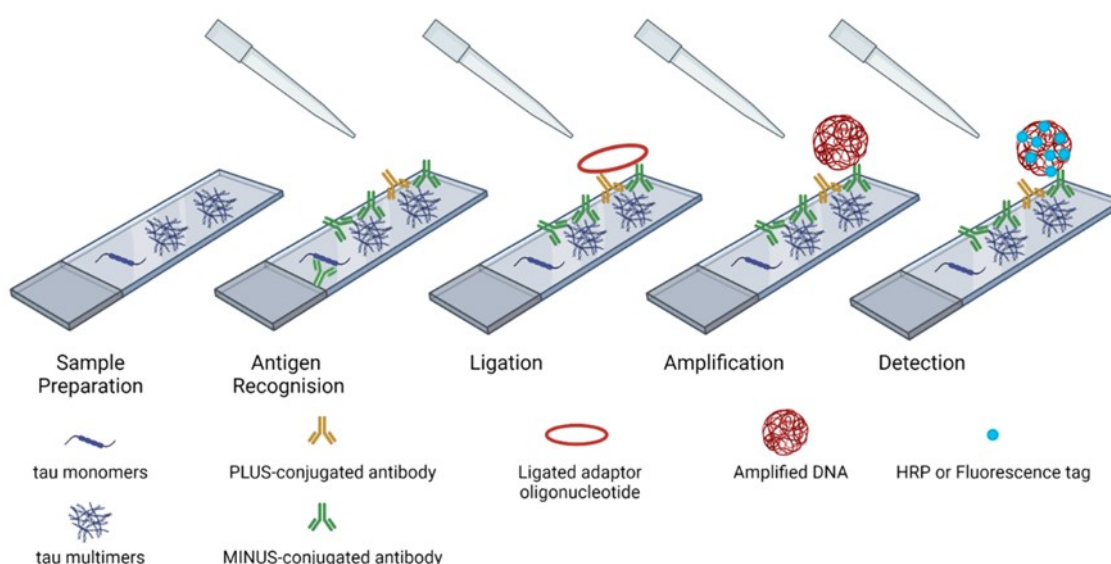
Figure 2.3. Semi-quantitative scale used for analysis. Semi-quantitative scale between 1 to 6 was used for semi-quantitative analysis.

Chapter 3: tau-PLA detects tau-tau interactions in *in vitro* systems

3.1 Introduction

The abnormal intraneuronal aggregation and misfolding of tau, a microtubule-associated protein, in the central nervous system (CNS) is the main pathological hallmarks of tauopathies, with AD being the most common neurodegenerative disorder (Goedert et al., 2017; Lee et al., 2001). Proximity ligation assay (PLA), first developed by Soderberg et al. in 2006, is a technique that allows the specific detection of endogenous protein interaction directly in normal cells and tissues (Söderberg et al., 2006). Based on a recently developed assay, the alpha-synuclein proximity ligation assay (AS-PLA), where multimers of alpha-synuclein but not monomers can be detected after conjugation of the same epitope-blocking monoclonal antibody with the PLA probes (Roberts et al., 2015), we tried to develop a method that would detect tau-tau interactions *in situ*. Following the PLA principles, every time two or more protein molecules interact one with the other, and the PLUS and MINUS PLA probes are in proximity (less than 40 nm away), ligation with a connector oligonucleotide is occurring, producing a circular DNA. This circular DNA serves as a template for the following step of amplification. However, at this point, we need to highlight that 50% of the binding events can be captured by tau-PLA as the PLUS-PLUS and MINUS-MINUS events do not lead to productive ligation. Successful ligations work as primers for a rolling cycle amplification reaction and the final DNA products are visualised as single dots after the addition of complementary labelled oligonucleotides tagged with HRP or fluorescent tag (Söderberg et al., 2006). Final products are visualised using brightfield or fluorescent microscopy, respectively. For the development of tau-PLA, tau5 antibody (ab80589, Abcam), a monoclonal pan-tau antibody that recognises the epitopes 218-225 amino acids of the non-phosphorylated full-length human tau was used for the generation of the tau-PLA conjugates with the PLA PLUS and MINUS Probes (Porzig et al., 2007). To validate the ability of tau-PLA to detect tau self-interactions but no monomeric tau, several *in vitro* systems were used including tau BiFC assay and tau multimerisation inducible systems like FKBP-FRB-rapamycin system and heparin-induced tau aggregation. The bimolecular fluorescence

complementation (BiFC) assay is based on the structural complementation of two fragments of GFP leading to the production of a bimolecular fluorescence complex when these two GFP splits are brought in proximity to each other after interaction between the proteins they are fused to (Brunello et al., 2016; Kerppola, 2013). These GFP splits encode the 10 first β -strands including the 1–214 amino acids and the 11th β -strand comprising of the 215–230 amino acids of GFP and can be fused with different molecules to visualise and investigate their interactions (Fig.3.2A). Another system commonly used for induced interactions between molecules is the FKBP-FRB-rapamycin system. Interaction between the FKBP (FK506 binding protein) and FRB (FKBP rapamycin binding) domain of mTOR is lacking. Rapamycin is a molecule (antibiotic) that can bind simultaneously and with high affinity to FKBP and FRB inducing the dimerisation of these two proteins (Fig.3.3A). Therefore, induced interactions between two molecules can be achieved by fusing these molecules with FKBP and FRB after the addition of rapamycin (Banaszynski et al., 2005; Inobe et al., 2015). Finally, numerous studies nowadays have proved that sulfated glycosaminoglycans like heparin, a poly-anionic cofactor, can be used as a tau multimerisation inducer in *in vitro* studies due to their ability to generate paired helical-like tau fibrils after interaction with non-phosphorylated tau (Fig.3.3A) (Falcon et al., 2019; Goedert et al., 1996; Lim et al., 2014; Ramachandran and Udgaonkar, 2011).



Created in BioRender.com 

Figure 3.1 Schematic representation of tau Proximity Ligation Assay (tau-PLA). Tau-PLA consists of four main steps: antigen recognition, ligation, amplification, and detection. During

antigen recognition, tau-PLA conjugates recognise and bind to tau antigens. For the production of tau-PLA conjugates, the tau5 antibody, a monoclonal pan-tau antibody was conjugated with PLA PLUS and tau-PLA MINUS probes. When two tau monomers interact one with the other, and the tau-PLA PLUS and tau-PLA MINUS probes are in proximity, ligation with a connector oligonucleotide is occurring, producing a circular DNA. This circular DNA serves as a template for the following step. 50% of the binding events can be captured by tau-PLA as the PLUS-PLUS and MINUS-MINUS events do not lead to productive ligation. During the amplification step, successful ligations work as primers for a rolling cycle amplification reaction. Finally, during the detection step, the final DNA product is visualised as a single dot after the addition of complementary labelled oligonucleotides with HRP or fluorescent tags. Created with BioRender.

3.2 Hypothesis and Aims

We hypothesise that tau-PLA can recognise tau-tau interactions but no monomers *in vitro*

Our aim for this chapter is to:

- To examine whether tau-PLA signal is co-localised with the GFP signal produced by BiFC complexes in transfected cells
- To test whether tau-PLA can detect the rapamycin-induced interactions between the tau molecules of the tau – FKBP – FRB system.
- To prove that the ability of tau-PLA to recognise tau multimers but no monomeric tau in the different protein interaction systems is not due to the tags fused to tau protein.

3.3 Tau-PLA detects tau-BiFC complexes

For the BiFC assay, HEK293 cells were co-transfected with two plasmid constructs, the pmGFP10C-tau (Addgene, 71433) and pmGFP11C-tau (Addgene, 71434), that encode tau protein fused with a fragment of GFP. Overexpression of plasmid constructs was used to induce the intracellular tau multimerisation (Fig 3.2A). Transfection of HEK293 cells with only the pmGFP10C-tau or pmGFP11C-tau plasmid led to the expression of only one GFP fragment, having as a consequence an impaired

fluorescence signal (Fig. 3.2B). However, overexpression of both plasmid constructs by co-transfecting the HEK293 cells induced tau-tau interactions, bringing the two complementary fragments in proximity, and therefore resulting in the production of fluorescence signal by the cells. No GFP signal was detected in the untransfected cells (Fig. 3.2B). Application of tau-PLA revealed that tau-PLA signal was detected in cells exhibiting BiFC fluorescence, while tau-PLA signal appeared to be absent in the untransfected cells as shown in Fig. 3.2C. This finding revealed that tau-PLA is characterised by high specificity for tau-tau interactions *in vitro*.

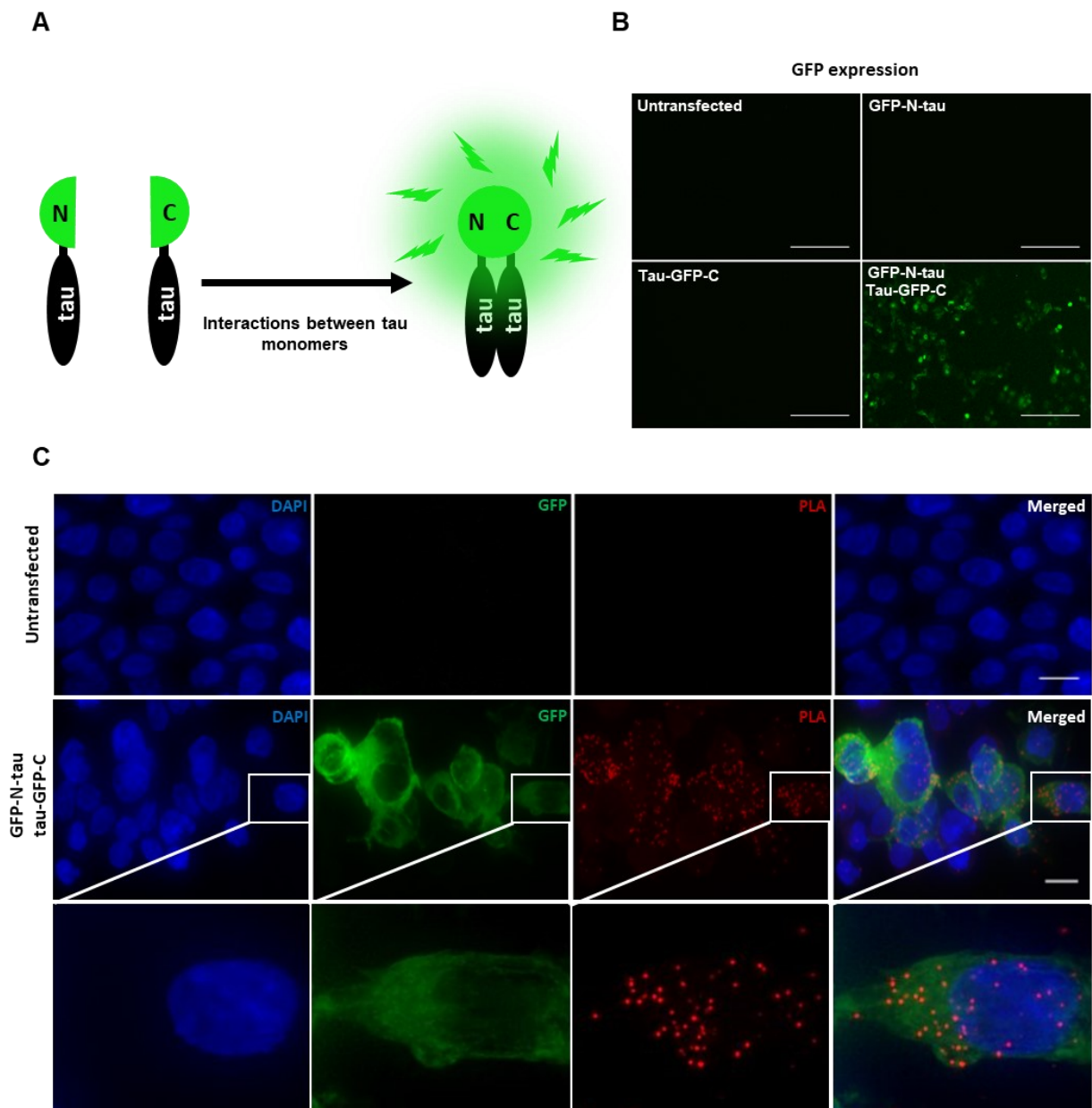


Figure 3.2 Tau-PLA detects tau-BiFC complexes. A) BiFC plasmid constructs encoding tau protein fused with a split of GFP reporter gene. Production of GFP activity

after structural complementation of the two GFP fragments when these complementary fragments are brought in proximity to each other after tau multimerisation. B) Fluorescent microscopy revealed that overexpression of both BiFC plasmid constructs in HEK293 cells induced intracellular tau multimerisation. C) GFP signal (green) in co-transfected HEK293 cells indicated tau-tau interactions. Tau-PLA signal (red) was detected in cells exhibiting BiFC fluorescence revealing tau-PLA specificity for tau-tau interactions *in vitro*. Cell nuclei were stained with DAPI (blue). Images captures are projections of z-stacks. Scale bar: 10 μm (Bengoa-Vergniory, N., Velentza-Almpani, E., et al., 2021).

3.4 Tau-PLA detects intracellular tau complexes but no monomeric

Another *in vitro* system used to test whether tau-PLA can detect tau multimers but no tau monomers was FKBP-FRB-rapamycin inducible system. This time, HEK293 cells were co-transfected with plasmid constructs expressing tau protein fused with FKBP or FRB, an inducible system where the presence of rapamycin leads to a conditional association between the two tau complexes (Fig. 3.3A). In contrast to the previous assay, where tau-tau interactions were induced with plasmid overexpression, this time the conditions of the experiment were modified in a way that low levels of plasmid expression were achieved to avoid spontaneous tau aggregation. In this case, the tau-PLA signal was negligible regardless of the existence of tau monomers (Fig. 3.3B). The addition of rapamycin to the system for 1 hour after plasmid co-transfection, induced tau multimerisation resulting in a significant increase in the dotted tau-PLA signal (Fig. 3.3B). This outcome indicated that tau-PLA detects tau self-interactions but not monomeric tau *in vitro*.

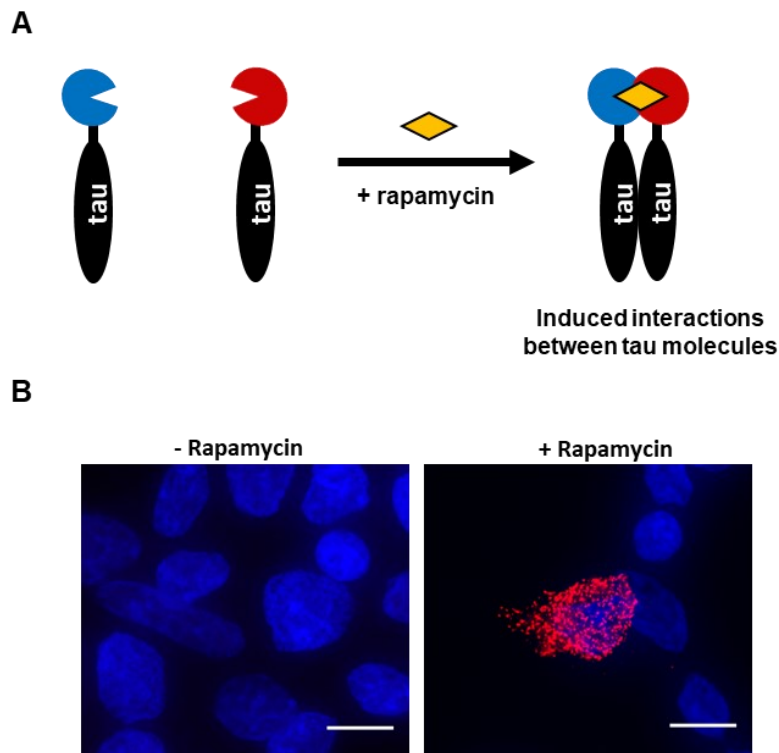


Figure 3.3 Tau-PLA can detect the rapamycin-induced interactions between the tau molecules of the tau-FKBP-FRB system. A) Tau-FKBP-FRB system is an inducible system where the presence of rapamycin leads to an association between two tau molecules fused with a split of the GFP reporter gene. B) HEK293 cells were co-transfected with plasmid constructs expressing tau protein fused with FKBP or FRB. Low levels of plasmid expression were achieved to avoid spontaneous tau aggregation. In the absence of rapamycin, no tau-PLA signal (red) was detected, while this signal was significantly increased after the addition of rapamycin indicating that tau-PLA has high specificity for tau-tau interactions but not monomers *in vitro*. Cell nuclei were stained with DAPI (blue). Images captured are projections of z-stacks. Scale bar: 10 μm (Bengoa-Vergniory, N., Velentza-Almpani, E., et al., 2021).

3.5 Tau-PLA detects tau multimerisation of recombinant tau but no monomers

In both previous assays, we used tau constructs fused with different tags. To exclude the possibility that the interactions between tau monomers are due to tags, untagged full-length human 4Rtau was shaken in the presence of heparin for 360 hours in total to

generate different tau aggregates (Fig. 3.4A). Before tau shaking, no tau aggregates were detected with TEM (Fig. 3.4B). Following 16 hours of protein shaking, globular tau aggregated structures were captured with TEM (Fig. 3.4B). After 360 hours of shaking a mixed population of tau aggregated species was detected, consisting of amorphous accumulations, globular structures, and filaments (Fig. 3.4B). Alpha-synuclein aggregates were also produced after protein shaking for 120 hours to be used as negative control and revealed that tau-PLA is highly specific for tau and not general protein accumulation. Application of tau-PLA and imaging of equal preparation amounts confirmed the specificity of tau-PLA for tau multimers but no tau monomers or alpha-synuclein fibrils. (Fig. 3.4B). Therefore, all these findings highlighted that tau-PLA detects tau-tau interactions with high specificity *in vitro*.

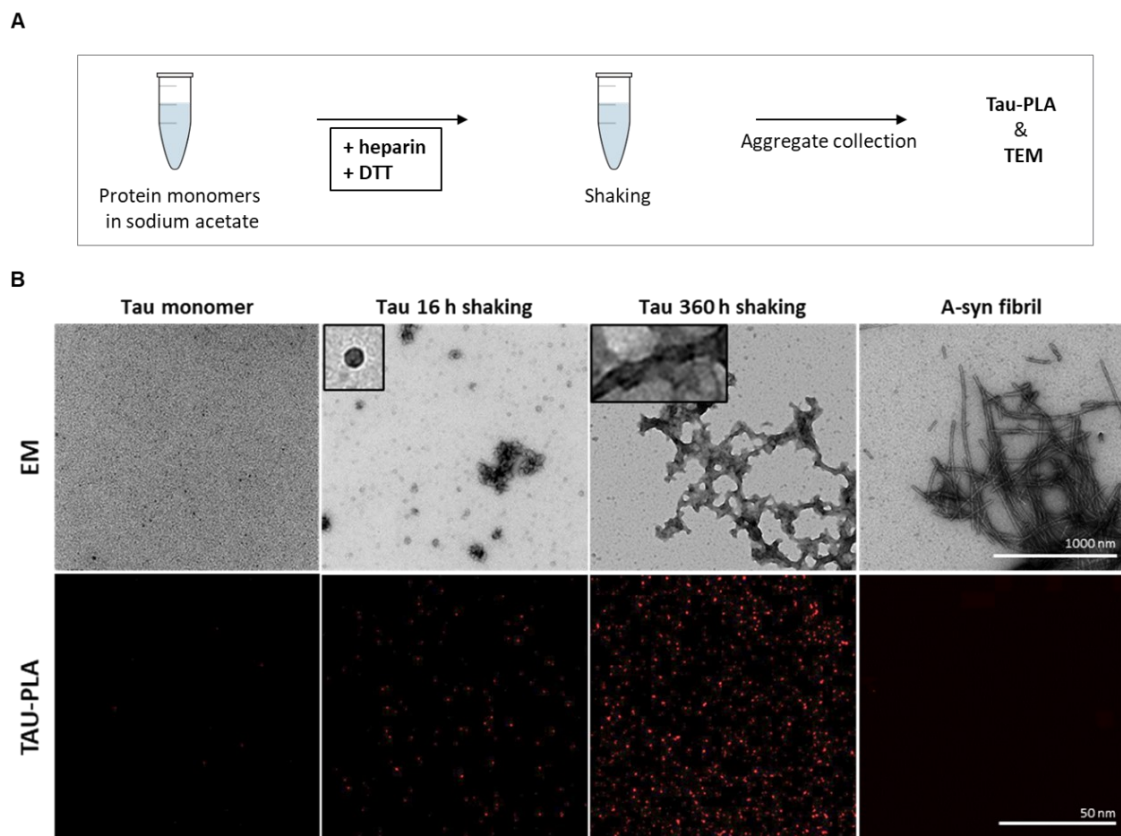


Figure 3.4 Tau-PLA detects tau multimerisation of recombinant tau but no monomers. A) Untagged full-length 4Rtau was shaken together with heparin to generate tau aggregates for 360 hours. The produced recombinant protein aggregates were subjected to TEM (Scale bar: 1000 nm) and tau-PLA (Scale bar: 50 nm). B) After 16 hours of protein shaking, globular tau aggregated structures were captured with TEM. After 360 hours of shaking a mixed population of multimeric tau complexes was detected. A-synuclein fibrils were formed after shaking for 120 hours, in the absence

of heparin, and were used as a negative control. Tau-PLA (red) recognized tau multimers but no monomers or alpha-synuclein fibrils.

3.6 Discussion

Tauopathies, with Alzheimer's disease as the most common neurodegenerative disorder, are caused by the abnormal folding and aggregation of tau molecules that seed themselves and spread throughout the brain in a prion-like manner causing, as they expand, irreversible neuronal cell death and progressive neurological symptoms (Goedert, Eisenberg, et al., 2017; Spillantini & Goedert, 2013). Accumulating evidence indicates that these oligomeric tau molecules, rather than NFT, are considered to be the toxic species, with seeding capacity, responsible for the prion-like spread of tau pathology, behaving as invisible killers, given that we lack a robust technique for their detection (Holmes et al., 2014; Kaufman et al., 2017; Lasagna-Reeves et al., 2012). Proximity ligation assay (PLA), first developed by Soderberg et al. in 2006, is a technique that allows the specific detection of endogenous protein-protein interactions directly in normal cells and tissues (Soderberg et al., 2006). Based on this assay, we have now developed a new technique, the tau proximity ligation assay (tau-PLA), which allows the *in situ* visualization of tau-tau interactions with high specificity and sensitivity without recognising tau monomers. For the build-up of the assay, a monoclonal epitope-blocking antibody was used, as suggested by previous studies, to ensure that each tau molecule is captured by one antibody, avoiding the binding of two or more antibodies on a single tau molecule, as this would result in a false positive PLA signal (Roberts et al., 2019, 2015). In line with Roberts et al. and according to manufacturers' instructions, an antibody in BSA- and azide-free buffer is essential to achieve the successful conjugation of the antibody with the PLA PLUS and MINUS Probes (Roberts et al., 2019, 2015). For all the aforementioned reasons, the tau5 antibody (ab80589, Abcam) was used. It has been reported that tau5 is a monoclonal pan-tau antibody that recognises the epitope consisting of the 218-225 amino acids of the non-phosphorylated full-length human tau, making it the best candidate for the detection of monomeric unphosphorylated tau and avoiding the limitations and restrictions that the other antibodies present for the development of a productive PLA signal (Porzig et al., 2007). To validate the ability of tau-PLA to detect tau

multimerisation but no monomers, several *in vitro* systems were used including Tau BiFC assay and Tau FKBP-FRB-rapamycin assay. Both assays revealed that tau-PLA recognised tau-tau interactions but no monomeric tau. In the first case, the tau-PLA signal was colocalised with BiCF fluorescence revealing the ability of tau-PLA to detect tau-tau interactions, while in the second one, the tau-PLA signal was significantly increased after the addition of rapamycin, highlighting the preference and specificity of the assay for tau-tau interactions but not tau monomers. The specificity and sensitivity of PLA for aggregated species but not monomeric have also been reported in previous studies investigating the interaction of homotypic proteins, supporting, therefore, the reliability and efficacy of the PLA approach (Mazzetti et al., 2020; Roberts et al., 2019, 2015; Sekiya et al., 2019). Although these assays are widely used for the investigation of protein multimerisation, the use of tags could be a limitation as evidence reports the possible interference of the molecular tags with the interactions of the proteins of interest, affecting the process of protein multimerisation and giving conflicting results (Kaniyappan et al., 2020; Lim et al., 2014). To exclude therefore the possibility that tau interactions are due to the tags, untagged full-length 4Rtau isoform was shaken together with heparin to generate different tau aggregates. Numerous studies support nowadays the use of heparin, a poly-anionic cofactor, as a tau multimerisation inducer for *in vitro* studies, due to its ability to generate paired helical-like tau fibrils after interaction with non-phosphorylated tau (Falcon et al., 2019; Goedert et al., 1996; Lim et al., 2014; Ramachandran and Udgaonkar, 2011). As expected, tau-PLA recognized tau multimers, capturing a range of tau aggregates, from small amorphous to filamentous species, but no monomeric tau. Overall, these findings highlight that tau-PLA detects self-interacting tau molecules *in vitro* and cell-based assays, but no tau monomers with high specificity and sensitivity, being a potentially useful tool for the investigation of endogenous disease-related tau-tau interactions in AD brain tissue

3.6.1 Limitations

Although much effort was applied to optimise the conditions of the assays, as mentioned previously, there was a limitation that needed to be addressed. Although BiFC assay and FKBP-FRB-rapamycin inducible system are well-established assays used for the investigation of protein-protein interactions, there is evidence supporting

that the tags fused with the proteins of interest could affect the interactions resulting in misleading outcomes (Kaniyappan et al., 2020; Lim et al., 2014). However, findings have reported that in contrast to other cell-based assays that use big protein tags like FRET, the aforementioned assays are characterised by the use of small-sized molecular tags that do not affect the procedure of protein aggregation (Kerppola, 2013; Lim et al., 2014; Roberts et al., 2015). In any case, to be completely confident with our findings and to exclude the possibility that tau interactions are due to the tags, we used a heparin-inducible tau aggregation system, where untagged tau molecules were used for the generation of the various multimeric tau species and assessment of the tau-PLA. Finally, to exclude the possibility of cross-reactivity of tau-PLA and detection of irrelevant protein molecules, other than tau, tau-PLA was also applied in solutions with alpha-synuclein soluble and aggregated species. As expected, no tau-PLA signal was observed indicating that our assay is tau-specific.

3.6.2 Conclusions

Here, we have developed a new assay, the tau-PLA, which allows the detection of tau-tau interactions with high specificity and sensitivity. Overall, our findings revealed that tau-PLA detects tau-BiFC complexes highlighting the high specificity of the assay for tau-tau interactions. In addition, the rapamycin inducible FRB-FKBP fusion protein system revealed that tau-PLA detects tau multimers, but no tau monomers. Finally, the detection of aggregated recombinant full-length unphosphorylated 4R tau molecules by tau-PLA proved that tau-PLA is able to detect a mixed population of aggregated tau species, including globular structures and filaments, mostly of short or intermediate length, but no tau monomers.

Chapter 4: *In situ* specificity of tau-PLA in animal and post-mortem human brain tissues

4.1 Introduction

MAPT KO mouse is an engineered mouse missing exon 1 in the *MAPT* gene after replacement with the neomycin-resistant cassette, resulting in the lack of tau protein expression. Although this mouse is developing normally and has reproductive ability, the lack of tau protein in the brain affects the growth and extension of axons and therefore neuronal maturation, leading to mild cognitive deficits (Dawson et al., 2001). This mouse is a very useful and widely used tool in research for the investigation of the physiological and pathological role of tau (Kraus et al., 2019; Metrick et al., 2020; Vargas-Caballero et al., 2017). P301S mutation, described in frontotemporal dementia and parkinsonism linked to chromosome 17 (FTDP-17), is detected in exon 10 of tau protein, affecting tau ability to induce microtubule assembly and promoting tau aggregation. This results, in an early onset of clinical symptoms and, has strong functional deficits in the individuals diagnosed with such mutation. (Allen et al., 2002; Goedert et al., 1996; Morris, 2001; Sperfeld et al., 1999). P301S mouse is a well-characterized mouse model of human tauopathy, expressing the shortest human four-repeat tau isoform (0N4R) with the P301S mutation on a wild-type mouse tau background featuring the main characteristics of the disease (Allen et al., 2002). This mouse model is widely used for the investigation of tauopathies like frontotemporal dementia and AD as it is characterised by the abnormal aggregation of hyperphosphorylated tau in NFT and NT resulting in the development of neuropathological effects, including neurodegeneration, synaptic loss, and neuroinflammation, as well as, the presence of severe behavioral deficits and clinical symptoms (Allen et al., 2002; Yoshiyama et al., 2007). In contrast to human cases, no hyperphosphorylated tau has been observed in glial cells (Bugiani, 1999). By the age of 5-6 months old, P301S transgenic mice have already developed severe motor symptoms with severe paraparesis, associated with the aggregation of hyperphosphorylated tau in the brainstem and spinal cord (Allen et al., 2002). By this age, this model is also characterised by the development of cognitive impairment. However, not until 6 months old is AT8 positive staining detected in the hippocampal

region of the mice (Holmes et al., 2014; Yoshiyama et al., 2007). AT8 is a phospho-tau antibody that recognises phosphorylation in both serine 202 and threonine 205 residues of the human tau protein and is considered to be the “Gold Standard marker” for tau-IHC and AD Braak staging (Alafuzoff et al., 2008; Braak et al., 2006). Neuronal cell death and neurodegeneration are far superior to the number of NFTs, suggesting that undetected tau aggregated complexes mediate toxicity (Ghag et al., 2018; Gómez-Isla et al., 1997). In recent studies on the P301S mouse model, researchers by using biomolecular assays detected increased tau seeding activity in brain regions that appeared to be unaffected based on conventional staining methods, with the onset of tau seeding activity being observed 4 months earlier to tau-immunoreactive staining (Holmes et al., 2014; Kaufman et al., 2016a). Therefore, *in situ* visualisation of these invisible early-type tau multimers in mouse models of human tauopathy could be a valuable tool for the investigation of tauopathies.

4.2 Hypothesis and Aims

We hypothesise that tau-PLA can detect tau multimers *in situ* with high specificity in animal and post-mortem human brain tissues.

Our aim for this chapter is to:

- To examine the *in situ* specificity of tau-PLA in the P301S transgenic mouse model of human tauopathy and *MAPT* KO mice.
- To prove that tau-PLA is a result of successful tau-PLA
- To prove that tau-PLA is an antibody-dependent assay

4.3 *In situ* specificity of tau-PLA in transgenic and *MAPT* KO mice

To determine whether tau-PLA can detect with high specificity self-interacting tau molecules *in situ*, brain tissue from *MAPT* KO mice that exhibit a lack of tau expression, P301S transgenic mice that represent an animal model of human tauopathy, and wild-type aged matched littermates C57BL/6, were investigated. Analysis with tau-PLA was performed in FFPE brain tissue sections from 2 months-old *MAPT* KO mice, alongside brain tissue from 6 months-old P301S transgenic mice and C57BL/6 age-matched

controls. Application of tau-PLA in the brain areas of the CA1 region of the hippocampus, striatum, and midbrain revealed that no positive tau-PLA signal was detected in *MAPT* KO, whereas the signal appeared to be quite strong in P301S mice. C57BL/6 mice showed a negligible load of tau-PLA (Fig. 4.1). Significant load of tau-PLA was also spotted in the area of striatal tracks of the P301S transgenic mice, where the axons of neuronal cells were detected (Fig. 4.1). AT8-IHC was also performed in animal tissue. In line with previous studies (Allen et al., 2002; Holmes et al., 2014), AT8 staining was prominent in the midbrain while the signal was missing from the areas of the hippocampus and striatum (Fig. 4.1). Therefore, the findings from AT8-IHC and tau-PLA revealed the presence of tau-tau interactions in anatomical brain regions of P301S mice that appeared to be unaffected and devoid of AT8 staining.

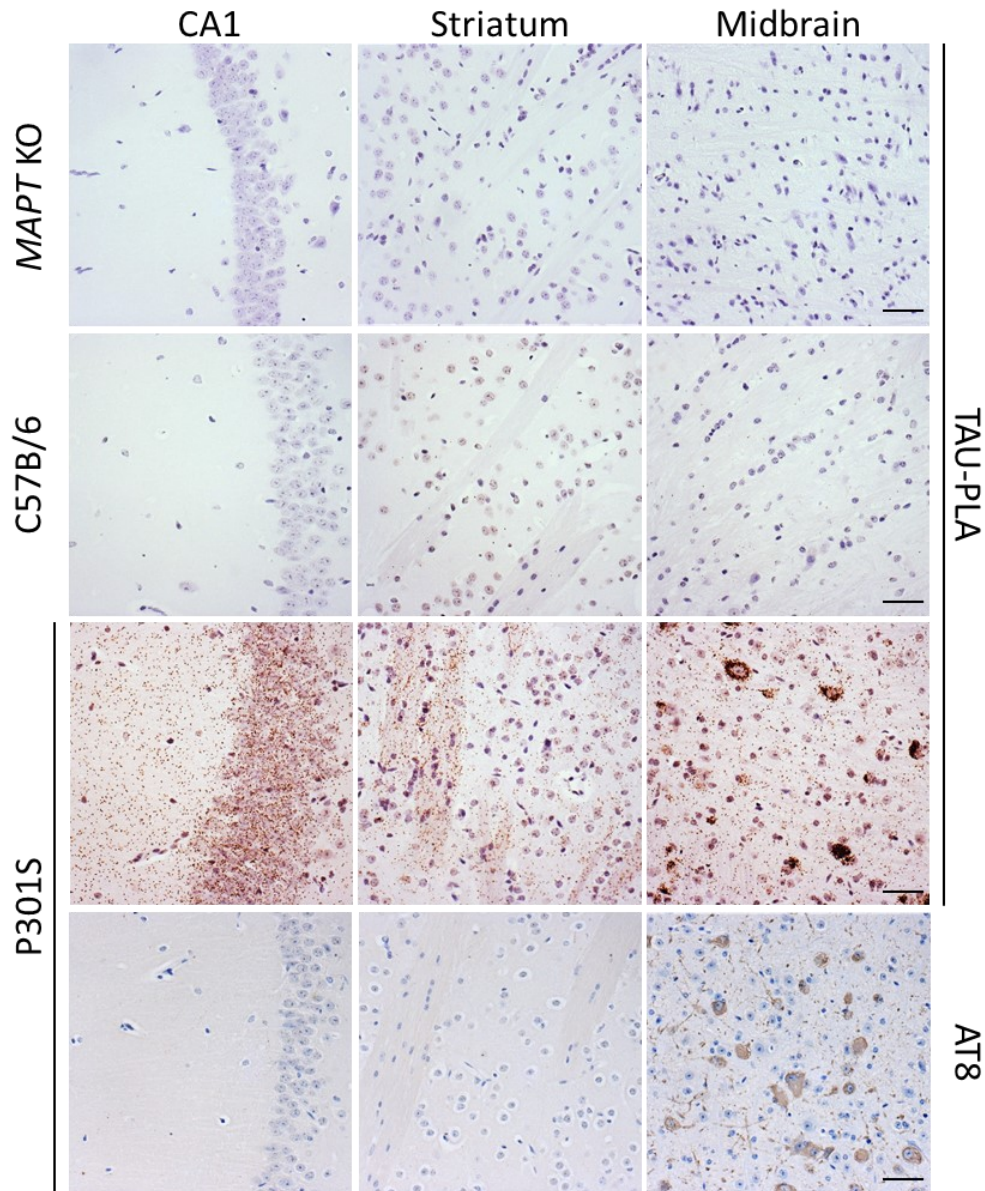


Figure 4.1 Demonstration of the *in situ* specificity of tau-PLA in mouse brain tissue. Brain regions of the hippocampus (CA1), striatum, and midbrain from 6 months old female and male *MAPT* KO (N=2) P301S tau (N=6), and C57BL/6 (N=6) mice stained for tau-PLA, AT8-IHC, and haematoxylin (nuclei). No positive tau-PLA signal was detected in *MAPT* K/O, whereas the signal appeared to be quite strong in P301S mice. C57BL/6 mice showed a negligible load of tau-PLA, demonstrating the *in situ* specificity of tau-PLA. Comparison with AT8-IHC revealed the presence of tau-tau interaction in anatomical brain regions of P301S mice that were devoid of AT8 staining. Scale bar 100 μ m.

Finally, brain tissue from 3, 6, and 9 months-old P301S mice was stained for Tau-PLA. The CA1 region of the hippocampus and midbrain presented a low tau-PLA signal in the 3 months-old mice, with the signal increasing to moderate levels in 6 months-old and high levels in 9 months-old mice. This result highlighted an age-dependent accumulation of tau-PLA signal in P301S animals (Fig. 4.2).

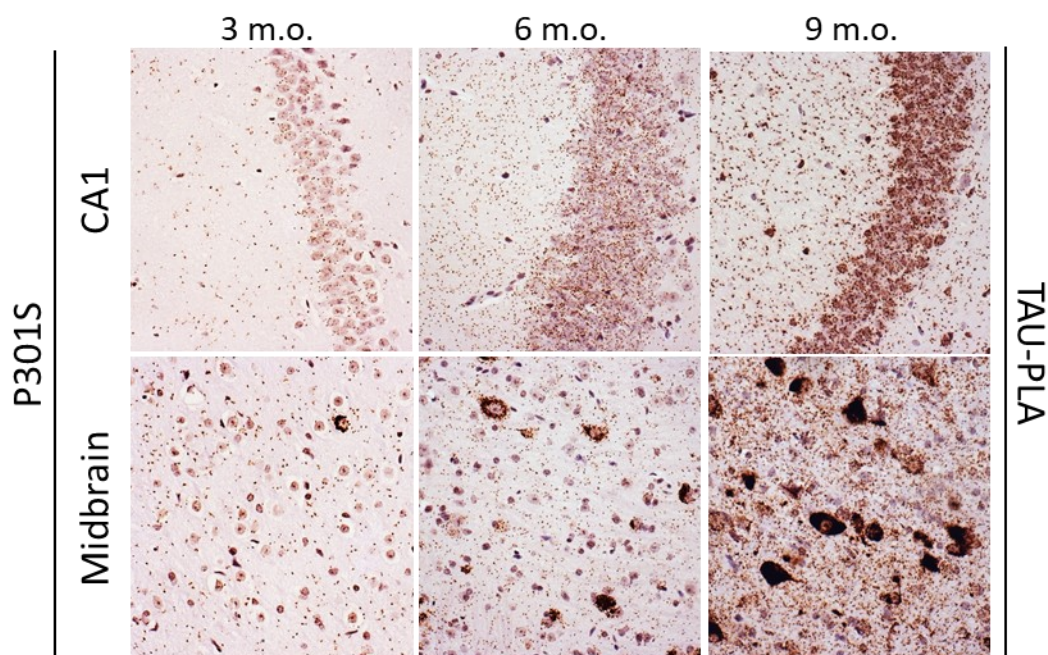


Figure 4.2 Age-dependent accumulation of tau-PLA signal in P301S transgenic mice. FFPE sections from the brain regions of the hippocampus (CA1) and midbrain from 3, 6, and 9 months-old P301S mice were stained for Tau-PLA and haematoxylin (nuclei). Tau-PLA analysis revealed that the tau-PLA signal accumulates with age in P301S animals. Scale bar 100 μ m.

Tau-PLA parameters were also accessed under fluorescent conditions to confirm that the signal obtained after the application of tau-PLA is due to successful tau-PLA staining and not due to autofluorescence caused by tissue processing and tissue preparation for the PLA. FFPE brain tissue sections from 2 months-old *MAPTKO* mice, together with 6 months-old P301S transgenic mice and C57BL/6 age-matched controls were analysed using fluorescent tau-PLA to examine the different parameters and conditions of the assay. Performance of fluorescent tau-PLA in the CA1 region of the

hippocampus revealed no positive tau-PLA signal in *MAPT* KO, while this signal appeared to be strong in P301S mice. Negligible levels of fluorescent tau-PLA were also observed in C57BL/6 mice (Fig. 4.3). These findings suggested that the tissue processing and preparation conditions for the tau-PLA assay didn't affect the outcome of the assay.

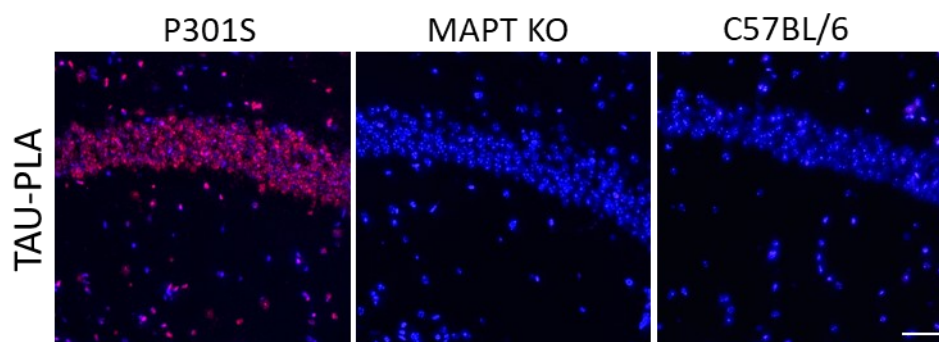


Figure 4.3 Fluorescent tau-PLA in mouse brain tissue. Brain regions of the CA1 region of hippocampus from 6 months old female and male *MAPT* KO (N=2) P301S tau (N=6), and C57BL/6 (N=6) mice stained for fluorescent tau-PLA (red) and DAPI (blue). No positive tau-PLA signal was detected in *MAPT* K/O, whereas the signal appeared to be quite strong in P301S mice. C57BL/6 mice showed a negligible load of tau-PLA. Cell nuclei were stained with DAPI. Scale bar 100 μ m.

4.4 *In situ* specificity of tau-PLA in human tissue

4.4.1 Tau-PLA is a result of productive tau-PLA

To further test whether the signal obtained was not a background staining and was a result of productive tau-PLA, the assay was also performed using no-ligase controls. In this case, FFPE brain tissue from the cortex of 6 months old P301S was stained with tau-PLA but this time the ligation step was removed. No staining was detected in the P301S tissue after excluding the ligation step (Fig. 4.4A). Similarly, FFPE post-mortem human sections from Braak stages 0 to VI were also examined in the same way. Once again, the removal of the ligase step from the tau-PLA protocol led to the absolute depletion of the PLA signal (Fig. 4.4B). Both findings suggested that the tau-PLA

signal was a result of productive tau-PLA and was dependent on the ligation of the two tau-PLA conjugates.

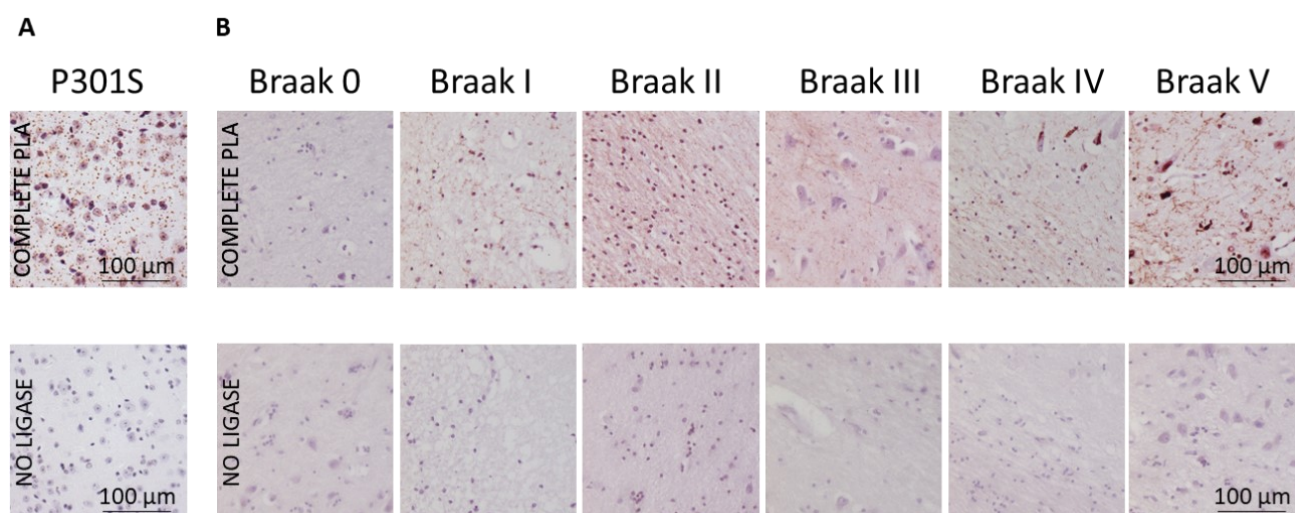


Figure 4.4 Tau-PLA is a result of productive tau-PLA. FFPE sections from the cortex of 6 months old P301S mice and post-mortem human brain tissue (Braak 0 – Braak VI) stained for tau-PLA in the presence (complete tau-PLA) or absence (no ligase control tau-PLA) of ligation step. Removal of the ligation step led to the absolute depletion of the PLA signal, highlighting that tau-PLA was a result of productive tau-PLA. Scale bar 100 μm.

4.4.2 Tau-PLA is an antibody-dependent assay

Next, to prove that tau-PLA is an antibody-dependent assay and to exclude the possibility of false positive results due to the PLA assay itself, PLA conjugates were produced after fusing PLUS and MINUS PLA probes with the 6xHisTag antibody. 6xHisTag is not physiologically produced in the human brain and therefore the 6xHisTag antibody wouldn't be able to detect any antigen to bind to. Indeed, no stain was detected after the performance of 6xHisTag-IHC to FFPE section from post-mortem human brain tissue (Fig. 4.5). No signal was also observed after 6xHisTag application to samples of Braak stage 0 and V (Fig. 4.5), indicating that tau-PLA is characterised by high *in situ* specificity for tau-tau interactions, without giving any non-specific background staining due to PLA elements and reagents themselves and is dependent on the antibody used for the assay.

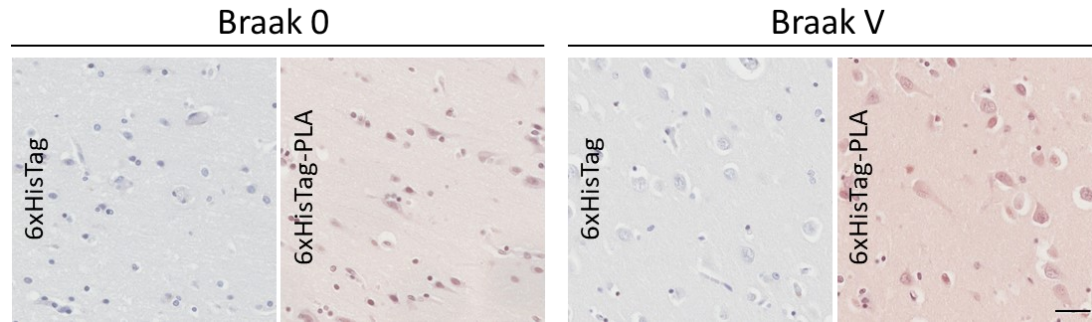


Figure 4.5 Application of 6xHisTag-PLA in post-mortem human brain tissue. FFPE sections from post-mortem human brain tissue from Braak stage 0 and V stained for 6xHisTag-IHC, 6xHisTag-PLA, and haematoxylin (nuclei). No positive signal was detected in both cases indicating that tau-PLA detected tau-tau interactions with high specificity *in situ* and is an antibody-dependent assay. Scale bar 50 μ m.

4.5 Discussion

The specificity of tau-PLA was further investigated using animal models. P301S is a mouse model of human tauopathy characterised by the expression of the shortest four-repeat (0N4R) human tau isoform with the P301S mutation. P301S mutation has been described in frontotemporal dementia and parkinsonism linked to chromosome 17 (FTDP-17) and appears to induce tau aggregation (Allen et al., 2002; Goedert et al., 1996; Morris, 2001). By the age of 6-month-old P301S mice develop neurological and clinical symptoms as a result of the accumulation of hyperphosphorylated large tau lesions in the brain and the spinal cord (Allen et al., 2002). Not until 6 months old AT8 positive tau lesions have been described in the brain of this mouse model (Allen et al., 2002; Holmes et al., 2014). Application of tau-PLA in the brain tissue of 6-month-old P301S mice revealed a strong tau-PLA signal in the regions of the hippocampus, striatum, and midbrain, highlighting that tau multimerisation has already started with tau self-aggregation being evident from the age of 3 months old. This finding is in line with previous cell-based studies where scientists detected high seeding activity of tau molecules extracted from the brain of P301S mice, with this spreading capacity being observed 4 months earlier than the appearance of the first immunoreactive species (Holmes et al., 2014; Kaufman et al., 2016b). Finally, analysis of mouse tissue revealed elevated levels of early-type tau multimers in the area of striatal tracks in the P301S

mice pointing out that axons might be the subcellular location where tau aggregation first takes place, an expected outcome given the fact that the main function of tau is microtubule stabilisation in the axonal projections (Kent et al., 2020; Wang and Mandelkow, 2016). To prove now that the signal obtained from tau-PLA is due to productive PLA capturing the actual tau pathology in this mouse model of human tauopathy, *MAPT KO* mice were analysed as well. These mice, due to *MAPT* gene modification, lack the expression of tau protein (Dawson et al., 2001). Indeed, the application of both AT8-IHC and tau-PLA in *MAPT KO* mice showed no positive staining signal. The lack of tau expression in these mice has been repeatedly described in previous studies using various staining, cell-based, and seed amplification assays (Dawson et al., 2001; Holmes et al., 2014; Kaufman et al., 2016b; Kraus et al., 2019; Saijo et al., 2017). This outcome highlights the specificity of our assay and the lack of non-specific background staining. Further analysis was also performed to prove that the PLA signal is a result of productive tau-PLA and that is an antibody-dependent assay. According to the PLA principles, every experimental step is crucial for the development of the PLA signal, and therefore depletion of one of these steps would result in the complete loss of this signal (Roberts et al., 2019; Söderberg et al., 2006). Indeed, the removal of the ligation step diminished the tau-PLA signal, highlighting that the staining obtained after the performance of the assay is a result of a productive PLA. Finally, the replacement of the tau5 antibody with an antibody detecting a protein molecule that is not normally expressed in the brain (anti-6x His tag), resulted in no PLA signal, supporting further the *in situ* specificity of the assay for the tau-tau interactions and indicating that tau-PLA is an antibody-dependent assay.

4.5.1 Limitations

After the development of tau-PLA, one of the major limitations was whether tau-PLA can detect tau-tau interactions *in situ* with high specificity. Previous studies have reported the low significance of the assay when used *in situ*, with the assay being prone to give false positive results under different conditions (Alsemarz et al., 2018). Moving to the *in situ* analysis, to exclude the possibility of non-specific binding and background staining of tau-PLA, we focused on the blocking and antigen retrieval steps by controlling the blocking time and the pH of the AR solution, achieving the best

experimental conditions to avoid having a non-specific background staining without losing at the same time the actual tau-PLA signal. Adjustment of antigen retrieval pH at 6.0 is crucial for the successful tau-PLA assay (Roberts et al., 2019). To further exclude the possibility of tau-PLA giving a false-positive signal, control experiments were also performed (6xHisTag-PLA).

4.5.2 Conclusions

Overall, the findings from the application of tau-PLA in animal and human brain tissue proved that tau-PLA is an antibody-dependent assay that detects tau-tau interactions, but no monomers, with high specificity. The assay is also characterised by high sensitivity and every experimental step (antigen recognition, ligation, amplification, and detection) should be performed carefully and according to the proposed protocols to achieve a productive PLA signal.

Chapter 5: tau-PLA recognised disease-related tau multimers

5.1 Introduction

Tau protein plays a dominant role in AD pathology as impaired tau has been proven to correlate better with AD symptoms. An increase in tau levels has been observed in AD cases (Hernández et al., 2018). Different potential mechanisms have been described to contribute to this increase including the rise in the *mapt* gene transcription (Morita and Sobue, 2009), the increase of tau protein translation (Keller, 2006), or/and the impaired tau degeneration (García-Escudero et al., 2017; Wang and Mandelkow, 2012). These events lead to tau accumulation promoting the formation of small or large tau aggregates, affecting the subcellular tau localisation, and disturbing the normal function and integrity of neuronal cells (Hernández et al., 2018; Silva and Haggarty, 2020; Spillantini and Goedert, 2013). However, not only do tau levels affect the progress of the disease, but tau structure is proven to play a pivotal role (Gerson et al., 2016; Nelson et al., 2002). Different forms of tau aggregates/strains spotted in the AD brain have been described as varying in morphology, size, structure, composition, location, and conformation (Gerson et al., 2016). These tau complexes could be soluble, including oligomers, protofibrils, and annular protofibrils (A. Lasagna-Reeves et al., 2011; Lasagna-Reeves et al., 2014, 2011b, 2011a) or insoluble tau fibrils consisting of PHFs and SFs (Grundke-Iqbal et al., 1986; Lee et al., 1991). Soluble tau oligomers rather than late-type tau fibrils are considered to be the main toxic species promoting neurotoxicity and inducing cell death, and therefore contributing to the disease progress (Berger et al., 2007; Ghag et al., 2018; Holmes et al., 2014; Kraus et al., 2019). The tau complexes are also characterised by anatomical and cellular specificity (Lasagna-Reeves et al., 2014). In addition, different tau forms may correlate with different stages of AD (Lasagna-Reeves et al., 2014). At a cellular level, tau oligomers could be observed both in neurons and glial cells (Gibbons et al., 2019). When in neurons, three distinguished but overlapping forms of tau maturities have been described with the help of different molecular markers (Baner et al., 1989). These tau forms are the pre-tangles, the mature NFTs, and the ghost tangles (Baner et al., 1991, 1989). Pre-tangle materials, NFTs, and NTs are intraneuronal aggregates, while ghost tangles are spotted in the extracellular environment as tau remnants after neuronal cell death (Moloney et al.,

2021). Neuritic plaque-associated tau is also detected in the extracellular space in interaction with amyloid-beta (Sarkar et al., 2020). Apart from neuronal cells, tau is also expressed by the glial cells, such as the astrocytes and oligodendrocytes but not microglia (Brunello et al., 2020; Narasimhan et al., 2017). Neuronal tau pathology can trigger glial tau pathology. Oligodendrocytes can present tau accumulations independently of tau multimerisation in neurons and can use their processes to achieve tau propagation (Narasimhan et al., 2020). However, this cannot happen in the case of astrocytes (Narasimhan 2020). Although microglial cells don't express tau protein, studies have revealed that tau aggregated species have been spotted inside the microglia of post-mortem AD brain tissue (Brunello et al., 2016). This is because the microglial cells are considered the primary phagocytes of the central nervous system (CNS), with a high phagocytotic activity that contribute to the clearance of tau deposits in the extracellular environment (Konishi et al., 2022). After phagocytosis, most of the tau is degraded, while the excess of tau could be released to the extracellular matrix through tau-containing exosomes, contributing to some extent to the propagation of tau (Juan R Perea 2018). This phagocytotic capacity has been lately described to astrocytic cells as well, which apart from the production of low levels of endogenous tau, they can also internalise tau molecules from the extracellular environment and ghost tangles (Fleeman and Proctor, 2021), preventing the spread of tau pathology (Fleeman and Proctor, 2021; Yamada, 2017). Although phagocytosis of tau from astrocytes could protect neurons from toxicity, the internalisation of pathological tau molecules could affect the function and integrity of astrocytes themselves (Kovacs, 2020). It is clear that tau aggregates could vary in many ways. Advanced and conservatory techniques have been used so far for the investigation of these tau structures and the process of tau multimerisation (Holmes et al., 2014; Kaufman et al., 2017; Kraus et al., 2019; Lasagna-Reeves et al., 2014; Metrick et al., 2020; Saijo et al., 2017). However, not all tau species could be spotted and visualised *in situ*. Direct visualisation of most tau pathology would help to better understand AD progress.

5.2 Hypothesis and Aims

We hypothesise that tau-PLA can detect endogenous disease-related tau multimers, labelling a range of tau structures in the AD brain.

Our aim for this chapter is to:

- To investigate the different tau staining patterns of tau-PLA in the AD human brain.
- To investigate the neurofibrillary tangle formation process using tau-PLA
- To examine the ability of tau-PLA to detect non-neuronal tau complexes in glial cells.

5.3 Tau-PLA labels a range of structures in the AD brain

Moving onto human tissue, we examined whether tau-PLA could recognise disease-related tau multimers, by analysing FFPE sections from post-mortem brain tissue of a Braak stage V patient. Sections from the grey and white matter of the hippocampal region and temporal isocortex were stained for tau-PLA and an analysis of the staining pattern was performed. Tau-PLA labelled a range of tau structures across the different areas of brain tissue. Apart from the late-type NFTs (Fig. 5.1i), the NTs (Fig. 5.1ii), and the neuritic plaque-associated tau (Fig. 5.1iii), tau-PLA also recognised a previously unreported diffuse tau pathology consisting of small-sized tau multimers (Fig. 5.1v). This form of tau pathology could be detected diffused in the neuropil, in the soma of the neuronal cells located in the cytoplasm or/and in the nuclei, and in the axonal projections of the neurons where tau-PLA dots could be spotted forming a rail track structure (Fig. 5.1iv, 5.1v, and 5.1vi). Both the white matter of the hippocampal region in the human tissue (Fig. 5.1vi), as well as, the area of striatal tracks in the P301S mice (Fig. 4.1) where the neuronal projections were located, presented a significant level load of tau pathology indicating that axons might be subcellular where tau multimerisation first takes place. This could be also supported by the fact that tau protein is physiologically characterised by an intra-axonal location, enhancing microtubule stability, regulating the number of protofilaments in microtubules and axonal growth, and contributing to synaptic plasticity (Pallas-Bazarra et al., 2016; Panda et al., 2003). This diffuse tau pathology could also be spotted in the cytoplasm of morphologically intact neuronal cells. Here, it is essential to highlight that these intra-neuronal accumulations of tau multimers were distinguished by the pre-tangle materials and lacked any AT8-IHC labelling (Fig. 5.1iv). Finally, apart from the neuronal staining, tau multimers in the perikarya of oligodendrocytes were also

observed (Fig. 5.1vi). Therefore, we can clearly say that tau-PLA could recognise a range of tau structures, from late-type large lesions to early-type, small-sized diffuse tau pathology.

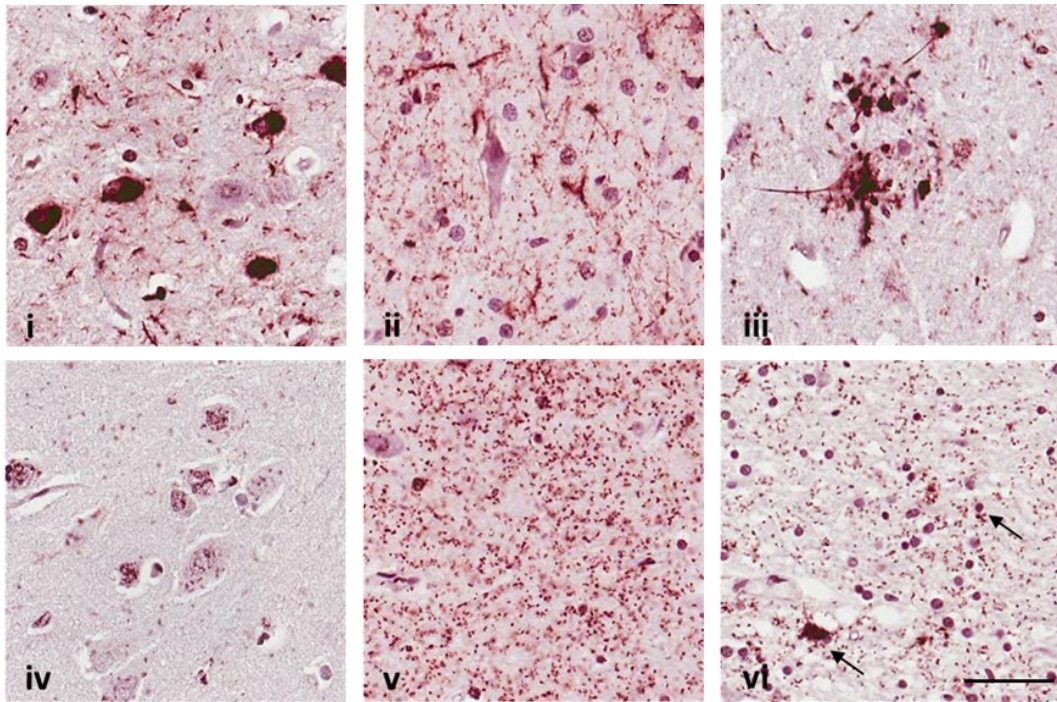


Figure 5.1 Tau-PLA recognises a range of tau structures, from large lesions to small-sized diffuse tau pathology. FFPE sections from post-mortem human brain tissue from a Braak stage V individual stained for tau-PLA. Tau-PLA detected (i) neurofibrillary tangles (CA1), (ii) neuropil threads (entorhinal cortex), (iii) neuritic plaque-associated tau (CA1), (iv) diffuse tau accumulations in morphologically intact neuronal cells lacking any AT8-IHC labelling and being distinguished from pre-tangles (CA1), (v) diffuse small-sized tau multimers (CA4), and (vi) the perikarya of a minority of oligodendrocytes (arrows, white matter). Scale bar 50 μ m.

5.4 NFT maturity characterised by Tau-PLA

Next, we examined the tau-PLA staining pattern on a cellular level focusing on NFT evolution. Once again, FFPE sections from post-mortem human brain tissue from a non-AD individual and a Braak stage V patient were stained for tau-PLA, and detailed analysis at a neuronal level was performed with the help of a brightfield microscope.

Application of tau-PLA revealed that tau-tau interactions start early in the formation of late-type intraneuronal tau aggregates even before the appearance of pre-tangle materials. During the early stages of NFTs maturity, tau-PLA labelled small-sized diffuse tau multimers forming small PLA dots that were detected in the cytoplasm of neuronal cells, as well as, in the extra-neuronal environment (Fig. 5.2 Diffuse). An increase in the levels of tau-tau interactions led to the formation of pre-tangle materials, also stained by tau-PLA (Fig. 5.2 Pretangle). As tau multimerisation continues, the tau-PLA positive pre-tangles could lead to the formation of mature NFTs. These large late-type tau lesions, consisting of paired helical tau filaments (PHFs) and straight tau filaments (SFs) including several PTMs (like hyperphosphorylation) and conformational changes, were also detected by tau-PLA (Fig. 5.2 Mature). The tau-PLA signal was eventually abolished at the level of ghost tangles where, after the neuronal cell death, the tau-tau interactions of tau fibrils appeared to be less dense and more distanced from each other preventing the development of the tau-PLA signal (Fig. 5.2 Ghost). No tau-PLA signal was detected in sections from the non-AD post-mortem human brain with the neurons appearing normal and physiologically intact (Fig 5.2 Normal). Therefore, we could clearly say that tau-PLA can characterise NFTs maturity revealing that tau-tau interactions start early in the formation of tangles, while this signal appeared to be absent at the level of lesions representing ghost tangles. The abolishment of the signal at the ghost tangle level also highlighted that to achieve a productive tau-PLA signal, the close proximity of tau molecules is essential.

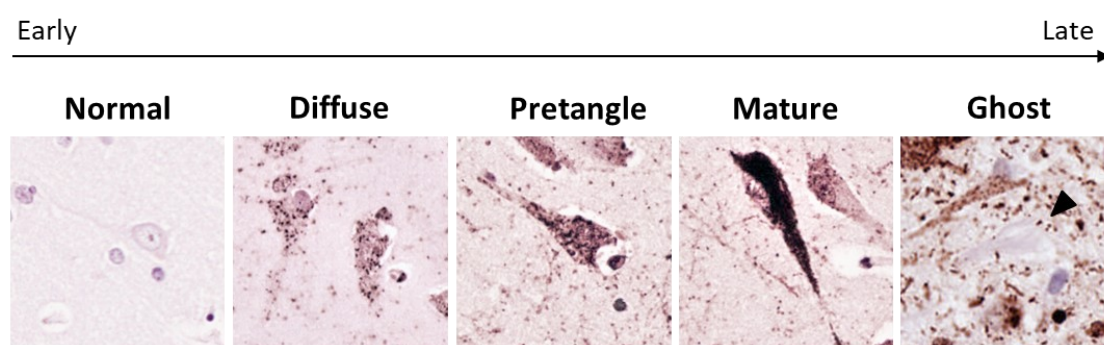


Figure 5.2 NFT maturity characterized by tau-PLA. FFPE sections from post-mortem human brain tissue from a non-AD case and a Braak stage V patient were stained for tau-PLA. Tau-PLA labelled small-sized diffuse tau multimers, pre-tangle

materials, mature NFTs, and but no ghost tangles. No tau-PLA signal was detected in neurons of the non-AD post-mortem human brain sections. Scale bar 50 μm .

5.5 Tau-PLA detects tau small complexes in glial cells

As mentioned previously, part of tau-PLA labelled pathology was also detected in the perikarya of oligodendrocytes (Fig. 5.1vi), structures that weren't visible with AT8-IHC as we will see in the following chapter. Based on this observation, we decide to examine if tau-tau interactions could be spotted in other glial cell types such as microglial cells and astrocytes. To answer this question, FFPE sections from post-mortem human brain tissue of Braak stage VI from the hippocampal region were examined by performing co-immunofluorescence for tau-PLA and Iba1 (a marker for microglial cells) or GFAP (a marker for astrocytes). The results of co-immunofluorescence revealed that apart from the neuronal location, a small portion of tau multimeric pathology could also be spotted in these brain immune cell types (Fig. 5.3). This finding suggested that diffuse small-sized tau structures could also be detected in glial cells.

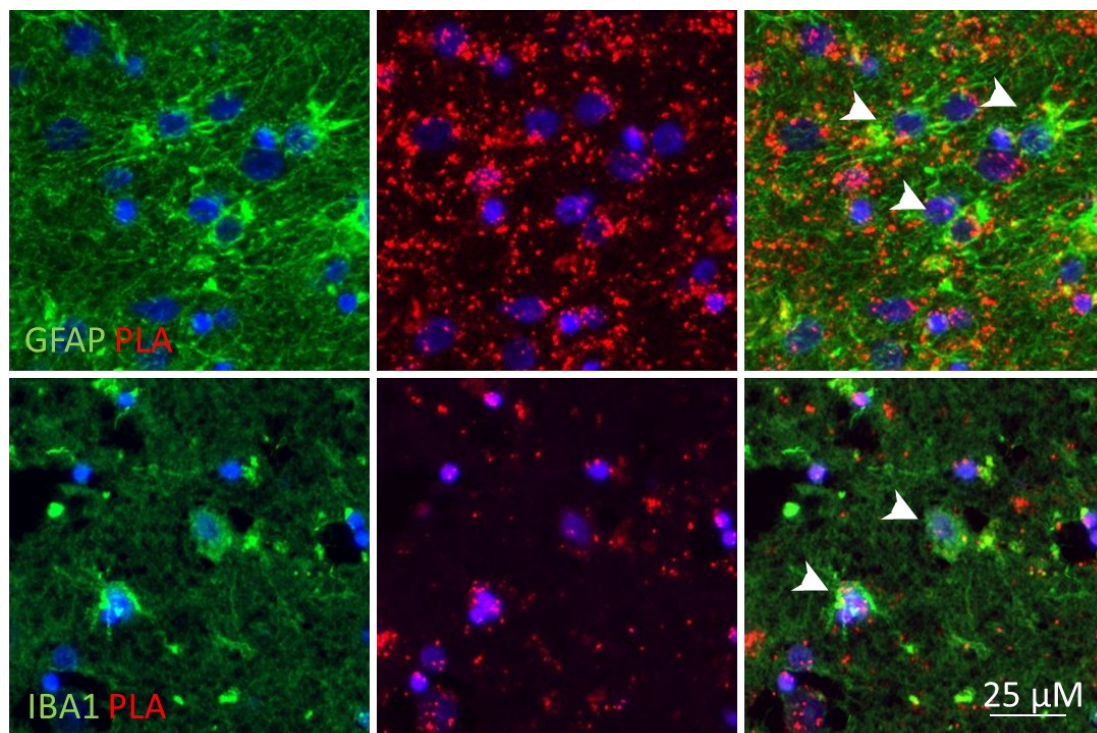


Figure 5.3 Tau-PLA detects tau small complexes in glial cells. FFPE sections from post-mortem human brain tissue of Braak stage VI from the hippocampal region after performing co-immunofluorescence for tau-PLA (red) and GFAP (green), an astrocytic marker or Iba1 (green), a microglial cell marker. Cell nuclei were stained with DAPI (blue). Arrows indicate astrocytes in the top panel and microglia in the bottom one. Scale bar 25 μm (Bengoa-Vergniory, N., Velentza-Almpani, E., et al., 2021).

5.6 Discussion

Application of tau-PLA in post-mortem human brain tissue revealed a range of tau pathology in the different Braak stages. Similar to other histopathological markers, tau-PLA detected insoluble fibrillar large tau lesions including NFTs, NTs, and neuritic plaque-associated tau (Alafuzoff et al., 2008; Goedert et al., 1996; Lasagna-Reeves et al., 2012). It also detected pretangle materials in the cytoplasm of intact neuronal cells. In contrast to previous studies that were unable to capture *in situ* an early-type tau pathology before the formation of pretangles (Alafuzoff et al., 2008; Braak et al., 2006; Weaver, 2000), tau-PLA detected a previously unreported tau pathology consisting of self-interacting monomeric tau. This early tau multimerisation has been described as well in previous studies investing the seeding capacity of tau and supporting that tau self-interaction is one of the earliest events occurring during the development of tau pathology before the generation of fibrillar hyperphosphorylated lesions (Holmes et al., 2014; Kaufman et al., 2016a; Kraus et al., 2019; Saijo et al., 2017). At a cellular level, tau-PLA labeled tau species were spotted both in neuronal and glial cells. When in neurons, tau-PLA captured a range of tau structures during NFTs maturity, from diffuse pathology to mature NFTs, with the tau-PLA signal being abolished at the level of ghost-tangles. The loss of the PLA signal in the ghost tangles could have three possible explanations. One of them supports that after the cell death and lysis of the cell membrane, the tau molecules are not densely packed, and therefore the PLA probes are not in close proximity to allow the production of PLA signal. The second and more possible explanation focuses on the epitope recognised by the tau5 antibody, the antibody used for the build-up of the assay. Tau5 antibody recognises an epitope located between the amino acids 218-225 of the full-length human tau, which has been reported to be lost in the ghost tangles preventing, therefore, their detection by tau-PLA

(Fitzpatrick et al., 2017; Porzig et al., 2007). Finally, the last explanation is based on the fact that the binding capacity of tau5 can be affected by the nearby phosphorylated sites (Nakano et al., 2004; Porzig et al., 2007). Therefore, reduced accessibility of the tau5 antibody to its epitope due to the increased levels of tau modification at this late stage of NFT maturity could be a possible explanation (Furcila et al., 2019). Apart from the neuronal staining, part of tau-PLA labelled pathology was also detected in the oligodendrocytes, astrocytes, and microglia suggesting a potential contribution of these cell types in tau propagation and spread through the brain. On the one hand, oligodendrocytes and astrocytes has been reported to contribute to the progress of tau pathology through the expression of tau molecules and the formation of tau aggregates (Brunello et al., 2020; Narasimhan et al., 2020, 2017). On the other hand, although the expression of tau has not been described in the microglial cells, these cells contribute actively to tau propagation through the mechanisms of phagocytosis, pinocytosis, and endocytosis with the release and reuptake of tau to and from the extracellular space (Brunello et al., 2016; Konishi et al., 2022). Here, we need to state that although tau-PLA provides significant information about the architectural morphology, aggregation level, maturity, and location of tau multimers, further experimental approaches are essential to define the properties and spreading behaviour of these molecules.

5.6.1 Limitations

Both the experimental work and analysis of the study contained limitations that needed to be addressed. Regarding the experimental procedure, the reduced availability and the high cost of the PLA kits were two major restrictions that delayed the analysis of the available tissue. For tau-PLA, a good quality tissue is essential as this assay is characterised by high sensitivity. Over-fixation has been reported to affect the immunochemical reactivity, however, the impact of the long fixation on the antigen recognition from the most widely used antibodies appeared to be significantly low (Webster et al., 2009). In addition, for the performance of co-immunofluorescence for tau-PLA and other histological markers (e.g. tau-PLA and GFAP or IBA1), we need to make sure that the antibodies used for the detection of the other markers do not affect or are not affected by tau-PLA. Therefore, optimisation of the protocol is essential. Regarding the tissue analysis, although tau-PLA revealed a previously unreported

early-type tau pathology, allowing the direct visualisation of this pathology *in situ*, it cannot provide direct details about the pathophysiological role of these molecules or the mechanisms that lead to the production of these species. However, the structure, maturity, and cellular and anatomical location can provide meaningful outcomes about their behaviour and function.

5.6.2 Conclusions

To sum up, tau-PLA detected *in situ* a range of tau structures, from large fibrillar tau lesions to a previously unreported early-type, small-sized, diffuse tau pathology. Characterisation of NFT maturity at a cellular level with tau-PLA revealed that the assay can capture the diffused tau pathology, pre-tangle materials, and mature NFTs, with the tau-PLA signal being abolished in the ghost tangles. Co-immunofluorescence for tau-PLA and glial cell markers revealed the existence of small tau molecules in these cell types.

Chapter 6: Extensive and early tau multimerisation revealed by tau-PLA in the development of tau pathology

6.1 Introduction

The abnormal aggregation and misfolding of tau in neurons in the central nervous system (CNS) is the main pathological hallmark of tauopathies, with AD the most common neurodegenerative disorder (Goedert et al., 2017; Lee et al., 2001). The intracellular aggregation of hyperphosphorylated tau in the NFTs, NTs, and neuritic plaque-associated tau, together with the extracellular amyloid beta plaques and the enhanced levels of neuroinflammation are the fundamental neuropathological characteristics of the AD (Braak et al., 2006; Selkoe and Hardy, 2016; Spillantini and Goedert, 2013). The progression of tau pathology in the AD brain is occurring gradually in synaptically connected brain regions and is apparent long before the appearance of the clinical symptoms (Alafuzoff et al., 2008; Braak et al., 2006; H. Braak and Braak, 1997a; Gauthier-Kemper et al., 2011). AD staging was first based on the modified silver staining proposed by Gallyas (Gallyas, 1971). According to Gallyas, silver staining is a method with high sensitivity in the detection of argyrophilic structures like NFTs and was used by Braak in this first proposed staging system (E. Braak and Braak, 1997; H. Braak and Braak, 1997a, 1997b, 1991; Heiko Braak and Braak, 1991). Due to its limitations, in 2006 Braak and his colleagues developed a new method for the staging of AD based on the immunoreaction using the AT8 antibody, for the detection of both soluble and insoluble hyperphosphorylated tau protein (Braak et al., 2006). According to this system, the intraneuronal hyperphosphorylated tau propagates from transentorhinal (Braak stage I) to entorhinal (Braak stage II) cortex to fusiform and lingual gyri (Braak stage III) and neocortical association areas (Braak stage IV). In the latest stages of the disease, the pathology expands to frontal, parietal, and occipital directions (Braak stage V) reaching the striate area of OC (Braak stage VI) (Braak et al., 2006). Based on this staging system and focusing on the density of NTs in the different brain regions, Alafuzoff and colleagues developed later on a modified Braak staging method to overcome the restrictions and limitations of the previously proposed system (Alafuzoff et al., 2008). This modified Braak staging system is based on AT8-immunoreactive NTs and the stages were defined as follows. Braak stage I is

characterised by at least low levels of AT8-immunopositive NTs in the region of transentorhinal. Involvement of the posterior hippocampal region is observed in Braak stage II with at least moderate levels of AT8-immunopositive NTs being spotted in the superficial layers of EC. In Braak stage III, pathology is expanded to the deeper layers of EC in the posterior hippocampus continuing to the fusiform gyrus and neocortex, while the severe involvement of the superficial and deeper layers of the middle TC is spotted in Braak stage IV. In Braak stages V and VI, the apparent involvement of the parastriate and striate areas of OC is observed, respectively (Alafuzoff et al., 2008). Although this staging system is well-established and widely used for the definition and characterisation of the different stages of the tau pathology, more sensitive recently developed techniques like the Fluorescence Resonance Energy Transfer (FRET) or the Real-time quaking-induced conversion (RT-QuIC) managed to capture the seeding activity of tau in brain regions free of hyperphosphorylated tau depositions (Holmes et al., 2014; Kaufman et al., 2017; Kraus et al., 2019; Metrick et al., 2020). This indicates that more sensitive techniques for the *in situ* visualisation of tau are needed, being able to detect the different tau structures in an early stage before the formation of late-type large tau lesions. Different antibodies have been developed today that can detect early-type tau pathology including oligomeric tau species exhibiting PTMs that occur early during neurofibrillary tangle maturity. Such antibodies are the phosphor-tau antibodies AT180, PHF-1, T217, and S422 and the conformational antibodies MC1 and Alz50 (Ercan-Herbst et al., 2019; Holmes et al., 2014; Li et al., 2016; Smolek et al., 2016; Weaver, 2000). However, the detection of tau-tau interactions, even before exhibiting any PTMs, would open a window for the investigation of the early-type multimeric tau pathology, the events that lead to the formation of the late-type large tau lesions, the driving mechanisms of the disease progression, and the tau propagation from cell to cell and from the one anatomical region to the other. Due to its *in situ* sensitivity and specificity, tau-PLA could be a potential tool and approach to investigate the distribution of tau pathology across the different stages of AD.

6.2 Hypothesis and Aims

We hypothesise that tau self-interaction is one of the earliest detectable molecular events occurring during the development of tau pathology, preceding tau hyperphosphorylation and misfolding, in the AD brain.

Our aim for this chapter is to:

- Determine the Braak stage of post-mortem human brain tissue obtained.
- Investigate the spatiotemporal distribution of tau-tau interactions in the AD post-mortem brain.
- Compare tau-PLA with other tau histopathological markers
- Investigate tau-PLA detection power in comparison to other tau antibodies during NFT maturity

6.3 Braak Staging of post-mortem human brain tissue according to BrainNet Europe diagnostic protocol

After defining the range of tau structures labelled by tau-PLA, we focused on determining the temporospatial distribution of tau-tau interactions in the post-mortem human brain across the different Braak stages as defined by the BrainNet Europe diagnostic protocol. To achieve this, we first had to determine the Braak stage of our cases according to the modified Braak staging system (Braak et al., 2006) based on AT8-immunoreactive NTs across the brain tissue (Alafuzoff et al., 2008). FFPE sections from the post-mortem brain tissue of 67 cases from the regions of the hippocampus, TC, and OC were analysed with AT8-IHC, and the Braak stage of each case was determined. Cases with other tauopathies other than AD (e.g., ARTAG, PART, etc) were excluded from the analysis (see Methods 2.2.3.2 Exclusion Criteria). Braak 0 cases were AT8-IHC negative, while at Braak stage I low levels of immunopositive NTs started being visible in the transentorhinal cortex of the hippocampus (Fig 6.1). Moderate levels of AT8-IHC labelled NTs were visible in the outer layers of EC in Braak stage II (Fig 6.1). Spread of the NTs from the hippocampus to the region of the temporal isocortex was observed in the Braak III cases, while severe involvement of the middle temporal cortex with a high load of positive-stained NTs

was detected in the Braak IV stage (Fig 6.1). The peristriate area of the OC was severely affected with at least moderate levels of positive AT8-IHC NTs at Braak stage V, followed by the severe involvement of the striate area of the OC at Braak stage VI (Fig 6.1). Positive AT8-IHC tangles and pre-tangle materials could be spotted in various areas of brain tissue, however, their presence didn't contribute to the staging process as according to BrainNet Europe diagnostic protocol NTs are the ones playing the decisive role in defining the stages of each case.

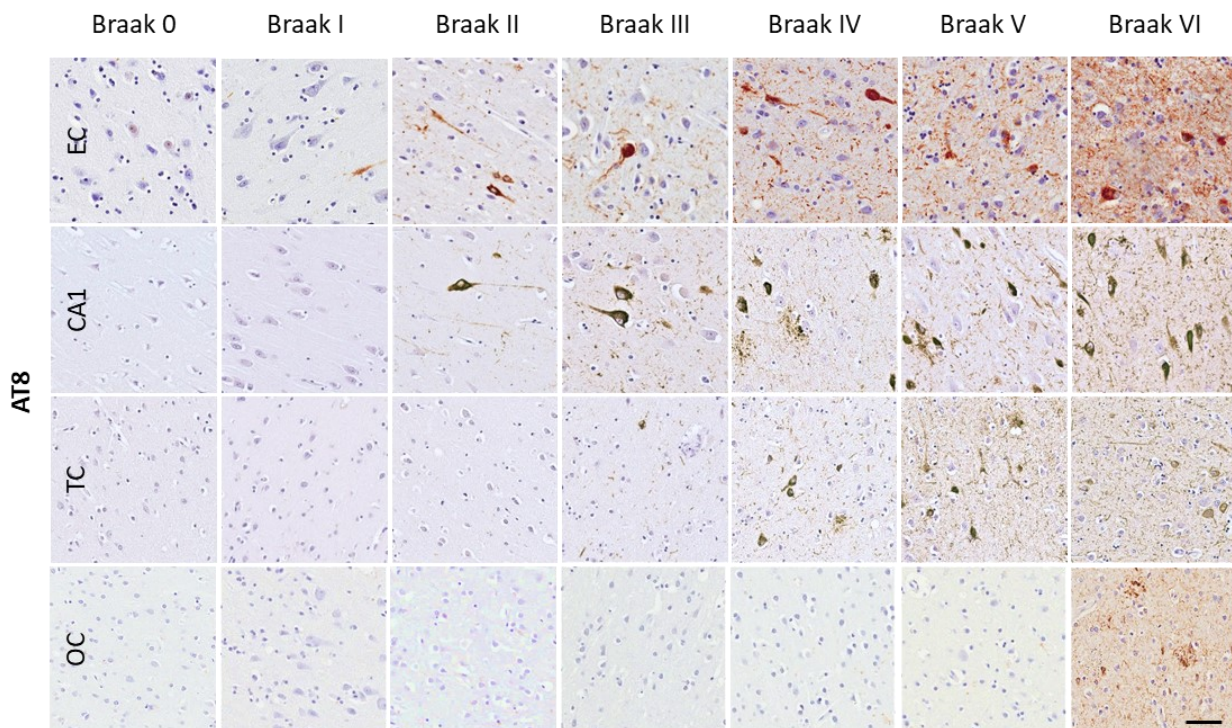


Figure 6.1 Tau aggregates labelled with AT8-IHC across the different Braak Stages as defined by BrainNet Europe diagnostic protocol. FFPE sections from post-mortem human brain tissue from the brain regions of the hippocampus, TC, and OC were stained for AT8-IHC. The Braak stage of each case was determined according to the modified Braak staging system (Braak et al., 2006) based on AT8-immunoreactive NTs across the brain tissue (Alafuzoff et al., 2008). Braak 0 cases were negative for AT8-IHC. Involvement of transentorhinal and EC was observed in Braak I and Braak II cases, respectively. AT8-IHC positive NTs were detected at low levels in the temporal isocortex in Braak III cases, while TC was severely affected in Braak IV cases. Parastriate and striate areas of OC were involved in Braak stages V and VI respectively. Scale bar 50 μ m. *EC Entorhinal cortex, TC Temporal cortex, OC Occipital cortex*

6.4 Spatiotemporal distribution of tau-PLA labelled structures across Braak Stages

We then moved on to determining the spatiotemporal distribution of tau-tau interactions across the different Braak stages. FFPE post-mortem tissue from Braak stage 0 to VI from the brain regions of the hippocampus, TC, and OC were labelled with tau-PLA and the staining pattern was analysed. Results from tau-PLA revealed that almost negligible levels of tau-PLA dots were detected in non-AD cases (Braak 0). (Fig 6.2 and 6.4). As proved previously with the *in vitro* assays, tau5 is an epitope-blocking antibody and therefore tau-PLA cannot detect monomeric tau species (Chapter 3). The fact that tau-PLA detected almost negligible levels of tau multimers in Braak 0 indicated that our assay is characterised by high specificity for self-interacting tau and does not detect endogenous tau monomers. It also suggested that tau multimerisation is not an event that occurs physiologically in the brain.

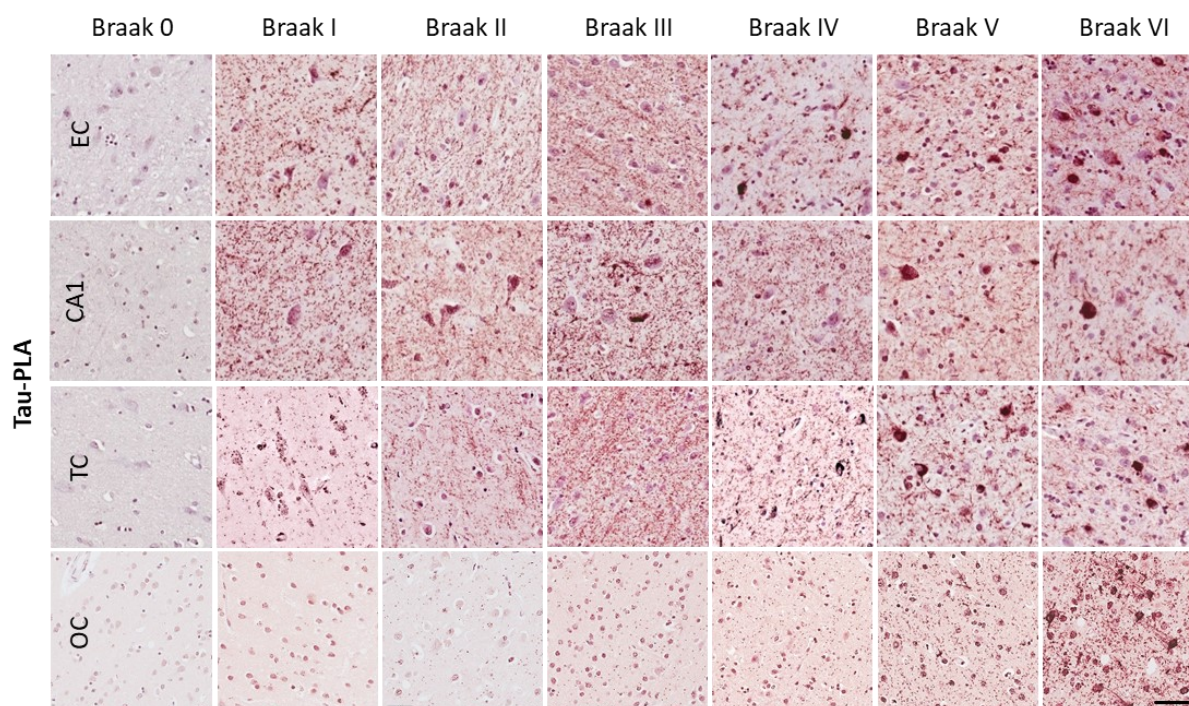


Figure 6.2 Tau-tau interactions labelled with tau-PLA across the different Braak Stages as defined by BrainNet Europe diagnostic protocol. FFPE sections from post-mortem human brain tissue from the brain regions of the hippocampus, TC, and OC were stained for tau-PLA. Almost negligible levels of tau-PLA were detected in Braak 0 cases. Involvement of hippocampus (EC and CA1) and TC was observed from Braak I to Braak VI. OC was involved in Braak stage III with the tau pathology increasing in

the following stages. Both diffuse small-sized tau multimers and large neurofibrillary-type lesions were detected. Scale bar 50 μ m. *EC Entorhinal cortex, TC Temporal cortex, OC Occipital cortex*

At this point, however, it is essential to highlight that although the load of tau-PLA dots in the majority of the Braak 0 cases was nil (Fig 6.2 and 6.4), individuals within the population in this group presented heterogeneity in the load of tau-PLA dots, with a minority of cases having moderate or even high levels of tau-PLA signal in the area of the hippocampus (Fig 6.3).

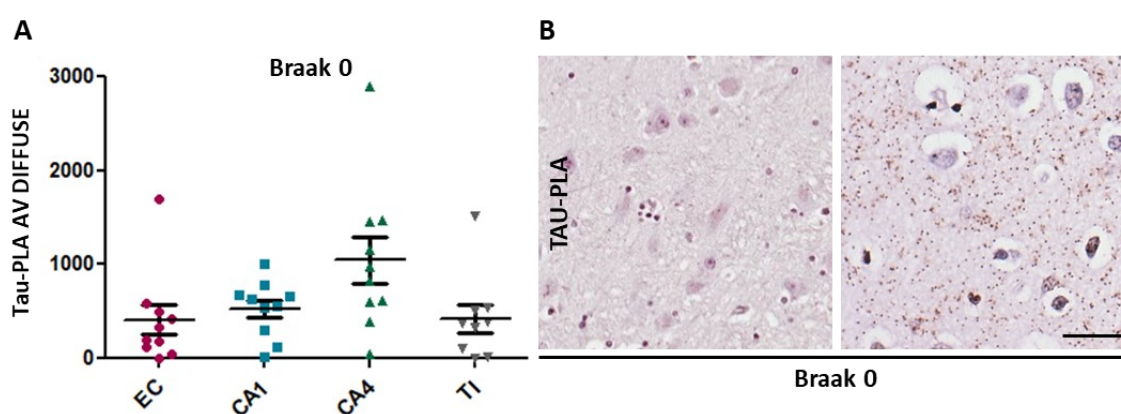
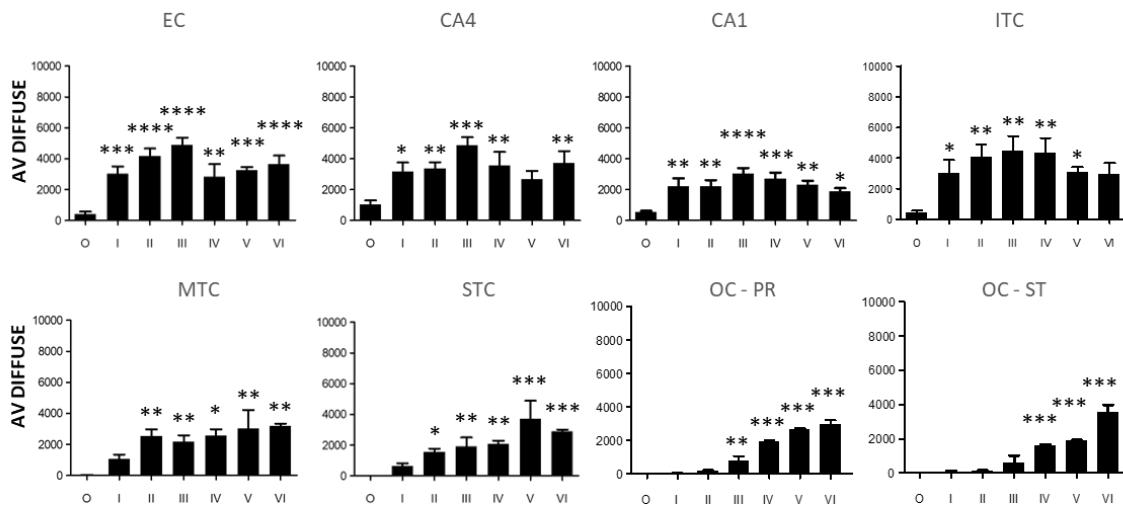


Figure 6.3 Tau-PLA revealed that cases in Braak 0 group presented heterogeneity as far as it concerns the levels of tau-PLA load in brain regions that are affected quite early in the development of pathology. A) Quantification of tau-PLA stained small-sized diffuse multimers in the different areas of the hippocampus, indicating the distribution of the population in the Braak 0 group. *AV*; average. B) Representative images of EC labelled with tau-PLA displaying the heterogeneity that characterises the Braak 0 group. Scale bar 50 μ m. *EC Entorhinal cortex, TI Temporal isocortex*

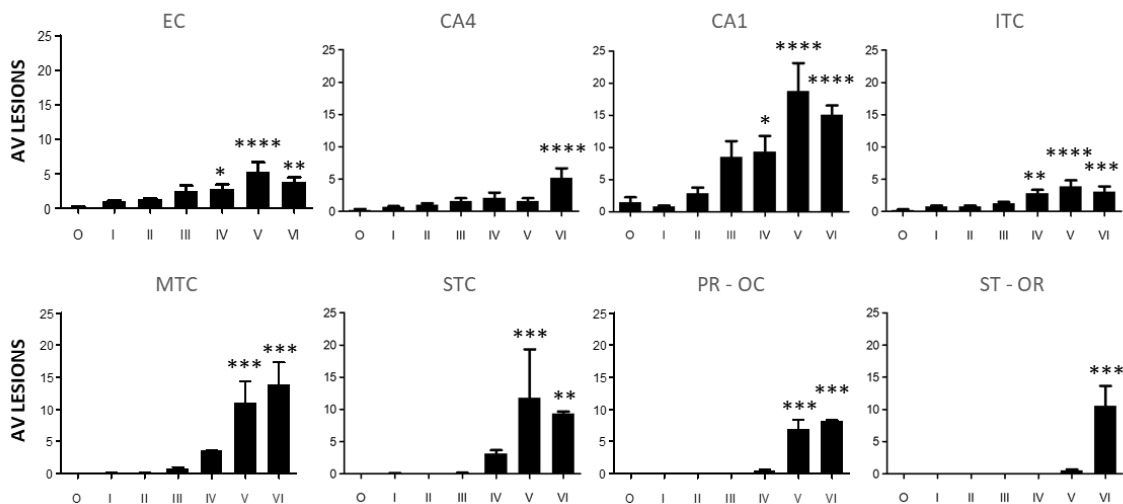
As detailed above, the staining pattern of tau-PLA can be mostly divided into two main groups: the diffuse small-sized tau pathology and the large tau lesions (Chapter 5.3). Moving now to Braak stage I, as far as it concerns the diffuse dotted pathology, high levels of the tau-PLA signal were detected in the EC without mostly being accompanied by AT8-IHC positive staining (Fig 6.2 and 6.4). This signal was significantly increased

through the Braak stages up to Braak stage III which displayed the highest levels of diffused pathology in EC (Fig 6.2 and 6.4A). TC was mostly affected by tau multimerisation in Braak stages III and IV, while OC presented the higher tau-PLA signal at Braak stages VI to VI, with the striate area being significantly involved at Braak stage IV (Fig 6.2 and 6.4A). The fact that in early Braak stages, tau-PLA diffuse pathology was present in anatomical brain regions devoid of AT8-IHC suggested that tau-tau interactions are one of the first events occurring during the progress of tau pathology in the AD brain. About the large perikarya neurofibrillary-type lesions, tau-PLA recognised the lesions following the same pattern (number and spatial distribution) as the AT8 antibody (Fig 6.4B and C).

A. Tau-PLA – Diffuse pathology



B. Tau-PLA – Lesions



C. AT8 – Lesions

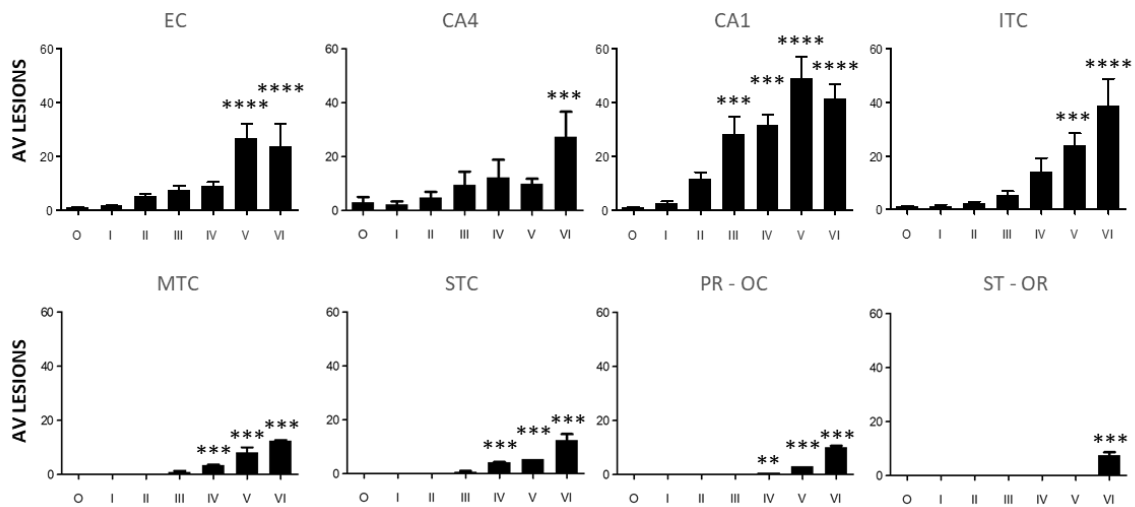


Figure 6.4 Quantification of tau-PLA labelled diffuse pathology and tau-PLA and AT8-IHC labelled large perikaryal neurofibrillary-type lesions in hippocampal regions, TC, and OC. Automated quantification of A) tau-PLA diffuse pathology, B) tau-PLA labelled large lesions, and C) AT8-IHC labelled large lesions across the different brain areas. All groups were compared to the control (Braak 0) through a ONE-WAY ANOVA (Dunnet). N = 11/12/12/9/7/8/8. * $p < 0.05$, ** $p < 0.01$, *** $p < 0.001$, **** $p < 0.0001$. EC Entorhinal cortex, ITC Inferior temporal cortex, MTC Middle temporal cortex, STC Superior temporal cortex, OC Occipital cortex, PR Parastriate area, ST Striate area, AV average

At this point, we need to point out that AT8-IHC seemed to be more sensitive to tau-PLA in the detection of large lesions (Fig 6.4B and C). To explain this event, an analysis of the cases with tau5 antibody was performed. FFPE sections from the different regions of the hippocampus were examined by performing tau5-IHC. Results showed that tau5-IHC and tau-PLA had an almost identical number of large lesions, indicating that the differences observed in tau-PLA and AT8-IHC labelled lesions were due to the superiority of AT8 to tau5 for large lesions (Fig 6.4 ad 6.5). This evidence was in line with previous studies which suggest that the binding capacity of tau5 antibody could be affected by the nearby post-translationally modified sites (Nakano et al., 2004; Porzig et al., 2007).

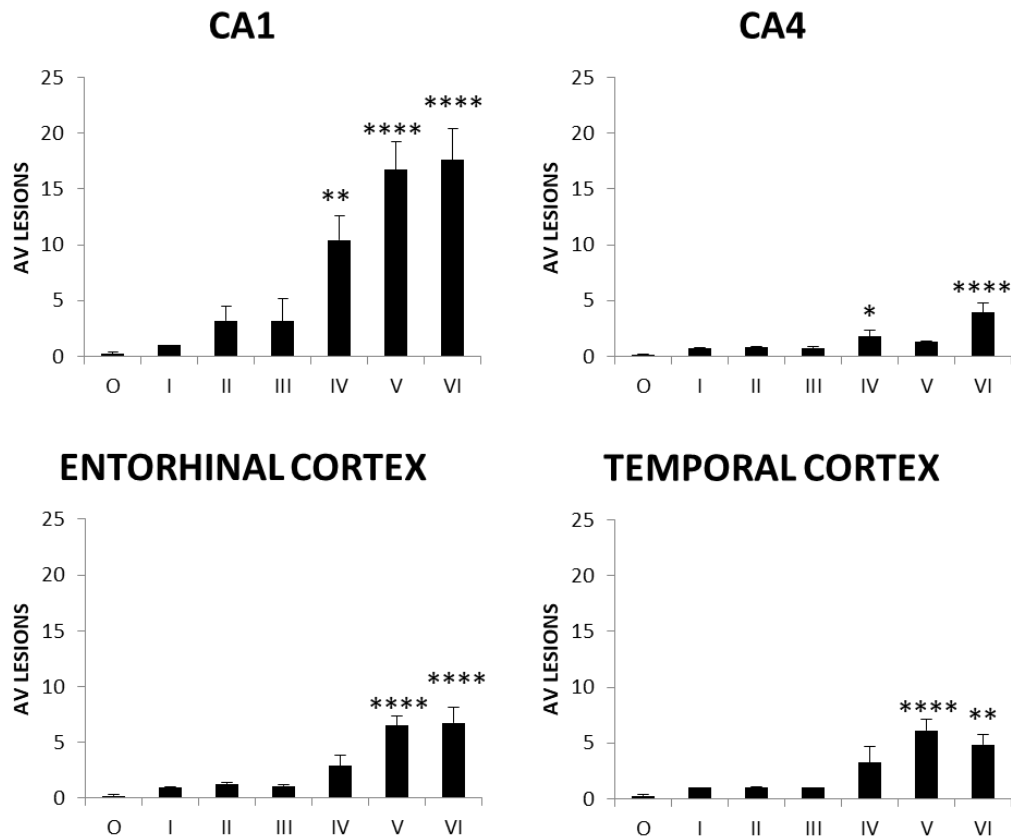


Figure 6.5 Quantification of large lesions labelled with tau5-IHC in the hippocampal and temporal region. Automated quantification of tau5-IHC labelled large lesions across the different hippocampal and temporal brain regions. All groups were compared to the control (Braak 0) through a ONE-WAY ANOVA (Dunnet). N = 11/12/12/9/7/8/8. *p < 0.05, **p < 0.01, ***p < 0.001, ****p < 0.0001.

Analysis of beta-amyloid levels in the regions of the hippocampus and the TC of the AD brain tissue was also performed. FFPE post-mortem human tissue was analysed by performing 4G8-IHC for the detection of beta-amyloid deposits. An increasing trend in the levels of a-beta was observed as we moved from the initial to the last Braak stages, with the EC and the TC being involved in Braak stage II (Fig 6.6).

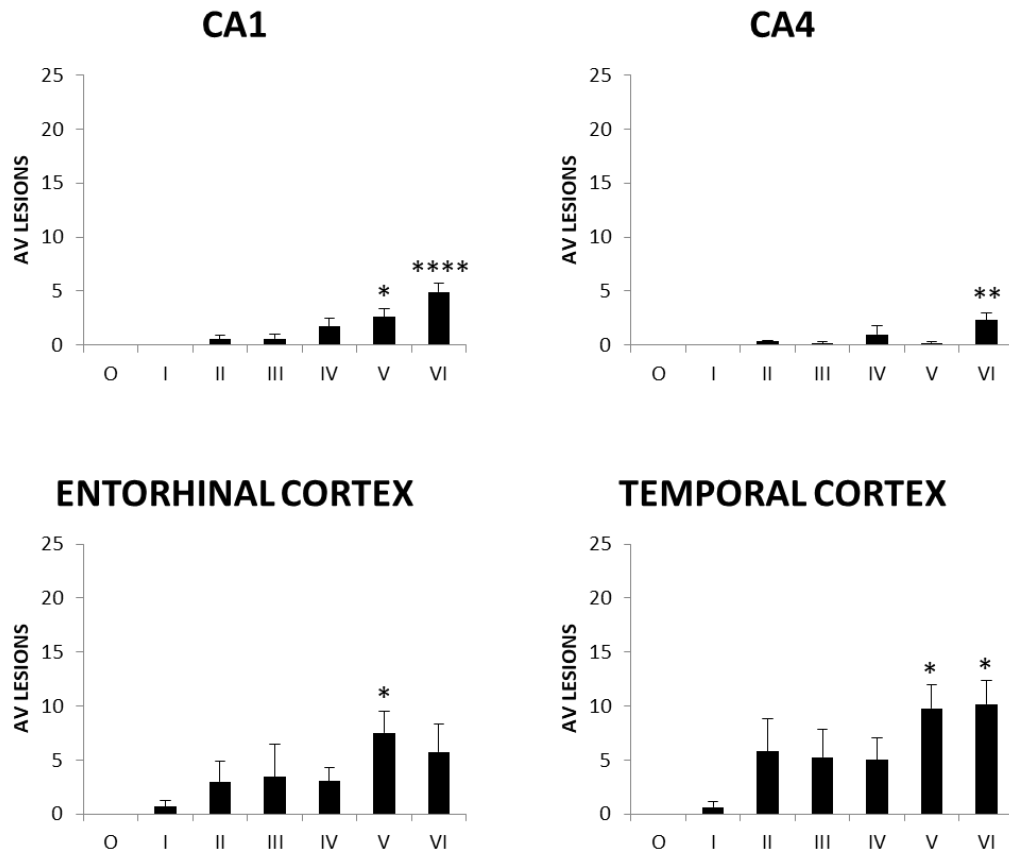


Figure 6.6 Quantification of lesions labelled with 4G8-IHC in the hippocampal and temporal region. Automated quantification of 4G8-IHC labelled lesions across the different hippocampal and temporal brain regions. All groups were compared to the control (Braak 0) through a ONE-WAY ANOVA (Dunnet). N = 11/12/12/9/7/8/8. * $p < 0.05$, ** $p < 0.01$, *** $p < 0.001$, **** $p < 0.0001$.

We could note from these findings, as well as, from the spatiotemporal distribution of tau-PLA labelled structures in the different brain regions across the different Braak stages (Fig 6.7), that tau multimerisation starts early in the development of tau pathology in the brain of AD individuals and is characterised as a pathological event that does not occur physiologically in the brain as it is mostly unaccompanied by AT8-IHC positive immunostaining.

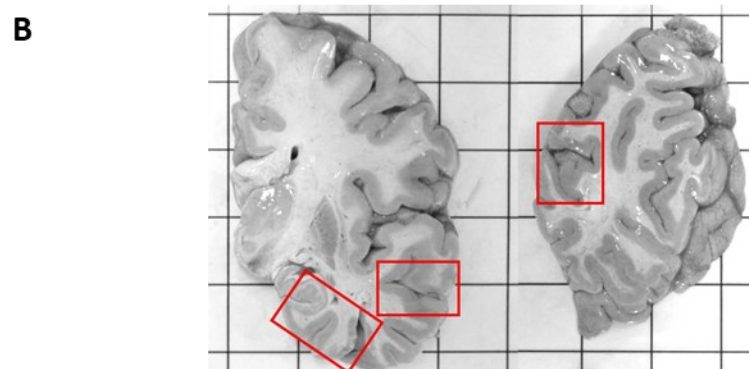
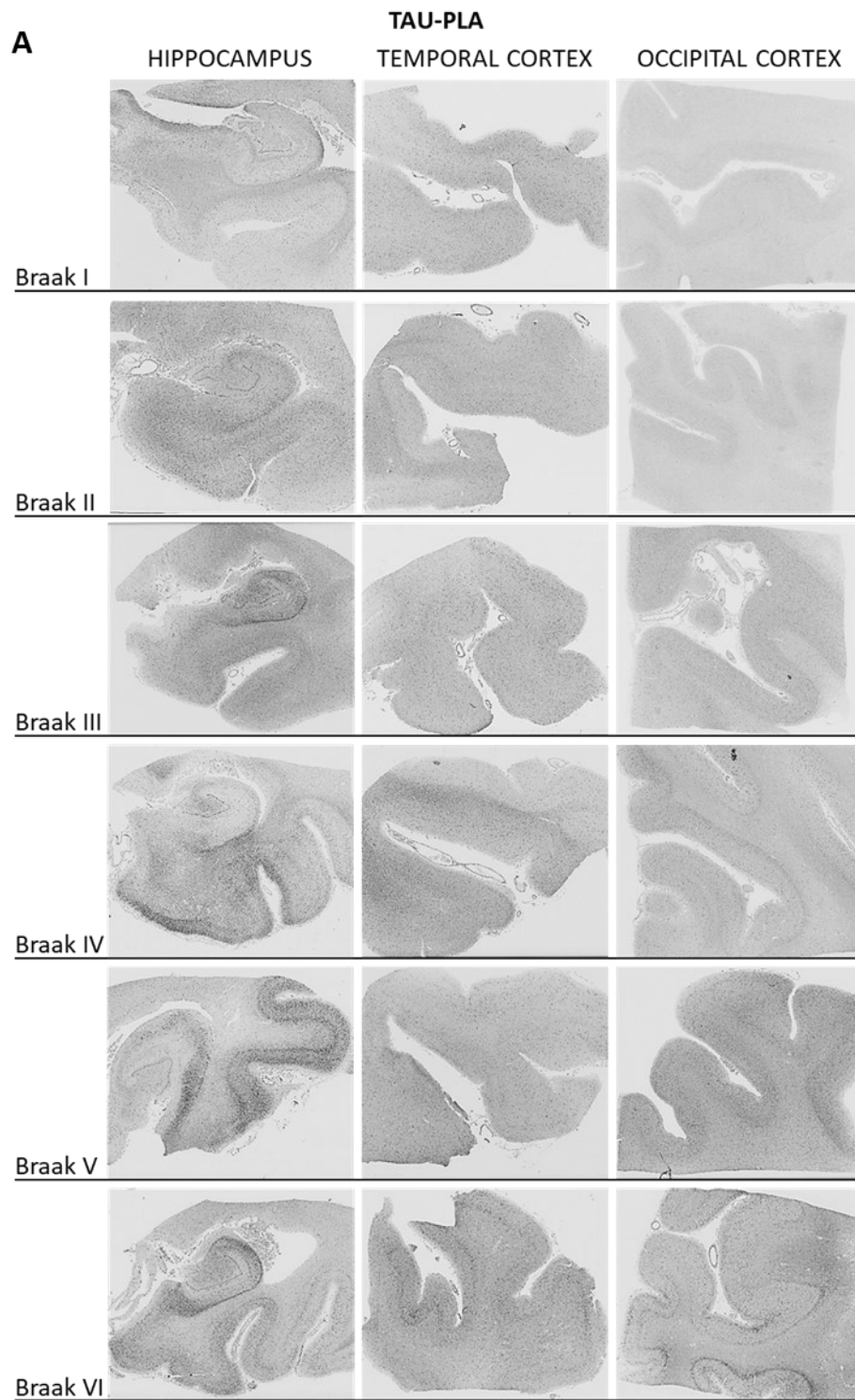


Figure 6.7 Scanned tau-PLA labelled post-mortem human brain tissue sections.

A) Sections from the hippocampal region, temporal cortex, and occipital cortex stained for tau-PLA. B) Macroscopically neuroanatomical regions of 1-posterior hippocampus, fusiform gyrus, and part of inferior temporal gyrus, 2-temporal cortex including parts of middle and superior temporal gyrus, and 3-occipital cortex including calcarine fissure.

6.5 Tau-PLA reveals early tau-tau interactions, prior to tau hyperphosphorylation and misfolding

Based on the previous analysis we could clearly say that the AT8 antibody, although is the gold standard marker for the diagnosis and staging of AD, is characterised by high specificity and preference for the large neurofibrillary-type lesions, mostly for NFTs, NTs, and neuritic plaque-associated tau. Nowadays, a number of antibodies have been described that detect tau post-translational modifications (PTMs) that occur early in the development of tau pathology in the AD brain which precedes hyperphosphorylation of tau in the Ser202/Thr205, the binding site of AT8 antibody (Ercan-Herbst et al., 2019; Lasagna-Reeves et al., 2012; Lasagna-Reeves et al., 2012). Well-known phospho-tau antibodies that recognise early PTMs are AT180 which recognises hyperphosphorylation of tau in the residue Thr231, PHF-1 which detects hyperphosphorylation in the double epitope Ser396/Ser404 of the paired helical filament of tau, and the T217 and S422 antibodies that detect hyperphosphorylation of tau in the Thr217 and Ser422 of the full-length tau, respectively. As mentioned previously, all these events have been described to occur early in the development of AD pathology preceding the formation of late-type aggregated tau species. Markers related to early tau misfolding and conformational changes have been also developed. Two widely used conformational antibodies are MC1 and Alz50. MC1 detects specific interactions of the amino acids within the residues 312-322, while Alz50 spots interactions between amino acids 2-10 and 312-342 of full-length tau. To start with, we first investigated the staining pattern of each candidate antibody. FFPE sections from post-mortem human brain tissue from the region of the hippocampus, TC, and OC were examined with IHC for these markers, and quantification of large tau structures was performed (Fig. 6.8). Both AT180 and T217 detected a significant number of tau lesions

from Braak stage II to VI in the hippocampal region, with the TC being involved in Braak Stage IV. Severe involvement of OC was observed in the late AD stages, mostly at Braak stage VI (Fig 6.8 and 6.9A & B). A similar staining pattern was also displayed in the PHF-1- and S422-IHC, however the sensitivity for the large lesions appeared to be lower compared to the previous ones, detecting fewer lesions in each brain region (Fig 6.8 and 6.9C & D). Focusing now on tau misfolding, IHC for MC1 and Alz50 was performed. The outcomes from the analysis revealed these antibodies detected the late-type large lesions in the same manner as the phospho-tau antibodies, but once again the amount of tau exposed per Braak stage in each anatomical brain area was lower, indicating either the weaker ability of the conformational antibodies to capture the large tau complexes or the existence of fewer tau structures exhibiting conformational modifications (Fig 6.8 and 6.9E & F). However, apart from these minor differences that characterised the aforementioned antibodies in detecting the fibrillar lesions, their staining pattern appeared to be similar to the one of AT8-IHC and tau-PLA for large lesions (Fig 6.4 and 6.9).

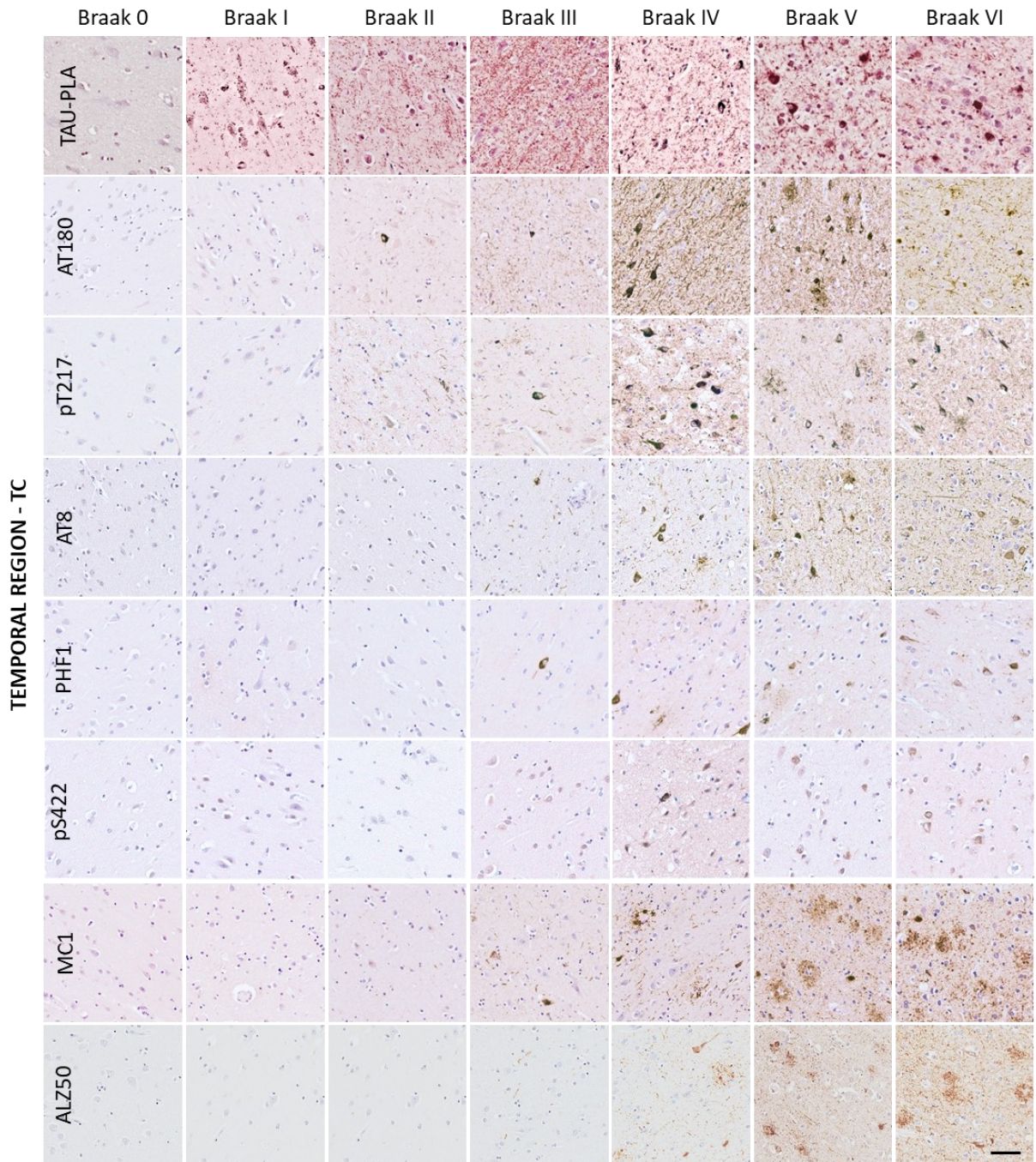
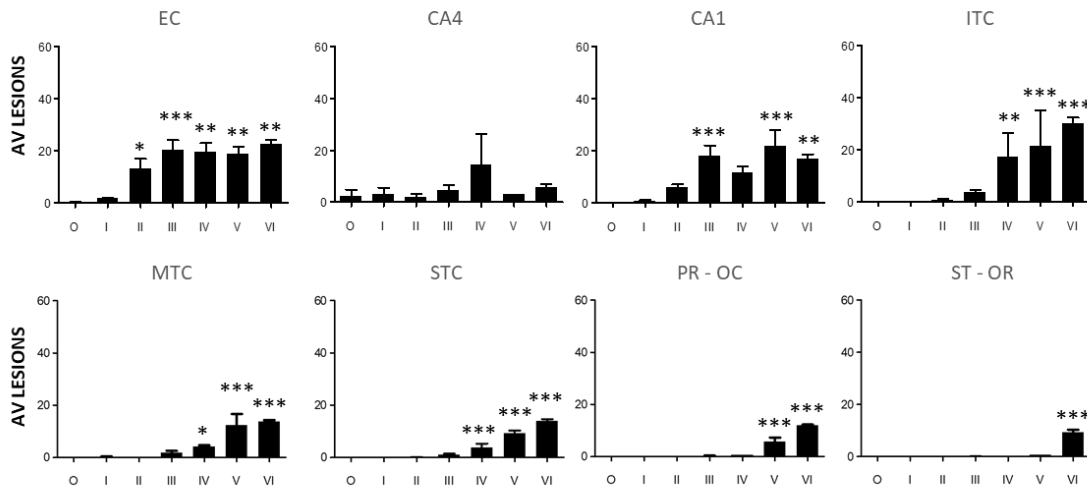
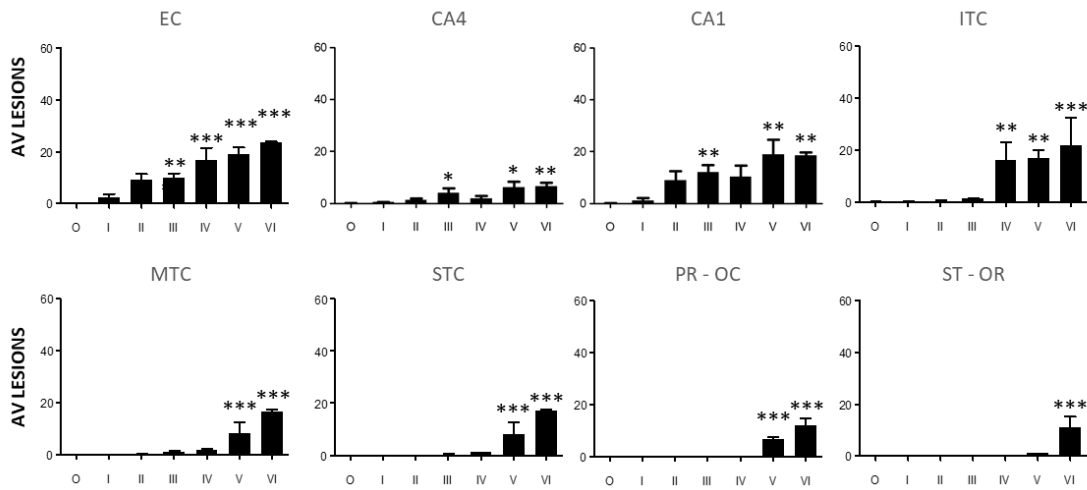


Figure 6.8 Tau aggregates labelled with different phospho-tau and conformational tau antibodies across the different Braak Stages as defined by BrainNet Europe diagnostic protocol. FFPE sections from post-mortem human brain tissue from the brain regions of the hippocampus, TC, and OC were stained for AT180-, T217-, PHF-1-, S422-, MC1-, and Alz50-IHC. Scale bar 50 μ m. *EC Entorhinal cortex, TC Temporal cortex, OC Occipital cortex*

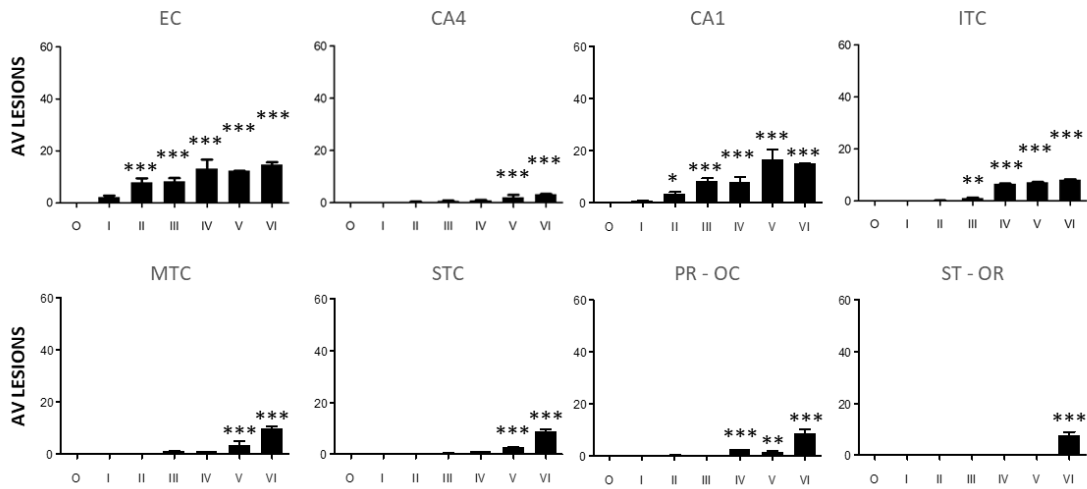
A. AT180 – Lesions



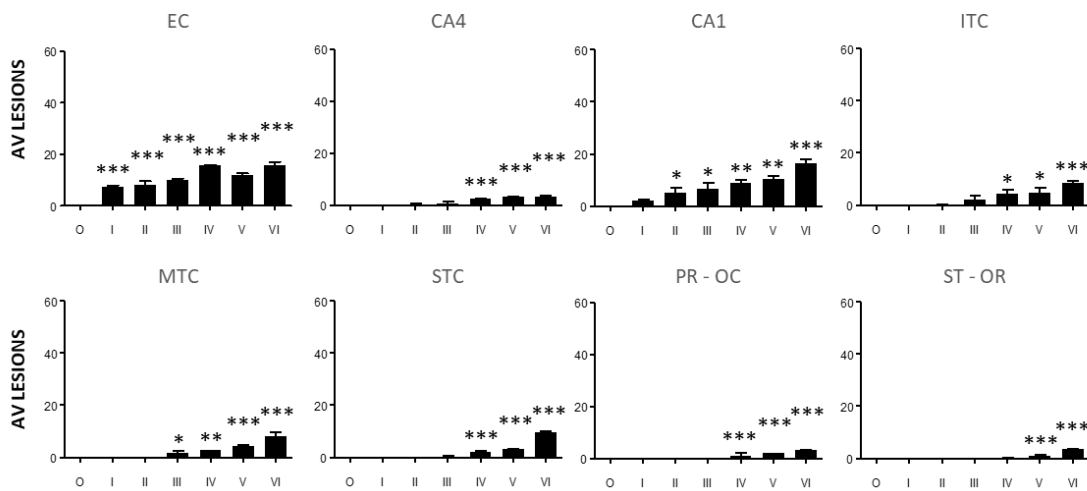
B. T217 – Lesions



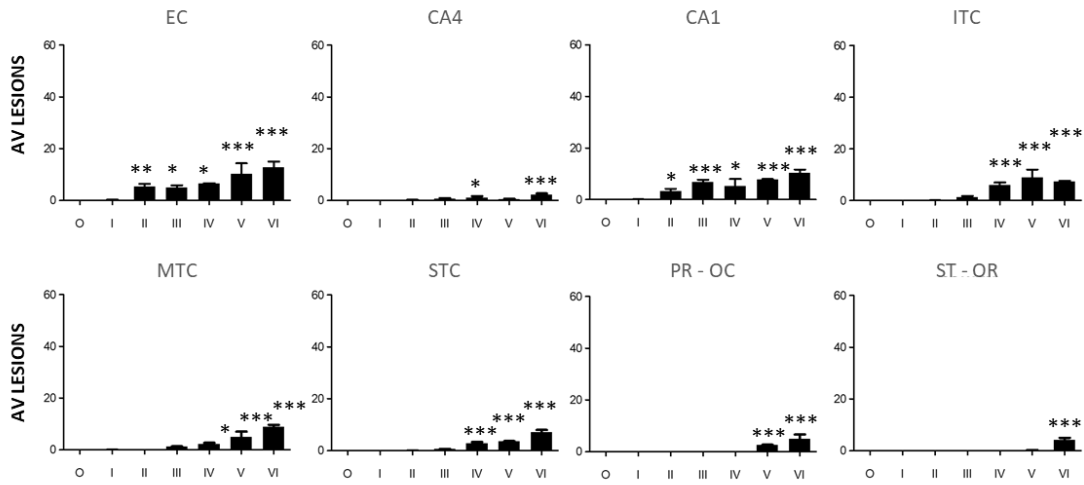
C. PHF1 – Lesions



D. S422 – Lesions



E. MC1 – Lesions



F. ALZ50 - Lesions

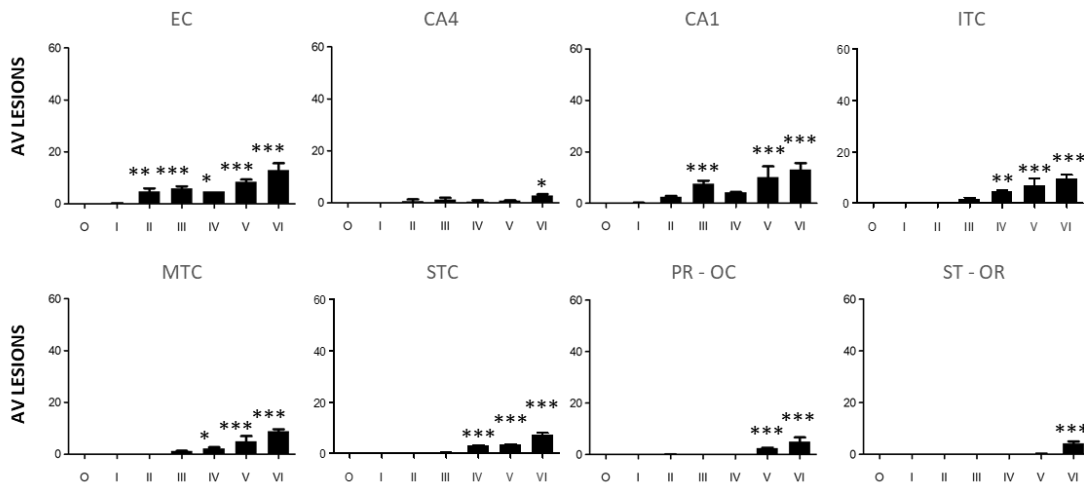
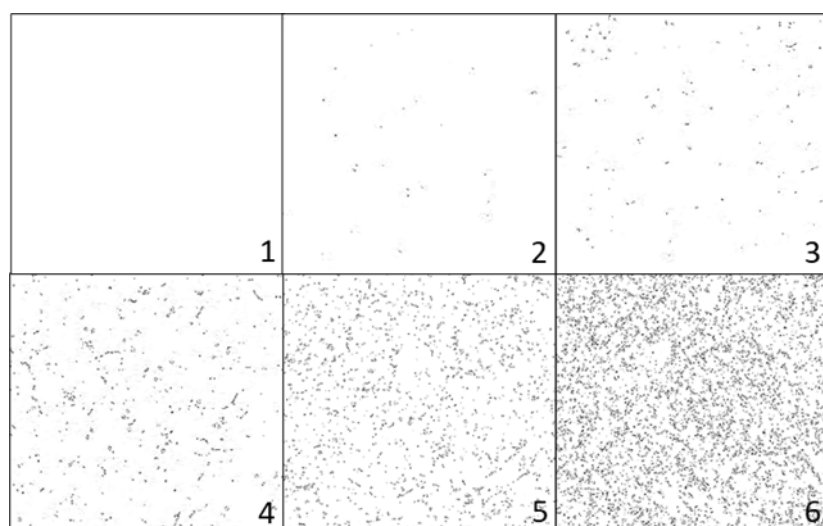


Figure 6.9 Quantification of AT180-, T217-, PHF-1, S422-, MC1- and Alz50-IHC labelled large perikaryal neurofibrillary-type lesions in hippocampal regions, TC, and OC. Automated quantification of A) AT180-, B) T217-, C) PHF-1-, D) S422-, E) MC1-, and F) Alz50-IHC labelled large lesions across the different brain areas. All groups were compared to the control (Braak 0) through a ONE-WAY ANOVA (Dunnet). N = 11/12/12/9/7/8/8. *p < 0.05, **p < 0.01, *p < 0.001, ****p < 0.0001. EC Entorhinal cortex, ITC Inferior temporal cortex, MTC Middle temporal cortex, STC Superior temporal cortex, OC Occipital cortex, PR Parastriate area, ST Striate area, AV average**

We next compared the ability of all these antibodies to detect the early-type diffuse tau pathology by performing semi-quantitative evaluation using density plates of the tau structures captured with tau-PLA and tau-IHC in the different brain areas, across the different Braak stages (Fig 6.8 and 6.10). Comparison of tau-PLA with tau-IHC revealed that tau-PLA has higher ability and sensitivity in detecting the early-type diffuse tau pathology in the hippocampal regions, TC, and OC compared to the other markers, being able to detect high levels of tau multimers in the hippocampus from Braak stage I and with the OC being severely affected in Braak stage III (Fig 6.10). These findings suggested that tau multimerisation is one of the earliest events occurring during the development of AD pathology. Essentially high levels of early-type diffuse tau pathology were also captured by AT180-IHC followed by T217-IHC, with a high load of small-sized tau molecules being spotted in the Braak stage II in the hippocampal region and the temporal isocortex (Fig 6.10). OC was mainly involved at Braak stage V with VI (Fig 6.10). the rest of the phospho-tau antibodies displayed weaker capacity in capturing tau diffuse pathology, while conformational markers presented a moderate preference for the small-sized tau species, firstly spotted in the hippocampus and TC in Braak stages II and III, respectively (Fig 6.10). Altogether these findings suggested that tau self-interaction is one of the earliest events occurring during the development of tau pathology in the AD brain, preceding the detectable molecular events of tau hyperphosphorylation and tau misfolding.



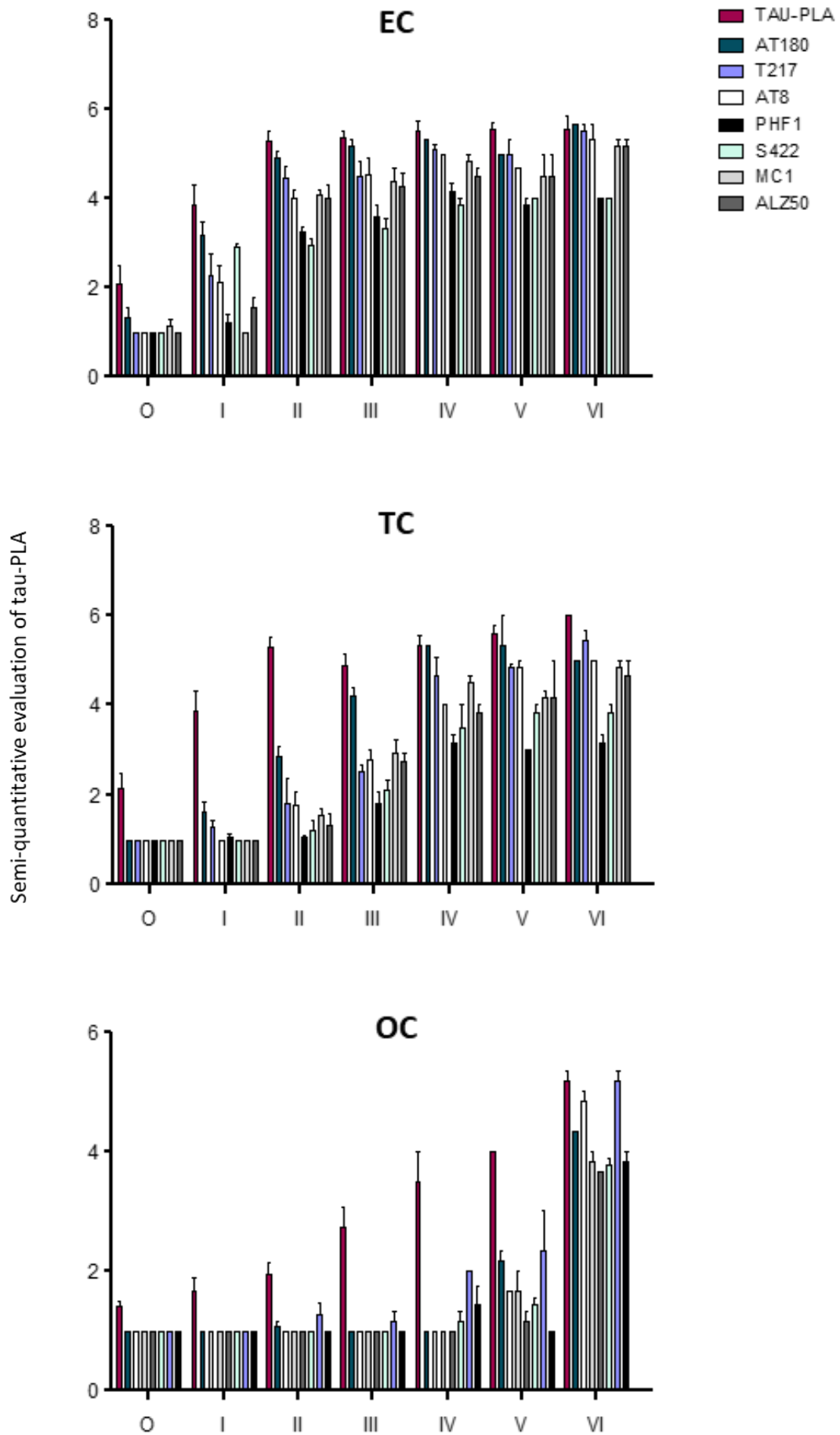


Figure 6.10 Widespread tau multimerization occurs early and prior to tau hyperphosphorylation and tau misfolding across EC, TC, and OC. Semi-quantitative scale between 1 to 6 was used for semi-quantitative analysis. FFPE sections from EC, TC, and OC from Braak 0 to VI were analysed with tau-PLA and immunohistochemistry for tau using different tau antibodies. Semi-quantitative evaluation of tau-PLA and tau-IHC labelled diffuse pathology. All groups in each Braak stage were compared to tau-PLA through a ONE-WAY ANOVA (Dunnet). N = 11/12/12/9/7/8/8. *p < 0.05, **p < 0.01, ***p < 0.001. *EC Entorhinal cortex, TC Temporal cortex, OC Occipital cortex, AV average*

6.6 Tau-PLA highlights tau multimerisation as one of the earliest events occurring during NFT maturity

Focusing now on the most powerful phospho-tau (AT180) and tau misfolding (MC1) antibody, we compared the detection power of tau-PLA with these markers and the gold diagnostic standard marker AT8 during the neurofibrillary tangle maturity. As described previously, NFT formation is characterised by four stages: diffused small-sized tau pathology, pretangle materials, mature neurofibrillary type tangles, and ghost tangles. Characterisation of these tau structures was performed by staining FFPE sections from post-mortem human brain tissue from the region of the hippocampus with tau-PLA, AT8-IHC, AT180-IHC, and MC1-IHC. Our finding suggested that tau-PLA has the highest detection power, able to detect high levels of tau diffuse pathology, even before the formation of pretangle materials inside the cytoplasm of intact neurons (Fig 6.11). Then followed the AT180 antibody which was also able to capture part of the diffuse pathology quite early in the dynamic lifespan of NFTs, earlier than AT8, whose staining was first detected at the stage of pretangle (Fig 6.11). Conformational changes recognised by MC1 also occurred early during tangle maturity, but not before the appearance of pretangle materials (Fig 6.11). Interestingly, ghost tangles were spotted by AT180- and AT8-IHC, but not by tau-PLA and MC1-IHC (Fig 6.11). These observations together with the previous findings supported that tau-tau interactions are one of the earliest detectable *in situ* events during the development of tau pathology in the AD brain, preceding the events of tau hyperphosphorylation and tau misfolding.

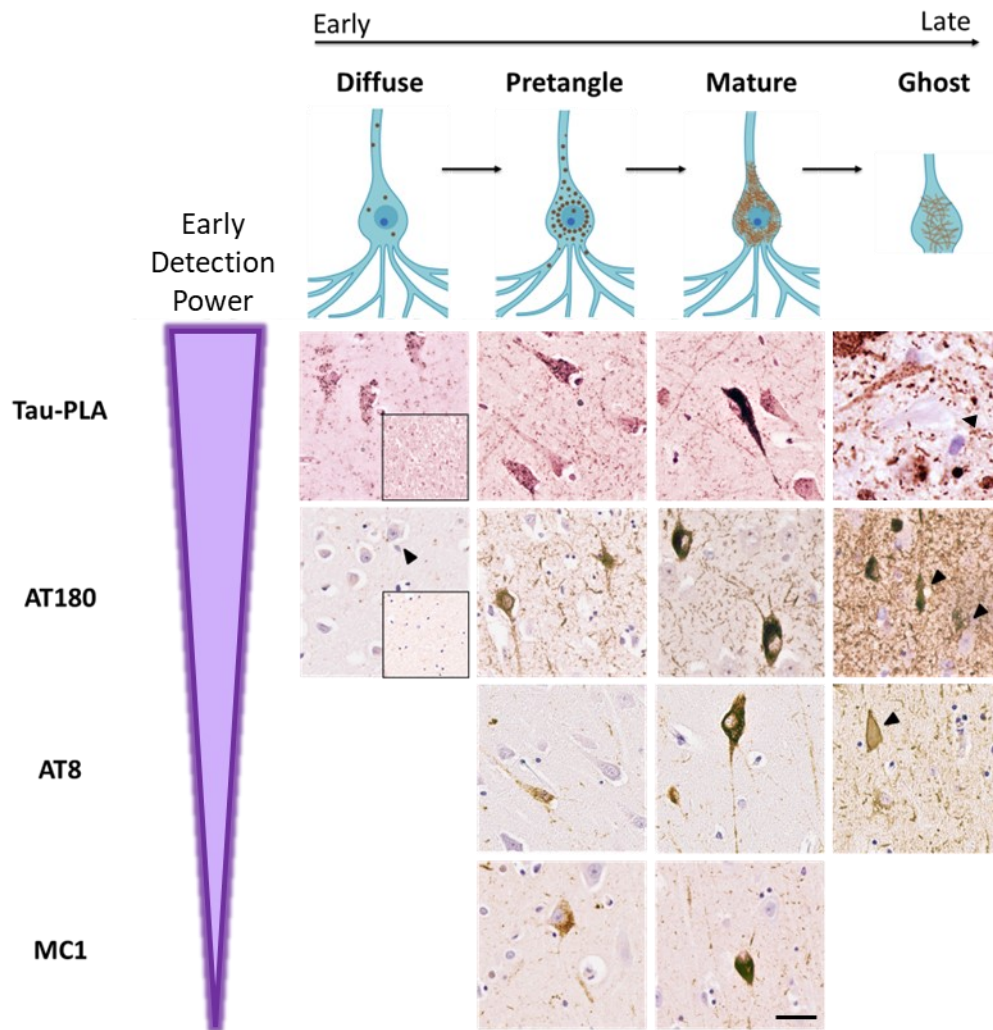


Figure 6.11 Tau multimerisation is one of the earliest detectable events occurring during the maturity of NFTs. Schematic representation and brightfield images of NFT lifespan. Representative images from FFPE sections from the hippocampal region across the different Braak stages stained for tau-PLA and AT180-, AT8-, and MC1-IHC. Tau-PLA showed that tau self-interaction is one of the earliest events occurring during neurofibrillary tangle maturity, highlighting its high detection power. Scale bar 50 μm . Schematic representation was created with BioRender (Bengoa-Vergniory, N., Velentza-Almpani, E., et al., 2021).

6.6 Discussion

To demonstrate the *in situ* specificity of our assay and its ability to recognise endogenous disease-related tau-tau interactions, FFPE sections from the brain region of the hippocampus, the temporal cortex, and the occipital cortex, from 67 cases from Braak stage 0 to VI were investigated using tau-PLA and tau-IHC. Until today, AT8-IHC is the gold standard for the clinical diagnosis and staging of AD, with the AT8 antibody recognising the phosphor-epitope pSer202/pThr205 and capturing hyperphosphorylated fibrillar lesions (Alafuzoff et al., 2008; Braak et al., 2006). For the detection of the early tau modifications, further tau antibodies have been developed like the phosphor-tau antibodies AT180 (pThr231), PHF-1 (pSer396/pSer404), T217 (pThr217), and S422 (pSer422), all of them being reported to capture phosphorylated events that occur early in the development of the AD pathology and the conformational antibodies MC1 and Alz50 detecting early misfolded tau (Ercan-Herbst et al., 2019; Li et al., 2016; Smolek et al., 2016; Weaver, 2000). With most of the histological antibodies failing to capture *in situ* the early tau multimerisation, tau-PLA allowed the direct visualisation and detection of a previously unreported early-type tau pathology consisting of self-interacting monomeric tau molecules. Under normal physiological conditions, no tau-PLA or tau-IHC signal was observed in the brain of the Braak stage 0 cases indicating that the majority of tau molecules are not modified and preserve their physiological monomeric state as has been previously reported (Alafuzoff et al., 2008; Kumar et al., 2015; Wang and Mandelkow, 2012). In contrast to the other early histopathological markers, tau-PLA revealed that although the PLA signal was negligible in most cases in the Braak 0 group, a minority of them presented moderate or even high levels of tau-PLA, indicating that in a subgroup of asymptomatic individuals with no tau aggregates defined by other tau antibodies, tau multimerisation has already started. However, at this point, we need to state that further experimental analysis is needed to conclude whether these diffuse tau multimers in the Braak 0 group are the outcome of pathological molecular events or are part of physiological procedures occurring in the brain such as aging (Wang and Mandelkow, 2016; Wegmann et al., 2016). As described in Chapter 5, tau-PLA staining pattern can be divided into two main subgroups: the early stage, small-sized, diffuse tau pathology, and the large fibrillar lesions. From the Braak stage I, tau-PLA detected high levels of diffuse tau pathology, mostly unaccompanied by tau-IHC, with the AT180 antibody

being able to capture, but with less sensitivity, a proportion of soluble aggregated tau molecules as has been previously described (Ercan-Herbst et al., 2019). The lack of signal obtained from the other histopathological markers in the early Braak stages suggested that the tau-PLA labelled multimers could lack any PTM related to hyperphosphorylation or conformational change. This finding supports that tau self-interaction is one of the earliest detectable events occurring during the development of tau pathology in the AD brain, a finding strongly supported by other biochemical and cellular assays investigating tau seeding capacity (Holmes et al., 2014; Kaufman et al., 2017; Metrick et al., 2020). Although the early tau multimerisation has been supported by other studies, these approaches lacked the structural preservation and regional location of the tau multimers provided by our assay (Ercan-Herbst et al., 2019; Kaufman et al., 2016b; Kraus et al., 2019; Metrick et al., 2020). In addition, some of these studies were characterised by reduced resolution as the Braak 0 and Braak I cases were grouped and treated as the control group, reducing, therefore, the resolution and significance in the determination of the sequence of the events in this crucial transition step (Ercan-Herbst et al., 2019). Moving to the following Braak stages, a significant increase of the tau-PLA signal was observed, with essentially high levels of diffused pathology being captured as well by the AT180- and T217-IHC. On a cellular level, tau-PLA proved to have the highest detection power suggesting that tau self-interaction is one of the earliest events occurring during neurofibrillary tangle maturity. Regarding the large tau lesions, the staining pattern of tau-PLA and tau-IHC presented minor differences in their sensitivity, with all markers detecting a significant number of tau lesions from Braak stage II to VI in the region of hippocampus and involvement of the temporal cortex in the Braak stage III-IV. PHF-1 and S422 presented reduced sensitivity for the large tau lesions compared to the other markers, followed by the conformational antibodies MC1 and Alz50 that detected fewer tau aggregates in each anatomical brain region. Regarding the detection of the large lesions by tau-PLA, our assay recognised these fibrillar aggregates following the same staining pattern as AT8-IHC, with the AT8 antibody being more sensitive and detecting a larger number of tau lesions than tau-PLA. This difference proved to be due to the superiority of the AT8 to the tau5 antibody for the large lesions, a fact supported by previous studies suggesting that the binding ability of the tau5 antibody, the antibody used for the build-up of our assay, can be affected by the nearby phosphorylated sites (Porzig et al., 2007). Therefore, the enhanced levels of tau PTMs at the late Braak stages could affect and

reduce the accessibility of the tau5 antibody to its epitope (Alquezar et al., 2021; Furcila et al., 2019; Wang and Mandelkow, 2016). Finally, focusing on the second pathological hallmark of AD, the extracellular deposition of a-beta and the formation of amyloid plaques, our study revealed an increasing trend in the levels of a-beta as we moved from the initial Braak stages to the last ones, with the involvement of the EC and TC in the Braak stage II, in line with previous reports (Liu et al., 2021; Thal et al., 2006).

6.6.1 Limitations

Both the experimental work and analysis of the study contained limitations that needed to be addressed. As far as it concerns the experimental procedure, one major limitation is the difficulty of obtaining the essential tissue for our study. Several brain regions from the different Braak stages were not available due to oversampling through the years. For this reason, we had to reduce the number of cases investigated in some groups. In addition, although most of the cases had been analysed both macroscopically and microscopically and all the findings were provided in detail by the brain tissue banks, re-examination of the cases revealed that some cases were inappropriate for experimental analysis as they were obtained years ago and kept in formalin for many decades, presenting alternations in their composition and structure that would affect the experimental procedures. Especially, in the case of tau-PLA, a good quality tissue is essential as this assay is characterised by high sensitivity. Over-fixation has been reported to affect the immunochemical reactivity, however, the impact of the long fixation on the antigen recognition from the most widely used antibodies appeared to be significantly low (Webster et al., 2009). In addition, the reduced availability of the PLA kits due to reduced production, prolonged periods of delivery from the USA, together with Brexit and COVID-19, delayed significantly the analysis of the available tissue and forced us to reduce the number of cases and brain regions for analysis to avoid running out of reagents during the performance of PLA. Finally, two major limitations of tau-PLA compared to immunohistochemistry are the much higher cost of the PLA and the longer duration of the experimental procedure. About the findings obtained from tau-PLA analysis, although tau-PLA uncovered a previously unreported early-type tau pathology in the post-mortem human brain, it cannot provide direct outcomes either about the pathological role of these species or the molecular

mechanisms that lead to their generation. Similarly, further study is essential to determine whether the tau-tau interactions spotted in the brain of Braak 0 cases are the outcome of early pathological events or part of the normal aging process. However, the cellular and anatomical location of these multimers, their temporal distribution, their morphology, their aggregation status, and their investigation with other histological markers can lead to some significant outcomes.

6.6.2 Conclusions

Overall, the lack of tau-PLA in the pure healthy control brain tissue revealed that our assay is highly specific for tau-tau interactions without detecting endogenous monomeric tau. This finding also supported that tau multimerisation does not occur physiologically in the brain of healthy young individuals. Tau-PLA also revealed that cases in the Braak 0 group, as defined by AT8-IHC, could present heterogeneity in the levels of tau-PLA load, indicating that in a subgroup of asymptomatic individuals tau self-interaction might have already started. Tau-PLA detected an extensive diffuse tau pathology within the early Braak stages, mostly accompanied by AT8-IHC. In addition, it recognised the large tau lesions following the same pattern as the AT8 antibody, with AT8-IHC being more sensitive due to the superiority of the AT8 to the tau5 antibody. Finally, tau-PLA revealed that tau-tau interactions are one of the earliest detectable events occurring during the development of tau pathology, preceding tau hyperphosphorylation and misfolding.

Chapter 7: Investigation of the seeding activity of self-interacting tau molecules

7.1 Introduction

Although late-type tau aggregates like NFTs and NTs are considered to be primarily responsible for the progression of tau pathology in the AD brain, accumulating evidence today supports that soluble aggregated tau molecules rather than NFTs are the toxic species with seeding capacity responsible for the prion-like spread of tau pathology, as neuronal loss appeared to be superior to the number of NFTs (Ghag et al., 2018; Gómez-Isla et al., 1997; Holmes et al., 2014; Kaufman et al., 2017; Liu et al., 2012; Metrick et al., 2020). Different studies have shown that injection of aggregated tau species in the brain of mouse models induced tau pathology that spread through the brain, in synaptically connected distant areas, following known neuronal networks. Like prion proteins, different tau assemblies with distinct physiochemical and biochemical properties induce the development of phenotypic diversity of tau pathology (Holmes et al., 2014; Kaufman et al., 2017). Although these different tau strains with different tau capacities are able to propagate from cell to cell in synaptically connected brain regions, no transmission between individuals or animals has been reported in epidemiological studies (Holmes et al., 2014; Kaniyappan et al., 2020; Kaufman et al., 2016a; Sanders et al., 2014). Given that these early self-propagating tau aggregates seem to play a pivotal role in the spread of tau pathology, a number of robust assays have been developed to exploit and investigate their seeding activity. Although the majority of the developed assays are unable to recognise tau-tau interactions *in situ*, these assays are more sensitive and can detect pathology earlier than standard conventional techniques like IHC (Metrick et al., 2020). Here, we need to highlight that both novel and conventional methods work complementary to each other to allow capturing the whole image of the pathology (Metrick et al., 2020). A well-known assay is the flow cytometric resonance energy transfer (FRET) biosensor assay, a technique that combines flow cytometry sensitivity and biosensor cell line stability and allows the detection of protein multimerisation. Researchers, by using FRET, detected increased tau seeding activity in anatomical brain regions that appeared to be unaffected based on standard staining methods (Kaufman et al., 2017, 2016a). Another novel assay that has

been recently developed is real-time quaking-induced conversion (RT-QuIC) (Atarashi et al., 2007; Kraus et al., 2019; Saborio et al., 2001). Scientists here built a sensitive and selective RT-QuIC assay for the investigation of tau aggregated complexes seeding activity (Tau RT-QuIC) (Kraus et al., 2019; Saijo et al., 2017). Analysis of AD and healthy post-mortem human brains showed that specimens extracted from sporadic and familial AD brains presented higher seeding activity and shorter lag phase compared to the non-AD brain tissue (Kraus et al., 2019). Although these assays are useful tools for the investigation of aggregated tau pathophysiological role, the fact that a robust technique for their visualisation *in situ* was missing, was the major limitation. On the other hand, the visualisation of tau multimers with tau-PLA could play a vital role in examining the pathophysiology of the early-type aggregates, but still, the investigation of the levels of toxicity and the seeding potential of these small diffuse multimers needs additional approaches. Therefore, coupling these two assays could be an interesting approach for the investigation of tau-tau interactions and their role in the progression of tau pathology in the AD brain.

7.2 Hypothesis and Aims

We hypothesise that the early-type tau multimers detected by tau-PLA are species with seeding activity that can propagate to synaptically connected brain regions contributing to the progression of AD pathology.

Our aim for this chapter is to:

- Characterise the τ_{306} plasmid construct.
- Purify and characterise the purified τ_{306} tau fragment to set up the tau RT-QuIC assay and test the ability of τ_{306} to aggregate *in vitro*.
- Generate the analysis groups for the tau RT-QuIC assay based on AT8 and tau-PLA findings.
- Investigate the seeding activity of the early-type tau multimers using tau RT-QuIC assay.

7.3 Characterisation of τ 306 plasmid construct

For the tau RT-QuIC with τ 306 substrate with a point mutation at 322 cysteine to serine, purification of the τ 306 tau fragment was essential. Bacterial cells expressing the τ 306 substrate were kindly provided by Byron Caughey. T306 fragment is comprised of tau residues 306-378 of the full-length 4R tau isoform, residues located in the core of tau fibrils. A point mutation has been engineered to residue 322 by the replacement of cysteine amino acid with serine. A stop codon was also inserted at residue 379 at the C terminal. As mentioned previously, studies have shown that the τ 306 fragment tends to aggregate faster in AD cases compared to non-AD controls (Kraus et al., 2019) making it an appropriate substrate for the tau RT-QuIC assay. This mutated cloning construct was inserted and cloned into the backbone of the pET-28a expression plasmid vector which carried a kanamycin resistance gene. A 6xHis Tag was also inserted into the sequence to assist later in the purification of the τ 306 fragment. pET-28a(+) τ 306 – His tag vector (5512 bp) was carried in the BL21(DE3) strain of Escherichia coli. To identify the identity of our plasmid construct, restriction enzyme digestion, as well as, sanger sequencing were performed. Therefore, the purification of a good quality plasmid DNA was essential. The pET-28a(+) τ 306 – His tag plasmid vector was amplified in BL21(DE3) bacterial cells and purified via QIAprep® Spin Miniprep Kit (Qiagen, 27106). The integrity, quality, and quantity of the plasmid DNA were subsequently determined. The purity and concentration of the plasmid DNA were determined using UV spectrophotometry. The ratio of absorbance at 260 nm and 280 nm of the purified plasmid DNA varied between 1.85-2.05, values indicative of pure DNA (a ratio of 1.8 – 2.1 indicates high purity DNA), while the plasmid DNA concentration was between ~30 ng/ μ l. Restriction enzyme digestion was then performed using the appropriate endonucleases according to the restriction maps of the plasmids (Fig 7.1A). Based on the plasmid map, the restriction enzyme used were XhoI and BglII, cutting the plasmid vector in a way that led to the production of two plasmid DNA fragments. The length of the obtained fragments was expected to be 5.125 kb and 0.387 kb. The size of acquired the DNA bands was determined using the Quick-Load Purple 2-Log DNA Ladder (0.1-10.0kb) (NEB, UK) (Fig 7.1B). Agarose gel electrophoresis revealed that the size and the number of the bands obtained were in line with the ones expected according to the plasmid restriction maps (Fig 7.1). The identity of the plasmid DNA was later confirmed with Sanger sequencing performed by

GENEWIZ, from Azenta Life Sciences, a genomics service company. DNA Dynamo and SnapGene Software were used for the analysis of the plasmid construct.

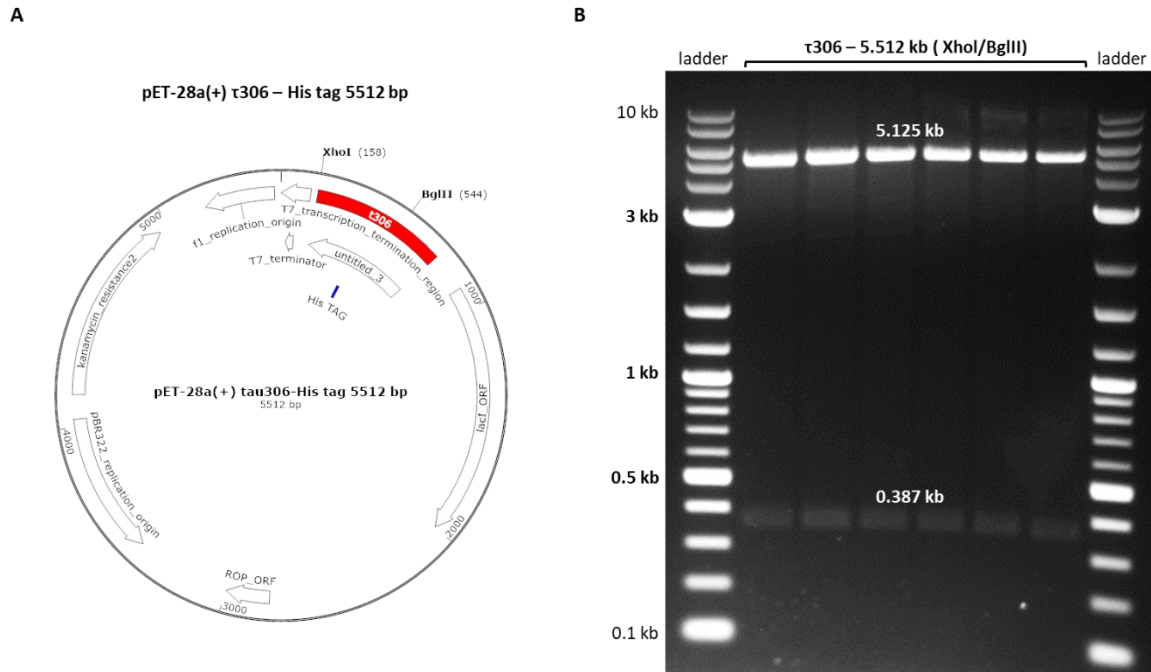


Figure 7.1 Characterisation of τ 306 plasmid construct. A) Map of τ 306 plasmid construct (pET-28a(+) τ 306 – His tag vector (5512 bp)). The restriction enzymes used for the restriction enzyme digest, XhoI and BglIII with their cutting sites are also presented. B) T306 plasmid construct digested with XhoI and BglIII restriction enzymes (double digestion) leading to the production of two bands with sizes 5.125 kb and 0.387 kb.

7.4 τ 306 protein fragment purification and aggregation

For tau RT-QuIC assay with τ 306 substrate, expression and purification of soluble monomeric recombinant tau τ 306 fragment was essential. T306 fragment expression from BL21(DE3) strain of *Escherichia coli* was performed based on the protocol previously described in (Saijo et al., 2017) following the overnight express autoinduction method (Studier, 2005). After protein overexpression, the τ 306 fragment was purified by performing FPLC and SEC. To confirm that monomeric soluble species

of τ 306 were obtained, transmission electron microscopy (TEM) was performed. No aggregated τ 306 species were captured with TEM (Fig. 7.2). To test whether our protein has also the ability to aggregate, the τ 306 fragment was shaking for 360 hours. TEM images showed that after intense shaking, a mixed population of tau aggregated species was detected consisting of amorphous accumulations, globular structures, and filaments (Fig. 7.2). Both soluble and aggregated τ 306 species were used for RT-QuIC assay.

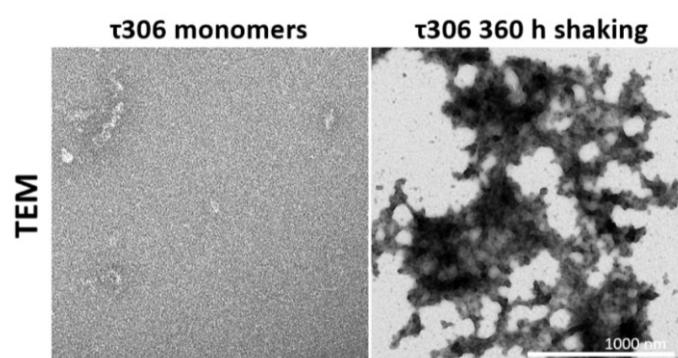


Figure 7.2 Transmission electron microscopy of recombinant τ 306 soluble monomers and τ 306 aggregated species. Aggregation of recombinant τ 306 fragment was induced by shaking for 360 hours. Scale bar 1000nm. *TEM* Transmission electron microscopy.

7.5 Tau RT-QuIC reveals high seeding activity of early tau multimerisation

For the investigation of the seeding activity of these early-type tau multimers detected by tau-PLA, tau RT-QuIC with τ 306 substrate was performed. Recent studies showed that τ 306 tends to aggregate faster in AD cases compared to non-AD controls (Kraus et al., 2019). Considering the fact that not all control cases characterised by AT8 antibody are pure healthy controls, we decided to split our cases further and generate three groups. Based on the results obtained from the analysis of the brain region of the temporal cortex with tau-PLA, we grouped our cases in the PLA-/AT8- group which was comprised of brain tissue where no tau aggregates were detected (N=6), PLA+/AT8- group where tau multimerization has already started in the temporal cortex but large fibrils were negligible or restricted to one or two in a couple of cases (N=5),

and PLA+/AT8+ group where both diffuse pathology and high levels of large lesions were detected in the temporal region(N=5). AT8, tau-PLA, and 4G8 large lesions, as well as, tau-PLA labelled diffuse pathology in each group were quantified and compared (Fig. 7.3).

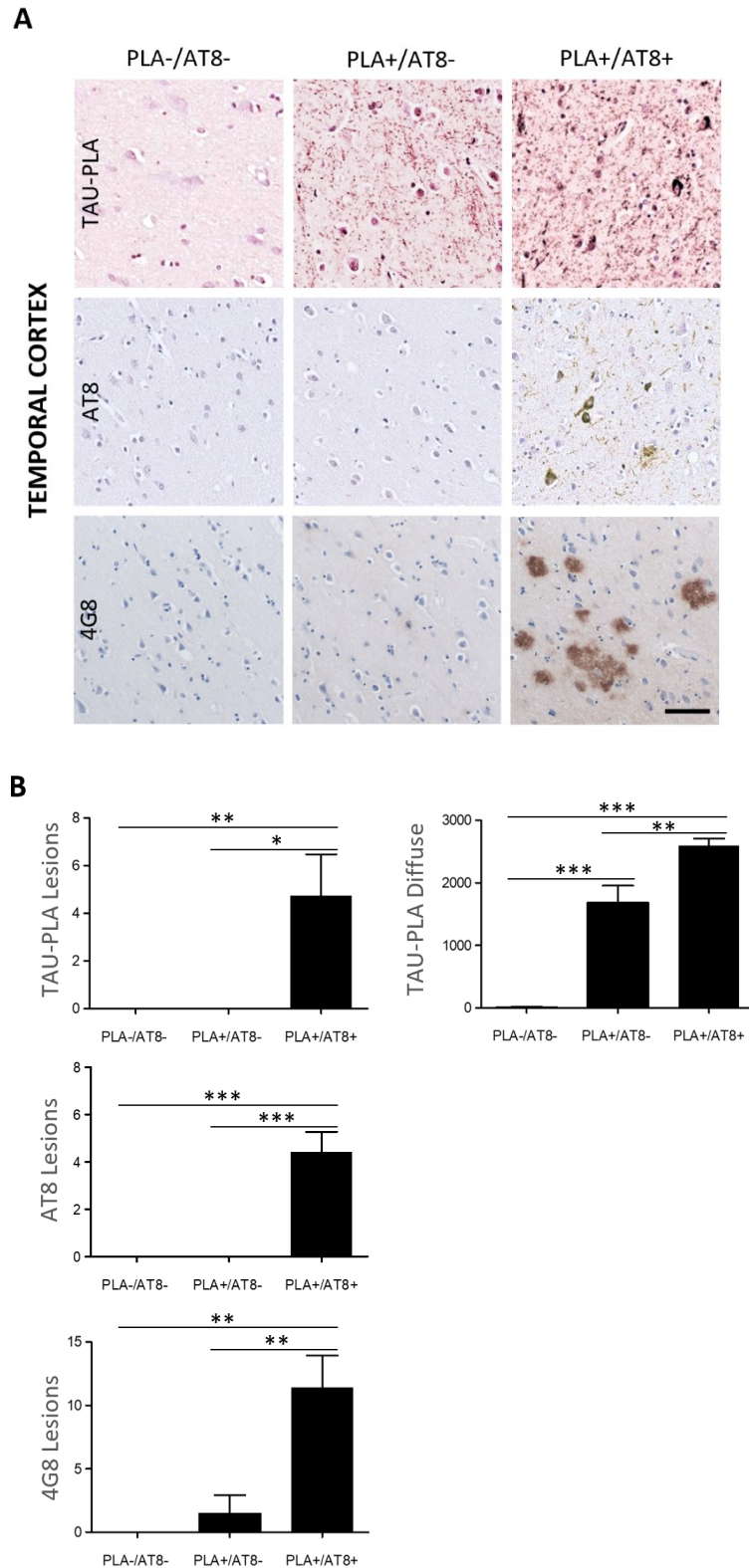


Figure 7.3 PLA-/AT8-, PLA+/AT8-, and PLA+/AT8+ groups. A) Representative images of temporal cortex from PLA-/AT8-, PLA+/AT8-, and PLA+/AT8+ groups stained with tau-PLA, AT8-IHC, and 4G8-IHC. Scale bar 50 μ m. B) Quantification of the number of lesions and diffuse pathology per field labelled with tau-PLA, AT8-IHC, and 4G8-IHC in the temporal cortex. All groups were assessed through ONE-WAY ANOVA (Tukey). N = 6/5/5. * $p < 0.05$, ** $p < 0.01$, *** $p < 0.001$.

At the first stage, tau RT-QuIC seeded with soluble τ 306 fragment or τ 306 aggregates, with or without the addition of tau KO mouse brain homogenate and N-2 supplement was performed to investigate the different conditions of the assay (Fig. 7.4A). Results showed that tau KO mouse brain homogenate and N-2 supplement are essential to prevent the spontaneous aggregation of τ 306 monomeric substrate. The addition of τ 306 aggregated species into the tau-RT-QuIC reaction solution led to rapid seeding activity of tau-based monomeric substrate (τ 306) resulting in the quick formation of τ 306 multimers (Fig. 7.4B).

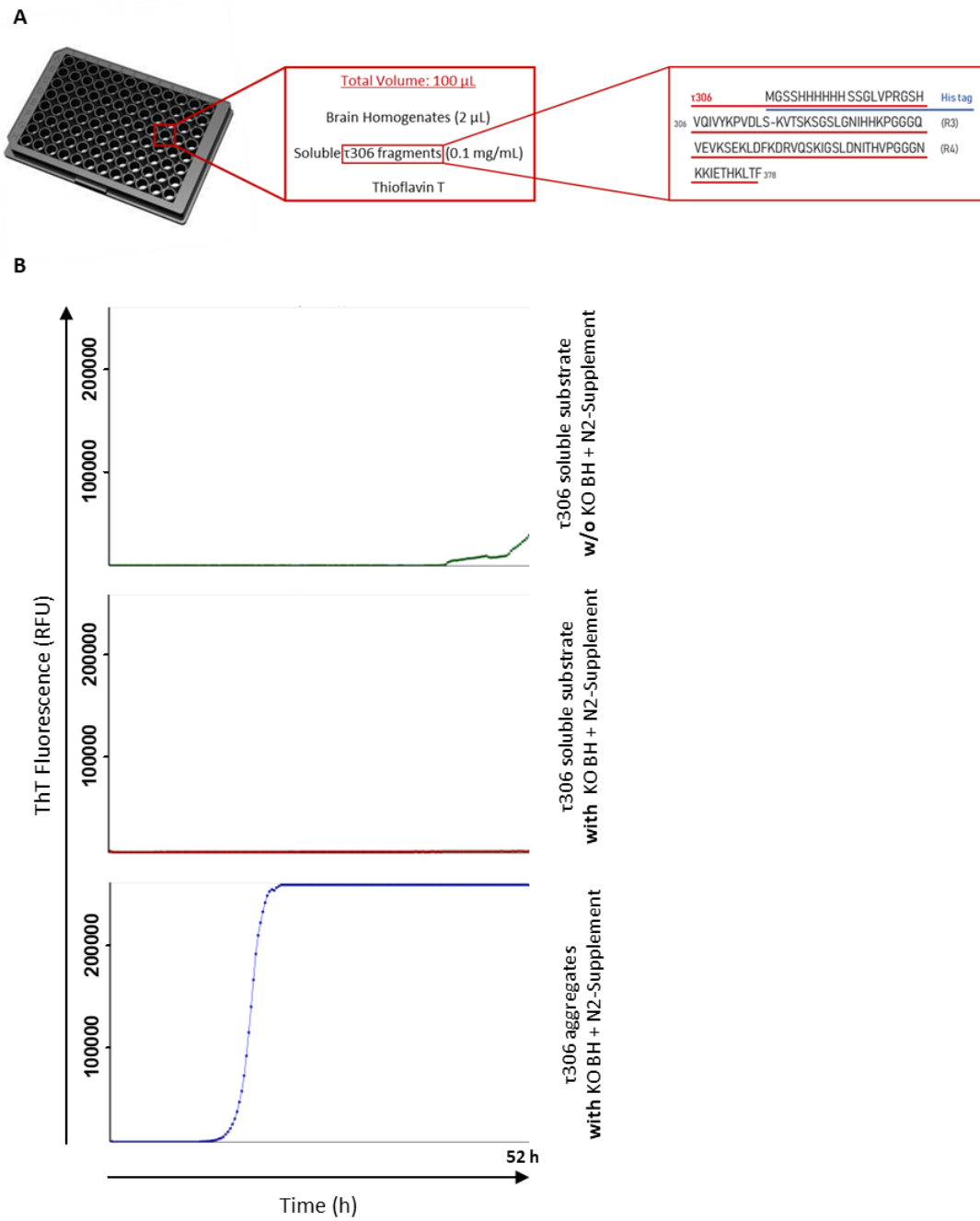


Figure 7.4 ThT fluorescence data of RT-QuIC analysis. A) Schematic representation of RT-QuIC reaction and τ 306 tau plasmid construct, consisting of residues 306–378 of full-length human tau isoform httau40 with a point mutation at residue 322 cysteine to serine. B) RT-QuIC analysis of τ 306 soluble fragments and τ 306 aggregates under different conditions (with or without N2-Supplement and KO BH). Each curve represents a single case, run in triplicate.

After assessing the assay conditions, tau-RT-QuIC analysis of brain homogenates from the temporal region of PLA-/AT8-, PLA+/AT8-, and PLA+/AT8+ cases was performed. T306 aggregates and tau KO mouse brain homogenate were used as positive and negative controls of the assay, respectively. The assay cut-off was determined to be 52 hours and had a reproducible endpoint before the spontaneous amyloid aggregation in the wells with the tau KO mouse brain homogenate. The endpoint of 52 hours was used for any data points with ThT fluorescence values at or greater than 52 hours. Brain homogenates of the PLA-/AT8- group showed slower seeding activity relative to brain tissue from PLA+/AT8- and PLA+/AT8+ groups in which τ 306 substrate presented a rapid seeding activity (Fig. 7.5A). Comparison of tau seeding activity of PLA-/AT8-, PLA+/AT8-, and PLA+/AT8+ brain homogenates of temporal cortex with RT-QuIC was performed by analysing the maximum ThT fluorescence (Fmax), the reaction time needed to reach a ThT fluorescence of the average baseline fluorescence + 5 SD (Standard Deviation) (lag time), the time to reach the maximum ThT fluorescence, and the maximum slope (Vmax). Groups with dilution 10^{-1} were assessed through ONE-WAY ANOVA (analysis of variance). The Fmax of PLA+/AT8- and PLA+/AT8+ groups were statistically higher compared to PLA-/AT8- group, with PLA+/AT8- group presenting the shortest time to reach the Fmax (Fig. 7.5B). Lag time analysis showed that the lag phase before reaching the ThT fluorescence threshold was significantly shorter in tau RT-QuIC reaction seeded with PLA+/AT8- and PLA+/AT8+ brain homogenates compared to PLA-/AT8- brain tissue (Fig. 7.5B). Finally, the Vmax of the kinetic curve of the PLA+/AT8- group was statistically higher compared to PLA-/AT8- group but not to the PLA+/AT8+ group. No statistical differences were detected between PLA-/AT8- and PLA+/AT8+ group (Fig. 7.5B). Overall, these data indicated higher seeding activity in PLA+/AT8- and PLA+/AT8+ temporal brain tissue compared to the pure healthy control lacking tau pathology.

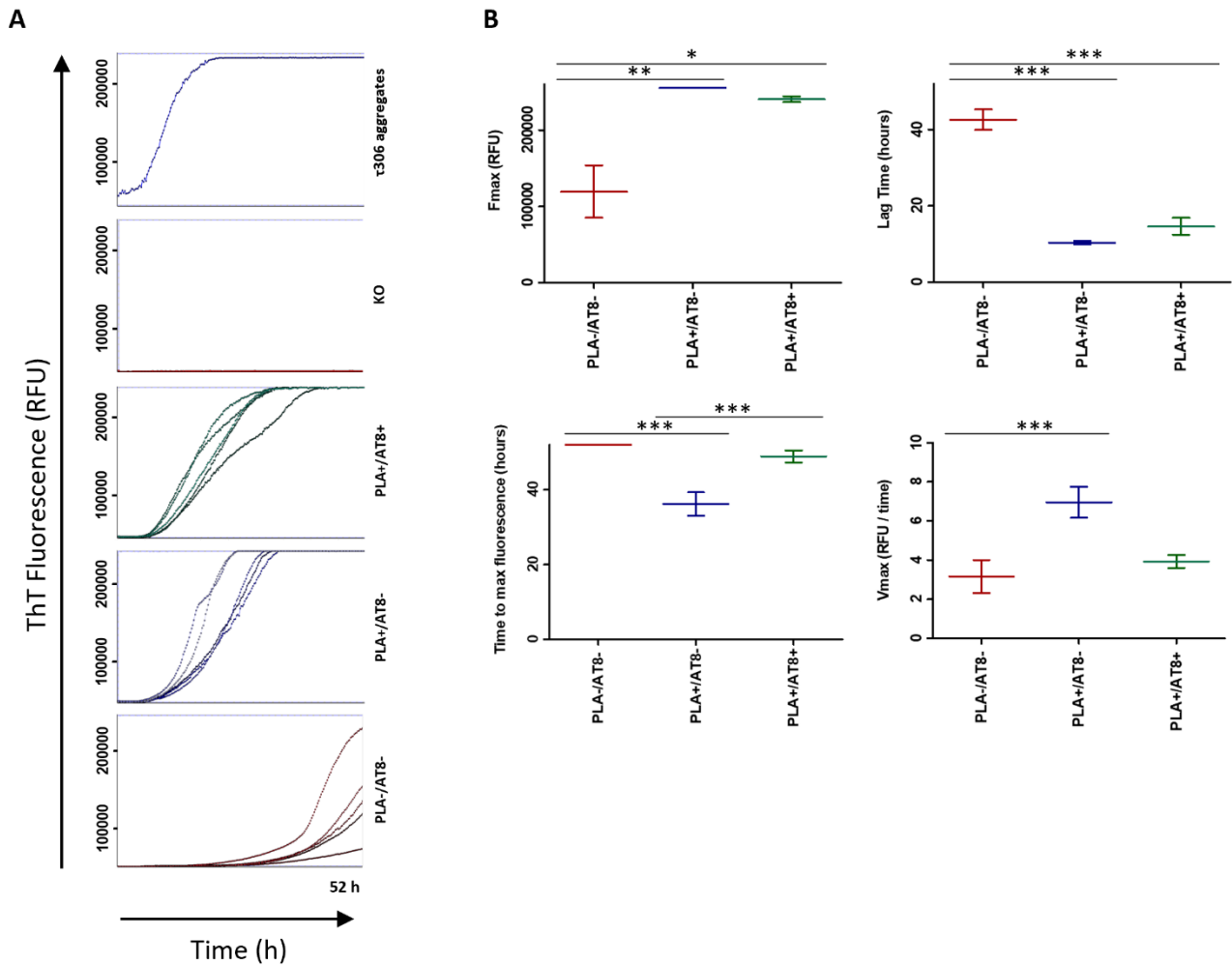


Figure 7.5 Tau RT-QuIC analysis. A) RT-QuIC dilution analysis of τ 306 aggregates, *MAPT* KO, PLA-/AT8-, PLA+/AT8-, and PLA+/AT8+ brain homogenates. Each curve represents a single case, run in triplicate. B) Comparison of tau seeding activity of PLA-/AT8-, PLA+/AT8-, and PLA+/AT8+ brain homogenates with RT-QuIC. Brain homogenates from the temporal cortex of PLA-/AT8-, PLA+/AT8-, and PLA+/AT8+ groups were analysed. Fmax (maximum ThT fluorescence), lag time (reaction time to exceed a ThT fluorescence threshold of the average baseline fluorescence + 5 SD), time to reach maximum ThT fluorescence, and Vmax (maximum slope) were analysed. The assay cut-off was determined to be 52 hours as a reproducible endpoint before the spontaneous amyloid aggregation in the wells with the tau KO mouse brain homogenate. The endpoint of 52 hours was used for any data points with ThT fluorescence values at or greater than 52 hours. Groups with dilution 1×10^{-1} were assessed through a ONE-WAY ANOVA (Bonferroni). N = 5. * $p < 0.05$, ** $p < 0.01$, *** $p < 0.001$, *AV Average*.

7.6 Discussion

After the detection of this previously unreported diffuse tau pathology, we then questioned whether these early-type tau multimers have a pathophysiological role and whether they are key drivers for the expansion of tau pathology in the AD brain. Previous findings reported that abnormal tau proteins tend to propagate and spread themselves from one brain region to the other through synaptically connected neuronal networks and other pathways where the involvement of the extracellular space and the contribution of other cell types is evident (Alafuzoff et al., 2008; Hromadkova et al., 2022; Silva and Haggarty, 2020; Yamada, 2017). To address this question we assessed the seeding capacity of multimeric tau in the AD brain using a novel but well-established seed amplification assay, the AD RT-QuIC (Kraus et al., 2019; Saijo et al., 2017). Recent research studies validated the specificity of the assay for AD tau aggregates by performing a number of experiments including seed capture experiments, examination of cross-seeding effects of other amyloid proteins like A β 42, and characterisation of the assay products (Kraus et al., 2019). T306 substrate and heparin were used to build up the assay according to previous reports (Kraus et al., 2019; Poggiolini et al., 2022). T306 is a tau fragment consisting of the residues 306-378 of the full-length 4R tau isoform with a point mutation to the residue 322, where cysteine amino acid is replaced with serine (Kraus et al., 2019; Metrick et al., 2020). The use of τ 306 substrate presents the following advantages. Firstly, in line with previous studies, fragmented monomeric tau proteins tend to aggregate more effectively compared to the total length protein (Barghorn and Mandelkow, 2002; Lim et al., 2014). Secondly, the addition of a point mutation in the tau gene also increases tau accumulation potency (Lim et al., 2014; Schweers et al., 1995). Finally, the use of heparin, a poly-anionic cofactor, promotes and enhances the formation of tau assemblies by generating paired helical-like tau fibrils (Falcon et al., 2019; Taniguchi et al., 2005). In agreement with previous findings, shaking of τ 306 fragments with heparin under defined conditions leads to the formation of tau fibrils and other polymorphic tau structures (Saijo et al., 2017). The addition of soluble τ 306 fragments or insoluble τ 306 aggregated complexes in the RT-QuIC reaction solution revealed enhanced levels of seeding activity of the monomeric tau substrate in the wells treated with tau aggregates, while the tau seeding activity appeared to be low to negligible in the wells treated with tau monomers. However, at this point, we need to mention that spontaneous accumulation of

monomeric tau was reported after hours of shaking since the τ 306 fragment has properties that facilitate self-multimerisation under specific conditions, fact that has been previously addressed by other research groups as well (Hromadkova et al., 2022; Kraus et al., 2019; Metrick et al., 2020). To avoid this spontaneous τ 306 aggregation, N-2 media supplement (Gibco 17502-048) and brain homogenate from *MAPT KO* mice were used. N-2 supplement is a serum-free media supplement essential for promoting cell growth in cell cultures. However, in this case, this reagent was used to prevent τ 306 fragments from binding to the walls of the wells of the reaction well plate resulting in the loss of monomeric substrate and the formation of random accumulations on the walls of the wells (Minikel, 2014). On the other hand, the addition of *MAPT KO* brain homogenate to the reaction solution has been reported to prevent the spontaneous substrate aggregation caused due to protein shaking under optimal conditions (protein concentration, temperature, and speed of shaking) (Kraus et al., 2019). Therefore, under these conditions, we could clearly say that the signal produced during RT-QuIC assay is the outcome of protein aggregation induced by the addition of protein seeds with defined properties (Poggiolini et al., 2022; Saijo et al., 2017). Indeed, the addition of these two elements in the assay reaction reduced the short-term assembly of the soluble tau fragments that occurred after a couple of days of shaking. Hence, the signal produced in the wells treated with the aggregated tau species indicated that these molecules are capable to induce enhanced levels of tau substrate multimerisation in a short period, in contrast to the soluble monomeric species that require more time until the first protein interactions start being evident. Based on this assay and after the *in situ* visualisation of tau multimers with the help of tau-PLA, we accessed whether these diffuse oligomeric tau molecules are potentially toxic species with seeding properties that can propagate to synaptically connected brain regions, being responsible for the progression of tau pathology in the AD brain. Analysis of the temporal cortex positive for diffuse tau pathology but negative for tau large lesions (PLA+/AT8-) revealed enhanced levels of tau seeding capacity and short RT-QuIC reaction lag phase, with values similar to the one obtained from the PLA+/AT8+ group. Here, we need to acknowledge that although in the PLA+/AT8- group a couple of cases presented a single tangle in the wider area of the temporal cortex, the comparison of these two groups proved that the existence of a single isolated tangle in some of the cases is not enough to induce enhanced levels of tau seeding activity, meaning that the lesions responsible for the seeding capacity of tau are the small-sized multimeric tau species

labelled by tau-PLA rather than the large late-type tau aggregates. If the latter were the responsible species, we would expect the PLA+/AT8+ group to present substantially higher levels of tau seeding capacity compared to the PLA+/AT8- group. In contrast to these two groups, low levels of spreading potency were reported in the pure healthy cases, indicating that these early-type tau multimers have a pathological role and could be potential targets for the development of more efficient therapeutic approaches. In agreement with these findings, is a large number of studies supporting the seeding properties and behaviour of tau multimers using various *in vivo* and *in vitro* systems for the investigation of their physiological and pathological role (Ghag et al., 2018; Holmes et al., 2014; Kaufman et al., 2017; Lasagna-Reeves et al., 2014; Metrick et al., 2020).

7.6.1 Limitations

Although much effort was applied to optimise the conditions of the assay and to ensure that our analysis remains unbiased, several limitations and restrictions needed to be addressed. Firstly, one major limitation was the lack of available frozen brain tissue due to the high demand over the years. For this reason, our analysis was restricted to 5 cases per group, a small sample number, but still powerful to allow the performance of the statistical analysis. Examination of further cases could help to establish a more validated image of the pathophysiological role of tau multimers. Another difficulty that needs to be addressed concerns the purification of τ 306 substrate, a tau protein fragment that is prone to aggregate, and the purification of pure monomeric species is a challenge (Kraus et al., 2019). To deal with this restriction, the whole experimental procedure of tau purification was performed at the low temperature of 4°C, modifying as well the steps that could facilitate the spontaneous tau assembly. Finally, focusing on the outcome of this analysis, although tau multimers are characterised by high seeding activity contributing to the progression of AD, more investigation concerning gene expression and modification should be done to uncover the underline mechanism that promotes the pathological behaviour of tau.

7.6.2 Conclusions

Overall, this analysis led to the following conclusions. Both tau RT-QuIC and tau-PLA assays detected tau-tau interactions in post-mortem human brain tissue from both AD and non-AD cases. Tau RT-QuIC revealed that the early-type tau multimers have high seeding activity and might be the potential toxic species contributing to the disease progression. In agreement with tau-PLA, tau RT-QuIC also highlighted an extensive early-type tau pathology in anatomical brain regions that appeared to be unaffected based on standard AT8-IHC. From an experimental aspect, the use of the τ 306 substrate proved to be crucial for the investigation of tau seeding activity due to its structural properties and its ability to induce aggregation, while the addition of N-2 supplement and *MAPT KO* brain homogenate to the reaction solution was critical to avoid the spontaneous assembly and binding of the tau monomeric substrate. Analysis of more cases is needed to validate further these findings.

Chapter 8: General Discussion

The abnormal intraneuronal aggregation and misfolding of tau, a microtubule-associated protein, in the central nervous system is one of the main pathological hallmarks of tauopathies, with AD being the most common neurodegenerative disorder (Goedert et al., 2017; Lee et al., 2001). Although the large tau lesions such as NFTs, NTs, and neuritic plaque-associated tau were considered to be primarily responsible for the progression of tau pathology in the AD brain, accumulating evidence nowadays supports that these soluble aggregated tau molecules, rather than the late-type tau large lesions, are the potential toxic species with seeding capacity that spread themselves in a prion-like manner, behaving as invisible killers given that we lack a robust technique for their detection (Ghag et al., 2018; Gómez-Isla et al., 1997; Holmes et al., 2014; Kaufman et al., 2017; Liu et al., 2012; Metrick et al., 2020).

Proximity ligation assay (PLA), first developed by Soderberg and his group in 2006, is a technique that allows the specific detection of protein-protein interactions directly in cells and tissues preserving the cellular and anatomical morphology (Söderberg et al., 2006). Although PLA was mainly used for the investigation of heterotypic protein interactions *in situ*, PLA is currently used for the detection and examination of homotypic protein multimerisation (Mazzetti et al., 2020; Roberts et al., 2019, 2015; Sekiya et al., 2019). Based on a recently developed assay, the alpha-synuclein proximity ligation assay (AS-PLA), for the specific visualisation of α -synuclein oligomers *in situ* (Roberts et al., 2019; Roberts, Wade-Martins, & Alegre-Abarategui, 2015), we have now developed a relevant assay for the histopathological detection of tau-tau interactions in animal and human tissue with anatomical and subcellular detail. This assay is called tau proximity ligation assay (tau-PLA) and enables the direct visualisation of tau multimerisation *in situ*.

Tau self-aggregation in FFPE sections from the brain regions of the hippocampus and temporal cortex from 67 post-mortem human brains from Braak stage 0 to VI was investigated using tau-PLA. The temporospatial distribution of tau-PLA labelled pathology was analysed and compared with other histopathological markers responsible for the detection of hyperphosphorylated and misfolded tau. Finally, the pathophysiological role of these tau multimers was examined by investigating their

seeding capacity using a seed amplification assay. As expected, our assay detected tau-tau interactions with high specificity and sensitivity, but no tau monomers. In addition, tau-PLA managed to capture a range of tau pathology, from large tau lesions to a previously unreported widespread diffuse tau pathology developed also in brain regions that appeared to be devoid of any other pathology, ahead and beyond the appearance of tau molecules exhibiting hyperphosphorylation and conformational changes from the earliest Braak stages. Finally, investigation of the pathophysiological role of these early-type tau aggregates revealed that these species are characterised by high seeding capacity, being able to induce tau aggregation, and could be the potential targets for the development of more efficient therapeutic approaches.

Although the PLA is a well-established assay for the detection of heterotypic protein interactions, the use of the assay for the investigation of homotypic protein multimerisation generates questions about the specificity of the assay, with several studies supporting the low significance of the *in situ* PLA (Alam, 2018; Alsemarz et al., 2018; Lindskog et al., 2020). To address this limitation, before moving to the analysis of the human brain tissue with tau-PLA, several experiments were performed to further support the specificity of the assay. As performed previously by Roberts and colleagues for the development of alpha-synuclein PLA (AS-PLA), with the use of various cell-based assays (BiFC assay and FKBP-FRB system) and tau aggregation inducible systems, we managed to prove that tau-PLA is a sensitive and selective tau multimerisation detection technology with high specificity for tau-tau interactions but no monomeric tau molecules (Roberts et al., 2019, 2015). Loss of tau-PLA signal after the depletion of the ligation step or replacement of the tau5 antibody with a different antibody detecting protein molecules that are not normally expressed in the brain, supported as well that the signal obtained is a result of productive tau-PLA and that tau-PLA is an antibody-dependent assay. Finally, to further validate our assay, analysis of animal brain tissue was performed. Brain tissue from *MAPT KO* mice, a mouse model that lacks the expression of tau protein in the brain due to genetic modifications, was investigated with tau-PLA. As expected, no tau-PLA signal was detected in the brain tissue of these mice highlighting the selectivity of our assay and excluding the possibility of the non-specific binding of the PLA elements. The lack of tau-tau interactions in the *MAPT KO* mice has also been described in other research studies where no tau seeding activity was spotted after the effort of inducing tau

multimerisation (Holmes et al., 2014; Kaufman et al., 2016b; Kraus et al., 2019; Saijo et al., 2017). In contrast, enhanced levels of tau-PLA signal were observed in the brain tissue of P301S mice, a mouse model of human tauopathy, where the formation of tau fibrillar lesions is evident by the age of 6 months old (Holmes et al., 2014; Kaufman et al., 2016b). Tau-PLA also captured tau-self interactions in anatomical brain regions that appeared to be unaffected based on standard histopathological markers, indicating that the process of tau multimerisation has already started (Allen et al., 2002; Holmes et al., 2014).

With most of the histopathological studies being unable to visualise these tau-tau interactions in tissue, tau-PLA allowed the detection of a previously unreported early-type, small-sized diffuse tau pathology. Tau-PLA labeled a range of tau structures, from the late-type large lesions that were also captured by other standard histological markers, to the early-type small-sized diffuse tau pathology whose visualisation until now was a challenge. We can therefore claim that the staining pattern of tau-PLA can be mostly divided into two main groups, the diffuse small-sized tau pathology, and the large tau lesions.

Moving to the analysis of the disease-related endogenous tau in the post-mortem human brain, after determining the Braak stage of each case based on the staging system proposed by Alafuzoff and colleagues (Alafuzoff et al., 2008), all cases were analysed with tau-PLA. In addition, each case was further examined with additional antibodies that detect early tau post-translational modifications and more precisely early hyperphosphorylated or misfolded tau.

Focusing on the large tau lesions, assessment of post-mortem human brain tissue from the different brain regions revealed that tau-PLA detected the large fibrillar tau lesions in a similar pattern with the AT8 antibody, presenting however reduced sensitivity compared to AT8-IHC for these large lesions. This difference in the detection power of these two assays proved to be due to the superiority of the AT8 antibody to the tau5 antibody for the large tau lesions, a fact supported by previous studies that suggest that the binding ability of the tau5 antibody, the antibody used for the build-up of our assay, can be affected by the nearby phosphorylated sites (Porzig et al., 2007). Following the same pattern as the other early histological markers, tau-PLA captured a significant number of large tau lesions from the Braak stage II to VI in the hippocampal region,

with the involvement of the TC in Braak stage III. Involvement of the OC was observed in the later Braak stages. Comparison of the detection power of the other tau markers for the large lesions showed, similarly to previous records, that the early phosphor-tau antibodies investigated presented higher sensitivity for the large lesions than the conformational antibodies (Ercan-Herbst et al., 2019; Holmes et al., 2014).

Moving to the diffuse tau multimerisation, under physiological conditions, no tau-PLA or tau-IHC staining signal was detected in the Braak stage 0 cases revealing that tau multimerisation does not occur physiologically in the brain and that the tau molecules remain monomeric lacking any PTM. At this point, we need to mention that in a minority of Braak 0 cases, tau-PLA revealed that tau self-interaction had already started. However, further investigation is essential to determine whether these multimers are pathological contributing to the disease progress, or have a physiological role (Wang and Mandelkow, 2016, 2012). From Braak stage I, high levels of diffuse tau pathology were captured by tau-PLA, followed by AT180-IHC. Until today AT180, was one of the best markers used for the detection of early-type tau pathology, being able to capture tau protein modification in the brain regions of the hippocampus from the earliest Braak stages (Ercan-Herbst et al., 2019). However, its sensitivity proved to be lower compared to tau-PLA, with tau-PLA being able to capture significantly high levels of the tau diffuse pathology from Braak stage I in the hippocampal area. The lack of positive staining signal from the rest of the histological markers in the early Braak stages revealed that tau multimerisation is one of the earliest detectable molecular events occurring during the development of tau pathology in the AD brain, preceding the events of tau hyperphosphorylation and misfolding. These tau-tau interactions have been described previously in various cell-based and seed amplification assays, however, the lack of the direct visualisation of these tau multimers was always a major limitation (Holmes et al., 2014; Kaufman et al., 2017; Kraus et al., 2019; Metrick et al., 2020; Saijo et al., 2017). Tau-PLA managed to overcome this limitation, providing essential information about the morphology, three-dimensional structure, folding, maturity, aggregation level, and cellular and anatomical location of these tau species. The tau-PLA signal was significantly increased from Braak stage I to III with the amount of the diffuse tau-PLA signal being slightly decreased in the later Braak stages. One possible explanation is that the NFTs could act as a sink for the tau multimers and therefore, the increase in the number of large tau lesions in the late Braak stages will

contribute to the further reduction in the levels of the earlier pathological tau species (Castellani et al., 2008; Kuchibhotla et al., 2014). Another possible explanation lies in the increase in the number of ghost tangles that seems to lack tau-PLA staining due to the loss of the epitope recognised by the tau5 antibody in the ghost tangles, and therefore, cannot be visualised *in situ* (Fitzpatrick et al., 2017; Porzig et al., 2007). Both explanations could be the case with the first one being stronger as reduced levels of tau multimerisation in the later Braak stages have been described as well in previous research studies investigating tau seeding activity (Metrick et al., 2020).

At this point, we need to admit that uncovering the temporospatial distribution of tau pathology from post-mortem brain tissue from AD and non-AD cases provided important information about AD progression, however, there are several questions and limitations that need to be addressed. The temporal sequence of the events as described by tau-PLA does not establish causality. We cannot state unequivocally that these early-type tau multimers will turn to hyperphosphorylated or misfolded large fibrillar lesions while the disease progresses as each tau molecule could follow a different distinct pathway and fate based on various genetic, epigenetic, and environmental factors. We could not also confirm whether these diffuse multimers used to be part of the large lesions. However, this hypothesis is not strong enough as we would expect the tau-PLA signal to be stronger in the areas around the large lesions, but this is not the case as enhanced levels of tau-PLA-labelled diffuse pathology are spotted in areas devoid of fibrillar tau lesions. Finally, tau-PLA cannot provide information about the pathophysiological role and the seeding capacity of these multimeric species, and therefore, we could not confirm whether these diffuse tau multimers are the potential toxic species promoting the neuronal cell death or whether this diffuse pathology could be part of the normal aging process. To address this question investigation of the pathophysiological role of these species was performed using a seed amplification assay, specific for the detection of tau seeding activity, the tau RT-QuIC.

Although RT-QuIC assay is a useful tool for the investigation of aggregated tau pathophysiological role, the use of heparin for the induction of aggregation had been described to be the major limitation of the assay, as the morphological architecture of the formed heparin-induced tau seeds seems to present differences with the structure from the aggregates extracted from the brain tissue of AD patients (Zhang 2019). For this reason, the development of a robust technique for the *in situ* visualisation of these

aggregated tau species can be the key to overcoming this limitation, providing us with information concerning the structural morphology and the anatomical location of these conformers. Such an assay is tau-PLA which allows the direct visualisation of tau-tau interactions with high specificity and sensitivity on normal cells and tissue. Although this assay overcomes the limitation of RT-QuIC, the investigation of the seeding potential of these small diffuse multimers needs additional approaches. Taking all these data together, we can clearly say that coupling these two assays could be an interesting approach for the investigation of tau-tau interactions and their role in the progression of tau pathology in the AD brain. Application of tau-PLA in human post-mortem brain tissue from individuals from Braak stage 0 to VI, revealed a previously unreported early type of tau pathology characterised by an extensive diffuse tau distribution in anatomical brain regions that appeared to be unaffected, with this pathology lacking specific early tau PTMs. Investigation of the seeding capacity of these early-type tau multimers (PLA+/AT8-) revealed an extensive ability of propagation in these tau conformers, similar to the one presented by the large tau lesions (PLA+/AT8+). This fact highlights that early-type tau multimers could be the major responsible factors for the progression of the pathology in the AD brain. The pathological role of tau-tau interactions has been investigated using cell-based assays, such as FRET, as demonstrated by DeVos et al. (DeVos et al., 2018). In agreement with our findings, the researchers here, by using biosensor cells for the detection of aggregated tau species in human brain lysate samples, found high levels of tau seeding in the entorhinal cortex, even in cases with rare neurofibrillary tangles. Similar to our study, tau seeding was also detected in non-pathological regions of the brain along the Braak tau pathway, suggesting the existence of soluble tau aggregates prior to the development of overt tau pathology (DeVos et al., 2018). Despite the promise of biosensor cell lines for investigating tau multimerisation, the use of large fluorescence molecular tags can interfere with tau interactions and potentially produce conflicting results, as highlighted by Lim et al. (Lim et al., 2014). A recent study published by Kaniyappan and colleagues proved that the FRET signal produced after the application of the FRET assay for the evaluation of the tau multimerisation process in AD is independent of the tau self-propagation, but other factors contribute to the development of this FRET signal (Kaniyappan 2020). Other assays, like the BiFC cell-based assay that was also used for the establishment of tau-PLA specificity, could be used instead as the GFP fragments/splits that are fused to the recombinant tau molecules have small size

reducing the interference of the tags in tau-tau interactions induced by the addition of brain homogenate extracts from the three groups (Kerppola, 2013; Lim et al., 2014). Regardless of the unanswered questions, we believe that our study will shed new light and open potential new avenues into the investigation of the early pathology and the driving mechanisms of AD, the development of therapies and biomarkers, and the establishment of preventive strategies.

8.1 Limitations

Both the experimental work and the tissue analysis of the study contained limitations that needed to be addressed. As far as it concerns the tau-PLA protocol, the high cost of the PLA kits, as well as the longer duration of the protocol are some of the main limitations of the assay. For a successful tau-PLA, good quality tissue is essential, and therefore tissue over-fixation should be avoided. Tissue kept in formalin for many decades should be re-examined as it might present alternations in its composition and structure that would affect the experimental procedures. Finally, the reduced availability of the PLA kits due to reduced production and prolonged periods of delivery from the USA delayed significantly the analysis of the available tissue and forced us to reduce the number of cases and brain regions investigated to avoid running out of reagents during the performance of tau-PLA. Regarding tissue availability, obtaining the essential frozen tissue for our study was also a minor restriction as several brain regions from the different Braak stages were not available due to oversampling through the years. For this reason, we had to reduce the number of cases investigated per group to 5, a small sample number, but still powerful to allow the performance of the statistical analysis. Regarding the brain tissue analysis, although tau-PLA can detect a previously unreported, early-type, small-sized diffuse tau pathology in animal and post-mortem human brain tissue providing information about the morphology of these multimers and their temporospatial distribution, it cannot provide direct outcomes about the pathophysiological role and the molecular mechanisms that lead to their generation. Although tau RT-QuIC tried to address this limitation by providing significant information about these multimeric tau species, their seeding activity, and their potential toxicity, more investigation focusing on the gene expression and modification

is essential to uncover the underline mechanisms that promote the pathological behaviour of tau.

8.2 Future directions

Therefore, in the future, it would be interesting to determine the differentially expressed genes related to the early-type tau multimerisation as we hypothesize that epigenetic changes are occurring in parallel or earlier with the early tau-tau interactions, and spotting them will help us to understand what is happening in the brain in the first place. To achieve this, DNA methylation analysis and single-cell RNA sequencing are currently being performed. DNA methylation analysis will help us to investigate how the methylation of different genes affects their expression (Yong et al., 2016), while single-cell RNA sequencing will provide the transcriptional profile of a large number of individual cells within a heterologous sample (Hwang et al., 2018). Our cases once again were separated into the three main groups as characterised by tau-PLA and AT8-IHC, one group with the pure healthy control cases (tau-PLA-/AT8-), one where tau multimerization has already started in the temporal cortex but large fibrils were negligible or restricted to the minimal presence of one or two isolated tangles in a couple of cases (tau-PLA+/AT8-), and one positive for both early-type and significant late-type tau pathology (tau-PLA+/AT8+). Next, we aim to further investigate the differentially expressed genes detected by the transcriptomics analysis and examine their expression *in situ* with IHC and Western Blot (levels of expression, subcellular location, etc.). Analysis of the inflammatory environment of the brain by investigation of the morphology, activation, and location of brain immune cells and the levels of pro-inflammatory and anti-inflammatory cytokines is one of the future goals of this project. Post-mortem human brain sections from tau-PLA+/AT8- and tau-PLA+/AT8+ brain regions from AD patients, as well as, the respective regions from controls (tau-PLA-/AT8-) will be analysed using specific markers for the detection of microglia (Iba1, TMEM199, CD68), astrocytes (GFAP), infiltrating leukocytes in the brain (CD45) and T and B cells (CD3, CD4, and CD8) (Cameron and Landreth, 2010; Di Benedetto et al., 2022; Heneka et al., 2015; Paouri et al., 2017; Wyss-Coray and Rogers, 2012). To further support our findings, western blotting analysis will be also employed for the same markers. The brain inflammatory environment will be investigated by analysing

the levels of pro- and anti-inflammatory cytokines and chemokines using ELISA (Heneka et al., 2015; Wyss-Coray and Rogers, 2012). Finally, the comparison of the post-mortem human brain tissue from patients with other tauopathies and neurodegenerative disorders with human tissue derived from AD patients is the last objective to be achieved. After detecting the brain regions that are most affected by the pathological lesions of each disease by performing IHC, we will stain them with tau-PLA and we will investigate and compare the tau pathology between AD and related disorders.

8.3 Conclusions

In conclusion, we have now developed a selective and sensitive assay, tau-PLA, that allows for the first time the direct visualisation of self-interacting tau molecules, but no monomeric, both *in vitro* and *in situ* with high specificity. Our assay detected a previously unreported early-type diffuse tau pathology in subcellular and anatomical brain regions ahead of other standard histopathological markers, revealing that tau multimerisation precedes tau hyperphosphorylation and conformational changes, being one of the earliest detectable molecular events of the AD tau pathology. Investigation of the pathophysiological role of these multimeric tau species also revealed their extensive seeding capacity, defining them as the potentially toxic species contributing to the disease progression. Further optimisation of the assay could allow the detection of tau-tau interactions in human biofluids like CSF, providing a powerful tool for the early diagnosis of AD and related tauopathies. Overall, this assay could open a window for the investigation of early-type tau pathology, the discovery of the driving mechanisms of disease, and the development of more effective therapeutic approaches and strategies.

Appendix

Table 2.6 - Solutions and Regents

	Reagent	Recipe
Bacterial Work	Kanamycin 50 µg/µl	1 g kanamycin powder (SIGMA, K4000) dissolved in 20 ml of ddH ₂ O. Filtered with a 0.22 µm syringe filter (Thermo, 723-2520), aliquoted in 1 ml aliquots, and stored at -20 °C.
	Luria-Bertani (LB) Broth	20 g LB Broth powder (SIGMA-ALDRICH, L3022) dissolved in 1 L of ddH ₂ O. Autoclaved and stored at RT.
	LB/agar kanamycin plates	10 g LB Broth powder (SIGMA-ALDRICH, L3022) and 7.5 g agarose dissolved in 500 ml of ddH ₂ O, autoclaved and cooled down in a water bath at 42 °C. The solution was supplemented with 500 µl kanamycin 50 µg/µl and poured into plates. Plates were stored at 4 °C for up to four weeks.
Molecular work	TAE buffer (1X)	20 ml TAE Buffer (50X) (AppliChemin, A1691,1000) was diluted in 1 L of ddH ₂ O total volume. Stored at RT.
	Quick-load purple 1 kb DNA ladder	10 µl 1 kb DNA Ladder (NEB, N3232) was mixed with 10 µl 6x Gel Loading Dye Purple (NEB, B7024S) and 40 µl of ddH ₂ O. Stored at -20 °C.
	1 M Isopropyl-β-D-thio-galactopyranoside (IPTG)	238.3 g of IPTG (Melford, 367-93-1) dissolved in 1 ml of ddH ₂ O. Stored at -20 °C.
	2ZY Component	10 g of Yeast Extract (SIGMA-ALDRICH, Y1625) and Bactotryptose (tryptone) (BD Bioscience, 211699) dissolved in 1 L ddH ₂ O. Autoclaved and stored at RT.
	1 M MgSO ₄	6.0185 g MgSO ₄ (SIGMA-ALDRICH, 229784) dissolved in 50 ml ddH ₂ O. Stored at RT.

20 x NPSC	5.35 g NH ₄ Cl (SIGMA-ALDRICH, V000113), 3.22 g Na ₂ SO ₄ (SIGMA-ALDRICH, 238597), 6.8 g KH ₂ PO ₄ (SIGMA-ALDRICH, P5655), and 7.1 g Na ₂ HPO ₄ (SIGMA-ALDRICH, S9763) dissolved in 100 ml ddH ₂ O. pH adjusted at 6.75. Autoclaved and stored at RT.
50 x LAC	10 ml α-Lactose (SIGMA-ALDRICH, L2643), 2.5 ml Glucose (SIGMA-ALDRICH, S8644), and 25 ml Glycerol (SIGMA-ALDRICH, G5516) dissolved in 70 ml ddH ₂ O. Glycerol was added in the end. The solution was filtered with a 0.22 μm syringe filter (Thermo, 723-2520). Extra ddH ₂ O was added to make up the final volume of 100 ml. Stored at RT.
Trace Elements	1.0 g FeSO ₄ · 7H ₂ O (SIGMA-ALDRICH, F8633), 8.8 g ZnSO ₄ · 7H ₂ O (SIGMA-ALDRICH, 227316), 0.4 g CuSO ₄ · 7H ₂ O (SIGMA-ALDRICH, C3036), 0.15 g MnSO ₄ · 4H ₂ O (SIGMA-ALDRICH, 229784), 0.1 g Na ₂ B ₄ O ₇ · 10H ₂ O (SIGMA-ALDRICH, S9640), and 0.05 g (NH ₄) ₆ Mo ₇ O ₂₄ · 4H ₂ O (SIGMA-ALDRICH, 12054-85-2) dissolved in ¾ of 1 L ddH ₂ O. 0.2 ml HCl was added to dissolve the crystals that appeared. ddH ₂ O was added to make up the final volume of 1 L. Filtered with a 0.22 μm syringe filter (Thermo, 723-2520). Stored at RT.
Autoinduction bacterial culture media: 2ZYM – 2 x LAC	372 ml 2ZY Component, 800 ml 1 M MgSO ₄ , 20 ml 20 x NPSC, 16 ml 50 x LAC, 400 μl Trace Elements. ddH ₂ O was added for the final volume of 400 ml. MgSO ₄ was added before 20 x NPSC to avoid precipitation. The medium was kept sterile and stored at RT.
10 mM Tris, pH 8.0	6.057 g Tris Base (SIGMA-ALDRICH, T1503) dissolved in 40 ml ddH ₂ O. pH adjusted to 8.0 using 1M HCl (SIGMA-ALDRICH, H9892). Extra ddH ₂ O was added to make up the final volume of 50 ml. Stored at RT.

PMSF Protease Inhibitor	20 mg PMSF Protease Inhibitor (ThermoFisher, 36978) dissolved in 1 ml ddH ₂ O. Stored at 4 °C.
FPLC Buffer A	25 mM Na ₂ HPO ₄ (SIGMA-ALDRICH, S9763), 150 mM NaCl (SIGMA-ALDRICH, S7653), 10 mM Tris, pH 8.0, and 10 mM Imidazole (SIGMA-ALDRICH, I2399). Stored at 4 °C.
FPLC Buffer B	25 mM Na ₂ HPO ₄ (SIGMA-ALDRICH, S9763), 150 mM NaCl (SIGMA-ALDRICH, S7653), 10 mM Tris pH 8.0, and 500 mM Imidazole (SIGMA-ALDRICH, I2399). Stored at 4 °C.
8 M guanidine hydrochloride in PBS	38.212 g guanidine hydrochloride (SIGMA-ALDRICH, G3272) dissolved in 50 ml PBS. Filtered with a 0.22 μm syringe filter (Thermo, 723-2520). Stored at 4 °C.
25 Mm Ammonium Hydrogen Carbonate	3.956 g Ammonium Hydrogen Carbonate (SIGMA-ALDRICH, 09830) dissolved in 2 L ddH ₂ O. Filtered with 0.22 μm syringe filter (Thermo, 723-2520). Stored at 4 °C.
10 x Running Buffer (10x Tris/Glycine/SDS Buffer pH 8.0)	30.2 g Tris Base (SIGMA-ALDRICH, T1503), 144 g Glycine (SIGMA-ALDRICH, G7126), and 10 g SDS (SIGMA-ALDRICH, L3771) were dissolved in 1 L ddH ₂ O. pH was adjusted at 8.0. using 1M NaOH. Stored at 4 °C.
1 x Running Buffer	100 ml of 10 x Running Buffer was diluted with 900 ml ddH ₂ O. Stored at RT.
100 Mm Sodium Acetate	0.82 g Sodium Acetate (SIGMA-ALDRICH, W302406) dissolved in 100 ml ddH ₂ O. pH adjusted to 7.4 using 1M NaOH. Stored at RT.
1 x PBS	5 PBS tablets (SIGMA-ALDRICH, P4417) in 1 L ddH ₂ O. Stored at RT.

1M NaOH	4 g NaOH (SIGMA-ALDRICH, S5881) dissolved in 100 ml ddH ₂ O. Stored at RT.
1 M Tris, pH 7.4 or pH 7.5	127 g Tris HCl (SIGMA-ALDRICH, T3253) and 23.6 g Tris Base (SIGMA-ALDRICH, T1503). pH adjusted to 7.4 or 7.5 using 1M NaOH. Stored at RT.
50 mM HEPES pH 7.4	0,119 g HEPES (SIGMA-ALDRICH, H3375) dissolved in 10 ml ddH ₂ O. The solution was vortexed and stored at 4 °C. pH was adjusted to 7.4 using 1M NaOH. Stored at 4 °C. Stored at 4 °C.
2 M NaCl	1.1688 g NaCl (SIGMA-ALDRICH, S9888) dissolved in 10 ml ddH ₂ O. Stored at 4 °C to be chilled before use.
10 mg/ml Heparin	0,1 g Heparin (SIGMA-ALDRICH, H6279) dissolved in 10 ml ddH ₂ O. Stored at 4 °C.
10 mM ThT stock	31.8 mg of ThT dissolved in 10 ml of Tris buffer, pH 8.0. 5% NaN ₃ (SIGMA-ALDRICH, S2002) was added so that the final NaN ₃ concentration was 0.01%. Filtered with a 0.22 µm syringe filter (Thermo, 723-2520) and stored at 4 °C.
500µM ThT	20 µL 10 mM ThT stock dissolved in 180 µL ddH ₂ O. Vortexed and stored at 4 °C.
10% W/V Knock-out mouse brain homogenate (KO BH)	For 50 ml homogenate buffer: 1.25 ml 1 M Tris, pH 7.4, 3,4 ml 2 M NaCl, and 0,135 ml 1M KCl dissolved in 50 ml ddH ₂ O. 4 ml homogenate buffer was added to 0.4 g frozen tissue from the KO mouse brain. Tissue Ruptor (Qiagen, 9002755) and disposable probes (Qiagen, 990890) were used to homogenate the tissue. After the solution was homogenous, the homogenate was split into tubes and centrifuged at 13300 rpm for 15 minutes at 4 °C.

		Supernatant was transferred to new tubes and stored at -80 °C.
	N2/HEPES	1 ml of 50 mM HEPES, pH 7.4. dissolved in 5 ml ddH ₂ O. 50 µL of 100 x N2 (Gibco 17502-048) was added in the 5 ml of 10 mM HEPES, pH 7.4.
	KO/N2/HEPES	27.7 µL K/O mouse brain homogenate added in 500 µL N2/HEPES, pH 7.4.
	Protease and Phosphatase Inhibitors in TBS	Pierce Protease and Phosphatase Inhibitor Mini Tablets (ThermoFisher, A32959) dissolved in 3 ml TBS.
Cellular work	EDTA - Trypsin (1X)	5 ml 10X EDTA-Trypsin (SIGMA-ALDRICH, T4174) in 45 ml Dulbecco's Phosphate Buffered Saline (SIGMA, D8537). Stored at 4 °C.
	Complete Dulbecco's Modified Eagle's Medium-high glucose (10% FCS)	10% Fetal calf serum (FCS) (SIGMA-ALDRICH, F7524), 1% 200 mM L-glutamine (SIGMA-ALDRICH, G7513), and 1% 100 U/ml Penicillin/Streptomycin (SIGMA-ALDRICH, P4333) in Dulbecco's Modified Eagle Media (SIGMA-ALDRICH, D6546). Stored at 4 °C.
	4% Paraformaldehyde (PFA)	4 g PFA (SIGMA-ALDRICH, P6148) dissolved in 70 ml ddH ₂ O and mixed by stirring at ~60 °C. 1 M NaOH was added dropwise until PFA is completely dissolved. pH adjusted to 7.4 using 1M NaOH. Extra ddH ₂ O was added to make up the final volume of 100 ml. Store in aliquots at -20°C. Once thawed, store at 4°C for up to 2 weeks.
	Poly-D-lysine stock solution (0.1 mg/ml)	5 mg Poly-D-lysine hydrobromide (SIGMA-ALDRICH, P6407) dissolved in 50 ml tissue culture (TC) H ₂ O bottle (SIGMA-ALDRICH, W3500). Store at 4°C.
	Poly-D-lysine (50 µg/ml)	Equal volumes of poly-D-lysine stock solution (0.1 mg/ml) mixed with TC H ₂ O (SIGMA-ALDRICH, W3500).

Animal work	4% PFA in PBS	4 g PFA (SIGMA-ALDRICH, P6148) dissolved in 70 ml ddH ₂ O and mixed by stirring at ~60 °C. 1 M NaOH was added dropwise until PFA is completely dissolved. The solution was supplemented with 5 PBS tablets (SIGMA-ALDRICH, P4417). pH adjusted to 7.2 using 1M NaOH. Extra ddH ₂ O was added to make up the final volume of 100 ml. Filtered through Whatman 3 mm Chromatography Paper (20 x 20 cm) (SLS, CHR1128) and kept in ice until use. Stored at -20 °C.
	30% sucrose – NaN ₃	3 PBS tablets (SIGMA-ALDRICH, P4417), 180 g Sucrose (SIGMA-ALDRICH, 84097), and 0.12 g NaN ₃ (SIGMA-ALDRICH, S2002) dissolved in 400 ml ddH ₂ O. Extra ddH ₂ O was added to make up the final volume of 600 ml ddH ₂ O. Stored at 4 °C.
Immunohistochemistry (IHC)	10 x TBS	80 g NaCl (SIGMA-ALDRICH, S7653) dissolved in 100 ml 1M Tris pH 7.5. Extra ddH ₂ O was added to make up the final volume of 100 ml. Stored at RT.
	1 x TBS	100 ml of TBS diluted in 900 ml ddH ₂ O. Stored at RT.
	0.3% H ₂ O ₂ in PBS	3 ml 30% H ₂ O ₂ (SIGMA-ALDRICH, H1009) diluted in 300 ml PBS final volume.
	3% H ₂ O ₂ in PBS	30 ml 30% H ₂ O ₂ (SIGMA-ALDRICH, H1009) diluted in 300 ml PBS final volume.
	Antigen Retrieval Buffer, pH 6.0	5 ml Antigen Retrieval Buffer 100x, pH 6.0 (Abcam, 93678) diluted in 500 ml final volume of ddH ₂ O. Stored at 4 °C.
	Normal Goat Serum (NGS) Blocking Buffer (for IHC)	10 ml NGS (Vector Laboratories, S-1000-20) diluted in 100 ml PBS or TBS final volume.
	Normal Horse Serum (NHS) Blocking Buffer (for IHC)	10 ml NHS (Vector Laboratories, S-2000-20) diluted in 100 ml PBS or TBS final volume.
	5% Milk Blocking Buffer	5 g Skim milk powder (Millipore, 70166) dissolved in 100 ml TBS final volume.

	TBS - 0.05% Tx Wash Buffer	250 μ l Triton-X-100 (SIGMA-ALDRICH, x100) dissolved in 500 ml TBS. Stored at RT.
	TBS - 0.1% Tx Wash Buffer	500 μ l Triton-X-100 (SIGMA-ALDRICH, x100) dissolved in 500 ml TBS. Stored at RT
PLA	10 % H ₂ O ₂ in PBS	80 ml 30% H ₂ O ₂ (SIGMA-ALDRICH, H1009) diluted in 240 ml ddH ₂ O final volume. Stored at 4 °C.
	TBS - 0.05% Tw Wash Buffer	250 μ l Tween 20 (SIGMA-ALDRICH, P9416) dissolved in 500 ml TBS. Stored at RT.
	TBS - 0.1% Tw Wash Buffer	500 μ l Tween 20 (SIGMA-ALDRICH, P9416) dissolved in 500 ml TBS. Stored at RT
	IF Blocking Buffer	75.07 g Glycine (SIGMA-ALDRICH, G7126) dissolved in 1 L TBS supplemented with 1ml Triton-X-100 (SIGMA-ALDRICH, x100). Stored at RT.
	NGS IF Blocking Buffer	10 ml NGS (Vector Laboratories, S-1000-20) diluted in 100 ml IF Blocking Buffer final volume.
	5x DUOLINK Wash Buffer B	0.5 g NaCl (SIGMA-ALDRICH, S7653) dissolved in 100 ml 1M Tris pH 7.5. Stored at RT.
	PLA ligation solution	120 μ l of PLA ligation solution was used per slide. For 120 μ l, 93 μ l ddH ₂ O, 24 μ l ligation stock, and 3 μ l ligase (SIGMA-ALDRICH, DUO92008) were mixed before use.
	PLA amplification solution	120 μ l of PLA amplification solution was used per slide. For 120 μ l, 94.5 μ l ddH ₂ O, 24 μ l amplification stock, and 1.5 μ l polymerase (SIGMA-ALDRICH, DUO92008) were mixed before use.
	PLA detection solution	120 μ l of PLA detection solution was used per slide. For 120 μ l, 96 μ l ddH ₂ O and 24 μ l detection stock (SIGMA-ALDRICH, DUO92008) were mixed before use.
	PLA substrate solution	120 μ l of PLA substrate solution was used per slide. For 120 μ l, 113.4 μ l ddH ₂ O, 1.8 μ l substrate A, 1.2 μ l substrate B, 1.2 μ l substrate C, 2.4 μ l substrate H ₂ O ₂ (SIGMA-ALDRICH, DUO92008) were mixed before use.

	1 µg/ml DAPI	DAPI Solution (1 mg/ml) (Thermo, 62248) 1:1000 diluted in PBS.
--	--------------	--

Table 2.7 - Commercial Kits

Kit	Source
QIAprep® Spin Miniprep Kit	Qiagen, 27106
VECTASTAIN® Elite® ABC-HRP Kit, Peroxidase (Standard)	Vector Laboratories, PK-6100
ImmPACT® DAB Substrate Kit, Peroxidase (HRP)	Vector Laboratories, SK-4105
Duolink® In Situ Probemaker PLUS	SIGMA-ALDRICH, DUO92009
Duolink® In Situ Probemaker MINUS	SIGMA-ALDRICH, DUO92010
Duolink® In Situ Detection Reagents Brightfield	SIGMA-ALDRICH, DUO92012
Duolink® In Situ Detection Reagents Red	SIGMA-ALDRICH, DUO92008

References

- 2020 Alzheimer's disease facts and figures, 2020. . *Alzheimers Dement.* 16, 391–460.
<https://doi.org/10.1002/alz.12068>
- 2022 Alzheimer's disease facts and figures, 2022. . *Alzheimers Dement.* 18, 700–789.
<https://doi.org/10.1002/alz.12638>
- A. Lasagna-Reeves, C., L. Castillo-Carranza, D., R. Jackson, G., Kaye, R., 2011. Tau Oligomers as Potential Targets for Immunotherapy for Alzheimers Disease and Tauopathies. *Curr. Alzheimer Res.* 8, 659–665.
<https://doi.org/10.2174/156720511796717177>
- Abell, J.G., Kivimäki, M., Dugravot, A., Tabak, A.G., Fayosse, A., Shipley, M., Sabia, S., Singh-Manoux, A., 2018. Association between systolic blood pressure and dementia in the Whitehall II cohort study: role of age, duration, and threshold used to define hypertension. *Eur. Heart J.* 39, 3119–3125.
<https://doi.org/10.1093/eurheartj/ehy288>
- Abreha, M.H., Dammer, E.B., Ping, L., Zhang, T., Duong, D.M., Gearing, M., Lah, J.J., Levey, A.I., Seyfried, N.T., 2018. Quantitative Analysis of the Brain Ubiquitylome in Alzheimer's Disease. *PROTEOMICS* 18, 1800108.
<https://doi.org/10.1002/pmic.201800108>
- Akincioglu, H., Gülçin, İ., 2020. Potent Acetylcholinesterase Inhibitors: Potential Drugs for Alzheimer's Disease. *Mini-Rev. Med. Chem.* 20, 703–715.
<https://doi.org/10.2174/1389557520666200103100521>
- Alafuzoff, I., Arzberger, T., Al-Sarraj, S., Bodi, I., Bogdanovic, N., Braak, H., Bugiani, O., Del-Tredici, K., Ferrer, I., Gelpi, E., Giaccone, G., Graeber, M.B., Ince, P., Kamphorst, W., King, A., Korkolopoulou, P., Kovács, G.G., Larionov, S., Meyronet, D., Monoranu, C., Parchi, P., Patsouris, E., Roggendorf, W., Seilhean, D., Tagliavini, F., Stadelmann, C., Streichenberger, N., Thal, D.R., Wharton, S.B., Kretzschmar, H., 2008. Staging of Neurofibrillary Pathology in Alzheimer's Disease: A Study of the BrainNet Europe Consortium. *Brain Pathol.* 0, 080509082911413-??? <https://doi.org/10.1111/j.1750-3639.2008.00147.x>
- Alam, M.S., 2018. Proximity Ligation Assay (PLA). *Curr. Protoc. Immunol.* 123, e58.
<https://doi.org/10.1002/cpim.58>

- Allen, B., Ingram, E., Takao, M., Smith, M.J., Jakes, R., Virdee, K., Yoshida, H., Holzer, M., Craxton, M., Emson, P.C., Atzori, C., Migheli, A., Crowther, R.A., Ghetti, B., Spillantini, M.G., Goedert, M., 2002. Abundant Tau Filaments and Nonapoptotic Neurodegeneration in Transgenic Mice Expressing Human P301S Tau Protein. *J. Neurosci.* 22, 9340–9351. <https://doi.org/10.1523/JNEUROSCI.22-21-09340.2002>
- Alquezar, C., Arya, S., Kao, A.W., 2021. Tau Post-translational Modifications: Dynamic Transformers of Tau Function, Degradation, and Aggregation. *Front. Neurol.* 11, 595532. <https://doi.org/10.3389/fneur.2020.595532>
- Alsemarz, A., Lasko, P., Fagotto, F., 2018. Limited significance of the in situ proximity ligation assay (preprint). *Cell Biology*. <https://doi.org/10.1101/411355>
- Amos, L.A., 2004. Microtubule structure and its stabilisation. *Org. Biomol. Chem.* 2, 2153. <https://doi.org/10.1039/b403634d>
- Andrade-Moraes, C.H., Oliveira-Pinto, A.V., Castro-Fonseca, E., da Silva, C.G., Guimaraes, D.M., Szczupak, D., Parente-Bruno, D.R., Carvalho, L.R.B., Polichiso, L., Gomes, B.V., Oliveira, L.M., Rodriguez, R.D., Leite, R.E.P., Ferretti-Rebustini, R.E.L., Jacob-Filho, W., Pasqualucci, C.A., Grinberg, L.T., Lent, R., 2013. Cell number changes in Alzheimer's disease relate to dementia, not to plaques and tangles. *Brain* 136, 3738–3752. <https://doi.org/10.1093/brain/awt273>
- Anstey, K.J., Ashby-Mitchell, K., Peters, R., 2017. Updating the Evidence on the Association between Serum Cholesterol and Risk of Late-Life Dementia: Review and Meta-Analysis. *J. Alzheimers Dis.* 56, 215–228. <https://doi.org/10.3233/JAD-160826>
- Apicco, D.J., Ash, P.E.A., Maziuk, B., LeBlang, C., Medalla, M., Al Abdullatif, A., Ferragud, A., Botelho, E., Ballance, H.I., Dhawan, U., Boudeau, S., Cruz, A.L., Kashy, D., Wong, A., Goldberg, L.R., Yazdani, N., Zhang, C., Ung, C.Y., Tripodis, Y., Kanaan, N.M., Ikezu, T., Cottone, P., Leszyk, J., Li, H., Luebke, J., Bryant, C.D., Wolozin, B., 2018. Reducing the RNA binding protein TIA1 protects against tau-mediated neurodegeneration in vivo. *Nat. Neurosci.* 21, 72–80. <https://doi.org/10.1038/s41593-017-0022-z>
- Apicco, D.J., Zhang, C., Maziuk, B., Jiang, L., Ballance, H.I., Boudeau, S., Ung, C., Li, H., Wolozin, B., 2019. Dysregulation of RNA Splicing in Tauopathies. *Cell Rep.* 29, 4377–4388.e4. <https://doi.org/10.1016/j.celrep.2019.11.093>

- Arbaciauskaite, M., Lei, Y., Cho, Y.K., 2021. High-specificity antibodies and detection methods for quantifying phosphorylated tau from clinical samples. *Antib. Ther.* 4, 34–44. <https://doi.org/10.1093/abt/tbab004>
- Arriagada, P.V., Growdon, J.H., Hedley-Whyte, E.T., Hyman, B.T., 1992. Neurofibrillary tangles but not senile plaques parallel duration and severity of Alzheimer's disease. *Neurology* 42, 631–631. <https://doi.org/10.1212/WNL.42.3.631>
- Atarashi, R., Moore, R.A., Sim, V.L., Hughson, A.G., Dorward, D.W., Onwubiko, H.A., Priola, S.A., Caughey, B., 2007. Ultrasensitive detection of scrapie prion protein using seeded conversion of recombinant prion protein. *Nat. Methods* 4, 645–650. <https://doi.org/10.1038/nmeth1066>
- Atri, A., 2019. Current and Future Treatments in Alzheimer's Disease. *Semin. Neurol.* 39, 227–240. <https://doi.org/10.1055/s-0039-1678581>
- Bain, H.D.C., Davidson, Y.S., Robinson, A.C., Ryan, S., Rollinson, S., Richardson, A., Jones, M., Snowden, J.S., Pickering-Brown, S., Mann, D.M.A., 2019. The role of lysosomes and autophagosomes in frontotemporal lobar degeneration. *Neuropathol. Appl. Neurobiol.* 45, 244–261. <https://doi.org/10.1111/nan.12500>
- Bakulski, K.M., Vadari, H.S., Faul, J.D., Heeringa, S.G., Kardia, S.L.R., Langa, K.M., Smith, J.A., Manly, J.J., Mitchell, C.M., Benke, K.S., Ware, E.B., 2021. Cumulative Genetic Risk and *APOE* $\epsilon 4$ Are Independently Associated With Dementia Status in a Multiethnic, Population-Based Cohort. *Neurol. Genet.* 7, e576. <https://doi.org/10.1212/NXG.0000000000000576>
- Banaszynski, L.A., Liu, C.W., Wandless, T.J., 2005. Characterization of the FKBP·Rapamycin·FRB Ternary Complex. *J. Am. Chem. Soc.* 127, 4715–4721. <https://doi.org/10.1021/ja043277y>
- Bancher, C., Brunner, C., Lassmann, H., Budka, H., Jellinger, K., Wiche, G., Seitelberger, F., Grundke-Iqbal, I., Iqbal, K., Wisniewski, H.M., 1989. Accumulation of abnormally phosphorylated τ precedes the formation of neurofibrillary tangles in Alzheimer's disease. *Brain Res.* 477, 90–99. [https://doi.org/10.1016/0006-8993\(89\)91396-6](https://doi.org/10.1016/0006-8993(89)91396-6)
- Bancher, C., Grundke-Iqbal, I., Iqbal, K., Fried, V.A., Smith, H.T., Wisniewski, H.M., 1991. Abnormal phosphorylation of tau precedes ubiquitination in neurofibrillary pathology of Alzheimer disease. *Brain Res.* 539, 11–18. [https://doi.org/10.1016/0006-8993\(91\)90681-K](https://doi.org/10.1016/0006-8993(91)90681-K)

- Barghorn, S., Mandelkow, E., 2002. Toward a Unified Scheme for the Aggregation of Tau into Alzheimer Paired Helical Filaments. *Biochemistry* 41, 14885–14896. <https://doi.org/10.1021/bi026469j>
- Barnes, D.E., Byers, A.L., Gardner, R.C., Seal, K.H., Boscardin, W.J., Yaffe, K., 2018. Association of Mild Traumatic Brain Injury With and Without Loss of Consciousness With Dementia in US Military Veterans. *JAMA Neurol.* 75, 1055. <https://doi.org/10.1001/jamaneurol.2018.0815>
- Bengoa-Vergniory, N., Velentza-Almpani, E., Silva, A.M., Scott, C., Vargas-Caballero, M., Sastre, M., Wade-Martins, R., Alegre-Abarrategui, J., 2021. Tau-proximity ligation assay reveals extensive previously undetected pathology prior to neurofibrillary tangles in preclinical Alzheimer's disease. *Acta Neuropathol. Commun.* 9, 18. <https://doi.org/10.1186/s40478-020-01117-y>
- Bennett, D.A., Schneider, J.A., Arvanitakis, Z., Kelly, J.F., Aggarwal, N.T., Shah, R.C., Wilson, R.S., 2006. Neuropathology of older persons without cognitive impairment from two community-based studies. *Neurology* 66, 1837–1844. <https://doi.org/10.1212/01.wnl.0000219668.47116.e6>
- Berger, Z., Roder, H., Hanna, A., Carlson, A., Rangachari, V., Yue, M., Wszolek, Z., Ashe, K., Knight, J., Dickson, D., Andorfer, C., Rosenberry, T.L., Lewis, J., Hutton, M., Janus, C., 2007. Accumulation of Pathological Tau Species and Memory Loss in a Conditional Model of Tauopathy. *J. Neurosci.* 27, 3650–3662. <https://doi.org/10.1523/JNEUROSCI.0587-07.2007>
- Bessey, L.J., Walaszek, A., 2019. Management of Behavioral and Psychological Symptoms of Dementia. *Curr. Psychiatry Rep.* 21, 66. <https://doi.org/10.1007/s11920-019-1049-5>
- Bi, X., Zhou, J., Lynch, G., 1999. Lysosomal Protease Inhibitors Induce Meganeurites and Tangle-like Structures in Entorhinohippocampal Regions Vulnerable to Alzheimer's Disease. *Exp. Neurol.* 158, 312–327. <https://doi.org/10.1006/exnr.1999.7087>
- Biessels, G.J., Despa, F., 2018. Cognitive decline and dementia in diabetes mellitus: mechanisms and clinical implications. *Nat. Rev. Endocrinol.* 14, 591–604. <https://doi.org/10.1038/s41574-018-0048-7>
- Blokh, D., Stambler, I., Lubart, E., Mizrahi, E.H., 2017. The application of information theory for the estimation of old-age multimorbidity. *GeroScience* 39, 551–556. <https://doi.org/10.1007/s11357-017-9996-4>

- Boluda, S., Iba, M., Zhang, B., Raible, K.M., Lee, V.M.-Y., Trojanowski, J.Q., 2015. Differential induction and spread of tau pathology in young PS19 tau transgenic mice following intracerebral injections of pathological tau from Alzheimer's disease or corticobasal degeneration brains. *Acta Neuropathol. (Berl.)* 129, 221–237. <https://doi.org/10.1007/s00401-014-1373-0>
- Boyko, S., Surewicz, W.K., 2022. Tau liquid–liquid phase separation in neurodegenerative diseases. *Trends Cell Biol.* 32, 611–623. <https://doi.org/10.1016/j.tcb.2022.01.011>
- Braak, E., Braak, H., 1997. Alzheimer's disease: transiently developing dendritic changes in pyramidal cells of sector CA1 of the Ammon's horn. *Acta Neuropathol. (Berl.)* 93, 323–325. <https://doi.org/10.1007/s004010050622>
- Braak, H., Alafuzoff, I., Arzberger, T., Kretschmar, H., Del Tredici, K., 2006. Staging of Alzheimer disease-associated neurofibrillary pathology using paraffin sections and immunocytochemistry. *Acta Neuropathol. (Berl.)* 112, 389–404. <https://doi.org/10.1007/s00401-006-0127-z>
- Braak, H., Braak, E., 1997a. Diagnostic Criteria for Neuropathologic Assessment of Alzheimer's Disease. *Neurobiol. Aging* 18, S85–S88. [https://doi.org/10.1016/S0197-4580\(97\)00062-6](https://doi.org/10.1016/S0197-4580(97)00062-6)
- Braak, H., Braak, E., 1997b. Frequency of Stages of Alzheimer-Related Lesions in Different Age Categories. *Neurobiol. Aging* 18, 351–357. [https://doi.org/10.1016/S0197-4580\(97\)00056-0](https://doi.org/10.1016/S0197-4580(97)00056-0)
- Braak, H., Braak, E., 1991. Neuropathological staging of Alzheimer-related changes. *Acta Neuropathol. (Berl.)* 82, 239–259. <https://doi.org/10.1007/BF00308809>
- Braak, Heiko, Braak, E., 1991. Demonstration of Amyloid Deposits and Neurofibrillary Changes in Whole Brain Sections. *Brain Pathol.* 1, 213–216. <https://doi.org/10.1111/j.1750-3639.1991.tb00661.x>
- Brandt, R., 1996. The tau proteins in neuronal growth and development. *Front. Biosci. J. Virtual Libr.* 1, d118-130. <https://doi.org/10.2741/a120>
- Brunello, C.A., Merezhko, M., Uronen, R.-L., Huttunen, H.J., 2020. Mechanisms of secretion and spreading of pathological tau protein. *Cell. Mol. Life Sci.* 77, 1721–1744. <https://doi.org/10.1007/s00018-019-03349-1>
- Brunello, C.A., Yan, X., Huttunen, H.J., 2016. Internalized Tau sensitizes cells to stress by promoting formation and stability of stress granules. *Sci. Rep.* 6, 30498. <https://doi.org/10.1038/srep30498>

- Buchman, A.S., Yu, L., Wilson, R.S., Lim, A., Dawe, R.J., Gaiteri, C., Leurgans, S.E., Schneider, J.A., Bennett, D.A., 2019. Physical activity, common brain pathologies, and cognition in community-dwelling older adults. *Neurology* 92, e811–e822. <https://doi.org/10.1212/WNL.0000000000006954>
- Bugiani, O., 1999. Pathogenesis of Alzheimer's disease and dementia. *Rev. Neurol. (Paris)* 155 Suppl 4, S28-32.
- By the American Geriatrics Society 2015 Beers Criteria Update Expert Panel, 2015. American Geriatrics Society 2015 Updated Beers Criteria for Potentially Inappropriate Medication Use in Older Adults. *J. Am. Geriatr. Soc.* 63, 2227–2246. <https://doi.org/10.1111/jgs.13702>
- Camero, S., Benítez, M.J., Barrantes, A., Ayuso, J.M., Cuadros, R., Ávila, J., Jiménez, J.S., 2014. Tau Protein Provides DNA with Thermodynamic and Structural Features which are Similar to those Found in Histone-DNA Complex. *J. Alzheimers Dis.* 39, 649–660. <https://doi.org/10.3233/JAD-131415>
- Cameron, B., Landreth, G.E., 2010. Inflammation, microglia, and alzheimer's disease. *Neurobiol. Dis.* 37, 503–509. <https://doi.org/10.1016/j.nbd.2009.10.006>
- Carlomagno, Y., Chung, D.C., Yue, M., Castanedes-Casey, M., Madden, B.J., Dunmore, J., Tong, J., DeTure, M., Dickson, D.W., Petrucelli, L., Cook, C., 2017. An acetylation–phosphorylation switch that regulates tau aggregation propensity and function. *J. Biol. Chem.* 292, 15277–15286. <https://doi.org/10.1074/jbc.M117.794602>
- Castellani, R.J., Nunomura, A., Lee, H., Perry, G., Smith, M.A., 2008. Phosphorylated Tau: Toxic, Protective, or None of the Above. *J. Alzheimers Dis.* 14, 377–383. <https://doi.org/10.3233/JAD-2008-14404>
- Chang, R., Yee, K.-L., Sumbria, R.K., 2017. Tumor necrosis factor α Inhibition for Alzheimer's Disease. *J. Cent. Nerv. Syst. Dis.* 9, 117957351770927. <https://doi.org/10.1177/1179573517709278>
- Chen, X., Li, Y., Wang, C., Tang, Y., Mok, S.-A., Tsai, R.M., Rojas, J.C., Karydas, A., Miller, B.L., Boxer, A.L., Gestwicki, J.E., Arkin, M., Cuervo, A.M., Gan, L., 2020. Promoting tau secretion and propagation by hyperactive p300/CBP via autophagy-lysosomal pathway in tauopathy. *Mol. Neurodegener.* 15, 2. <https://doi.org/10.1186/s13024-019-0354-0>
- Chêne, G., Beiser, A., Au, R., Preis, S.R., Wolf, P.A., Dufouil, C., Seshadri, S., 2015. Gender and incidence of dementia in the Framingham Heart Study from mid-

- adult life. *Alzheimers Dement.* 11, 310–320.
<https://doi.org/10.1016/j.jalz.2013.10.005>
- Cherbuin, N., Kim, S., Anstey, K.J., 2015. Dementia risk estimates associated with measures of depression: a systematic review and meta-analysis. *BMJ Open* 5, e008853. <https://doi.org/10.1136/bmjopen-2015-008853>
- Chesser, A.S., Pritchard, S.M., Johnson, G.V.W., 2013. Tau Clearance Mechanisms and Their Possible Role in the Pathogenesis of Alzheimer Disease. *Front. Neurol.* 4. <https://doi.org/10.3389/fneur.2013.00122>
- Clavaguera, F., Lavenir, I., Falcon, B., Frank, S., Goedert, M., Tolnay, M., 2013. “Prion-Like” Templated Misfolding in Tauopathies: Tau and Templated Misfolding. *Brain Pathol.* 23, 342–349. <https://doi.org/10.1111/bpa.12044>
- Cook, C., Carlomagno, Y., Gendron, T.F., Dunmore, J., Scheffel, K., Stetler, C., Davis, M., Dickson, D., Jarpe, M., DeTure, M., Petrucelli, L., 2014. Acetylation of the KXGS motifs in tau is a critical determinant in modulation of tau aggregation and clearance. *Hum. Mol. Genet.* 23, 104–116. <https://doi.org/10.1093/hmg/ddt402>
- Cripps, D., Thomas, S.N., Jeng, Y., Yang, F., Davies, P., Yang, A.J., 2006. Alzheimer Disease-specific Conformation of Hyperphosphorylated Paired Helical Filament-Tau Is Polyubiquitinated through Lys-48, Lys-11, and Lys-6 Ubiquitin Conjugation. *J. Biol. Chem.* 281, 10825–10838. <https://doi.org/10.1074/jbc.M512786200>
- Cummings, J., Lee, G., Ritter, A., Sabbagh, M., Zhong, K., 2019. Alzheimer’s disease drug development pipeline: 2019. *Alzheimers Dement. Transl. Res. Clin. Interv.* 5, 272–293. <https://doi.org/10.1016/j.trci.2019.05.008>
- Cummings, J., Lee, G., Ritter, A., Zhong, K., 2018. Alzheimer’s disease drug development pipeline: 2018. *Alzheimers Dement. Transl. Res. Clin. Interv.* 4, 195–214. <https://doi.org/10.1016/j.trci.2018.03.009>
- David, D.C., Layfield, R., Serpell, L., Narain, Y., Goedert, M., Spillantini, M.G., 2002. Proteasomal degradation of tau protein: Tau and the proteasome. *J. Neurochem.* 83, 176–185. <https://doi.org/10.1046/j.1471-4159.2002.01137.x>
- Dawson, H.N., Ferreira, A., Eyster, M.V., Ghoshal, N., Binder, L.I., Vitek, M.P., 2001. Inhibition of neuronal maturation in primary hippocampal neurons from τ deficient mice. *J. Cell Sci.* 114, 1179–1187. <https://doi.org/10.1242/jcs.114.6.1179>

- Dent, E.W., Baas, P.W., 2014. Microtubules in neurons as information carriers. *J. Neurochem.* 129, 235–239. <https://doi.org/10.1111/jnc.12621>
- DeTure, M.A., Dickson, D.W., 2019. The neuropathological diagnosis of Alzheimer's disease. *Mol. Neurodegener.* 14, 32. <https://doi.org/10.1186/s13024-019-0333-5>
- DeVos, S.L., Corjuc, B.T., Oakley, D.H., Nobuhara, C.K., Bannan, R.N., Chase, A., Commins, C., Gonzalez, J.A., Dooley, P.M., Frosch, M.P., Hyman, B.T., 2018. Synaptic Tau Seeding Precedes Tau Pathology in Human Alzheimer's Disease Brain. *Front. Neurosci.* 12, 267. <https://doi.org/10.3389/fnins.2018.00267>
- Di Benedetto, G., Burgaletto, C., Bellanca, C.M., Munafò, A., Bernardini, R., Cantarella, G., 2022. Role of Microglia and Astrocytes in Alzheimer's Disease: From Neuroinflammation to Ca²⁺ Homeostasis Dysregulation. *Cells* 11, 2728. <https://doi.org/10.3390/cells11172728>
- Dickey, C.A., Yue, M., Lin, W.-L., Dickson, D.W., Dunmore, J.H., Lee, W.C., Zehr, C., West, G., Cao, S., Clark, A.M.K., Caldwell, G.A., Caldwell, K.A., Eckman, C., Patterson, C., Hutton, M., Petrucelli, L., 2006. Deletion of the Ubiquitin Ligase CHIP Leads to the Accumulation, But Not the Aggregation, of Both Endogenous Phospho- and Caspase-3-Cleaved Tau Species. *J. Neurosci.* 26, 6985–6996. <https://doi.org/10.1523/JNEUROSCI.0746-06.2006>
- Dickson, D.W., 1997. The Pathogenesis of Senile Plaques: *J. Neuropathol. Exp. Neurol.* 56, 321–339. <https://doi.org/10.1097/00005072-199704000-00001>
- Ding, H., Dolan, P.J., Johnson, G.V.W., 2008. Histone deacetylase 6 interacts with the microtubule-associated protein tau. *J. Neurochem.* 106, 2119–2130. <https://doi.org/10.1111/j.1471-4159.2008.05564.x>
- Drazic, A., Myklebust, L.M., Ree, R., Arnesen, T., 2016. The world of protein acetylation. *Biochim. Biophys. Acta BBA - Proteins Proteomics* 1864, 1372–1401. <https://doi.org/10.1016/j.bbapap.2016.06.007>
- Dujardin, S., Bégard, S., Caillierez, R., Lachaud, C., Carrier, S., Lieger, S., Gonzalez, J.A., Deramecourt, V., Déglon, N., Maurage, C.-A., Frosch, M.P., Hyman, B.T., Colin, M., Buée, L., 2018. Different tau species lead to heterogeneous tau pathology propagation and misfolding. *Acta Neuropathol. Commun.* 6, 132. <https://doi.org/10.1186/s40478-018-0637-7>
- Dujardin, S., Commins, C., Lathuiliere, A., Beerepoot, P., Fernandes, A.R., Kamath, T.V., De Los Santos, M.B., Klickstein, N., Corjuc, D.L., Corjuc, B.T., Dooley,

- P.M., Viode, A., Oakley, D.H., Moore, B.D., Mullin, K., Jean-Gilles, D., Clark, R., Atchison, K., Moore, R., Chibnik, L.B., Tanzi, R.E., Frosch, M.P., Serrano-Pozo, A., Elwood, F., Steen, J.A., Kennedy, M.E., Hyman, B.T., 2020. Tau molecular diversity contributes to clinical heterogeneity in Alzheimer's disease. *Nat. Med.* 26, 1256–1263. <https://doi.org/10.1038/s41591-020-0938-9>
- Dunker, A.K., Silman, I., Uversky, V.N., Sussman, J.L., 2008. Function and structure of inherently disordered proteins. *Curr. Opin. Struct. Biol.* 18, 756–764. <https://doi.org/10.1016/j.sbi.2008.10.002>
- Eimer, W.A., Vijaya Kumar, D.K., Navalpur Shanmugam, N.K., Rodriguez, A.S., Mitchell, T., Washicosky, K.J., György, B., Breakefield, X.O., Tanzi, R.E., Moir, R.D., 2018. Alzheimer's Disease-Associated β -Amyloid Is Rapidly Seeded by Herpesviridae to Protect against Brain Infection. *Neuron* 99, 56–63.e3. <https://doi.org/10.1016/j.neuron.2018.06.030>
- Ercan-Herbst, E., Ehrig, J., Schöndorf, D.C., Behrendt, A., Klaus, B., Gomez Ramos, B., Prat Oriol, N., Weber, C., Ehrnhoefer, D.E., 2019. A post-translational modification signature defines changes in soluble tau correlating with oligomerization in early stage Alzheimer's disease brain. *Acta Neuropathol. Commun.* 7, 192. <https://doi.org/10.1186/s40478-019-0823-2>
- Eric Vallabh Minikel, 2014. RT-QuIC protocols in detail.
- Falcon, B., Zivanov, J., Zhang, W., Murzin, A.G., Garringer, H.J., Vidal, R., Crowther, R.A., Newell, K.L., Ghetti, B., Goedert, M., Scheres, S.H.W., 2019. Novel tau filament fold in chronic traumatic encephalopathy encloses hydrophobic molecules. *Nature* 568, 420–423. <https://doi.org/10.1038/s41586-019-1026-5>
- Falnes, P.Ø., Jakobsson, M.E., Davydova, E., Ho, A., Małeckı, J., 2016. Protein lysine methylation by seven- β -strand methyltransferases. *Biochem. J.* 473, 1995–2009. <https://doi.org/10.1042/BCJ20160117>
- Fan, L., Mao, C., Hu, X., Zhang, S., Yang, Z., Hu, Z., Sun, H., Fan, Y., Dong, Y., Yang, J., Shi, C., Xu, Y., 2020. New Insights Into the Pathogenesis of Alzheimer's Disease. *Front. Neurol.* 10, 1312. <https://doi.org/10.3389/fneur.2019.01312>
- Fann, J.R., Ribe, A.R., Pedersen, H.S., Fenger-Grøn, M., Christensen, J., Benros, M.E., Vestergaard, M., 2018. Long-term risk of dementia among people with traumatic brain injury in Denmark: a population-based observational cohort study. *Lancet Psychiatry* 5, 424–431. [https://doi.org/10.1016/S2215-0366\(18\)30065-8](https://doi.org/10.1016/S2215-0366(18)30065-8)

- Farlow, M., Anand, R., Messina Jr, J., Hartman, R., Veach, J., 2000. A 52-Week Study of the Efficacy of Rivastigmine in Patients with Mild to Moderately Severe Alzheimer's Disease. *Eur. Neurol.* 44, 236–241. <https://doi.org/10.1159/000008243>
- Feinstein, S.C., Wilson, L., 2005. Inability of tau to properly regulate neuronal microtubule dynamics: a loss-of-function mechanism by which tau might mediate neuronal cell death. *Biochim. Biophys. Acta BBA - Mol. Basis Dis.* 1739, 268–279. <https://doi.org/10.1016/j.bbadis.2004.07.002>
- Ferrer, I., Aguiló García, M., Carmona, M., Andrés-Benito, P., Torrejón-Escribano, B., Garcia-Esparcia, P., del Rio, J.A., 2019. Involvement of Oligodendrocytes in Tau Seeding and Spreading in Tauopathies. *Front. Aging Neurosci.* 11, 112. <https://doi.org/10.3389/fnagi.2019.00112>
- Ferrer, I., Andrés-Benito, P., Zelaya, M.V., Aguirre, M.E.E., Carmona, M., Ausín, K., Lachén-Montes, M., Fernández-Irigoyen, J., Santamaría, E., del Rio, J.A., 2020. Familial globular glial tauopathy linked to MAPT mutations: molecular neuropathology and seeding capacity of a prototypical mixed neuronal and glial tauopathy. *Acta Neuropathol. (Berl.)* 139, 735–771. <https://doi.org/10.1007/s00401-019-02122-9>
- Finley, D., 2009. Recognition and Processing of Ubiquitin-Protein Conjugates by the Proteasome. *Annu. Rev. Biochem.* 78, 477–513. <https://doi.org/10.1146/annurev.biochem.78.081507.101607>
- Fitzpatrick, A.W.P., Falcon, B., He, S., Murzin, A.G., Murshudov, G., Garringer, H.J., Crowther, R.A., Ghetti, B., Goedert, M., Scheres, S.H.W., 2017. Cryo-EM structures of tau filaments from Alzheimer's disease. *Nature* 547, 185–190. <https://doi.org/10.1038/nature23002>
- Fleeman, R.M., Proctor, E.A., 2021. Astrocytic Propagation of Tau in the Context of Alzheimer's Disease. *Front. Cell. Neurosci.* 15, 645233. <https://doi.org/10.3389/fncel.2021.645233>
- Folch, J., Petrov, D., Ettcheto, M., Abad, S., Sánchez-López, E., García, M.L., Olloquequi, J., Beas-Zarate, C., Auladell, C., Camins, A., 2016. Current Research Therapeutic Strategies for Alzheimer's Disease Treatment. *Neural Plast.* 2016, 1–15. <https://doi.org/10.1155/2016/8501693>
- Furcila, D., Domínguez-Álvaro, M., DeFelipe, J., Alonso-Nanclares, L., 2019. Subregional Density of Neurons, Neurofibrillary Tangles and Amyloid Plaques

- in the Hippocampus of Patients With Alzheimer's Disease. *Front. Neuroanat.* 13, 99. <https://doi.org/10.3389/fnana.2019.00099>
- Gallyas, F., 1971. Silver staining of Alzheimer's neurofibrillary changes by means of physical development. *Acta Morphol. Acad. Sci. Hung.* 19, 1–8.
- García-Escudero, V., Gargini, R., Martín-Maestro, P., García, E., García-Escudero, R., Avila, J., 2017. Tau mRNA 3'UTR-to-CDS ratio is increased in Alzheimer disease. *Neurosci. Lett.* 655, 101–108. <https://doi.org/10.1016/j.neulet.2017.07.007>
- García-Sierra, F., Mondragón-Rodríguez, S., Basurto-Islas, G., 2008. Truncation of Tau Protein and its Pathological Significance in Alzheimer's Disease. *J. Alzheimers Dis.* 14, 401–409. <https://doi.org/10.3233/JAD-2008-14407>
- Gauthier-Kemper, A., Weissmann, C., Golovyashkina, N., Sebö-Lemke, Z., Drewes, G., Gerke, V., Heinisch, J.J., Brandt, R., 2011. The frontotemporal dementia mutation R406W blocks tau's interaction with the membrane in an annexin A2-dependent manner. *J. Cell Biol.* 192, 647–661. <https://doi.org/10.1083/jcb.201007161>
- Gerson, J.E., Mudher, A., Kaye, R., 2016. Potential mechanisms and implications for the formation of tau oligomeric strains. *Crit. Rev. Biochem. Mol. Biol.* 51, 482–496. <https://doi.org/10.1080/10409238.2016.1226251>
- Ghag, G., Bhatt, N., Cantu, D.V., Guerrero-Munoz, M.J., Ellsworth, A., Sengupta, U., Kaye, R., 2018. Soluble tau aggregates, not large fibrils, are the toxic species that display seeding and cross-seeding behavior: Generation of tau aggregates via sonication. *Protein Sci.* 27, 1901–1909. <https://doi.org/10.1002/pro.3499>
- Gibbons, G.S., Lee, V.M.Y., Trojanowski, J.Q., 2019. Mechanisms of Cell-to-Cell Transmission of Pathological Tau: A Review. *JAMA Neurol.* 76, 101. <https://doi.org/10.1001/jamaneurol.2018.2505>
- Giménez, C., 1998. [Composition and structure of the neuronal membrane: molecular basis of its physiology and pathology]. *Rev. Neurol.* 26, 232–239.
- Goedert, M., Eisenberg, D.S., Crowther, R.A., 2017. Propagation of Tau Aggregates and Neurodegeneration. *Annu. Rev. Neurosci.* 40, 189–210. <https://doi.org/10.1146/annurev-neuro-072116-031153>
- Goedert, M., Spillantini, M.G., Hasegawa, M., Jakes, R., Crowther, R.A., Klug, A., 1996. Molecular dissection of the neurofibrillary lesions of Alzheimer's disease. *Cold Spring Harb. Symp. Quant. Biol.* 61, 565–573.

- Goedert, M., Spillantini, M.G., Jakes, R., Rutherford, D., Crowther, R.A., 1989. Multiple isoforms of human microtubule-associated protein tau: sequences and localization in neurofibrillary tangles of Alzheimer's disease. *Neuron* 3, 519–526. [https://doi.org/10.1016/0896-6273\(89\)90210-9](https://doi.org/10.1016/0896-6273(89)90210-9)
- Goldman, J.S., Hahn, S.E., Catania, J.W., Larusse-Eckert, S., Butson, M.Barber., Rumbaugh, M., Strecker, M.N., Roberts, J.S., Burke, W., Mayeux, R., Bird, T., 2011. Genetic counseling and testing for Alzheimer disease: Joint practice guidelines of the American College of Medical Genetics and the National Society of Genetic Counselors. *Genet. Med.* 13, 597–605. <https://doi.org/10.1097/GIM.0b013e31821d69b8>
- Gómez-Isla, T., Wasco, W., Pettingell, W.P., Gurubhagavatula, S., Schmidt, S.D., Jondro, P.D., McNamara, M., Rodes, L.A., Diblasi, T., Growdon, W.B., Seubert, P., Schenk, D., Growdon, J.H., Hyman, B.T., Tanzi, R.E., 1997. A novel presenilin-1 mutation: Increased β -amyloid and neurofibrillary changes: Novel PS1 Gene Mutation. *Ann. Neurol.* 41, 809–813. <https://doi.org/10.1002/ana.410410618>
- Goñi, F., Herline, K., Peyser, D., Wong, K., Ji, Y., Sun, Y., Mehta, P., Wisniewski, T., 2013. Immunomodulation targeting of both A β and tau pathological conformers ameliorates Alzheimer's disease pathology in TgSwDI and 3xTg mouse models. *J. Neuroinflammation* 10, 914. <https://doi.org/10.1186/1742-2094-10-150>
- Goodwin, M.S., Croft, C.L., Futch, H.S., Ryu, D., Ceballos-Diaz, C., Liu, X., Paterno, G., Mejia, C., Deng, D., Menezes, K., Londono, L., Arjona, K., Parianos, M., Truong, V., Rostonics, E., Hernandez, A., Boye, S.L., Boye, S.E., Levites, Y., Cruz, P.E., Golde, T.E., 2020. Utilizing minimally purified secreted rAAV for rapid and cost-effective manipulation of gene expression in the CNS. *Mol. Neurodegener.* 15, 15. <https://doi.org/10.1186/s13024-020-00361-z>
- Grundke-Iqbal, I., Iqbal, K., Tung, Y.C., Quinlan, M., Wisniewski, H.M., Binder, L.I., 1986. Abnormal phosphorylation of the microtubule-associated protein tau (tau) in Alzheimer cytoskeletal pathology. *Proc. Natl. Acad. Sci.* 83, 4913–4917. <https://doi.org/10.1073/pnas.83.13.4913>
- Grynspan, F., Griffin, W.R., Cataldo, A., Katayama, S., Nixon, R.A., 1997. Active site-directed antibodies identify calpain II as an early-appearing and pervasive

- component of neurofibrillary pathology in Alzheimer's disease. *Brain Res.* 763, 145–158. [https://doi.org/10.1016/S0006-8993\(97\)00384-3](https://doi.org/10.1016/S0006-8993(97)00384-3)
- Guo, H., Albrecht, S., Bourdeau, M., Petzke, T., Bergeron, C., LeBlanc, A.C., 2004. Active Caspase-6 and Caspase-6-Cleaved Tau in Neuropil Threads, Neuritic Plaques, and Neurofibrillary Tangles of Alzheimer's Disease. *Am. J. Pathol.* 165, 523–531. [https://doi.org/10.1016/S0002-9440\(10\)63317-2](https://doi.org/10.1016/S0002-9440(10)63317-2)
- Han, X., Sekino, Y., Babasaki, T., Goto, K., Inoue, S., Hayashi, T., Teishima, J., Sakamoto, N., Sentani, K., Oue, N., Yasui, W., Matsubara, A., 2020. Microtubule-associated protein tau (MAPT) is a promising independent prognostic marker and tumor suppressive protein in clear cell renal cell carcinoma. *Urol. Oncol. Semin. Orig. Investig.* 38, 605.e9-605.e17. <https://doi.org/10.1016/j.urolonc.2020.02.010>
- Hanger, D.P., Anderton, B.H., Noble, W., 2009. Tau phosphorylation: the therapeutic challenge for neurodegenerative disease. *Trends Mol. Med.* 15, 112–119. <https://doi.org/10.1016/j.molmed.2009.01.003>
- Harada, A., Oguchi, K., Okabe, S., Kuno, J., Terada, S., Ohshima, T., Sato-Yoshitake, R., Takei, Y., Noda, T., Hirokawa, N., 1994. Altered microtubule organization in small-calibre axons of mice lacking tau protein. *Nature* 369, 488–491. <https://doi.org/10.1038/369488a0>
- Haroutunian, V., Davies, P., Vianna, C., Buxbaum, J.D., Purohit, D.P., 2007. Tau protein abnormalities associated with the progression of alzheimer disease type dementia. *Neurobiol. Aging* 28, 1–7. <https://doi.org/10.1016/j.neurobiolaging.2005.11.001>
- Harris, L.D., Jasem, S., Licchesi, J.D.F., 2020. The Ubiquitin System in Alzheimer's Disease, in: Barrio, R., Sutherland, J.D., Rodriguez, M.S. (Eds.), *Proteostasis and Disease, Advances in Experimental Medicine and Biology*. Springer International Publishing, Cham, pp. 195–221. https://doi.org/10.1007/978-3-030-38266-7_8
- He, H.J., Wang, X.S., Pan, R., Wang, D.L., Liu, M.N., He, R.Q., 2009. The proline-rich domain of tau plays a role in interactions with actin. *BMC Cell Biol.* 10, 81. <https://doi.org/10.1186/1471-2121-10-81>
- He W., Goodkind D., Kowal P., 2016. *An Aging World: 2015*, U.S. Gov. Publ. Off. Wash.

- Hebert, L.E., Bienias, J.L., Aggarwal, N.T., Wilson, R.S., Bennett, D.A., Shah, R.C., Evans, D.A., 2010. Change in risk of Alzheimer disease over time. *Neurology* 75, 786–791. <https://doi.org/10.1212/WNL.0b013e3181f0754f>
- Hendriks, S., Peetoom, K., Bakker, C., van der Flier, W.M., Papma, J.M., Koopmans, R., Verhey, F.R.J., de Vugt, M., Köhler, S., Young-Onset Dementia Epidemiology Study Group, Withall, A., Parlevliet, J.L., Uysal-Bozkir, Ö., Gibson, R.C., Neita, S.M., Nielsen, T.R., Salem, L.C., Nyberg, J., Lopes, M.A., Dominguez, J.C., De Guzman, M.F., Egeberg, A., Radford, K., Broe, T., Subramaniam, M., Abidin, E., Bruni, A.C., Di Lorenzo, R., Smith, K., Flicker, L., Mol, M.O., Basta, M., Yu, D., Masika, G., Petersen, M.S., Ruano, L., 2021. Global Prevalence of Young-Onset Dementia: A Systematic Review and Meta-analysis. *JAMA Neurol.* 78, 1080. <https://doi.org/10.1001/jamaneurol.2021.2161>
- Heneka, M.T., Carson, M.J., Khoury, J.E., Landreth, G.E., Brosseron, F., Feinstein, D.L., Jacobs, A.H., Wyss-Coray, T., Vitorica, J., Ransohoff, R.M., Herrup, K., Frautschy, S.A., Finsen, B., Brown, G.C., Verkhratsky, A., Yamanaka, K., Koistinaho, J., Latz, E., Halle, A., Petzold, G.C., Town, T., Morgan, D., Shinohara, M.L., Perry, V.H., Holmes, C., Bazan, N.G., Brooks, D.J., Hunot, S., Joseph, B., Deigendesch, N., Garaschuk, O., Boddeke, E., Dinarello, C.A., Breitner, J.C., Cole, G.M., Golenbock, D.T., Kummer, M.P., 2015. Neuroinflammation in Alzheimer’s disease. *Lancet Neurol.* 14, 388–405. [https://doi.org/10.1016/S1474-4422\(15\)70016-5](https://doi.org/10.1016/S1474-4422(15)70016-5)
- Hernández, F., Llorens-Martín, M., Bolós, M., Pérez, M., Cuadros, R., Pallas-Bazarrá, N., Zabala, J.C., Avila, J., 2018. New Beginnings in Alzheimer’s Disease: The Most Prevalent Tauopathy. *J. Alzheimers Dis.* 64, S529–S534. <https://doi.org/10.3233/JAD-179916>
- Hirano, A., 1994. Hirano bodies and related neuronal inclusions. *Neuropathol. Appl. Neurobiol.* 20, 3–11. <https://doi.org/10.1111/j.1365-2990.1994.tb00951.x>
- Hithersay, R., Startin, C.M., Hamburg, S., Mok, K.Y., Hardy, J., Fisher, E.M.C., Tybulewicz, V.L.J., Nizetic, D., Strydom, A., 2019. Association of Dementia With Mortality Among Adults With Down Syndrome Older Than 35 Years. *JAMA Neurol.* 76, 152. <https://doi.org/10.1001/jamaneurol.2018.3616>
- Ho, C.-Y., Lin, Y.-T., Chen, H.-H., Ho, W.-Y., Sun, G.-C., Hsiao, M., Lu, P.-J., Cheng, P.-W., Tseng, C.-J., 2020. CX3CR1-microglia mediates neuroinflammation and

- blood pressure regulation in the nucleus tractus solitarii of fructose-induced hypertensive rats. *J. Neuroinflammation* 17, 185. <https://doi.org/10.1186/s12974-020-01857-7>
- Holmes, B.B., DeVos, S.L., Kfoury, N., Li, M., Jacks, R., Yanamandra, K., Ouidja, M.O., Brodsky, F.M., Marasa, J., Bagchi, D.P., Kotzbauer, P.T., Miller, T.M., Papy-Garcia, D., Diamond, M.I., 2013. Heparan sulfate proteoglycans mediate internalization and propagation of specific proteopathic seeds. *Proc. Natl. Acad. Sci.* 110. <https://doi.org/10.1073/pnas.1301440110>
- Holmes, B.B., Furman, J.L., Mahan, T.E., Yamasaki, T.R., Mirbaha, H., Eades, W.C., Belaygorod, L., Cairns, N.J., Holtzman, D.M., Diamond, M.I., 2014. Proteopathic tau seeding predicts tauopathy in vivo. *Proc. Natl. Acad. Sci.* 111. <https://doi.org/10.1073/pnas.1411649111>
- Holper, S., Watson, R., Yassi, N., 2022. Tau as a Biomarker of Neurodegeneration. *Int. J. Mol. Sci.* 23, 7307. <https://doi.org/10.3390/ijms23137307>
- Holtzman, D.M., Morris, J.C., Goate, A.M., 2011. Alzheimer's Disease: The Challenge of the Second Century. *Sci. Transl. Med.* 3. <https://doi.org/10.1126/scitranslmed.3002369>
- Hromadkova, L., Siddiqi, M.K., Liu, H., Safar, J.G., 2022. Populations of Tau Conformers Drive Prion-like Strain Effects in Alzheimer's Disease and Related Dementias. *Cells* 11, 2997. <https://doi.org/10.3390/cells11192997>
- Humphrey, S.J., James, D.E., Mann, M., 2015. Protein Phosphorylation: A Major Switch Mechanism for Metabolic Regulation. *Trends Endocrinol. Metab. TEM* 26, 676–687. <https://doi.org/10.1016/j.tem.2015.09.013>
- Hutton, M., 2006. Molecular Genetics of Chromosome 17 Tauopathies. *Ann. N. Y. Acad. Sci.* 920, 63–73. <https://doi.org/10.1111/j.1749-6632.2000.tb06906.x>
- Hwang, B., Lee, J.H., Bang, D., 2018. Single-cell RNA sequencing technologies and bioinformatics pipelines. *Exp. Mol. Med.* 50, 1–14. <https://doi.org/10.1038/s12276-018-0071-8>
- Hyman, B.T., Phelps, C.H., Beach, T.G., Bigio, E.H., Cairns, N.J., Carrillo, M.C., Dickson, D.W., Duyckaerts, C., Frosch, M.P., Masliah, E., Mirra, S.S., Nelson, P.T., Schneider, J.A., Thal, D.R., Thies, B., Trojanowski, J.Q., Vinters, H.V., Montine, T.J., 2012. National Institute on Aging–Alzheimer's Association guidelines for the neuropathologic assessment of Alzheimer's disease. *Alzheimers Dement.* 8, 1–13. <https://doi.org/10.1016/j.jalz.2011.10.007>

- Hyman, B.T., Van Hoesen, G.W., Damasio, A.R., Barnes, C.L., 1984. Alzheimer's Disease: Cell-Specific Pathology Isolates the Hippocampal Formation. *Science* 225, 1168–1170. <https://doi.org/10.1126/science.6474172>
- Ikeda, K., Akiyama, H., Arai, T., Kondo, H., Haga, C., Iritani, S., Tsuchiya, K., 1998. Alz-50/Gallyas-positive lysosome-like intraneuronal granules in Alzheimer's disease and control brains. *Neurosci. Lett.* 258, 113–116. [https://doi.org/10.1016/S0304-3940\(98\)00867-2](https://doi.org/10.1016/S0304-3940(98)00867-2)
- Inobe, T., Nozaki, M., Nukina, N., 2015. Artificial regulation of p53 function by modulating its assembly. *Biochem. Biophys. Res. Commun.* 467, 322–327. <https://doi.org/10.1016/j.bbrc.2015.09.162>
- Iqbal, K., Liu, F., Gong, C.-X., Alonso, A. del C., Grundke-Iqbal, I., 2009. Mechanisms of tau-induced neurodegeneration. *Acta Neuropathol. (Berl.)* 118, 53–69. <https://doi.org/10.1007/s00401-009-0486-3>
- Jack, C.R., Petersen, R.C., Xu, Y.C., O'Brien, P.C., Smith, G.E., Ivnik, R.J., Boeve, B.F., Waring, S.C., Tangalos, E.G., Kokmen, E., 1999. Prediction of AD with MRI-based hippocampal volume in mild cognitive impairment. *Neurology* 52, 1397–1397. <https://doi.org/10.1212/WNL.52.7.1397>
- Jackson, J., Bianco, G., Rosa, A.O., Cowan, K., Bond, P., Anichtchik, O., Fern, R., 2018. White matter tauopathy: Transient functional loss and novel myelin remodeling. *Glia* 66, 813–827. <https://doi.org/10.1002/glia.23286>
- Jadhav, S., Avila, J., Schöll, M., Kovacs, G.G., Kövari, E., Skrabana, R., Evans, L.D., Kontsekova, E., Malawska, B., de Silva, R., Buee, L., Zilka, N., 2019. A walk through tau therapeutic strategies. *Acta Neuropathol. Commun.* 7, 22. <https://doi.org/10.1186/s40478-019-0664-z>
- Jansen, W.J., Ossenkoppele, R., Knol, D.L., Tijms, B.M., Scheltens, P., Verhey, F.R.J., Visser, P.J., Aalten, P., Aarsland, D., Alcolea, D., Alexander, M., Almdahl, I.S., Arnold, S.E., Baldeiras, I., Barthel, H., van Berckel, B.N.M., Bibeau, K., Blennow, K., Brooks, D.J., van Buchem, M.A., Camus, V., Cavedo, E., Chen, K., Chetelat, G., Cohen, A.D., Drzezga, A., Engelborghs, S., Fagan, A.M., Fladby, T., Fleisher, A.S., van der Flier, W.M., Ford, L., Förster, S., Fortea, J., Foskett, N., Frederiksen, K.S., Freund-Levi, Y., Frisoni, G.B., Froelich, L., Gabryelewicz, T., Gill, K.D., Gkatzima, O., Gómez-Tortosa, E., Gordon, M.F., Grimmer, T., Hampel, H., Hausner, L., Hellwig, S., Herukka, S.-K., Hildebrandt, H., Ishihara, L., Ivanoiu, A., Jagust, W.J., Johannsen, P.,

- Kandimalla, R., Kapaki, E., Klimkiewicz-Mrowiec, A., Klunk, W.E., Köhler, S., Koglin, N., Kornhuber, J., Kramberger, M.G., Van Laere, K., Landau, S.M., Lee, D.Y., de Leon, M., Lisetti, V., Lleó, A., Madsen, K., Maier, W., Marcusson, J., Mattsson, N., de Mendonça, A., Meulenbroek, O., Meyer, P.T., Mintun, M.A., Mok, V., Molinuevo, J.L., Møllergård, H.M., Morris, J.C., Mroczko, B., Van der Mussele, S., Na, D.L., Newberg, A., Nordberg, A., Nordlund, A., Novak, G.P., Paraskevas, G.P., Parnetti, L., Perera, G., Peters, O., Popp, J., Prabhakar, S., Rabinovici, G.D., Ramakers, I.H.G.B., Rami, L., Resende de Oliveira, C., Rinne, J.O., Rodrigue, K.M., Rodríguez-Rodríguez, E., Roe, C.M., Rot, U., Rowe, C.C., Rütther, E., Sabri, O., Sanchez-Juan, P., Santana, I., Sarazin, M., Schröder, J., Schütte, C., Seo, S.W., Soetewey, F., Soininen, H., Spuru, L., Struyfs, H., Teunissen, C.E., Tsolaki, M., Vandenberghe, R., Verbeek, M.M., Villemagne, V.L., Vos, S.J.B., van Waalwijk van Doorn, L.J.C., Waldemar, G., Wallin, A., Wallin, Å.K., Wiltfang, J., Wolk, D.A., Zboch, M., Zetterberg, H., 2015. Prevalence of Cerebral Amyloid Pathology in Persons Without Dementia: A Meta-analysis. *JAMA* 313, 1924. <https://doi.org/10.1001/jama.2015.4668>
- Jiang, L., Ash, P.E.A., Maziuk, B.F., Ballance, H.I., Boudeau, S., Abdullatif, A.A., Orlando, M., Petrucelli, L., Ikezu, T., Wolozin, B., 2019. TIA1 regulates the generation and response to toxic tau oligomers. *Acta Neuropathol. (Berl.)* 137, 259–277. <https://doi.org/10.1007/s00401-018-1937-5>
- Kamer, A.R., Pirraglia, E., Tsui, W., Rusinek, H., Vallabhajosula, S., Mosconi, L., Yi, L., McHugh, P., Craig, R.G., Svetcov, S., Linker, R., Shi, C., Glodzik, L., Williams, S., Corby, P., Saxena, D., de Leon, M.J., 2015. Periodontal disease associates with higher brain amyloid load in normal elderly. *Neurobiol. Aging* 36, 627–633. <https://doi.org/10.1016/j.neurobiolaging.2014.10.038>
- Kanaan, N.M., Hamel, C., Grabinski, T., Combs, B., 2020. Liquid-liquid phase separation induces pathogenic tau conformations in vitro. *Nat. Commun.* 11, 2809. <https://doi.org/10.1038/s41467-020-16580-3>
- Kang, S.-G., Han, Z.Z., Daude, N., McNamara, E., Wohlgemuth, S., Molina-Porcel, L., Safar, J.G., Mok, S.-A., Westaway, D., 2021. Pathologic tau conformer ensembles induce dynamic, liquid-liquid phase separation events at the nuclear envelope. *BMC Biol.* 19, 199. <https://doi.org/10.1186/s12915-021-01132-y>

- Kaniyappan, S., Tepper, K., Biernat, J., Chandupatla, R.R., Hübschmann, S., Irsen, S., Bicher, S., Klatt, C., Mandelkow, E.-M., Mandelkow, E., 2020. FRET-based Tau seeding assay does not represent prion-like templated assembly of Tau filaments. *Mol. Neurodegener.* 15, 39. <https://doi.org/10.1186/s13024-020-00389-1>
- Kaufman, S.K., Sanders, D.W., Thomas, T.L., Ruchinskas, A.J., Vaquer-Alicea, J., Sharma, A.M., Miller, T.M., Diamond, M.I., 2016a. Tau Prion Strains Dictate Patterns of Cell Pathology, Progression Rate, and Regional Vulnerability In Vivo. *Neuron* 92, 796–812. <https://doi.org/10.1016/j.neuron.2016.09.055>
- Kaufman, S.K., Sanders, D.W., Thomas, T.L., Ruchinskas, A.J., Vaquer-Alicea, J., Sharma, A.M., Miller, T.M., Diamond, M.I., 2016b. Tau Prion Strains Dictate Patterns of Cell Pathology, Progression Rate, and Regional Vulnerability In Vivo. *Neuron* 92, 796–812. <https://doi.org/10.1016/j.neuron.2016.09.055>
- Kaufman, S.K., Thomas, T.L., Del Tredici, K., Braak, H., Diamond, M.I., 2017. Characterization of tau prion seeding activity and strains from formaldehyde-fixed tissue. *Acta Neuropathol. Commun.* 5, 41. <https://doi.org/10.1186/s40478-017-0442-8>
- Kawas, C.H., Kim, R.C., Sonnen, J.A., Bullain, S.S., Trieu, T., Corrada, M.M., 2015. Multiple pathologies are common and related to dementia in the oldest-old: The 90+ Study. *Neurology* 85, 535–542. <https://doi.org/10.1212/WNL.0000000000001831>
- Keller, J., 2006. Age-related neuropathology, cognitive decline, and Alzheimer's disease. *Ageing Res. Rev.* 5, 1–13. <https://doi.org/10.1016/j.arr.2005.06.002>
- Kellogg, E.H., Hejab, N.M.A., Poepsel, S., Downing, K.H., DiMaio, F., Nogales, E., 2018. Near-atomic model of microtubule-tau interactions. *Science* 360, 1242–1246. <https://doi.org/10.1126/science.aat1780>
- Kent, S.A., Spires-Jones, T.L., Durrant, C.S., 2020. The physiological roles of tau and A β : implications for Alzheimer's disease pathology and therapeutics. *Acta Neuropathol. (Berl.)* 140, 417–447. <https://doi.org/10.1007/s00401-020-02196-w>
- Keren-Shaul, H., Spinrad, A., Weiner, A., Matcovitch-Natan, O., Dvir-Szternfeld, R., Ulland, T.K., David, E., Baruch, K., Lara-Astaiso, D., Toth, B., Itzkovitz, S., Colonna, M., Schwartz, M., Amit, I., 2017. A Unique Microglia Type

- Associated with Restricting Development of Alzheimer's Disease. *Cell* 169, 1276-1290.e17. <https://doi.org/10.1016/j.cell.2017.05.018>
- Kerppola, T.K., 2013. Bimolecular Fluorescence Complementation (BiFC) Analysis of Protein Interactions in Live Cells. *Cold Spring Harb. Protoc.* 2013, pdb.prot076497. <https://doi.org/10.1101/pdb.prot076497>
- Kfoury, N., Holmes, B.B., Jiang, H., Holtzman, D.M., Diamond, M.I., 2012. Trans-cellular Propagation of Tau Aggregation by Fibrillar Species. *J. Biol. Chem.* 287, 19440–19451. <https://doi.org/10.1074/jbc.M112.346072>
- Klein, C., Krämer, E.-M., Cardine, A.-M., Schraven, B., Brandt, R., Trotter, J., 2002. Process Outgrowth of Oligodendrocytes Is Promoted by Interaction of Fyn Kinase with the Cytoskeletal Protein Tau. *J. Neurosci.* 22, 698–707. <https://doi.org/10.1523/JNEUROSCI.22-03-00698.2002>
- Ko, L., Ko, E.C., Nacharaju, P., Liu, W.-K., Chang, E., Kenessey, A., Yen, S.-H.C., 1999. An immunochemical study on tau glycation in paired helical filaments. *Brain Res.* 830, 301–313. [https://doi.org/10.1016/S0006-8993\(99\)01415-8](https://doi.org/10.1016/S0006-8993(99)01415-8)
- Kocisko, D.A., Come, J.H., Priola, S.A., Chesebro, B., Raymond, G.J., Lansbury, P.T., Caughey, B., 1994. Cell-free formation of protease-resistant prion protein. *Nature* 370, 471–474. <https://doi.org/10.1038/370471a0>
- Konishi, H., Koizumi, S., Kiyama, H., 2022. Phagocytic astrocytes: Emerging from the shadows of microglia. *Glia* 70, 1009–1026. <https://doi.org/10.1002/glia.24145>
- Kopeikina, K.J., Carlson, G.A., Pitstick, R., Ludvigson, A.E., Peters, A., Luebke, J.I., Koffie, R.M., Frosch, M.P., Hyman, B.T., Spires-Jones, T.L., 2011. Tau Accumulation Causes Mitochondrial Distribution Deficits in Neurons in a Mouse Model of Tauopathy and in Human Alzheimer's Disease Brain. *Am. J. Pathol.* 179, 2071–2082. <https://doi.org/10.1016/j.ajpath.2011.07.004>
- Kovacech, B., Skrabana, R., Novak, M., 2010. Transition of Tau Protein from Disordered to Misordered in Alzheimer's Disease. *Neurodegener. Dis.* 7, 24–27. <https://doi.org/10.1159/000283478>
- Kovacs, G.G., 2020. Astroglia and Tau: New Perspectives. *Front. Aging Neurosci.* 12, 96. <https://doi.org/10.3389/fnagi.2020.00096>
- Kraus, A., Saijo, E., Metrick, M.A., Newell, K., Sigurdson, C.J., Zanusso, G., Ghetti, B., Caughey, B., 2019. Seeding selectivity and ultrasensitive detection of tau aggregate conformers of Alzheimer disease. *Acta Neuropathol. (Berl.)* 137, 585–598. <https://doi.org/10.1007/s00401-018-1947-3>

- Kuchibhotla, K.V., Wegmann, S., Kopeikina, K.J., Hawkes, J., Rudinskiy, N., Andermann, M.L., Spires-Jones, T.L., Bacskai, B.J., Hyman, B.T., 2014. Neurofibrillary tangle-bearing neurons are functionally integrated in cortical circuits in vivo. *Proc. Natl. Acad. Sci.* 111, 510–514. <https://doi.org/10.1073/pnas.1318807111>
- Kumar, A., Singh, A., Ekavali, 2015. A review on Alzheimer's disease pathophysiology and its management: an update. *Pharmacol. Rep.* 67, 195–203. <https://doi.org/10.1016/j.pharep.2014.09.004>
- Kuret, J., Congdon, E.E., Li, G., Yin, H., Yu, X., Zhong, Q., 2005. Evaluating triggers and enhancers of tau fibrillization. *Microsc. Res. Tech.* 67, 141–155. <https://doi.org/10.1002/jemt.20187>
- Lacovich, V., Espindola, S.L., Alloatti, M., Pozo Devoto, V., Cromberg, L.E., Čarná, M.E., Forte, G., Gallo, J.-M., Bruno, L., Stokin, G.B., Avale, M.E., Falzone, T.L., 2017. Tau Isoforms Imbalance Impairs the Axonal Transport of the Amyloid Precursor Protein in Human Neurons. *J. Neurosci.* 37, 58–69. <https://doi.org/10.1523/JNEUROSCI.2305-16.2016>
- Lasagna-Reeves, C.A., Castillo-Carranza, D.L., Sengupta, U., Clos, A.L., Jackson, G.R., Kaye, R., 2011a. Tau oligomers impair memory and induce synaptic and mitochondrial dysfunction in wild-type mice. *Mol. Neurodegener.* 6, 39. <https://doi.org/10.1186/1750-1326-6-39>
- Lasagna-Reeves, C.A., Castillo-Carranza, D.L., Sengupta, U., Clos, A.L., Jackson, G.R., Kaye, R., 2011b. Tau oligomers impair memory and induce synaptic and mitochondrial dysfunction in wild-type mice. *Mol. Neurodegener.* 6, 39. <https://doi.org/10.1186/1750-1326-6-39>
- Lasagna-Reeves, C.A., Castillo-Carranza, D.L., Sengupta, U., Guerrero-Munoz, M.J., Kiritoshi, T., Neugebauer, V., Jackson, G.R., Kaye, R., 2012. Alzheimer brain-derived tau oligomers propagate pathology from endogenous tau. *Sci. Rep.* 2, 700. <https://doi.org/10.1038/srep00700>
- Lasagna-Reeves, C.A., Castillo-Carranza, D.L., Sengupta, U., Sarmiento, J., Troncoso, J., Jackson, G.R., Kaye, R., 2012. Identification of oligomers at early stages of tau aggregation in Alzheimer's disease. *FASEB J.* 26, 1946–1959. <https://doi.org/10.1096/fj.11-199851>
- Lasagna-Reeves, C.A., Sengupta, U., Castillo-Carranza, D., Gerson, J.E., Guerrero-Munoz, M., Troncoso, J.C., Jackson, G.R., Kaye, R., 2014. The formation of

- tau pore-like structures is prevalent and cell specific: possible implications for the disease phenotypes. *Acta Neuropathol. Commun.* 2, 56. <https://doi.org/10.1186/2051-5960-2-56>
- Lathuiliere, A., Hyman, B.T., 2021. Quantitative Methods for the Detection of Tau Seeding Activity in Human Biofluids. *Front. Neurosci.* 15, 654176. <https://doi.org/10.3389/fnins.2021.654176>
- Launer, L.J., Andersen, K., Dewey, M.E., Letenneur, L., Ott, A., Amaducci, L.A., Brayne, C., Copeland, J.R.M., Dartigues, J.-F., Kragh-Sorensen, P., Lobo, A., Martinez-Lage, J.M., Stijnen, T., Hofman, A., 1999. Rates and risk factors for dementia and Alzheimer's disease: Results from EURODEM pooled analyses. *Neurology* 52, 78–78. <https://doi.org/10.1212/WNL.52.1.78>
- Lee, V.M.-Y., Balin, B.J., Otvos, L., Trojanowski, J.Q., 1991. A68: a Major Subunit of Paired Helical Filaments and Derivatized Forms of Normal Tau. *Science* 251, 675–678. <https://doi.org/10.1126/science.1899488>
- Lee, V.M.-Y., Goedert, M., Trojanowski, J.Q., 2001. Neurodegenerative Tauopathies. *Annu. Rev. Neurosci.* 24, 1121–1159. <https://doi.org/10.1146/annurev.neuro.24.1.1121>
- Li, C., Götz, J., 2017. Somatodendritic accumulation of Tau in Alzheimer's disease is promoted by Fyn-mediated local protein translation. *EMBO J.* 36, 3120–3138. <https://doi.org/10.15252/emj.201797724>
- Li, D., Cho, Y.K., 2020. High specificity of widely used phospho-tau antibodies validated using a quantitative whole-cell based assay. *J. Neurochem.* 152, 122–135. <https://doi.org/10.1111/jnc.14830>
- Li, M., Zhou, S., Wang, G., Qiao, L., Yi, S., Li, T., Pan, X., Liu, X., Tang, Z., 2022. Calpain Inhibitor Calpeptin Improves Alzheimer's Disease-Like Cognitive Impairments and Pathologies in a Diabetes Mellitus Rat Model. *Neurotox. Res.* 40, 1248–1260. <https://doi.org/10.1007/s12640-022-00561-z>
- Li, T., Braunstein, K.E., Zhang, J., Lau, A., Sibener, L., Deeble, C., Wong, P.C., 2016. The neuritic plaque facilitates pathological conversion of tau in an Alzheimer's disease mouse model. *Nat. Commun.* 7, 12082. <https://doi.org/10.1038/ncomms12082>
- Lim, S., Haque, Md.M., Kim, D., Kim, D.J., Kim, Y.K., 2014. Cell-based Models To Investigate Tau Aggregation. *Comput. Struct. Biotechnol. J.* 12, 7–13. <https://doi.org/10.1016/j.csbj.2014.09.011>

- Lindskog, C., Backman, M., Zieba, A., Asplund, A., Uhlén, M., Landegren, U., Pontén, F., 2020. Proximity Ligation Assay as a Tool for Antibody Validation in Human Tissues. *J. Histochem. Cytochem.* 68, 515–529. <https://doi.org/10.1369/0022155420936384>
- Liu, C.W., Lee, G., Jay, D.G., 1999. Tau is required for neurite outgrowth and growth cone motility of chick sensory neurons. *Cell Motil. Cytoskeleton* 43, 232–242. [https://doi.org/10.1002/\(SICI\)1097-0169\(1999\)43:3<232::AID-CM6>3.0.CO;2-7](https://doi.org/10.1002/(SICI)1097-0169(1999)43:3<232::AID-CM6>3.0.CO;2-7)
- Liu, H., Kim, C., Haldiman, T., Sigurdson, C.J., Nyström, S., Nilsson, K.P.R., Cohen, M.L., Wisniewski, T., Hammarström, P., Safar, J.G., 2021. Distinct conformers of amyloid beta accumulate in the neocortex of patients with rapidly progressive Alzheimer's disease. *J. Biol. Chem.* 297, 101267. <https://doi.org/10.1016/j.jbc.2021.101267>
- Liu, L., Drouet, V., Wu, J.W., Witter, M.P., Small, S.A., Clelland, C., Duff, K., 2012. Trans-Synaptic Spread of Tau Pathology In Vivo. *PLoS ONE* 7, e31302. <https://doi.org/10.1371/journal.pone.0031302>
- Lott, I.T., Dierssen, M., 2010. Cognitive deficits and associated neurological complications in individuals with Down's syndrome. *Lancet Neurol.* 9, 623–633. [https://doi.org/10.1016/S1474-4422\(10\)70112-5](https://doi.org/10.1016/S1474-4422(10)70112-5)
- Loy, C.T., Schofield, P.R., Turner, A.M., Kwok, J.B., 2014. Genetics of dementia. *The Lancet* 383, 828–840. [https://doi.org/10.1016/S0140-6736\(13\)60630-3](https://doi.org/10.1016/S0140-6736(13)60630-3)
- Lu, Y., He, H.-J., Zhou, J., Miao, J.-Y., Lu, J., He, Y.-G., Pan, R., Wei, Y., Liu, Y., He, R.-Q., 2013. Hyperphosphorylation Results in Tau Dysfunction in DNA Folding and Protection. *J. Alzheimers Dis.* 37, 551–563. <https://doi.org/10.3233/JAD-130602>
- Luo, G., Sui, D., Wang, K., Chae, J., 2015. Neuron anatomy structure reconstruction based on a sliding filter. *BMC Bioinformatics* 16, 342. <https://doi.org/10.1186/s12859-015-0780-0>
- Luptovčiak, I., Komis, G., Takáč, T., Ovečka, M., Šamaj, J., 2017. Katanin: A Sword Cutting Microtubules for Cellular, Developmental, and Physiological Purposes. *Front. Plant Sci.* 8, 1982. <https://doi.org/10.3389/fpls.2017.01982>
- Ma, Q.-L., Zuo, X., Yang, F., Ubeda, O.J., Gant, D.J., Alaverdyan, M., Kioseas, N.C., Nazari, S., Chen, P.P., Nothias, F., Chan, P., Teng, E., Frautschy, S.A., Cole, G.M., 2014. Loss of MAP Function Leads to Hippocampal Synapse Loss and

- Deficits in the Morris Water Maze with Aging. *J. Neurosci.* 34, 7124–7136.
<https://doi.org/10.1523/JNEUROSCI.3439-13.2014>
- Maina, M.B., Bailey, L.J., Wagih, S., Biasetti, L., Pollack, S.J., Quinn, J.P., Thorpe, J.R., Doherty, A.J., Serpell, L.C., 2018. The involvement of tau in nucleolar transcription and the stress response. *Acta Neuropathol. Commun.* 6, 70.
<https://doi.org/10.1186/s40478-018-0565-6>
- Mandelkow, E.-M., Mandelkow, E., 2012. Biochemistry and Cell Biology of Tau Protein in Neurofibrillary Degeneration. *Cold Spring Harb. Perspect. Med.* 2, a006247–a006247. <https://doi.org/10.1101/cshperspect.a006247>
- Masters, C.L., Bateman, R., Blennow, K., Rowe, C.C., Sperling, R.A., Cummings, J.L., 2015. Alzheimer’s disease. *Nat. Rev. Dis. Primer* 1, 15056.
<https://doi.org/10.1038/nrdp.2015.56>
- Matsuo, E.S., Shin, R.-W., Billingsley, M.L., Van deVoorde, A., O’Connor, M., Trojanowski, J.Q., Lee, V.M.Y., 1994. Biopsy-derived adult human brain tau is phosphorylated at many of the same sites as Alzheimer’s disease paired helical filament tau. *Neuron* 13, 989–1002. [https://doi.org/10.1016/0896-6273\(94\)90264-X](https://doi.org/10.1016/0896-6273(94)90264-X)
- Mazzetti, S., Basellini, M.J., Ferri, V., Cassani, E., Cereda, E., Paolini, M., Calogero, A.M., Bolliri, C., De Leonardis, M., Sacilotto, G., Cilia, R., Cappelletti, G., Pezzoli, G., 2020. α -Synuclein oligomers in skin biopsy of idiopathic and monozygotic twin patients with Parkinson’s disease. *Brain* 143, 920–931.
<https://doi.org/10.1093/brain/awaa008>
- McDowell, I., Xi, G., Lindsay, J., Tierney, M., 2007. Mapping the connections between education and dementia. *J. Clin. Exp. Neuropsychol.* 29, 127–141.
<https://doi.org/10.1080/13803390600582420>
- McGeer, P.L., Rogers, J., McGeer, E.G., 2016. Inflammation, Antiinflammatory Agents, and Alzheimer’s Disease: The Last 22 Years. *J. Alzheimers Dis.* 54, 853–857. <https://doi.org/10.3233/JAD-160488>
- McKhann, G.M., Knopman, D.S., Chertkow, H., Hyman, B.T., Jack, C.R., Kawas, C.H., Klunk, W.E., Koroshetz, W.J., Manly, J.J., Mayeux, R., Mohs, R.C., Morris, J.C., Rossor, M.N., Scheltens, P., Carrillo, M.C., Thies, B., Weintraub, S., Phelps, C.H., 2011. The diagnosis of dementia due to Alzheimer’s disease: Recommendations from the National Institute on Aging-Alzheimer’s

- Association workgroups on diagnostic guidelines for Alzheimer's disease. *Alzheimers Dement.* 7, 263–269. <https://doi.org/10.1016/j.jalz.2011.03.005>
- Mergenthaler, P., Lindauer, U., Dienel, G.A., Meisel, A., 2013. Sugar for the brain: the role of glucose in physiological and pathological brain function. *Trends Neurosci.* 36, 587–597. <https://doi.org/10.1016/j.tins.2013.07.001>
- Metrick, M.A., Ferreira, N. do C., Saijo, E., Kraus, A., Newell, K., Zanusso, G., Vendruscolo, M., Ghetti, B., Caughey, B., 2020. A single ultrasensitive assay for detection and discrimination of tau aggregates of Alzheimer and Pick diseases. *Acta Neuropathol. Commun.* 8, 22. <https://doi.org/10.1186/s40478-020-0887-z>
- Mez, J., Daneshvar, D.H., Kiernan, P.T., Abdolmohammadi, B., Alvarez, V.E., Huber, B.R., Alosco, M.L., Solomon, T.M., Nowinski, C.J., McHale, L., Cormier, K.A., Kubilus, C.A., Martin, B.M., Murphy, L., Baugh, C.M., Montenegro, P.H., Chaisson, C.E., Tripodis, Y., Kowall, N.W., Weuve, J., McClean, M.D., Cantu, R.C., Goldstein, L.E., Katz, D.I., Stern, R.A., Stein, T.D., McKee, A.C., 2017. Clinicopathological Evaluation of Chronic Traumatic Encephalopathy in Players of American Football. *JAMA* 318, 360. <https://doi.org/10.1001/jama.2017.8334>
- Michaelson, D.M., 2014. *APOE* ε4: The most prevalent yet understudied risk factor for Alzheimer's disease. *Alzheimers Dement.* 10, 861–868. <https://doi.org/10.1016/j.jalz.2014.06.015>
- Min, S.-W., Chen, X., Tracy, T.E., Li, Y., Zhou, Y., Wang, C., Shirakawa, K., Minami, S.S., Defensor, E., Mok, S.A., Sohn, P.D., Schilling, B., Cong, X., Ellerby, L., Gibson, B.W., Johnson, J., Krogan, N., Shamloo, M., Gestwicki, J., Masliah, E., Verdin, E., Gan, L., 2015. Critical role of acetylation in tau-mediated neurodegeneration and cognitive deficits. *Nat. Med.* 21, 1154–1162. <https://doi.org/10.1038/nm.3951>
- Min, S.-W., Cho, S.-H., Zhou, Y., Schroeder, S., Haroutunian, V., Seeley, W.W., Huang, E.J., Shen, Y., Masliah, E., Mukherjee, C., Meyers, D., Cole, P.A., Ott, M., Gan, L., 2010. Acetylation of Tau Inhibits Its Degradation and Contributes to Tauopathy. *Neuron* 67, 953–966. <https://doi.org/10.1016/j.neuron.2010.08.044>
- Min, S.-W., Sohn, P.D., Li, Y., Devidze, N., Johnson, J.R., Krogan, N.J., Masliah, E., Mok, S.-A., Gestwicki, J.E., Gan, L., 2018. SIRT1 Deacetylates Tau and

- Reduces Pathogenic Tau Spread in a Mouse Model of Tauopathy. *J. Neurosci.* 38, 3680–3688. <https://doi.org/10.1523/JNEUROSCI.2369-17.2018>
- Mirra, S.S., Heyman, A., McKeel, D., Sumi, S.M., Crain, B.J., Brownlee, L.M., Vogel, F.S., Hughes, J.P., Belle, G. v., Berg, L., participating CERAD neuropathologists, 1991. The Consortium to Establish a Registry for Alzheimer's Disease (CERAD): Part II. Standardization of the neuropathologic assessment of Alzheimer's disease. *Neurology* 41, 479–479. <https://doi.org/10.1212/WNL.41.4.479>
- Miyasaka, T., Sato, S., Tatebayashi, Y., Takashima, A., 2010. Microtubule destruction induces tau liberation and its subsequent phosphorylation. *FEBS Lett.* 584, 3227–3232. <https://doi.org/10.1016/j.febslet.2010.06.014>
- Moloney, C.M., Lowe, V.J., Murray, M.E., 2021. Visualization of neurofibrillary tangle maturity in Alzheimer's disease: A clinicopathologic perspective for biomarker research. *Alzheimers Dement.* 17, 1554–1574. <https://doi.org/10.1002/alz.12321>
- Mondragón-Rodríguez, S., Perry, G., Luna-Muñoz, J., Acevedo-Aquino, M.C., Williams, S., 2014. Phosphorylation of tau protein at sites Ser³⁹⁶⁻⁴⁰⁴ is one of the earliest events in Alzheimer's disease and Down syndrome: Phosphorylation was found to be the earliest event in AD and Down syndrome. *Neuropathol. Appl. Neurobiol.* 40, 121–135. <https://doi.org/10.1111/nan.12084>
- Moore, L.D., Le, T., Fan, G., 2013. DNA Methylation and Its Basic Function. *Neuropsychopharmacology* 38, 23–38. <https://doi.org/10.1038/npp.2012.112>
- Morishima-Kawashima, M., Hasegawa, M., Takio, K., Suzuki, M., Titani, K., Ihara, Y., 1993. Ubiquitin is conjugated with amino-terminally processed tau in paired helical filaments. *Neuron* 10, 1151–1160. [https://doi.org/10.1016/0896-6273\(93\)90063-W](https://doi.org/10.1016/0896-6273(93)90063-W)
- Morita, T., Sobue, K., 2009. Specification of Neuronal Polarity Regulated by Local Translation of CRMP2 and Tau via the mTOR-p70S6K Pathway. *J. Biol. Chem.* 284, 27734–27745. <https://doi.org/10.1074/jbc.M109.008177>
- Morris, H.R., 2001. The Genetic and Pathological Classification of Familial Frontotemporal Dementia. *Arch. Neurol.* 58, 1813. <https://doi.org/10.1001/archneur.58.11.1813>
- Morris, M., Knudsen, G.M., Maeda, S., Trinidad, J.C., Ioanoviciu, A., Burlingame, A.L., Mucke, L., 2015. Tau post-translational modifications in wild-type and

- human amyloid precursor protein transgenic mice. *Nat. Neurosci.* 18, 1183–1189. <https://doi.org/10.1038/nn.4067>
- Na, R., Yang, J., Yeom, Y., Kim, Y.J., Byun, S., Kim, K., Kim, K.W., 2019. A Systematic Review and Meta-Analysis of Nonpharmacological Interventions for Moderate to Severe Dementia. *Psychiatry Investig.* 16, 325–335. <https://doi.org/10.30773/pi.2019.02.11.2>
- Nachman, E., Wentink, A.S., Madiona, K., Bousset, L., Katsinelos, T., Allinson, K., Kampinga, H., McEwan, W.A., Jahn, T.R., Melki, R., Mogk, A., Bukau, B., Nussbaum-Krammer, C., 2020. Disassembly of Tau fibrils by the human Hsp70 disaggregation machinery generates small seeding-competent species. *J. Biol. Chem.* 295, 9676–9690. <https://doi.org/10.1074/jbc.RA120.013478>
- Nakano, H., Kobayashi, K., Sugimori, K., Shimazaki, M., Miyazu, K., Hayashi, M., Furuta, H., 2004. Regional Analysis of Differently Phosphorylated Tau Proteins in Brains from Patients with Alzheimer's Disease. *Dement. Geriatr. Cogn. Disord.* 17, 122–131. <https://doi.org/10.1159/000076344>
- Narasimhan, S., Changolkar, L., Riddle, D.M., Kats, A., Stieber, A., Weitzman, S.A., Zhang, B., Li, Z., Roberson, E.D., Trojanowski, J.Q., Lee, V.M.Y., 2020. Human tau pathology transmits glial tau aggregates in the absence of neuronal tau. *J. Exp. Med.* 217, e20190783. <https://doi.org/10.1084/jem.20190783>
- Narasimhan, S., Guo, J.L., Changolkar, L., Stieber, A., McBride, J.D., Silva, L.V., He, Z., Zhang, B., Gathagan, R.J., Trojanowski, J.Q., Lee, V.M.Y., 2017. Pathological Tau Strains from Human Brains Recapitulate the Diversity of Tauopathies in Nontransgenic Mouse Brain. *J. Neurosci.* 37, 11406–11423. <https://doi.org/10.1523/JNEUROSCI.1230-17.2017>
- Narita, T., Weinert, B.T., Choudhary, C., 2019. Functions and mechanisms of non-histone protein acetylation. *Nat. Rev. Mol. Cell Biol.* 20, 156–174. <https://doi.org/10.1038/s41580-018-0081-3>
- Nathan, J.A., Tae Kim, H., Ting, L., Gygi, S.P., Goldberg, A.L., 2013. Why do cellular proteins linked to K63-polyubiquitin chains not associate with proteasomes? *EMBO J.* 32, 552–565. <https://doi.org/10.1038/emboj.2012.354>
- Neddens, J., Temmel, M., Flunkert, S., Kerschbaumer, B., Hoeller, C., Loeffler, T., Niederkofler, V., Daum, G., Attems, J., Hutter-Paier, B., 2018. Phosphorylation of different tau sites during progression of Alzheimer's disease. *Acta Neuropathol. Commun.* 6, 52. <https://doi.org/10.1186/s40478-018-0557-6>

- Nelson, P.T., Stefansson, K., Gulcher, J., Saper, C.B., 2002. Molecular Evolution of τ Protein: Implications for Alzheimer's Disease. *J. Neurochem.* 67, 1622–1632. <https://doi.org/10.1046/j.1471-4159.1996.67041622.x>
- Niewidok, B., Igaev, M., Sündermann, F., Janning, D., Bakota, L., Brandt, R., 2016. Presence of a carboxy-terminal pseudorepeat and disease-like pseudohyperphosphorylation critically influence tau's interaction with microtubules in axon-like processes. *Mol. Biol. Cell* 27, 3537–3549. <https://doi.org/10.1091/mbc.e16-06-0402>
- Nixon, R.A., Yang, D.-S., 2011. Autophagy failure in Alzheimer's disease—locating the primary defect. *Neurobiol. Dis.* 43, 38–45. <https://doi.org/10.1016/j.nbd.2011.01.021>
- Oddo, S., Billings, L., Kesslak, J.P., Cribbs, D.H., LaFerla, F.M., 2004. A β Immunotherapy Leads to Clearance of Early, but Not Late, Hyperphosphorylated Tau Aggregates via the Proteasome. *Neuron* 43, 321–332. <https://doi.org/10.1016/j.neuron.2004.07.003>
- Olsson, B., Lautner, R., Andreasson, U., Öhrfelt, A., Portelius, E., Bjerke, M., Hölttä, M., Rosén, C., Olsson, C., Strobel, G., Wu, E., Dakin, K., Petzold, M., Blennow, K., Zetterberg, H., 2016. CSF and blood biomarkers for the diagnosis of Alzheimer's disease: a systematic review and meta-analysis. *Lancet Neurol.* 15, 673–684. [https://doi.org/10.1016/S1474-4422\(16\)00070-3](https://doi.org/10.1016/S1474-4422(16)00070-3)
- Otvos, L., Feiner, L., Lang, E., Szendrei, G.I., Goedert, M., Lee, V.M.-Y., 1994. Monoclonal antibody PHF-1 recognizes tau protein phosphorylated at serine residues 396 and 404. *J. Neurosci. Res.* 39, 669–673. <https://doi.org/10.1002/jnr.490390607>
- Pallas-Bazarra, N., Jurado-Arjona, J., Navarrete, M., Esteban, J.A., Hernández, F., Ávila, J., Llorens-Martín, M., 2016. Novel function of Tau in regulating the effects of external stimuli on adult hippocampal neurogenesis. *EMBO J.* 35, 1417–1436. <https://doi.org/10.15252/emj.201593518>
- Panda, D., Samuel, J.C., Massie, M., Feinstein, S.C., Wilson, L., 2003. Differential regulation of microtubule dynamics by three- and four-repeat tau: Implications for the onset of neurodegenerative disease. *Proc. Natl. Acad. Sci.* 100, 9548–9553. <https://doi.org/10.1073/pnas.1633508100>
- Paouri, E., Tzara, O., Kartalou, G.-I., Zenelak, S., Georgopoulos, S., 2017. Peripheral Tumor Necrosis Factor-Alpha (TNF- α) Modulates Amyloid Pathology by

- Regulating Blood-Derived Immune Cells and Glial Response in the Brain of AD/TNF Transgenic Mice. *J. Neurosci.* 37, 5155–5171. <https://doi.org/10.1523/JNEUROSCI.2484-16.2017>
- Park, S.A., Ahn, S.I., Gallo, J.-M., 2016. Tau mis-splicing in the pathogenesis of neurodegenerative disorders. *BMB Rep.* 49, 405–413. <https://doi.org/10.5483/BMBRep.2016.49.8.084>
- Parsons, C.G., Stöffler, A., Danysz, W., 2007. Memantine: a NMDA receptor antagonist that improves memory by restoration of homeostasis in the glutamatergic system - too little activation is bad, too much is even worse. *Neuropharmacology* 53, 699–723. <https://doi.org/10.1016/j.neuropharm.2007.07.013>
- Perl, D.P., 2010. Neuropathology of Alzheimer's Disease: D. P. PERL: NEUROPATHOLOGY OF ALZHEIMER'S DISEASE. *Mt. Sinai J. Med. J. Transl. Pers. Med.* 77, 32–42. <https://doi.org/10.1002/msj.20157>
- Perry, G., Friedman, R., Shaw, G., Chau, V., 1987. Ubiquitin is detected in neurofibrillary tangles and senile plaque neurites of Alzheimer disease brains. *Proc. Natl. Acad. Sci.* 84, 3033–3036. <https://doi.org/10.1073/pnas.84.9.3033>
- Petersen, R.C., Lopez, O., Armstrong, M.J., Getchius, T.S.D., Ganguli, M., Gloss, D., Gronseth, G.S., Marson, D., Pringsheim, T., Day, G.S., Sager, M., Stevens, J., Rae-Grant, A., 2018. Practice guideline update summary: Mild cognitive impairment: Report of the Guideline Development, Dissemination, and Implementation Subcommittee of the American Academy of Neurology. *Neurology* 90, 126–135. <https://doi.org/10.1212/WNL.0000000000004826>
- Piguet, O., Double, K.L., Kril, J.J., Harasty, J., Macdonald, V., McRitchie, D.A., Halliday, G.M., 2009. White matter loss in healthy ageing: A postmortem analysis. *Neurobiol. Aging* 30, 1288–1295. <https://doi.org/10.1016/j.neurobiolaging.2007.10.015>
- Poepsel, S., Sprengel, A., Sacca, B., Kaschani, F., Kaiser, M., Gatsogiannis, C., Raunser, S., Clausen, T., Ehrmann, M., 2015. Determinants of amyloid fibril degradation by the PDZ protease HTRA1. *Nat. Chem. Biol.* 11, 862–869. <https://doi.org/10.1038/nchembio.1931>
- Poggiolini, I., Gupta, V., Lawton, M., Lee, S., El-Turabi, A., Querejeta-Coma, A., Trenkwalder, C., Sixel-Döring, F., Foubert-Samier, A., Pavy-Le Traon, A., Plazzi, G., Biscarini, F., Montplaisir, J., Gagnon, J.-F., Postuma, R.B., Antelmi,

- E., Meissner, W.G., Mollenhauer, B., Ben-Shlomo, Y., Hu, M.T., Parkkinen, L., 2022. Diagnostic value of cerebrospinal fluid alpha-synuclein seed quantification in synucleinopathies. *Brain* 145, 584–595. <https://doi.org/10.1093/brain/awab431>
- Porzig, R., Singer, D., Hoffmann, R., 2007. Epitope mapping of mAbs AT8 and Tau5 directed against hyperphosphorylated regions of the human tau protein. *Biochem. Biophys. Res. Commun.* 358, 644–649. <https://doi.org/10.1016/j.bbrc.2007.04.187>
- Preman, P., Alfonso-Triguero, M., Alberdi, E., Verkhratsky, A., Arranz, A.M., 2021. Astrocytes in Alzheimer's Disease: Pathological Significance and Molecular Pathways. *Cells* 10, 540. <https://doi.org/10.3390/cells10030540>
- Qian, W., Shi, J., Yin, X., Iqbal, K., Grundke-Iqbal, I., Gong, C.-X., Liu, F., 2010. PP2A Regulates Tau Phosphorylation Directly and also Indirectly via Activating GSK-3 β . *J. Alzheimers Dis.* 19, 1221–1229. <https://doi.org/10.3233/JAD-2010-1317>
- Quinn, J.P., Corbett, N.J., Kellett, K.A.B., Hooper, N.M., 2018. Tau Proteolysis in the Pathogenesis of Tauopathies: Neurotoxic Fragments and Novel Biomarkers. *J. Alzheimers Dis.* 63, 13–33. <https://doi.org/10.3233/JAD-170959>
- Rady, R.M., Zinkowski, R.P., Binder, L.I., 1995. Presence of tau in isolated nuclei from human brain. *Neurobiol. Aging* 16, 479–486. [https://doi.org/10.1016/0197-4580\(95\)00023-8](https://doi.org/10.1016/0197-4580(95)00023-8)
- Rajan, K.B., Weuve, J., Barnes, L.L., McAninch, E.A., Wilson, R.S., Evans, D.A., 2021. Population estimate of people with clinical Alzheimer's disease and mild cognitive impairment in the United States (2020–2060). *Alzheimers Dement.* 17, 1966–1975. <https://doi.org/10.1002/alz.12362>
- Ramachandran, G., Udgaonkar, J.B., 2011. Understanding the Kinetic Roles of the Inducer Heparin and of Rod-like Protofibrils during Amyloid Fibril Formation by Tau Protein. *J. Biol. Chem.* 286, 38948–38959. <https://doi.org/10.1074/jbc.M111.271874>
- Ramazi, S., Zahiri, J., 2021. Posttranslational modifications in proteins: resources, tools and prediction methods. *Database J. Biol. Databases Curation* 2021, baab012. <https://doi.org/10.1093/database/baab012>
- Ramirez-Rios, S., Denarier, E., Prezel, E., Vinit, A., Stoppin-Mellet, V., Devred, F., Barbier, P., Peyrot, V., Sayas, C.L., Avila, J., Peris, L., Andrieux, A., Serre, L.,

- Fourest-Lieuvin, A., Arnal, I., 2016. Tau antagonizes end-binding protein tracking at microtubule ends through a phosphorylation-dependent mechanism. *Mol. Biol. Cell* 27, 2924–2934. <https://doi.org/10.1091/mbc.E16-01-0029>
- Rauch, J.N., Chen, J.J., Sorum, A.W., Miller, G.M., Sharf, T., See, S.K., Hsieh-Wilson, L.C., Kampmann, M., Kosik, K.S., 2018. Tau Internalization is Regulated by 6-O Sulfation on Heparan Sulfate Proteoglycans (HSPGs). *Sci. Rep.* 8, 6382. <https://doi.org/10.1038/s41598-018-24904-z>
- Rizzo, M.A., Springer, G.H., Granada, B., Piston, D.W., 2004. An improved cyan fluorescent protein variant useful for FRET. *Nat. Biotechnol.* 22, 445–449. <https://doi.org/10.1038/nbt945>
- Roberts, R.F., Bengoa-Vergniory, N., Alegre-Abarrategui, J., 2019. Alpha-Synuclein Proximity Ligation Assay (AS-PLA) in Brain Sections to Probe for Alpha-Synuclein Oligomers, in: Bartels, T. (Ed.), *Alpha-Synuclein, Methods in Molecular Biology*. Springer New York, New York, NY, pp. 69–76. https://doi.org/10.1007/978-1-4939-9124-2_7
- Roberts, R.F., Wade-Martins, R., Alegre-Abarrategui, J., 2015. Direct visualization of alpha-synuclein oligomers reveals previously undetected pathology in Parkinson's disease brain. *Brain* 138, 1642–1657. <https://doi.org/10.1093/brain/awv040>
- Robertson, L.A., Moya, K.L., Breen, K.C., 2004. The potential role of tau protein O-glycosylation in Alzheimer's disease. *J. Alzheimers Dis.* 6, 489–495. <https://doi.org/10.3233/JAD-2004-6505>
- Romero, J.P., Benito-León, J., Louis, E.D., Bermejo-Pareja, F., 2014. Under reporting of dementia deaths on death certificates: a systematic review of population-based cohort studies. *J. Alzheimers Dis. JAD* 41, 213–221. <https://doi.org/10.3233/JAD-132765>
- Rossi, G., Conconi, D., Panzeri, E., Redaelli, S., Piccoli, E., Paoletta, L., Dalprà, L., Tagliavini, F., 2013. Mutations in MAPT Gene Cause Chromosome Instability and Introduce Copy Number Variations Widely in the Genome. *J. Alzheimers Dis.* 33, 969–982. <https://doi.org/10.3233/JAD-2012-121633>
- Russ, T.C., Stamatakis, E., Hamer, M., Starr, J.M., Kivimäki, M., Batty, G.D., 2013. Socioeconomic status as a risk factor for dementia death: individual participant meta-analysis of 86 508 men and women from the UK. *Br. J. Psychiatry* 203, 10–17. <https://doi.org/10.1192/bjp.bp.112.119479>

- Ryman, D.C., Acosta-Baena, N., Aisen, P.S., Bird, T., Danek, A., Fox, N.C., Goate, A., Frommelt, P., Ghetti, B., Langbaum, J.B.S., Lopera, F., Martins, R., Masters, C.L., Mayeux, R.P., McDade, E., Moreno, S., Reiman, E.M., Ringman, J.M., Salloway, S., Schofield, P.R., Sperling, R., Tariot, P.N., Xiong, C., Morris, J.C., Bateman, R.J., And the Dominantly Inherited Alzheimer Network, 2014. Symptom onset in autosomal dominant Alzheimer disease: A systematic review and meta-analysis. *Neurology* 83, 253–260. <https://doi.org/10.1212/WNL.0000000000000596>
- Saborio, G.P., Permanne, B., Soto, C., 2001. Sensitive detection of pathological prion protein by cyclic amplification of protein misfolding. *Nature* 411, 810–813. <https://doi.org/10.1038/35081095>
- Saijo, E., Ghetti, B., Zanusso, G., Oblak, A., Furman, J.L., Diamond, M.I., Kraus, A., Caughey, B., 2017. Ultrasensitive and selective detection of 3-repeat tau seeding activity in Pick disease brain and cerebrospinal fluid. *Acta Neuropathol. (Berl.)* 133, 751–765. <https://doi.org/10.1007/s00401-017-1692-z>
- Samieri, C., Perier, M.-C., Gaye, B., Proust-Lima, C., Helmer, C., Dartigues, J.-F., Berr, C., Tzourio, C., Empana, J.-P., 2018. Association of Cardiovascular Health Level in Older Age With Cognitive Decline and Incident Dementia. *JAMA* 320, 657. <https://doi.org/10.1001/jama.2018.11499>
- Sanches Machado d’Almeida, K., Ronchi Spillere, S., Zuchinali, P., Corrêa Souza, G., 2018. Mediterranean Diet and Other Dietary Patterns in Primary Prevention of Heart Failure and Changes in Cardiac Function Markers: A Systematic Review. *Nutrients* 10, 58. <https://doi.org/10.3390/nu10010058>
- Sanders, D.W., Kaufman, S.K., DeVos, S.L., Sharma, A.M., Mirbaha, H., Li, A., Barker, S.J., Foley, A.C., Thorpe, J.R., Serpell, L.C., Miller, T.M., Grinberg, L.T., Seeley, W.W., Diamond, M.I., 2014. Distinct Tau Prion Strains Propagate in Cells and Mice and Define Different Tauopathies. *Neuron* 82, 1271–1288. <https://doi.org/10.1016/j.neuron.2014.04.047>
- Sarkar, S., Raymick, J., Cuevas, E., Rosas-Hernandez, H., Hanig, J., 2020. Modification of methods to use Congo-red stain to simultaneously visualize amyloid plaques and tangles in human and rodent brain tissue sections. *Metab. Brain Dis.* 35, 1371–1383. <https://doi.org/10.1007/s11011-020-00608-0>
- Schweers, O., Mandelkow, E.M., Biernat, J., Mandelkow, E., 1995. Oxidation of cysteine-322 in the repeat domain of microtubule-associated protein tau

- controls the in vitro assembly of paired helical filaments. *Proc. Natl. Acad. Sci.* 92, 8463–8467. <https://doi.org/10.1073/pnas.92.18.8463>
- Sekiya, H., Kowa, H., Koga, H., Takata, M., Satake, W., Futamura, N., Funakawa, I., Jinnai, K., Takahashi, M., Kondo, T., Ueno, Y., Kanagawa, M., Kobayashi, K., Toda, T., 2019. Wide distribution of alpha-synuclein oligomers in multiple system atrophy brain detected by proximity ligation. *Acta Neuropathol. (Berl.)* 137, 455–466. <https://doi.org/10.1007/s00401-019-01961-w>
- Selkoe, D.J., Hardy, J., 2016. The amyloid hypothesis of Alzheimer’s disease at 25 years. *EMBO Mol. Med.* 8, 595–608. <https://doi.org/10.15252/emmm.201606210>
- Serrano-Pozo, A., Frosch, M.P., Masliah, E., Hyman, B.T., 2011. Neuropathological Alterations in Alzheimer Disease. *Cold Spring Harb. Perspect. Med.* 1, a006189–a006189. <https://doi.org/10.1101/cshperspect.a006189>
- Siahaan, V., Krattenmacher, J., Hyman, A.A., Diez, S., Hernández-Vega, A., Lansky, Z., Braun, M., 2019. Kinetically distinct phases of tau on microtubules regulate kinesin motors and severing enzymes. *Nat. Cell Biol.* 21, 1086–1092. <https://doi.org/10.1038/s41556-019-0374-6>
- Silva, M.C., Haggarty, S.J., 2020. Tauopathies: Deciphering Disease Mechanisms to Develop Effective Therapies. *Int. J. Mol. Sci.* 21, 8948. <https://doi.org/10.3390/ijms21238948>
- Simón, D., García-García, E., Gómez-Ramos, A., Falcón-Pérez, J.M., Díaz-Hernández, M., Hernández, F., Avila, J., 2012. Tau Overexpression Results in Its Secretion via Membrane Vesicles. *Neurodegener. Dis.* 10, 73–75. <https://doi.org/10.1159/000334915>
- Sipe, J.D., Cohen, A.S., 2000. Review: History of the Amyloid Fibril. *J. Struct. Biol.* 130, 88–98. <https://doi.org/10.1006/jsbi.2000.4221>
- Sjogren, T., Sjogren, H., Lindgren, A.G., 1952. Morbus Alzheimer and morbus Pick; a genetic, clinical and patho-anatomical study. *Acta Psychiatr. Neurol. Scand. Suppl.* 82, 1–152.
- Skachokova, Z., Martinisi, A., Flach, M., Sprenger, F., Naegelin, Y., Steiner-Monard, V., Sollberger, M., Monsch, A.U., Goedert, M., Tolnay, M., Winkler, D.T., 2019. Cerebrospinal fluid from Alzheimer’s disease patients promotes tau aggregation in transgenic mice. *Acta Neuropathol. Commun.* 7, 72. <https://doi.org/10.1186/s40478-019-0725-3>

- Smet-Nocca, C., Broncel, M., Wieruszeski, J.-M., Tokarski, C., Hanouille, X., Leroy, A., Landrieu, I., Rolando, C., Lippens, G., Hackenberger, C.P.R., 2011. Identification of O-GlcNAc sites within peptides of the Tau protein and their impact on phosphorylation. *Mol. Biosyst.* 7, 1420. <https://doi.org/10.1039/c0mb00337a>
- Smolek, T., Madari, A., Farbakova, J., Kandrak, O., Jadhav, S., Cente, M., Brezovakova, V., Novak, M., Zilka, N., 2016. Tau hyperphosphorylation in synaptosomes and neuroinflammation are associated with canine cognitive impairment: Synaptic tau in canine dementia. *J. Comp. Neurol.* 524, 874–895. <https://doi.org/10.1002/cne.23877>
- Söderberg, O., Gullberg, M., Jarvius, M., Ridderstråle, K., Leuchowius, K.-J., Jarvius, J., Wester, K., Hydbring, P., Bahram, F., Larsson, L.-G., Landegren, U., 2006. Direct observation of individual endogenous protein complexes in situ by proximity ligation. *Nat. Methods* 3, 995–1000. <https://doi.org/10.1038/nmeth947>
- Sofroniew, M.V., Vinters, H.V., 2010. Astrocytes: biology and pathology. *Acta Neuropathol. (Berl.)* 119, 7–35. <https://doi.org/10.1007/s00401-009-0619-8>
- Sotiropoulos, I., Galas, M.-C., Silva, J.M., Skoulakis, E., Wegmann, S., Maina, M.B., Blum, D., Sayas, C.L., Mandelkow, E.-M., Mandelkow, E., Spillantini, M.G., Sousa, N., Avila, J., Medina, M., Mudher, A., Buee, L., 2017. Atypical, non-standard functions of the microtubule associated Tau protein. *Acta Neuropathol. Commun.* 5, 91. <https://doi.org/10.1186/s40478-017-0489-6>
- Sperfeld, A.D., Collatz, M.B., Baier, H., Palmbach, M., Storch, A., Schwarz, J., Tatsch, K., Reske, S., Joosse, M., Heutink, P., Ludolph, A.C., 1999. FTDP-17: An early-onset phenotype with parkinsonism and epileptic seizures caused by a novel mutation. *Ann. Neurol.* 46, 708–715. [https://doi.org/10.1002/1531-8249\(199911\)46:5<708::AID-ANA5>3.0.CO;2-K](https://doi.org/10.1002/1531-8249(199911)46:5<708::AID-ANA5>3.0.CO;2-K)
- Sperling, R.A., Aisen, P.S., Beckett, L.A., Bennett, D.A., Craft, S., Fagan, A.M., Iwatsubo, T., Jack, C.R., Kaye, J., Montine, T.J., Park, D.C., Reiman, E.M., Rowe, C.C., Siemers, E., Stern, Y., Yaffe, K., Carrillo, M.C., Thies, B., Morrison-Bogorad, M., Wagster, M.V., Phelps, C.H., 2011. Toward defining the preclinical stages of Alzheimer's disease: Recommendations from the National Institute on Aging-Alzheimer's Association workgroups on diagnostic

- guidelines for Alzheimer's disease. *Alzheimers Dement.* 7, 280–292.
<https://doi.org/10.1016/j.jalz.2011.03.003>
- Sperling, R.A., Donohue, M.C., Raman, R., Sun, C.-K., Yaari, R., Holdridge, K., Siemers, E., Johnson, K.A., Aisen, P.S., for the A4 Study Team, 2020. Association of Factors With Elevated Amyloid Burden in Clinically Normal Older Individuals. *JAMA Neurol.* 77, 735.
<https://doi.org/10.1001/jamaneurol.2020.0387>
- Spillantini, M.G., Goedert, M., 2013. Tau pathology and neurodegeneration. *Lancet Neurol.* 12, 609–622. [https://doi.org/10.1016/S1474-4422\(13\)70090-5](https://doi.org/10.1016/S1474-4422(13)70090-5)
- Stern, Y., Arenaza-Urquijo, E.M., Bartrés-Faz, D., Belleville, S., Cantilon, M., Chetelat, G., Ewers, M., Franzmeier, N., Kempermann, G., Kremen, W.S., Okonkwo, O., Scarmeas, N., Soldan, A., Udeh-Momoh, C., Valenzuela, M., Vemuri, P., Vuoksimaa, E., and the Reserve, Resilience and Protective Factors PIA Empirical Definitions and Conceptual Frameworks Workgroup, 2020. Whitepaper: Defining and investigating cognitive reserve, brain reserve, and brain maintenance. *Alzheimers Dement.* 16, 1305–1311.
<https://doi.org/10.1016/j.jalz.2018.07.219>
- Stopschinski, B.E., Holmes, B.B., Miller, G.M., Manon, V.A., Vaquer-Alicea, J., Prueitt, W.L., Hsieh-Wilson, L.C., Diamond, M.I., 2018. Specific glycosaminoglycan chain length and sulfation patterns are required for cell uptake of tau versus α -synuclein and β -amyloid aggregates. *J. Biol. Chem.* 293, 10826–10840. <https://doi.org/10.1074/jbc.RA117.000378>
- Studier, F.W., 2005. Protein production by auto-induction in high-density shaking cultures. *Protein Expr. Purif.* 41, 207–234.
<https://doi.org/10.1016/j.pep.2005.01.016>
- Sündermann, F., Fernandez, M.-P., Morgan, R.O., 2016. An evolutionary roadmap to the microtubule-associated protein MAP Tau. *BMC Genomics* 17, 264.
<https://doi.org/10.1186/s12864-016-2590-9>
- Suresh, B., Lee, J., Kim, K.-S., Ramakrishna, S., 2016. The Importance of Ubiquitination and Deubiquitination in Cellular Reprogramming. *Stem Cells Int.* 2016, 1–14. <https://doi.org/10.1155/2016/6705927>
- Tahami Monfared, A.A., Byrnes, M.J., White, L.A., Zhang, Q., 2022. Alzheimer's Disease: Epidemiology and Clinical Progression. *Neurol. Ther.* 11, 553–569.
<https://doi.org/10.1007/s40120-022-00338-8>

- Taniguchi, N., Takahashi, M., Kizuka, Y., Kitazume, S., Shuvaev, V.V., Ookawara, T., Furuta, A., 2016. Glycation vs. glycosylation: a tale of two different chemistries and biology in Alzheimer's disease. *Glycoconj. J.* 33, 487–497. <https://doi.org/10.1007/s10719-016-9690-2>
- Taniguchi, S., Suzuki, N., Masuda, M., Hisanaga, S., Iwatsubo, T., Goedert, M., Hasegawa, M., 2005. Inhibition of Heparin-induced Tau Filament Formation by Phenothiazines, Polyphenols, and Porphyrins. *J. Biol. Chem.* 280, 7614–7623. <https://doi.org/10.1074/jbc.M408714200>
- Tejada-Vera, B., 2013. Mortality from Alzheimer's disease in the United States: data for 2000 and 2010. *NCHS Data Brief* 1–8.
- Tepper, K., Biernat, J., Kumar, S., Wegmann, S., Timm, T., Hübschmann, S., Redecke, L., Mandelkow, E.-M., Müller, D.J., Mandelkow, E., 2014. Oligomer Formation of Tau Protein Hyperphosphorylated in Cells. *J. Biol. Chem.* 289, 34389–34407. <https://doi.org/10.1074/jbc.M114.611368>
- Thal, D.R., Capetillo-Zarate, E., Del Tredici, K., Braak, H., 2006. The development of amyloid beta protein deposits in the aged brain. *Sci. Aging Knowl. Environ.* SAGE KE 2006, re1. <https://doi.org/10.1126/sageke.2006.6.re1>
- The US Burden of Disease Collaborators, Mokdad, A.H., Ballestros, K., Echko, M., Glenn, S., Olsen, H.E., Mullany, E., Lee, A., Khan, A.R., Ahmadi, A., Ferrari, A.J., Kasaeian, A., Werdecker, A., Carter, A., Zipkin, B., Sartorius, B., Serdar, B., Sykes, B.L., Troeger, C., Fitzmaurice, C., Rehm, C.D., Santomauro, D., Kim, D., Colombara, D., Schwebel, D.C., Tsoi, D., Kolte, D., Nsoesie, E., Nichols, E., Oren, E., Charlson, F.J., Patton, G.C., Roth, G.A., Hosgood, H.D., Whiteford, H.A., Kyu, H., Erskine, H.E., Huang, H., Martopullo, I., Singh, J.A., Nacheha, J.B., Sanabria, J.R., Abbas, K., Ong, K., Tabb, K., Krohn, K.J., Cornaby, L., Degenhardt, L., Moses, M., Farvid, M., Griswold, M., Criqui, M., Bell, M., Nguyen, M., Wallin, M., Mirarefin, M., Qorbani, M., Younis, M., Fullman, N., Liu, P., Briant, P., Gona, P., Havmoller, R., Leung, R., Kimokoti, R., Bazargan-Hejazi, S., Hay, S.I., Yadgir, S., Biryukov, S., Vollset, S.E., Alam, T., Frank, T., Farid, T., Miller, T., Vos, T., Bärnighausen, T., Gebrehiwot, T.T., Yano, Y., Al-Aly, Z., Mehari, A., Handal, A., Kandel, A., Anderson, B., Biroscak, B., Mozaffarian, D., Dorsey, E.R., Ding, E.L., Park, E.-K., Wagner, G., Hu, G., Chen, H., Sunshine, J.E., Khubchandani, J., Leasher, J., Leung, J., Salomon, J., Unutzer, J., Cahill, L., Cooper, L., Horino, M., Brauer, M.,

- Breitborde, N., Hotez, P., Topor-Madry, R., Soneji, S., Stranges, S., James, S., Amrock, S., Jayaraman, S., Patel, T., Akinyemiju, T., Skirbekk, V., Kinfu, Y., Bhutta, Z., Jonas, J.B., Murray, C.J.L., 2018. The State of US Health, 1990-2016: Burden of Diseases, Injuries, and Risk Factors Among US States. *JAMA* 319, 1444. <https://doi.org/10.1001/jama.2018.0158>
- Thornton, C., Bright, N.J., Sastre, M., Muckett, P.J., Carling, D., 2011. AMP-activated protein kinase (AMPK) is a tau kinase, activated in response to amyloid β -peptide exposure. *Biochem. J.* 434, 503–512. <https://doi.org/10.1042/BJ20101485>
- Tint, I., Slaughter, T., Fischer, I., Black, M.M., 1998. Acute Inactivation of Tau Has No Effect on Dynamics of Microtubules in Growing Axons of Cultured Sympathetic Neurons. *J. Neurosci.* 18, 8660–8673. <https://doi.org/10.1523/JNEUROSCI.18-21-08660.1998>
- Trabzuni, D., Wray, S., Vandrovцова, J., Ramasamy, A., Walker, R., Smith, C., Luk, C., Gibbs, J.R., Dillman, A., Hernandez, D.G., Arepalli, S., Singleton, A.B., Cookson, M.R., Pittman, A.M., de Silva, R., Weale, M.E., Hardy, J., Ryten, M., 2012. MAPT expression and splicing is differentially regulated by brain region: relation to genotype and implication for tauopathies. *Hum. Mol. Genet.* 21, 4094–4103. <https://doi.org/10.1093/hmg/dds238>
- Trojanowski, J.Q., Lee, V.M.-Y., 2005. Pathological tau: a loss of normal function or a gain in toxicity? *Nat. Neurosci.* 8, 1136–1137. <https://doi.org/10.1038/nn0905-1136>
- Ungar, L., Altmann, A., Greicius, M.D., 2014. Apolipoprotein E, gender, and Alzheimer's disease: an overlooked, but potent and promising interaction. *Brain Imaging Behav.* 8, 262–273. <https://doi.org/10.1007/s11682-013-9272-x>
- U.S. Census Bureau. 2014 National Population Projections, 2021.
- Vanderweyde, T., Apicco, D.J., Youmans-Kidder, K., Ash, P.E.A., Cook, C., Lummertz da Rocha, E., Jansen-West, K., Frame, A.A., Citro, A., Leszyk, J.D., Ivanov, P., Abisambra, J.F., Steffen, M., Li, H., Petrucelli, L., Wolozin, B., 2016. Interaction of tau with the RNA-Binding Protein TIA1 Regulates tau Pathophysiology and Toxicity. *Cell Rep.* 15, 1455–1466. <https://doi.org/10.1016/j.celrep.2016.04.045>
- Vargas-Caballero, M., Denk, F., Wobst, H.J., Arch, E., Pegasiou, C.-M., Oliver, P.L., Shipton, O.A., Paulsen, O., Wade-Martins, R., 2017. Wild-Type, but Not

- Mutant N296H, Human Tau Restores A β -Mediated Inhibition of LTP in Tau $-/-$ mice. *Front. Neurosci.* 11, 201. <https://doi.org/10.3389/fnins.2017.00201>
- Velazquez, R., Ferreira, E., Tran, A., Turner, E.C., Belfiore, R., Branca, C., Oddo, S., 2018. Acute tau knockdown in the hippocampus of adult mice causes learning and memory deficits. *Aging Cell* 17, e12775. <https://doi.org/10.1111/acel.12775>
- Vermunt, L., Sikkes, S.A.M., Hout, A., Handels, R., Bos, I., Flier, W.M., Kern, S., Ousset, P., Maruff, P., Skoog, I., Verhey, F.R.J., Freund-Levi, Y., Tsolaki, M., Wallin, Å.K., Olde Rikkert, M., Soininen, H., Spuru, L., Zetterberg, H., Blennow, K., Scheltens, P., Muniz-Terrera, G., Visser, P.J., for the Alzheimer Disease Neuroimaging Initiative, AIBL Research Group, ICTUS/DSA study groups, 2019. Duration of preclinical, prodromal, and dementia stages of Alzheimer's disease in relation to age, sex, and *APOE* genotype. *Alzheimers Dement.* 15, 888–898. <https://doi.org/10.1016/j.jalz.2019.04.001>
- Violet, M., Delattre, L., Tardivel, M., Sultan, A., Chauderlier, A., Caillierez, R., Talahari, S., Nessler, F., Lefebvre, B., Bonnefoy, E., Bu \ddot{A} , L., Galas, M.-C., 2014. A major role for Tau in neuronal DNA and RNA protection in vivo under physiological and hyperthermic conditions. *Front. Cell. Neurosci.* 8. <https://doi.org/10.3389/fncel.2014.00084>
- Walker, K.A., Ficek, B.N., Westbrook, R., 2019. Understanding the Role of Systemic Inflammation in Alzheimer's Disease. *ACS Chem. Neurosci.* 10, 3340–3342. <https://doi.org/10.1021/acchemneuro.9b00333>
- Wang, Y., Mandelkow, E., 2016. Tau in physiology and pathology. *Nat. Rev. Neurosci.* 17, 5–21. <https://doi.org/10.1038/nrn.2015.1>
- Wang, Y., Mandelkow, E., 2012. Degradation of tau protein by autophagy and proteasomal pathways. *Biochem. Soc. Trans.* 40, 644–652. <https://doi.org/10.1042/BST20120071>
- Ward, A., Tardiff, S., Dye, C., Arrighi, H.M., 2013. Rate of Conversion from Prodromal Alzheimer's Disease to Alzheimer's Dementia: A Systematic Review of the Literature. *Dement. Geriatr. Cogn. Disord. Extra* 3, 320–332. <https://doi.org/10.1159/000354370>
- Weaver, C., 2000. Conformational change as one of the earliest alterations of tau in Alzheimer's disease. *Neurobiol. Aging* 21, 719–727. [https://doi.org/10.1016/S0197-4580\(00\)00157-3](https://doi.org/10.1016/S0197-4580(00)00157-3)

- Webster, J.D., Miller, M.A., DuSold, D., Ramos-Vara, J., 2009. Effects of Prolonged Formalin Fixation on Diagnostic Immunohistochemistry in Domestic Animals. *J. Histochem. Cytochem.* 57, 753–761. <https://doi.org/10.1369/jhc.2009.953877>
- Wee, M., Chegini, F., Power, J.H.T., Majd, S., 2018. Tau Positive Neurons Show Marked Mitochondrial Loss and Nuclear Degradation in Alzheimer’s Disease. *Curr. Alzheimer Res.* 15, 928–937. <https://doi.org/10.2174/1567205015666180613115644>
- Wegmann, S., Nicholls, S., Takeda, S., Fan, Z., Hyman, B.T., 2016. Formation, release, and internalization of stable tau oligomers in cells. *J. Neurochem.* 139, 1163–1174. <https://doi.org/10.1111/jnc.13866>
- Welsh, K.J., Kirkman, M.S., Sacks, D.B., 2016. Role of Glycated Proteins in the Diagnosis and Management of Diabetes: Research Gaps and Future Directions. *Diabetes Care* 39, 1299–1306. <https://doi.org/10.2337/dc15-2727>
- Wendeln, A.-C., Degenhardt, K., Kaurani, L., Gertig, M., Ulas, T., Jain, G., Wagner, J., Häslar, L.M., Wild, K., Skodras, A., Blank, T., Staszewski, O., Datta, M., Centeno, T.P., Capece, V., Islam, Md.R., Kerimoglu, C., Staufenbiel, M., Schultze, J.L., Beyer, M., Prinz, M., Jucker, M., Fischer, A., Neher, J.J., 2018. Innate immune memory in the brain shapes neurological disease hallmarks. *Nature* 556, 332–338. <https://doi.org/10.1038/s41586-018-0023-4>
- Weuve, J., Barnes, L.L., Mendes de Leon, C.F., Rajan, K.B., Beck, T., Aggarwal, N.T., Hebert, L.E., Bennett, D.A., Wilson, R.S., Evans, D.A., 2018. Cognitive Aging in Black and White Americans: Cognition, Cognitive Decline, and Incidence of Alzheimer Disease Dementia. *Epidemiology* 29, 151–159. <https://doi.org/10.1097/EDE.0000000000000747>
- Weuve, J., Bennett, E.E., Ranker, L., Gianattasio, K.Z., Pedde, M., Adar, S.D., Yanosky, J.D., Power, M.C., 2021. Exposure to Air Pollution in Relation to Risk of Dementia and Related Outcomes: An Updated Systematic Review of the Epidemiological Literature. *Environ. Health Perspect.* 129, 096001. <https://doi.org/10.1289/EHP8716>
- Wisniewski, T., Goñi, F., 2015. Immunotherapeutic Approaches for Alzheimer’s Disease. *Neuron* 85, 1162–1176. <https://doi.org/10.1016/j.neuron.2014.12.064>

- Wong, E., Cuervo, A.M., 2010. Integration of Clearance Mechanisms: The Proteasome and Autophagy. *Cold Spring Harb. Perspect. Biol.* 2, a006734–a006734. <https://doi.org/10.1101/cshperspect.a006734>
- Wong, Esther, Cuervo, A.M., 2010. Autophagy gone awry in neurodegenerative diseases. *Nat. Neurosci.* 13, 805–811. <https://doi.org/10.1038/nn.2575>
- Wyss-Coray, T., Rogers, J., 2012. Inflammation in Alzheimer Disease--A Brief Review of the Basic Science and Clinical Literature. *Cold Spring Harb. Perspect. Med.* 2, a006346–a006346. <https://doi.org/10.1101/cshperspect.a006346>
- Xu, J., Murphy, S.L., Kockanek, K.D., Arias, E., 2020. Mortality in the United States, 2018. *NCHS Data Brief* 1–8.
- Yamada, K., 2017. Extracellular Tau and Its Potential Role in the Propagation of Tau Pathology. *Front. Neurosci.* 11, 667. <https://doi.org/10.3389/fnins.2017.00667>
- Yamada, K., Holth, J.K., Liao, F., Stewart, F.R., Mahan, T.E., Jiang, H., Cirrito, J.R., Patel, T.K., Hochgräfe, K., Mandelkow, E.-M., Holtzman, D.M., 2014. Neuronal activity regulates extracellular tau in vivo. *J. Exp. Med.* 211, 387–393. <https://doi.org/10.1084/jem.20131685>
- Yan, S.D., Chen, X., Schmidt, A.M., Brett, J., Godman, G., Zou, Y.S., Scott, C.W., Caputo, C., Frappier, T., Smith, M.A., 1994. Glycated tau protein in Alzheimer disease: a mechanism for induction of oxidant stress. *Proc. Natl. Acad. Sci.* 91, 7787–7791. <https://doi.org/10.1073/pnas.91.16.7787>
- Yasuhara, O., Kawamata, T., Aimi, Y., McGeer, E.G., McGeer, P.L., 1994. Two types of dystrophic neurites in senile plaques of alzheimer disease and elderly non-demented cases. *Neurosci. Lett.* 171, 73–76. [https://doi.org/10.1016/0304-3940\(94\)90608-4](https://doi.org/10.1016/0304-3940(94)90608-4)
- Yiannopoulou, K.G., Papageorgiou, S.G., 2020. Current and Future Treatments in Alzheimer Disease: An Update. *J. Cent. Nerv. Syst. Dis.* 12, 117957352090739. <https://doi.org/10.1177/1179573520907397>
- Yiannopoulou, K.G., Papageorgiou, S.G., 2013. Current and future treatments for Alzheimer's disease. *Ther. Adv. Neurol. Disord.* 6, 19–33. <https://doi.org/10.1177/1756285612461679>
- Yong, W.-S., Hsu, F.-M., Chen, P.-Y., 2016. Profiling genome-wide DNA methylation. *Epigenetics Chromatin* 9, 26. <https://doi.org/10.1186/s13072-016-0075-3>
- Yoshiyama, Y., Higuchi, M., Zhang, B., Huang, S.-M., Iwata, N., Saido, T.C., Maeda, J., Suhara, T., Trojanowski, J.Q., Lee, V.M.-Y., 2007. Synapse Loss and

- Microglial Activation Precede Tangles in a P301S Tauopathy Mouse Model. *Neuron* 53, 337–351. <https://doi.org/10.1016/j.neuron.2007.01.010>
- Yu, W., Qiang, L., Solowska, J.M., Karabay, A., Korulu, S., Baas, P.W., 2008. The Microtubule-severing Proteins Spastin and Katanin Participate Differently in the Formation of Axonal Branches. *Mol. Biol. Cell* 19, 1485–1498. <https://doi.org/10.1091/mbc.e07-09-0878>
- Yuan, A., Kumar, A., Peterhoff, C., Duff, K., Nixon, R.A., 2008. Axonal Transport Rates In Vivo Are Unaffected by Tau Deletion or Overexpression in Mice. *J. Neurosci.* 28, 1682–1687. <https://doi.org/10.1523/JNEUROSCI.5242-07.2008>
- Zayia, L.C., Tadi, P., 2022. Neuroanatomy, Motor Neuron, in: StatPearls. StatPearls Publishing, Treasure Island (FL).
- Zhou, X., Wang, L., Xiao, W., Su, Z., Zheng, C., Zhang, Z., Wang, Y., Xu, B., Yang, X., Hoi, M.P.M., 2019. Memantine Improves Cognitive Function and Alters Hippocampal and Cortical Proteome in Triple Transgenic Mouse Model of Alzheimer's Disease. *Exp. Neurobiol.* 28, 390–403. <https://doi.org/10.5607/en.2019.28.3.390>